

**MITOCHONDRIAL FUNCTION, OXIDATIVE
STRESS AND PARKINSON'S DISEASE**

SUBMITTED BY:

MESFER M. AL SHAHRANI

INBORN ERRORS OF METABOLISM

GENETICS AND GENOMIC MEDICINE PROGRAMME

GREAT ORMOND STREET INSTITUTE OF CHILD HEALTH

UNIVERSITY COLLEGE LONDON

OCTOBER 2018

**THE RESEARCH DOCUMENTED IN THIS THESIS WAS FUNDED BY THE
KING KHALID UNIVERSITY (SAUDI ARABIA)**

**THIS THESIS IS SUBMITTED FOR THE DEGREE OF DOCTOR OF
PHILOSOPHY (PH.D.) AWARDED BY UNIVERSITY COLLEGE LONDON**

Declaration

I, Mesfer Al Shahrani, confirm that the work presented in this thesis is my own. Where information has been derived from other sources, I confirm that this has been indicated in the thesis. Some ideas and figures have been previously published in the following publications (see Appendix):

- ❖ **Al Shahrani, M.**; Heales, S.; Hargreaves, I.; Orford, M. Oxidative Stress: Mechanistic Insights into Inherited Mitochondrial Disorders and Parkinson’s Disease. *J. Clin. Med.* **2017**, 6, 100.

- ❖ Hargreaves, I.; **Al Shahrani, M.**; Wainwright, L.; Heales, S. Drug-Induced Mitochondrial Toxicity. *Drug Saf.* **2016**, 39, 661–674

Signed.....Date

***THIS THESIS IS DEDICATED TO THE MEMORY OF MY DEAR
MOTHER (1964–2015), IN GRATITUDE FOR ALL SHE GAVE
TO ME.***

Abstract

The loss of the activity of mitochondrial respiratory chain (MRC) complexes, particularly complex I, has been implicated in Parkinson's disease (PD) pathogenesis. However, it is still uncertain whether altered MRC activity is an early event in the pathophysiology of PD, or a late consequence of cellular stress. Therefore, this thesis contributes differently from other studies as to the ongoing investigations about MRC activity in PD post-mortem brain based on pathological severity. This study demonstrates that loss of complex I activity occurs in regions with both moderate and mild pathology in PD brain. Furthermore, multiple complex defects were noted in the moderate pathology region. However, the activity of complex II which is entirely encoded by nuclear DNA appeared to be preserved.

The exact mechanism of multiple complex defects remain elusive. However, the possibility arises that impairment of complex I results in secondary damage to the other complexes. Here, neuroblastoma cells were employed to study the effect of pharmacologically induced MRC complex I deficiency upon the activity of the other complexes. In this model, rotenone-treated (100 nM; 24-48 hours) SH-SY5Y cells induced an inhibition of complex I. At 24 hours no effect was observed on the other complexes. However at 48 hours, multiple complex defects were noted, but the activity of complex II appeared to be preserved. Additionally, bioenergetics and glutathione status were compromised. By utilizing this model, the effectiveness of antioxidants in alleviating the progression of complex I deficiency on other complexes were

also evaluated. Furthermore, the use of the Oxygraph-2K® instrument together with a step-wise protocol was developed to assess the integrated mitochondrial function in cultured SH-SY5Y cells. Additionally, the focus of attention was also to validate the fibroblast growth factor-21 ELISA assay. Based on the results, this assay appears to be a useful as a biomarker for mitochondrial dysfunction.

Impact Statement

A central role for mitochondria is energy production by the process of oxidative phosphorylation. Damage to this process might dramatically increase the generation of harmful free radicals and impair energy production. Indeed, the central nervous system depends upon mitochondrial function because neurons demand a high amount of energy to be metabolically active. Consequently, impaired mitochondrial function, increases free radicals and oxidative stress may contribute to decrease in ATP production, and eventually lead to age-related disorder such as Parkinson Disease (PD).

PD is a chronic and progressive neurodegenerative disorder, affecting approximately 1%, almost exclusively in the aged 60 years or older. As the aging population and life expectancy are projected to rapidly grow over the next few decades, the prevalence of this disorder is expected to increase to 50% by 2030. In addition, the cost of illness may possibly escalate further as the proportion of individuals in Western societies aged over 60 dramatically increases. Furthermore, the medical costs attributable to PD occur when the disease reaches more advanced stages and symptoms become more pronounced. Therefore, there is a need for the development of early diagnostic biomarkers and new therapeutic strategies to minimise the impact of disease progression and improve quality of life in patients.

Despite the precise mechanism associated with neurodegeneration in PD is not yet fully understood, the inhibition of mitochondrial complexes, particularly, complex I has been invoked as a potential contributor to the pathophysiology

of PD. The findings presented here provide further evidence of reduced mitochondrial complexes activities which is directly associated with pathological PD severity. This could potentially lead to the development of an early therapeutic intervention aimed at slowing down PD progression.

At the level of the mitochondrial complexes, the neuronal model presented here which successfully mimicked PD brain, not only provides a possible approach to study the biochemical consequences of complex I deficiency in neurodegenerative disorders such as PD, but also could be potentially applicable to study other inherited mitochondrial disorders as well as monitoring therapeutic interventions.

Furthermore, it has been reported that at the time of PD diagnosis, the majority of dopaminergic neurons have been already lost. Consequently, any antioxidant interventions at this stage would be unable to prevent subsequent neuronal death. This suggests that antioxidant intervention at early stage of PD may halt or slow down the neurodegenerative process. Taken together, the findings presented here adds to a growing body of literature on the positive impact of early intervention of antioxidants which may be helpful at slowing down disease progression.

Furthermore, although muscle biopsy remains a gold standard diagnostic tool for patients with mitochondrial disorders, it is still an invasive costly procedure that requires both a surgical technique and anesthesia. In order to limit the need for an invasive muscle biopsy, FGF-21 ELISA assay is being validated in this thesis as a potential mitochondrial biomarker. Results so far have been very promising and suggesting that this assay may potentially be useful clinically as a biomarker of mitochondrial disorders.

Table of Contents

Declaration	2
Abstract	4
Impact Statement	6
Table of Contents	8
List of Figures	15
List of Tables	21
List of Abbreviations	23
Acknowledgment	26

CHAPTER 1

Introduction	29
1.1 Mitochondrial Function and Structure	30
1.2 Mitochondrial Respiratory Chain (MRC).....	33
1.2.1 MRC Complex I [EC 1.6.5.3].....	36
1.2.2 MRC Complex II [EC 1.3.5.1].....	42
1.2.3 MRC Complex III [EC 1.10.2.2].....	43
1.2.4 MRC Complex IV [EC 1.9.3.1]	45
1.3 MRC Supercomplexes	46
1.4 ATP Synthase [EC 3.6.3.14]	47
1.5 Citrate Synthase [EC 2.3.3.1].....	51
1.6 Oxidative Stress.....	53
1.7 Mitochondria are a Major Site of ROS Production and Target of ROS-mediated Dysfunction	56
1.8 Mitochondrial Targets of Oxidative Stress and Association with Inherited Disorders and PD.....	58

1.8.1 Mitochondrial DNA	59
1.8.1.1 Leber's Hereditary Optic Neuropathy.....	60
1.8.1.2 Myoclonic Epilepsy with Ragged Red Fibers	61
1.8.2 Mitochondrial Cardiolipin.....	62
1.8.2.1 Barth Syndrome.....	64
1.8.3 Mitochondrial Aconitase	66
1.8.3.1 Friedreich Ataxia	68
1.8.4 Parkinson Disease	70
1.8.4.1 Mitochondrial Dysfunction and PD.....	71
1.8.4.2 The Interplay among PINK1, Parkin and DJ-1 during Mitochondrial Quality Control.....	77
1.8.4.3 A Potential Link between Neuroinflammation and Mitochondrial Dysfunction in the Pathogenesis of PD.....	78
1.8.4.4 Iron and Mitochondrial Dysfunction: Cross-Talk in PD.....	79
1.8.5 PD Treatments.....	84
1. 9 Parkinson Therapies Induced MRC Toxicity	86
1.9.1 Levodopa (L-dopa).....	86
1.9.2 Catechol-O-methyltransferase (COMT)	88
1.10 The Role of Antioxidants in the Prevention of Oxidative Damage	89
1.10.1 Coenzyme Q ₁₀	89
1.10.2 Glutathione (GSH).....	93
1.11 Oxidative Stress Biomarkers as Indicators for Mitochondria Disorders	98
Aims and the Scope of this Thesis	100

CHAPTER 2

Materials and Methods.....	101
2.1 Materials.....	102
2.2 Cell culture	103
2.2.1 Human SH-SY5Y Neuroblastoma Cell Line	103
2.2.2 SH-SY5Y Cell Storage and Recovery	104

2.2.3 SH-SY5Y Cell Thawing and Passaging	105
2.2.4 SH-SY5Y Cell Harvesting for Biochemical Assays	106
2.2.5 Cell treatments.....	107
2.4 Total Protein Determination	108
2.5 Mitochondrial Enzymatic Assays.....	110
2.5.1 Background.....	110
2.5.2 Analytical Equipment	111
2.5.3 Analytical Procedure	111
2.5.3.1 MRC Complex I [EC 1.6.5.3]	111
2.5.3.2 MRC Complex II [EC 1.3.5.1]	114
2.5.3.3 MRC Complex II-III	117
2.5.3.4 MRC Complex IV [EC 1.9.3.1].....	119
2.5.3.5 Citrate Synthase [EC 2.3.3.1]	121
2.6 High Performance Liquid Chromatography (HPLC)	124
2.6.1 Background.....	124
2.6.2 Measurement of Cellular Energy Charge (EC)	125
2.6.2.1 Analytical Equipment	127
2.6.2.2 Analytical Procedure.....	127
2.6.2.3 Cell treatment and Extraction	128
2.6.2.4 Adenine Nucleotides Derivatization	128
2.6.2.5 Data Analysis.....	129
2.6.3 Measurement of Coenzyme Q10	131
2.6.3.1 Analytical Equipment	131
2.6.3.2 Analytical Procedure.....	131
2.6.3.3 Data Analysis.....	132
2.6.4 Measurement of Reduced Glutathione (GSH)	133
2.6.4.1 Analytical Equipment	134
2.6.4.2 Analytical Procedure.....	134
2.6.3.4 Data Analysis.....	137
2.7 Statistical Analysis	138

CHAPTER 3

Evaluation of Mitochondrial Enzyme Complex Activities in Post-Mortem Brain Tissue from Patients with Parkinson’s Disease	139
3.1 Background	140
3.2 Aims	143
3.3 Methods	144
3.3.1 Brain samples	144
3.3.2 PD brain cases and control groups	144
3.3.3 Brain Tissue Homogenization	144
3.3.4 Mitochondrial Enzymatic Assays.....	145
3.3.5 Statistical Analysis	145
3.4 Results	149
3.5 Discussion.....	155
3.6 Conclusion	158

CHAPTER 4

Development of a Neuronal Cell model to Investigate Mitochondrial Respiratory Chain Dysfunction in Parkinson’s Disease	159
4.1 Background	160
4.2 Aims	162
4.3 Methods	163
4.3.1 Cell Culture	163
4.3.2 Total Protein Concentration	163
4.3.3 Mitochondrial Enzymatic Assays.....	163
4.3.4 Measurement of Cellular Energy Charge	163
4.3.5 Measurement of Coenzyme Q ₁₀	164
4.3.6 Measurement of Reduced Glutathione (GSH)	164
4.3.7 Statistical Analysis	164
4.4 Results	165
4.4.1 Mitochondrial Enzymatic Assays.....	165

4.4.2 Measurement of Cellular Energy Charge.....	169
4.4.3 Measurement of Coenzyme Q ₁₀	171
4.4.4 Measurement of Reduced Glutathione (GSH)	173
4.5 Discussion.....	174
4.6 Conclusion	178

CHAPTER 5

Evaluation of the Efficacy of Antioxidants on Mitochondrial Respiratory Chain Dysfunction in a Neuronal Cell Model

5.1 Background.....	180
5.1.1 Ascorbic Acid (Vitamin C)	181
5.1.2 α -Tocopherol and its Analogue	183
5.1.3 Reduced Glutathione and its Analogue	184
5.2 Aims.....	187
5.3 Methods	187
5.3.1 Cell Culture	187
5.3.2 Antioxidant Treatment.....	187
5.3.3 Mitochondrial Enzymatic Assays	188
5.3.4 Statistical Analysis	188
5.4 Results	190
5.4.1 Evaluation of the Protective Effects of Ascorbate on MRC Complex I, II-III and IV Activity	190
5.4.2 Evaluation of the Protective Effects of Trolox on MRC Complex I, II-III and IV Activity	192
5.4.3 Evaluation of the Protective Effects of NAC on MRC Complex I, II-III and IV Activity	194
5.5 Discussion.....	197
5.6 Conclusion	201

CHAPTER 6

Mitochondrial Cellular Respiration Measurement Using High Resolution Respirometry 203

6.1 Background	204
6.1.1 Mitochondrial Respiration States	207
6.1.2 The Measurement of Mitochondrial Respiration.....	210
6.1.3 The Assessment of Integrated Mitochondrial Function in Cultured Cells.....	215
6.2 Aim.....	216
6.3 Methods	216
6.3.1 Cell culture	216
6.3.2 Mitochondrial Cellular Respiration Measurement.....	217
6.3.3 Analytical Protocol.....	217
6.3.4 Data Analysis	225
6.4 Results	225
6.5 Discussion.....	227
6.6 Conclusion	229

CHAPTER 7

Development of an Accurate and Robust Assay for Fibroblast Growth Factor-21 230

7.1 Background	231
7.2 Aims	239
7.3 Methods	239
7.3.1 Background.....	239
7.3.2 Patient Samples	240
7.3.3 Analytical Procedure	241
7.3.4 Statistical Analysis	242
7.4 Results	243
7.4.1 Validation Process	243

7.4.2 The Induction of FGF21 in Mitochondrial Disorders Patients.....	248
7.4.3 Association between FGF21 Levels and Age and Biochemical Parameters in Peadiatric Patients with Genetically Confirmed Mitochondrial Disease	253
7.5 Discussion.....	263
7.6 Conclusions	268

CHAPTER 8

General Discussion, Conclusion and Further Work.....	269
8.1 Discussion.....	270
8.2 Conclusion	286
8.3 Further work.....	287
8.3.1 Neuronal Cell Model	287
8.3.2 Antioxidant Treatments	289
8.3.3 The Measurement of Mitochondrial Respiration Using O2K	289
8.3.4 FGF-21	290
List of References	291
Appendix.....	348
Section 1	348
Validation FGF-21 kit agreement and team	348
Section 2	350
Validation FGF-21 Plan	350
Published Conference Abstracts Related to this Thesis	358
Published Review Articles Related to this Thesis	359

List of Figures

Figure 1 Illustrates some of fundamental roles of mitochondria beyond of being primary energy source for the cellular metabolism	31
Figure 2 A typical the structure of mitochondria.....	33
Figure 3 A schematic underling bioenergetics of the MRC and OXPHOS pathways.	35
Figure 4 The structural components of MRC complex I in mammalian mitochondria.....	37
Figure 5 Illustrates the possible events associated with mitochondrial $O_2^{\bullet-}$ production, particularly from MRC complex I.....	41
Figure 6 Schematic illustrating the Q-cycle of the cytochrome bc_1 complex..	45
Figure 7 Illustrates the subunit organisation in ATP synthase	50
Figure 8 Schematic illustration of the TCA cycle.....	52
Figure 9 A schematic underlies the pathway of mitochondrial free radical generation and their enzymatic antioxidant defences.....	58
Figure 10 The chemical structure of CL.....	63
Figure 11 A potential mechanism of oxidation inactivation of m-aconitase by mitochondrial $O_2^{\bullet-}$	68
Figure 12 Schematic illustrating the potential role of mitochondrial dysfunction in the PD pathogenesis	74
Figure 13 The potential interaction between PD-related genes and their potential impact on mitochondrial function.....	75
Figure 14 A potential mechanism of dopamine metabolism and OH^{\bullet} radical formation in the striatum of PD patients as a result of iron accumulation and decline in GSH levels.	81
Figure 15 A summary of oxidative stress-induced mitochondrial damage is a common mechanistic link in the pathogenesis of inherited mitochondrial disorders and PD.....	83
Figure 16 A schematic underlying the current treatment options for Parkinson's patients.	85
Figure 17 The chemical structure of CQ_{10} and its two redox forms	90

Figure 18 Illustrating the biosynthesis of GSH and its transport to mitochondria.....	95
Figure 19 Highlights some of the most common oxidative stress biomarkers for cellular molecules oxidation..	99
Figure 20 Microscope image of control human SH-SY5Y cells captured at 20x magnification using Olympus IX71 inverted microscope	104
Figure 21 A schematic illustration of the preparation of SH-SY5Y cells for biochemical assays	107
Figure 22 Dose response reduction of MRC complex I activity by rotenone	108
Figure 23 A typical standard curve for the Lowry assay showing the plot of BSA standard protein concentration against absorbance at 750nm.....	110
Figure 24 A simple diagram showing the basic components of a UV/Visible spectrophotometer instrument.....	111
Figure 25 The reaction of MRC complex I activity	112
Figure 26 The standard curve of the MRC complex I activity (nmol/min/ml) plots against protein content (mg/ml)	114
Figure 27 The reaction of MRC complex II activity	115
Figure 28 The standard curve of the MRC complex II activity (nmol/min/ml) plots against protein content (mg/ml)	116
Figure 29 The reaction of MRC complex II-III activity.....	117
Figure 30 The standard curve of the MRC complex II-III activity (nmol/min/ml) plots against protein concentration (mg/ml).....	119
Figure 31 The reaction of MRC complex IV.....	120
Figure 32 The standard curve of the MRC complex IV activity (k/min/ml) plots against protein content (mg/ml).....	121
Figure 33 The reaction of CS activity.....	122
Figure 34 The standard curve of CS activity (nmol/min/ml) plots against protein content (mg/ml).	123
Figure 35 A simple diagram showing the basic components of a HPLC system.....	125
Figure 36 The reaction of chloroacetaldehyde with adenine forming N6-etheno derivatives.	126

Figure 37 Representative Chromatogram of adenine nucleotides.	130
Figure 38 Representative chromatogram of CoQ ₁₀ in control SH-SY5Y cells and internal standard (IS) with RT at 11.4 and 14.3 min, respectively.	133
Figure 39 The oxidation peak potential of 5μM GSH standard from +200 to +600 mV was monitored via voltammogram.....	136
Figure 40 Representative chromatogram of the external GSH standard (5μM) with RT at 10.7 min.....	136
Figure 41 The standard curve of the external GSH standard (μM) plots against peak area.....	137
Figure 42 MRC complex I activity in post-mortem brain regions of control (C) and the Parkinson's disease (PD) with different pathological severity.....	150
Figure 43 MRC complex II-III activity in post-mortem brain regions of control (C) and the Parkinson's disease (PD) with different pathological severity...	151
Figure 44 MRC complex IV activity in post-mortem brain regions of control (C) and the Parkinson's disease (PD) with different pathological severity...	152
Figure 45 MRC complex II activity in post-mortem brain regions of control (C) and the Parkinson's disease (PD) with different pathological severity.....	153
Figure 46 MRC complexes activities are expressed as a ratio to CS activity in SHSY5Y cells treated with 100 nM of rotenone for 24 and 48 hrs.....	166
Figure 47 CS activity in SH-SY5Y cells treated with 100 nM of rotenone for 24 and 48 hrs.....	168
Figure 48 Adenine nucleotides status in SH-SY5Y cells treated with 100 nM of rotenone for 24 and 48 hrs.	170
Figure 49 CoQ ₁₀ level in SH-SY5Y cells treated with 100 nM of rotenone for 24 and 48 hrs.....	171
Figure 50 CoQ ₁₀ level is expressed as a ratio to CS activity in SHSY5Y cells treated with 100 nM of rotenone for 48 hr.....	172
Figure 51 GSH status in SH-SY5Y cells treated with 100 nM of rotenone for 24 and 48 hrs.....	173
Figure 52 Vitamin C acts as a powerful antioxidant alone or synergistically with other free radical antioxidants, such as GSH and α-tocopherol.	182
Figure 53 The reaction which α-tocopherol terminates lipid peroxidation reaction by scavenging the chain-carrying LOO•.....	183

Figure 54 The potential mechanism of the membrane-permeable cysteine precursor, N-acetylcysteine (NAC).....	185
Figure 55 Schematic underlying the experimental design for rotenone and antioxidants treatment.....	189
Figure 56 Effect of ascorbate (1.0 mM; 24 hr) on MRC complex I, II-III and IV activity after 24 hr exposure of SH-SY5Y cells to rotenone.....	191
Figure 57 Effect of Trolox (500 μ M; 24 hr) on MRC complex I, II-III, and IV activity after 24 hr exposure of SH-SY5Y cells to rotenone.....	193
Figure 58 Effect of NAC (500 μ M; 24 hr) on MRC complex I, II-III and IV activity after 24 hr exposure of SH-SY5Y cells to rotenone.....	195
Figure 59 The schematic diagram outlines the MRC and OXPHOS pathways with substrates (electron donors) shown in rectangular box and inhibitors in circular box.....	205
Figure 60 An experimental example of polarographic oxygen consumption showing mitochondrial respiration states upon addition of substrates.....	208
Figure 61 A schematic representation of Clark amperometric sensor for determining dissolved O ₂ in biological sample.	211
Figure 62 The Oxygraph-2K [®] (O2k) for high-resolution respirometry (HRR) instrument	214
Figure 63 Illustrate (A) the calibrating of oxygen concentration in two chambers (1A and 1B) at air saturation (R1), constant temperature (37 °C), and stirrer speeds of 750 rpm in culture media. The slope uncorrected value for R1 should be within (\pm 1.0) [pmol/(s*ml)] as shown in circular box (B)...	218
Figure 64 The routine respiration; [R] state was evaluated after a 10 minutes period under SH-SY5Y cell media.....	219
Figure 65 The leak respiration [L] state was consequently induced after inhibiting complex V	220
Figure 66 The uncoupler FCCP enhanced respiration rate, which reflects the maximal of electron transfer system (ETS; [E]) state..	221
Figure 67 Rotenone blocks the mitochondrial respiration and induced residual oxygen consumption (ROX) state after inhibits MRC complex I.....	222
Figure 68 Representative oxygraph traces of oxygen consumptions in SH-SY5Y cells.....	224

Figure 69 Mitochondrial respiration rates in cultured SH-SY5Y cells.....	226
Figure 70 Mitochondrial respiration states in cultured SH-SY5Y cells after corrected to residual oxygen consumption (ROX).	226
Figure 71 The potential action of FGF-21 on glucose metabolism in various organs and tissues.	235
Figure 72 FGF-21 acts as a novel regulator and adaptor against physiological and pathological stress.....	236
Figure 73 The putative mechanism of the induction of FGF-21 protein in response to the mitochondrial stress stimuli in muscle cells.....	237
Figure 74 A typical Sandwich ELISA assay.	240
Figure 75 The standard curve for the FGF-21 ELISA assay showing the plot of FGF-21 standard concentration against absorbance at 450 nm.....	243
Figure 76 The standard curve for dilution of serum sample.....	246
Figure 77 Serum FGF-21 levels (pg/ml) in both disease controls and patients with suspected MD.	247
Figure 78 FGF-21 levels in paediatric patients with genetically confirmed mitochondrial disease.....	250
Figure 79 A Flow chart illustrates the serum level of FGF-21 in 38 adult patients.....	251
Figure 80 FGF-21 levels in adult patients genetically and clinically diagnosed with mitochondrial disease.	252
Figure 81 Correlation between serum FGF-21 levels (pg/ml) and age (days) in paediatric patients with genetically confirmed mitochondrial disease ($n= 63$)	254
Figure 82 Correlation between serum FGF-21 levels (pg/ml) and lactate levels (mmol/L) in paediatric patients with genetically confirmed mitochondrial disease ($n= 60$).....	255
Figure 83 Correlation between serum FGF-21 levels (pg/ml) and CK levels (U/L) in paediatric patients with genetically confirmed mitochondrial disease ($n= 50$).....	256
Figure 84 Correlation between serum FGF-21 levels (pg/ml) and alanine levels ($\mu\text{mol/L}$) in paediatric patients with genetically confirmed mitochondrial disease ($n= 49$).....	257

Figure 85 Correlation between serum FGF-21 levels (pg/ml) and ALT levels (U/L) in paediatric patients with genetically confirmed mitochondrial disease (<i>n</i> = 57).....	258
Figure 86 Correlation between serum FGF-21 levels (pg/ml) and ALP levels (U/L) in paediatric patients with genetically confirmed mitochondrial disease (<i>n</i> = 51).....	259
Figure 87 Correlation between serum FGF-21 levels (pg/ml) and creatinine levels (µmol/L) in paediatric patients with genetically confirmed mitochondrial disease (<i>n</i> = 58).	260
Figure 88 Correlation between serum FGF-21 levels (pg/ml) urea levels (mmol/L) in paediatric patients with genetically confirmed mitochondrial disease (<i>n</i> = 50)	261
Figure 89 Correlation between serum FGF-21 levels (pg/ml) glucose levels (mmol/L) in paediatric patients with genetically confirmed mitochondrial disease (<i>n</i> = 40)..	262
Figure 90 Summarised of the biochemical consequences associated with short and long-terms exposure to 100 nM of rotenone-induced MRC complex I deficiency	279

List of Tables

Table 1 List of some reactive species generated during metabolism	54
Table 2 List of some enzymatic and non-enzymatic antioxidant defence.....	55
Table 3 Gene products implicated in etiopathogenesis of familial PD.....	71
Table 4 HPLC mobile phase buffers (A and B) gradient profile utilized for the elution of adenine nucleotides from the HPLC column.	128
Table 5 Demographic data of the post-mortem PD cases used in this study	146
Table 6 MRC complex I, II-III and IV activities are expressed as a ratio to CS activity in post-mortem brain regions of control (C) and the Parkinson's disease (PD) with different pathological severity.	154
Table 7 MRC complex I, II-III and IV activities are expressed as a ratio to CS activity in SHSY5Y cells treated with 100 nM of rotenone for 24 and 48 hrs	167
Table 8 The structure and function of antioxidants ascorbate, Trolox and NAC	186
Table 9 The protective effects of ascorbate, Trolox and NAC on MRC activity in rotenone-treated cells	196
Table 10 The most commonly used substrates, inhibitors, and uncouplers of MRC function.....	210
Table 11 Mitochondrial respiratory rates in cultured SH-SY5Y cells	227
Table 12 Non-invasive biochemical parameters for evaluating mitochondrial disorders (MDs)	234
Table 13 Two serum samples of known concentration were assayed on one plate to assess intra-assay precision of Human FGF-21 ELISA assay.....	244
Table 14 Pooled serum sample of known concentration was assayed on different plates to assess inter-assay precision of Human FGF-21 ELISA assay	245
Table 15 Two serum samples were spiked with known concentration of human fibroblast growth factor (FGF-21) and assayed	246
Table 16 Paediatric patients with genetically confirmed mitochondrial disease	249

Table 17 MRC complex I, II-III and IV inhibitions in post-mortem PD brain regions with different pathological severity..... 273

Table 18 MRC complex I, II-III and IV inhibitions in SHSY5Y cells treated with 100 nM of rotenone for 24 and 48 hrs 275

Table 19 Summarised of key findings of energy charge, CoQ10 and GSH status upon exposure SH-SY5Y cells to 100 nM of rotenone for 24 and 48 hrs 277

List of Abbreviations

$\Delta\Psi_m$	Mitochondrial membrane potential
Acetyl-CoA	Acetyl-Coenzyme A
ADP	Adenosine diphosphate
ALP	Alkaline phosphatase
ALT	Alanine transaminase
AMP	Adenosine monophosphate
ANOVA	Analysis of Variance
ATP	Adenosine triphosphate
BSA	Bovine serum albumin
CNS	Central nervous system
CoQ	Coenzyme Q (ubiquinone)
CoQH ₂	Reduced CoQ (ubiquinol)
CS	Citrate synthase
CSF	Cerebrospinal fluid
CV	Coefficient of Variation
DA	Dopaminergic
DAT	Dopamine transporter
DMEM	Dulbecco's modified Eagle's medium
DNA	Deoxyribonucleic acid
dsDNA	Double stranded DNA
DTNB	5, 5'-dithio-bis (2-nitrobenzoic acid)
e^-	Electron
ETF	Electron-transferring-flavoprotein
ETF-QO	Electron-transferring-flavoprotein quinone oxidase
FA	Friedreich's Ataxia
FAD	Flavin adenosine dinucleotide
FADH ₂	Flavin adenosine dinucleotide (reduced)
FBS	Fetal Bovine Serum
FCCP	Carbonyl cyanide-(trifluoromethoxy) phenylhydrazone
GSH	Reduced Glutathione

GSSG.....Glutathione (oxidized form)
 GTP.....Guanosine triphosphate
 H⁺.....Proton
 H₂O₂.....Hydrogen peroxide
 HPLC.....High performance liquid chromatography
 IS.....Internal standard
k.....Rate order constant
 KCN.....Potassium cyanide
 LBs.....Lewy bodies
 LNs.....Lewy Neurites
 MAO.....Monoamine oxidase
 MnSOD:.....Manganese superoxide dismutase
 MPP⁺.....1-methyl-4phenyl-2,3-dihydropyridium ion
 MPTP.....1-methyl-4-phenyl-1,2,3,6-tetrahydropyridine
 MRCs.....Mitochondrial respiratory chain(s)
 mtDNA.....Mitochondrial Deoxyribonucleic acid
 NAD⁺.....Nicotinamide adenine dinucleotide (oxidised)
 NADH.....Nicotinamide adenine dinucleotide (reduced)
 NADPH.....Nicotinamide adenine dinucleotide phosphate (reduced)
 nDNA.....Nuclear Deoxyribonucleic acid
 NO.....Nitric Oxide
 NO•.....Nitric oxide radical
 O₂^{•-}.....Superoxide radical
 OAA.....Oxaloacetic acid
 OH•.....Hydroxyl radical
 PD.....Parkinson's disease
 PMF.....Proton motive force
 PTP.....Permeability transition pore
 RNA.....Ribonucleic acid
 ROS.....Reactive oxygen species
 SD.....Standard Deviation
 SEM.....Standard error of the
 mean

SNpc..... Substantia nigra pars compacta
SOD..... Superoxide dismutase
tRNA..... Transfer ribonucleic acid
UV Ultraviolet

Acknowledgment

This endeavour becomes reality with the kind of assistance and support of many individuals. I would like to extend my sincere gratitude to everyone who in different ways has contributed to this doctoral thesis.

Foremost, I would like to express my deepest gratitude to my principal supervisor Prof. Simon Heales for his guidance, advice, keen insight and encouragement he has generously provided throughout my PhD studies.

I wish to place on record my sincere and heartfelt thanks to my secondary supervisors Dr. Michael Orford, and Dr. Iain Hargreaves who always care of my PhD study, who always open their heart before their door to me if I have any questions or concerns. I can't thank them enough for everything that they have done for making this journey a possible one. Their tremendous supporting hand paved a way to the completion of this doctoral thesis. The timeless inspiration and encouragement that they gave has put me through this journey. I owe both of you a world of gratitude for all you have done for me.

Very special thanks to all the members of staff at Neurometabolic Unit, National Hospital for Neurology and Neurosurgery, for their help and support during my PhD journey, particularly Viruna Neergheen, Annapurna Chalasani and Dr. Simon Pope.

I express my thanks to Dr. Sonia Gandhi for providing post-mortem flash frozen brain tissues obtained from PD patients to evaluate the activity of mitochondrial respiratory chain complexes.

I would like to express my gratitude and appreciation to Prof. Shamima Rahman for providing the serum samples and numerous patient results she supplied me with for FGF-21.

Many thanks to all the members of staff at Clinical Immunology Laboratory, Great Ormond Street Hospital, for providing me all materials and assistance relating to FGF-21 Sandwich ELISA assay, particularly, Dr. Kimberly Gilmour and Elizabeth Ralph.

A special thanks to Dr. Kevin Mills and Dr. Francesca Mazzacuva for their continued support and help during my mother's death. Words cannot express my sincere appreciation to them for their support to get through this extremely difficult time of my life.

This journey would not have been possible without the boundless support and help from my colleagues. Thus, I would like to give my special gratitude to Aziza Khabbush, and Carmen De La Fuente who I shared my PhD journey with from start to finish.

Along with a great job and staying all night to extract a lot of the biochemical data for the FGF-21 correlation for me in a timely manner, I am extremely grateful to Fatma Taha, a true friend who walks into my life when my life has walked out during my difficult times at last year. She has been more like a sister than a friend to me. I can't thank her enough for everything that she has done for making this final stages a possible one.

A Heartfelt thanks to my family for their endless support, inspiration and love. They always support me spiritually and financially throughout my PhD journey.

Finally, I am highly indebted to the King Khalid University, Saudi Arabia, not only for providing the funding which allowed me to undertake this research, but also for giving me the opportunity to attend scientific conferences and connect with many outstanding researchers of similar interests, on a social level as well as a professional one.

CHAPTER 1

Introduction

1.1 Mitochondrial Function and Structure

Mitochondria (singular, mitochondrion) are evolutionary believed to be coined from an alpha-proteobacterium around a million years ago (reviewed by Gray, 2012). Over 150 years ago, mitochondria were first scientifically identified in avian flight muscles and liver. In 1890, Richard Altman provided the first description of mitochondria as cell organelles using a dye staining procedure, and subsequently referred to them as “bioblasts” (reviewed by O’Rourke, 2010). In 1898, the German scientist Carl Benda replaced the term of bioblast with mitochondrion (Greek: mitos—thread; chondros—granule). More progress in the area of mitochondria was made by Eugene Kennedy and Albert Lehninger after discovering that mitochondria are the site of the energy producing machinery, namely the oxidative phosphorylation pathway (OXPHOS) (reviewed by Pagliarini and Rutter, 2013). Over subsequent years, mitochondria have widely become known as the “powerhouse of the cells” following their description by Philip Siekevitz (reviewed by Verschoor et al., 2013). Mitochondria have caught the attention of most biochemists. They have been intensively investigated not only because they are “powerhouse of the cell”, but more recently due to their fast-growing involvement in the metabolic medicine area. In addition to their primary function to generate cellular energy in the form of ATP by means of the respiratory transport chains and OXPHOS, they also exhibit fascinating involvements in fatty acid oxidation and urea cycle metabolism, heme biosynthesis and intracellular calcium homeostasis as well as regulation of apoptosis, signal transduction, and the cell cycle (Figure 1) (Lionaki et al., 2015; Smith et al., 2012).

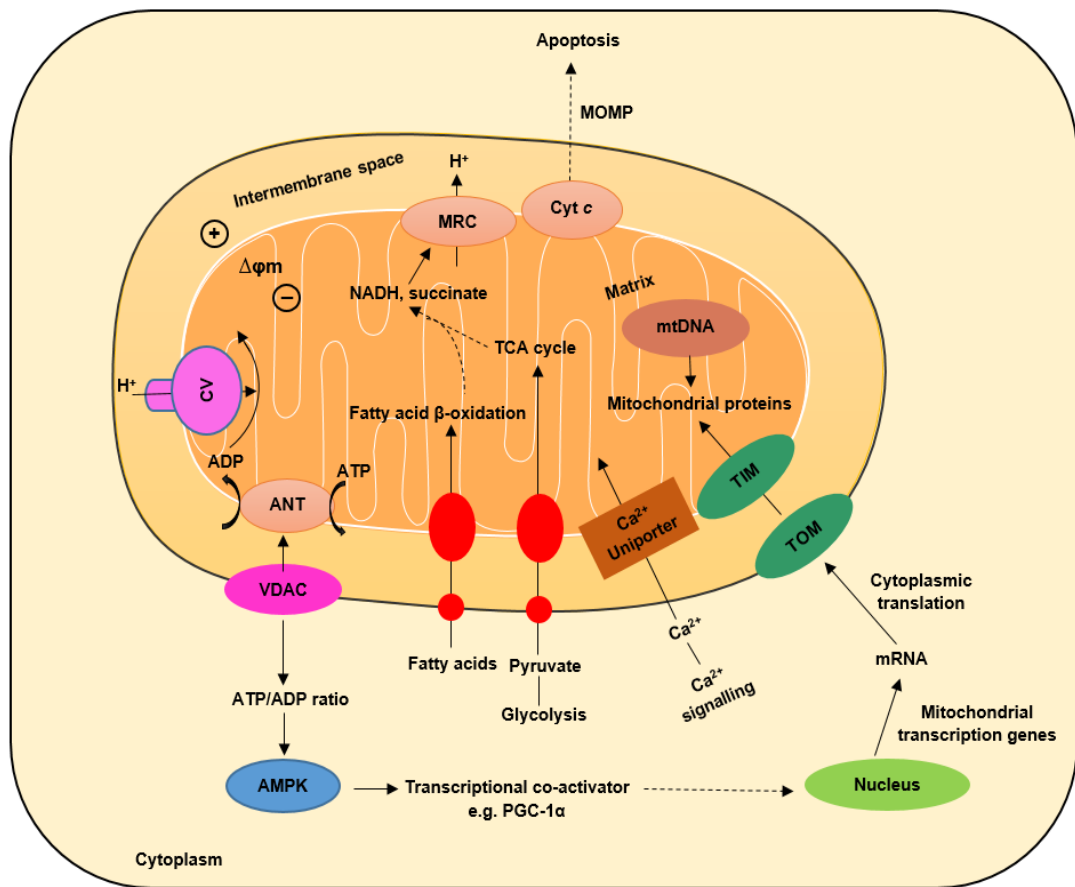


Figure 1 Illustrates some of fundamental roles of mitochondria beyond of being primary energy source for the cellular metabolism. In the cytosol, glucose is initially converted by glycolysis pathway to pyruvate. The Outer mitochondrial membrane (OMM) contains porin channels, also identified as voltage-dependent anion channels (VDACs) which allow small molecules to freely diffuse into the intermembrane space. The reduction of the cytosolic ATP/ADP ratio via alteration in ADP concentration consequently leads to activate the metabolic sensor, AMP-dependent protein kinase (AMPK), which subsequently stimulates the expression of the co-activator peroxisome proliferator-activated receptor γ coactivator 1 α (PGC-1 α). The mtDNA contains 13 genes that encode MRC complexes and ATP synthase. The other proteins which are encoded by nDNA genes are imported into mitochondrial matrix through translocases in both the outer and inner mitochondrial membrane, TOM and TIM, respectively. The adenine nucleotide translocase or adenine nucleotide translocator (ANT) acts as a protein carrier

in inner mitochondrial membrane (IMM), exchanging mitochondrial matrix ATP for cytosolic ADP. Mitochondria plays a significant role in the dynamic of Ca^{2+} signalling machinery by taking up Ca^{2+} from the cytosol into the mitochondrial matrix via the mitochondrial Ca^{2+} uniporter. In addition to its prominent roles in cell survival, mitochondria also contributes to programmed cell death (apoptosis) pathway by regulating the pro-apoptotic proteins. During apoptosis, mitochondrial outer membrane permeabilization (MOMP) forms pores in the IMM which subsequently causes depolarization of the mitochondrial membrane potential. These events ultimately lead to cell death via the release of pro-apoptotic mitochondrial proteins, such as cytochrome c into cytosol. Figure was adapted from (Smith et al., 2012).

Mitochondria have a unique structure, quite distinct from other cellular organelles with a size that varies from 1 μm to 4 μm (Kennady et al.; 2004). These organelles are bound by a double-layered phospholipid membrane arrangement, separating mitochondria into four compartments including the outer and inner membranes, the inter-membrane space (IMS) and matrix (Figure 2) (Kühlbrandt, 2015). The matrix is a viscous compartment bound by the inner membrane which contains not only the mitochondrial DNA and ribosomes, but also hundreds of enzymes utilized in both the TCA and urea cycles, the oxidation of long chain fatty acids and the synthesis and oxidation of various amino acids (Figure 1) (Prasai, 2017). The outer mitochondrial membrane (OMM) contains an abundant protein, (known as porin), which allows material to freely diffuse into the intermembrane space. By contrast, the inner mitochondrial membrane (IMM) serves as a barrier, selectively blocking or limiting the passage of most molecules. The IMM which houses the respiratory chain complexes is also highly folded into cristae which consequently increase the surface area of the membrane (Mannella, 2006).

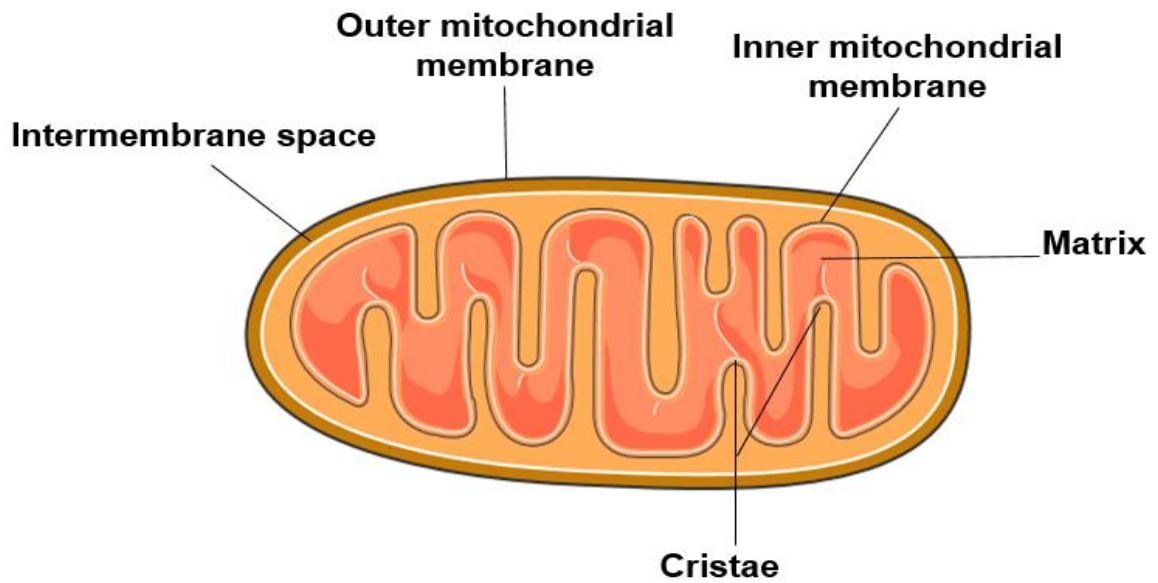


Figure 2 A typical the structure of mitochondria

1.2 Mitochondrial Respiratory Chain (MRC)

The high-energy electron carriers, which are produced by the cytosolic glycolysis pathway (NADH) and the mitochondrial TCA cycle (NADH and FADH_2) are both respectively oxidized by the mitochondrial respiratory chain (MRC) complex I (NADH: ubiquinone reductase; EC 1.6.5.3) and non-pumping proton complex II (succinate: ubiquinone reductase; EC 1.3.5.1). This oxidation process results in electrons flowing to an electron carrier, coenzyme Q_{10} (CoQ_{10}) (ubiquinone) and then on an onward shuttle to MRC complex III (ubiquinol: cytochrome c reductase; EC 1.10.2.2) (Land et al., 2004). Together with the electron transfer flavoprotein (ETF), electron transfer flavoprotein:ubiquinone oxidoreductase (ETF-QO; EC 1.5.5.1) forms a short electrons pathway short, which serves to shuttle electrons from FAD-dependent acyl-CoA dehydrogenases of fatty acid β -oxidation to CoQ_{10} and

then similarly on to MRC complex III (Nicholas and Frank, 2010). The electrons are ultimately carried by another mobile electron carrier, cytochrome *c* to MRC complex IV (cytochrome *c* oxidase; EC 1.9.3.1) where dissolved oxygen is reduced to form water. As a result of the passage of electrons passing between chains, protons or hydrogen ions (H^+) are pumped out of the basic and negatively charged mitochondrial matrix and into the acidic and positively charged intermembrane space through MRC complexes I, III, and IV. This consequently creates a membrane potential ($\Delta\phi_m$) of an approximate 160 mV and subsequent proton-motive force (PMF). This latter potential energy is harnessed by the mitochondrial ATPase enzyme, complex V as the protons, driven by the PMF, pass through enzyme complex resulting in the direct phosphorylation of ADP to ATP (Hargreaves et al., 2016). While inorganic phosphate shuttles from the cytoplasm to the matrix via the phosphate carrier, ATP then exchanges with ADP between the mitochondrial matrix and the cytoplasm via the adenine nucleotide translocase (ANT) (Smith et al., 2012). The complex V in conjunction with the other four multi-subunit proteins of the MRC is collectively defined as the OXPHOS pathway where up to 90 % of cellular metabolic energy is generated (Al Shahrani et al., 2017) (Figure 3). Notably, the mitochondrial respiratory enzyme complexes and ATP synthase are encoded by both nuclear and mitochondrial genes. However, the MRC complex II is entirely encoded by nuclear genes (Figure 3).

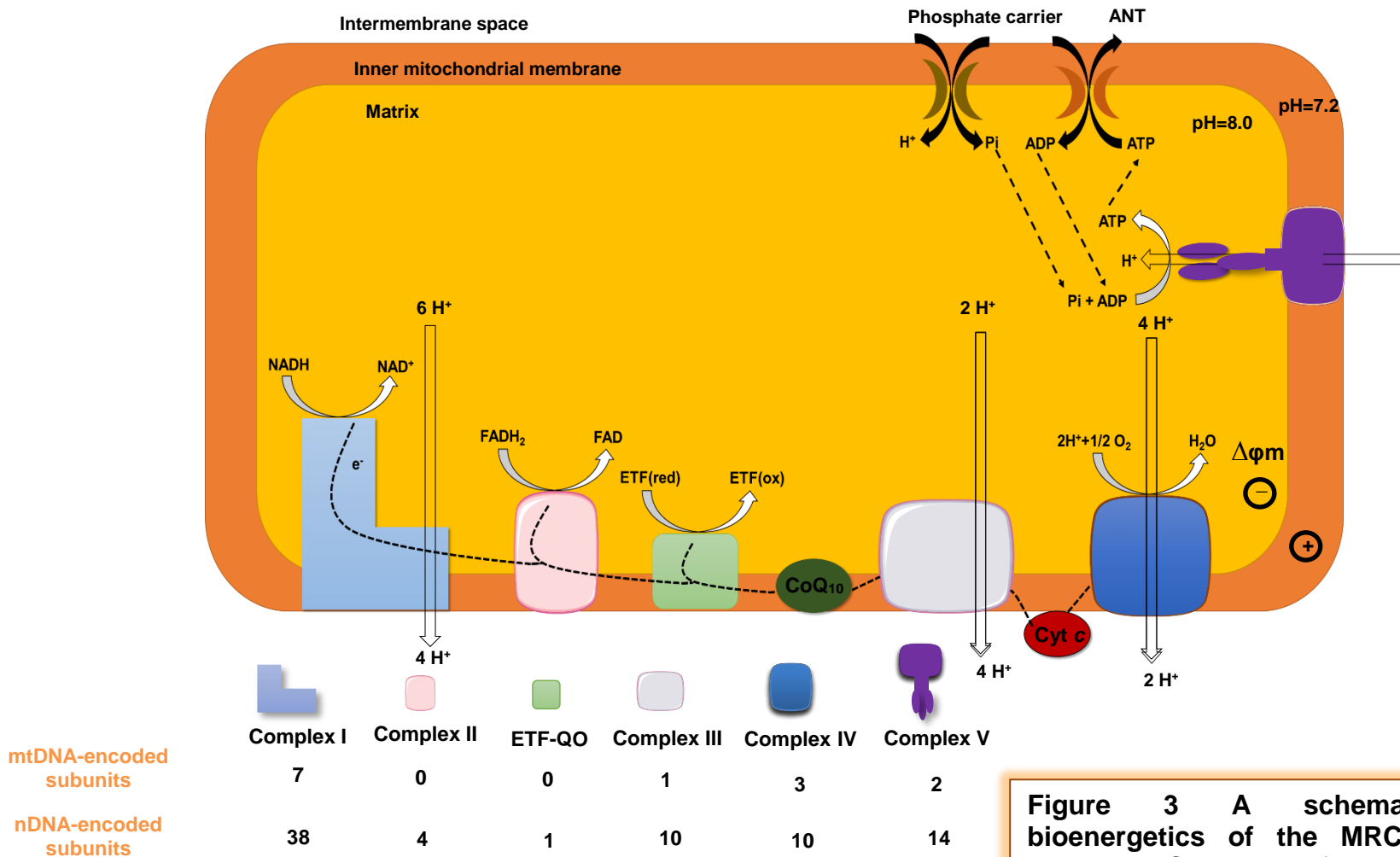


Figure 3 A schematic underlying bioenergetics of the MRC and OXPHOS pathways. See the text for more details.

1.2.1 MRC Complex I [EC 1.6.5.3]

The proton pumping, MRC complex I is the first step in the energy-generating pathway in mitochondria. Thus, it is considered to be rate-limiting step in mitochondrial respiration. In addition to being the largest complex in mammalian mitochondrial chains with a size of 980 kDa (Judy et al., 2003), it consists of a hydrophobic membrane arm and a hydrophilic peripheral arm, creating a unique L-shaped structure, as was previously showed by three-dimensional electron microscopy (Guenebaut. et al., 1997). Together with eight iron–sulfur clusters and a non-covalently bound FMN, this L-shaped complex is also comprised of 45 different multisubunit proteins of which 37 subunits are encoded by nuclear gene, while the remaining 7 hydrophobic subunits are encoded by mtDNA (Christophe et al., 2016). As summarized in (Figure 4), recent studies have also identified the human homologues of all the above subunits in bovine complex I (Sharma et al., 2009).

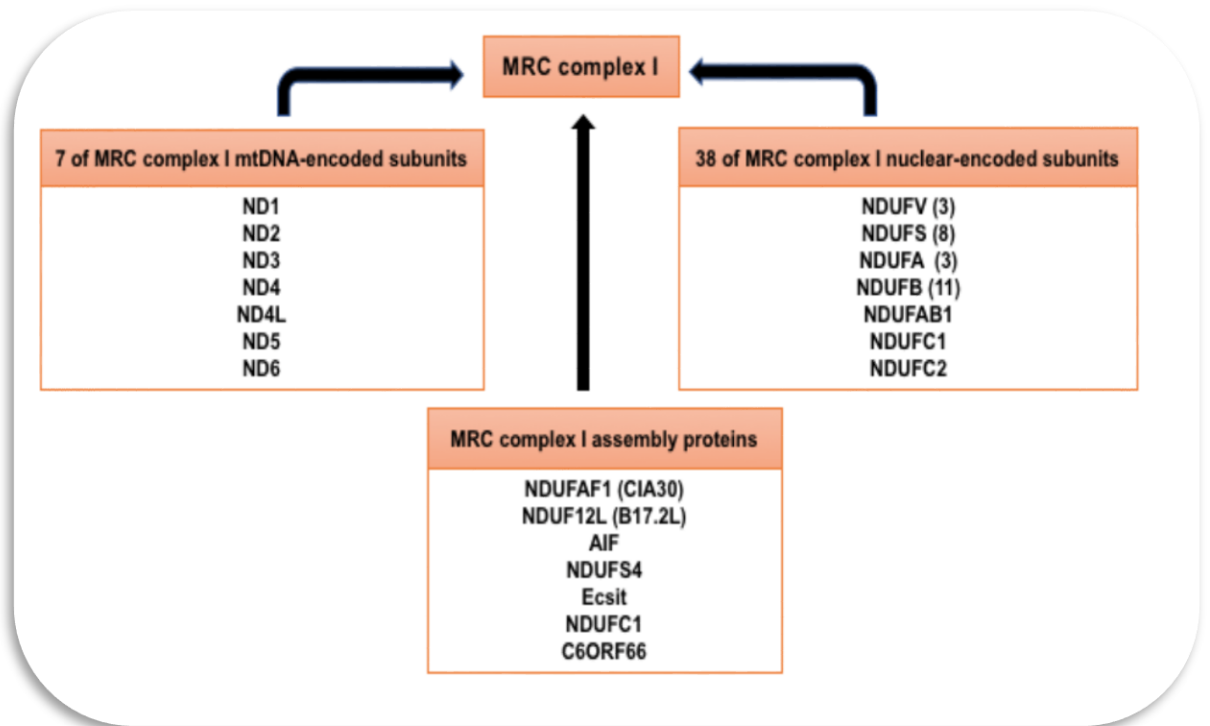


Figure 4 The structural components of MRC complex I in mammalian mitochondria. Together with assembly proteins, the set of MRC complex I subunits encoded by mtDNA and nuclear are shown. The prefix: “ND” indicates subunits of NADH-dehydrogenase; “F” and “S” indicate the prosthetic groups, flavin and iron–sulfur clusters, respectively. The Numbers in parentheses indicate the number of MRC complex I subunits.

The redox energy of NADH is produced primarily by both of intermediate chemical reactions within the TCA cycle as well as by the β -oxidation of fatty acids and are directly fed into the MRC complex I of the OXPHOS pathway. With the participation of iron–sulfur clusters and FMN cofactors, the transfer of two electrons from reduced NADH to CoQH₂ is catalysed by complex I, and is coupled to the pumping out 4 H⁺ across the IMM and into the IMS, which contributes to the generation of a PMF which is ultimately utilized to synthesise ATP by the process of OXPHOS.

The MRC complex I is well known to be a major source of mitochondrial reactive oxygen species (ROS) production in the cell, particularly in the form of superoxide (O_2^-). This free radical O_2^- is produced predominantly in the matrix by MRC complex I (reviewed by Al Shahrani et al., 2017). Several lines of evidence suggest two sites of the O_2^- production by MRC complex I including the Q-binding site, supported by observations made in intact mitochondria or submitochondrial particles (SMPs) and the reduced FMN in the active site for NADH oxidation, supported by observation made in isolated MRC complex I (Judy et al., 2008).

Together the reduction in the CoQ pool coincides with a high PMF by mitochondrial oxidizing succinate, the first description of MRC complex I-enhancing ROS was demonstrated in SMPs in which uncoupling proteins (UCPs) induced H_2O_2 (Hinkle et al., 1967). This observation suggests that MRC complex I is also a source of oxygen-derived radical H_2O_2 in addition to O_2^- . In the presence of NADH, O_2^- production was subsequently demonstrated in isolated MRC complex I. This was moreover enhanced further by the complex I inhibitor, rotenone a (Q-site inhibitor) known to block the electron transfer from NADH to CoQ_1 indicating that the production of O_2^- by isolated complex I is due to the reaction of O_2 with fully reduced FMN and is governed by the redox state NADH/NAD⁺ (Cadenas et al., 1977). This also provides an explanation as to why rotenone-induced complex I inhibition increases the generation of O_2^- since rotenone binding consequently forces the electrons back into FMN, which in turn generates O_2^- (Kussmaul et al., 2006). Similar findings were also observed in MRC complex I within intact mitochondria

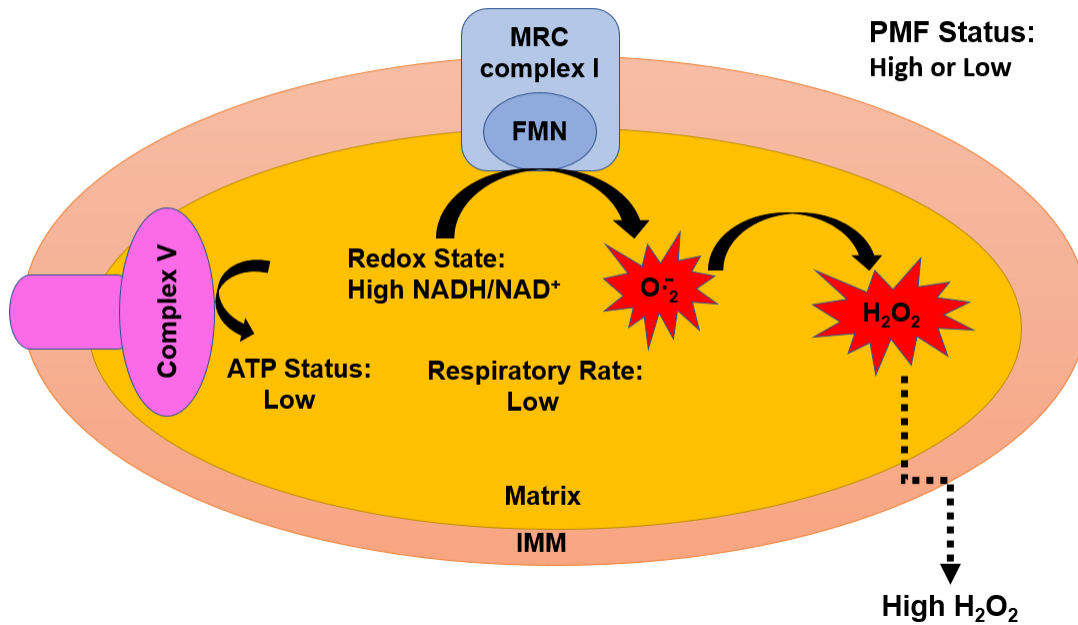
(Kudin et al., 2004 and Kussmaul et al., 2006). Therefore, impairment of MRC function caused by abnormal conditions such as dysfunction of cytochrome *c*, mutations, ischemia, or accumulate of NADH as a result of depleted ATP levels or reduction of respiration rate, could lead to an exaggerated redox state NADH/NAD⁺ ratio and consequently lead to enhanced O₂⁻ production.

Another plausible mechanism which may be linked to MRC complex I-mediated O₂⁻ production is reverse electron transport (RET) (Adam-Vizi and Chinopoulos, 2006). This occurs at high PMF status, once the CoQ pool becomes fully reduced and electron flows back from CoQH₂ into MRC complex I, resulting in the reduction of NAD at the FMN site (Chance and Hollunger, 1961). The first description of RET linked to H₂O₂ production was observed in SMPs supplied by succinate (Hinkle et al., 1967). The O₂⁻ was observed later in isolated complex I through RET (Cino and Del Maestro, 1989). Under the RET condition, therefore, the mitochondrial O₂⁻ production rate seems to be the highest that may occur within mitochondria (Hurd et al., 2007).

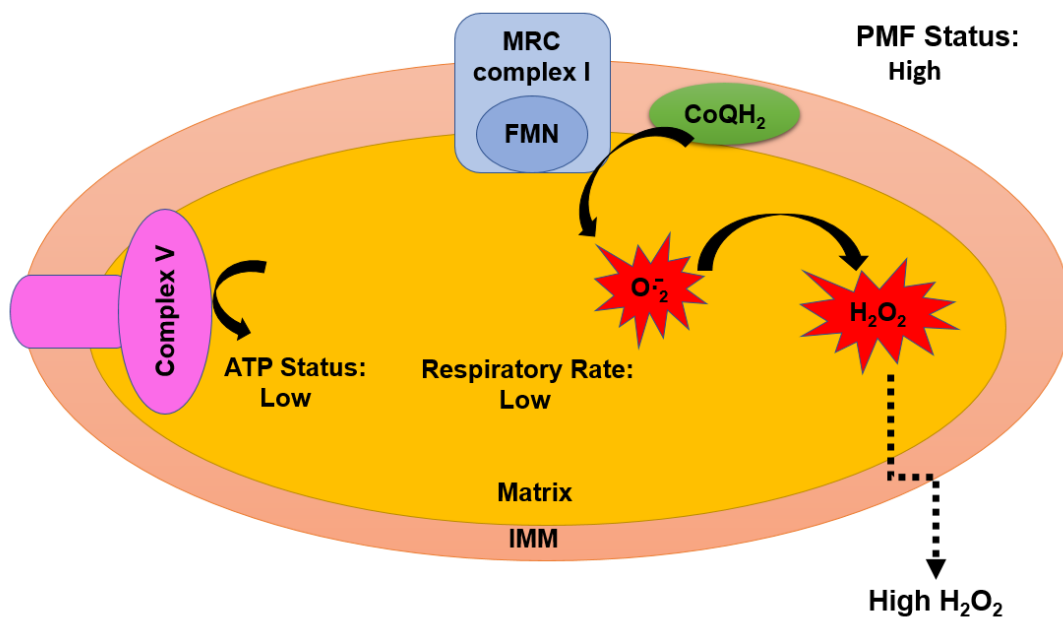
Taken together, two possible mechanisms can be associated with an excessive production of O₂⁻ from MRC complex I: (i) when the mitochondrial matrix redox state NADH/NAD⁺ ratio is high, which in turn, leads to a reduction of the redox cofactor FMN site at MRC complex I (Figure 5-A) (ii) when mitochondrial ATP levels are low, resulting in a reduction of the CoQ pool and increase in PMF status, which ultimately leads to a RET in MRC complex I (Figure 5-B). (iii) To a lesser extent, O₂⁻ production in the case

where mitochondria produce sufficient amounts of ATP level, although the PMF status and redox state NADH/NAD⁺ ratio are both low (Figure 5-C) (Murphy, 2009).

A- High Mitochondrial Matrix Redox State NADH/NAD⁺ Ratio



B- The Reduction in CoQ Pool Coincides with a High PMF



C- Normal Physiological Condition

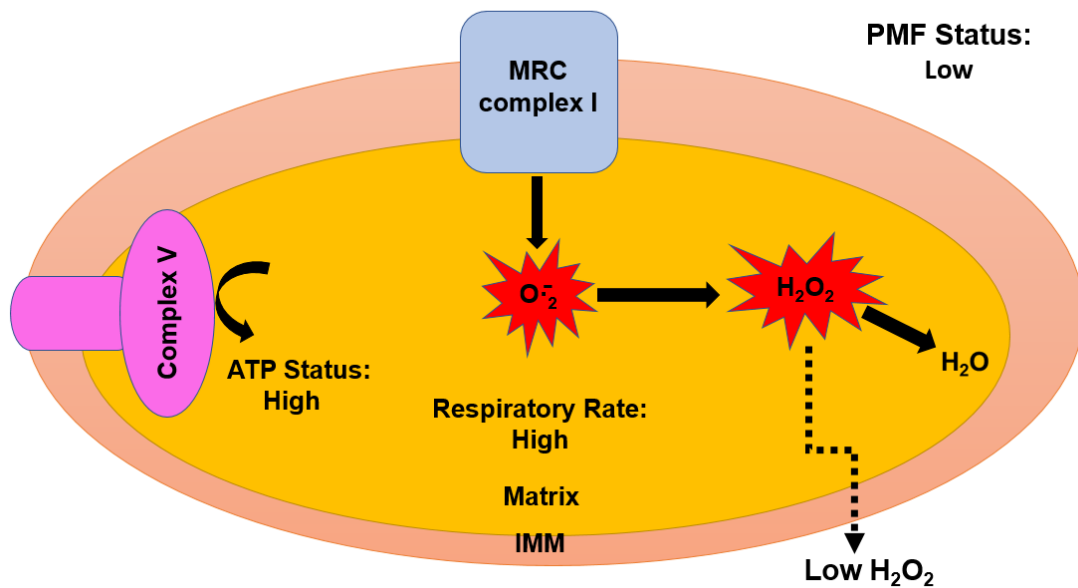


Figure 5 Illustrates the possible events associated with mitochondrial O_2^- production, particularly from MRC complex I. **(A)** When the mitochondrial matrix redox state NADH/NAD⁺ ratio is high, this in turn, reduces the redox cofactor FMN site at MRC complex I. **(B)** When mitochondrial ATP levels are low, resulting in a reduction of the CoQ pool and increase in PMF status, this ultimately leads to RET in MRC complex I. **(C)** A decreased level of O_2^- production occurs in cases where mitochondria produce sufficient amounts of ATP levels, and subsequently the PMF status and redox state NADH/NAD⁺ ratio are both low, in comparison with events **(A)** and **(B)**. Figures were adapted from (Murphy, 2009).

1.2.2 MRC Complex II [EC 1.3.5.1]

In addition to its functional role as succinate dehydrogenase (SDH) in the TCA cycle, the MRC complex II or succinate: quinone oxidoreductase (SQR) is another entry point into the MRC pathway, catalyzing both of the following reactions: (i) The oxidation of succinate to fumarate and (ii) the reduction of ubiquinone (CoQ) to ubiquinol (CoQH₂) (Rutter et al., 2010). Hence, MRC complex II represents a common hub of two key mitochondrial pathways.

Unlike to other MRC enzyme complexes, human MRC complex II is entirely encoded by nuclear DNA (Rutter et al., 2010). This nDNA-encoded complex is heterotetrameric containing two hydrophilic and two hydrophobic subunits (Iverson et al., 2012). Together with a flavoprotein (SDHA), and an iron-sulfur protein (SDHB) form a hydrophilic subunit, which protrudes into the mitochondrial matrix. In addition to a covalently attached flavin adenine dinucleotide (FAD) cofactor, SDHA also contains the succinate binding site. However, the two hydrophobic subunits, SDHC and SDHD are embedded in the inner mitochondrial membrane. Additionally, these subunits contain one haem *b* group and a CoQ-binding site (Dröse, 2013). In the hydrophobic space below the heme *b*, two phospholipid molecules which play central role in the structure and function of mitochondria, namely cardiolipin (CL) and phosphatidylethanolamine (PE), are also found (Sun et al., 2005).

During the oxidation reaction of succinate to fumarate, the covalently bonded FAD cofactor accepts hydrogens to yield FADH₂. Electrons from the reducing equivalents of FADH₂ are then passed on through a series of the iron-sulphur clusters to reduce CoQ to CoQH₂. Overall, these reactions are catalyzed by MRC complex II. In contrast with MRC complex I, III and IV, MRC complex II

does not to pump protons (Grimm, 2013). Fewer ATP molecules are therefore produced from the oxidation of FADH₂ than from NADH.

1.2.3 MRC Complex III [EC 1.10.2.2]

Complex III, also called (cytochrome *bc*₁ complex; ubiquinol: cytochrome *c* oxidoreductase) is the third enzyme complex in the MRC pathway. Its a multi-subunit transmembrane protein which is encoded by both mtDNA (cytochrome *b*) and nDNA (all other subunits). The cytochrome *bc*₁ complex also consists of eleven subunits including, three respiratory subunits (cytochrome *b*, cytochrome *c*₁, and Rieske protein), two core proteins and six low-molecular weight proteins (Crofts et al., 2017).

The MRC complex III operates via the mechanism known as the quinone cycle (Q-cycle) which was first proposed by Peter Mitchell (Mitchell, 1975). Proton transfer is dependent on the oxidation of quinol (QH₂) in a bifurcated reaction at the quinol oxidation site (Qo-site) in which two electrons from QH₂ are shuttled by two different routes. The first electron from QH₂ is transferred to the Rieske iron-sulfur protein, which subsequently feeds electrons through cytochrome *c*₁ in complex III onto cytochrome *c*, a mobile electron carrier. This ultimately leads to reduce a terminal electron acceptor (complex IV). Furthermore, a semiquinone (QH•) intermediate which is very unstable, is formed following this reaction. Consequently, this intermediate donates the second electron to two cytochromes *b* molecules (*b*_L and *b*_H), and then onto a second processing site, the quinol reduction site (Qi-site). At this site, Q is subsequently reduced via a two-electron gate to QH₂. Since this reaction requires two electrons for the complete reduction of Q at the Qi-site, in two turns the Qo-site fully oxidizes two QH₂ molecules. The second electron that is

delivered to the Qi-site reduces the unstable QH[•] to QH₂. At the end of the completion of one Q-cycle, two QH₂ molecules are oxidized at the Qo-site, Q molecule is reduced at Qi-site (Crofts et al., 2017; Bleier and Dröse, 2013). Therefore, the net result of the movement of two electrons from QH₂ to cytochrome *c* is that two molecules of cytochrome *c* are subsequently reduced, four H⁺ are pumped into intermembrane space, and two H⁺ are removed from the mitochondrial matrix (Figure 6).

Historically, MRC Complex III was documented to be the first mitochondrial site producing ROS in the form of O₂^{•-} (Jensen, 1966). It is believed that one electron donor, the unstable QH[•] formed at the Qi-site is responsible for the mitochondrial O₂^{•-} production (Turrens et al., 1985). This O₂^{•-} which is indeed generated at the Qo site and not at the Qi site has been experimentally observed by the use of specific inhibitors of the *bc1* complex that bind to the two distinct Q-binding sites. Several studies using intact mitochondria, or SMPs have demonstrated that the O₂^{•-} production at MRC complex III is stimulated upon addition of a Qi-site inhibitor, e.g. antimycin A (Muller et al., 2002; Bleier and Dröse, 2013). However, antimycin A-induced O₂^{•-} production is blocked by the addition of Qo site inhibitors e.g. myxothiazol and stigmatellin, thereby preventing the formation of QH[•] (Muller et al., 2003).

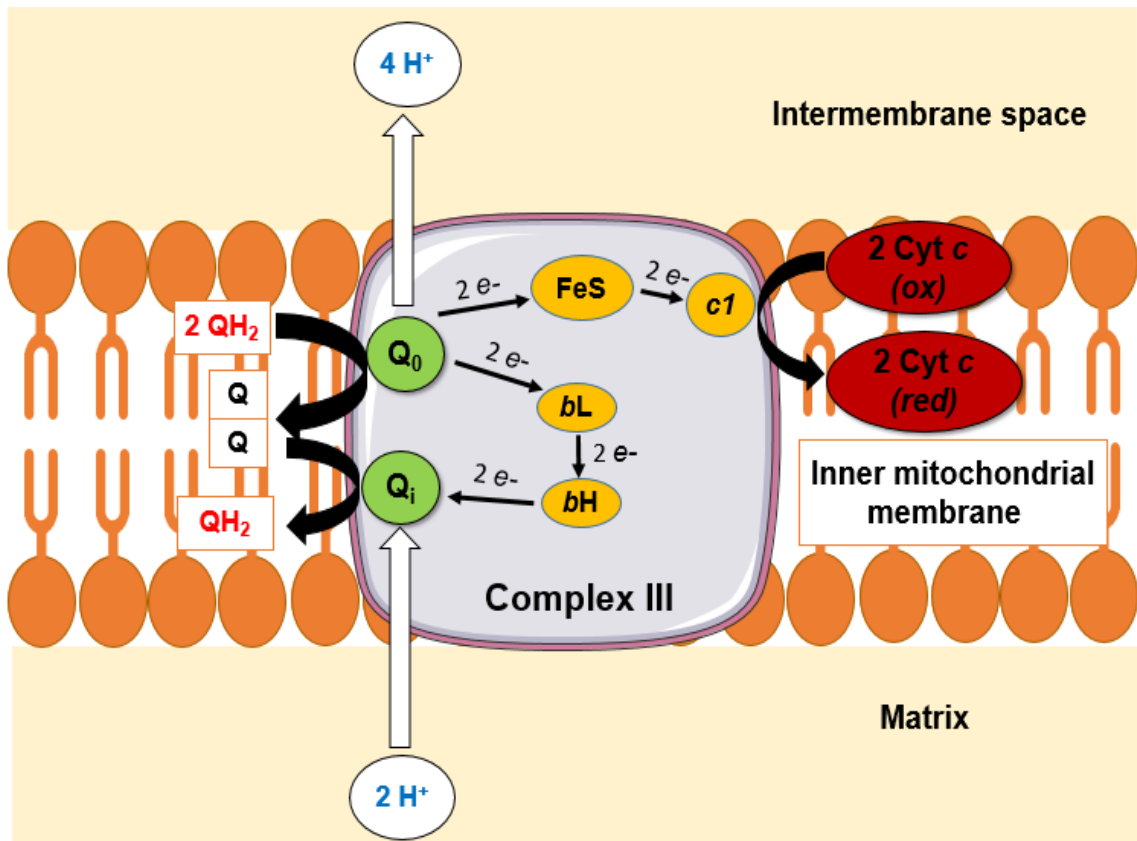


Figure 6 Schematic illustrating the Q-cycle of the cytochrome *bc*₁ complex. The net result of the movement of two electrons from QH₂ to cytochrome *c* is that two molecules of cytochrome *c* are subsequently reduced, four H⁺ are pumped into intermembrane space, and two H⁺ are removed from the mitochondrial matrix. Cyt, cytochrome; Oxd, oxidized; red, reduced.

1.2.4 MRC Complex IV [EC 1.9.3.1]

Complex IV also known as cytochrome *c* oxidase (COX) is the last enzyme complex in the MRC pathway. It consists of 14 protein subunits, three of which encoded by mtDNA and the remainder encoded by nDNA (Balsa et al., 2012). In addition to these subunits, COX also contains several metal containing prosthetic groups including, two haems, cytochrome *a* and *a*₃, and two copper centres (CuA and CuB) (Tsukihara et al, 1995).

Complex IV receives electron from each of four reduced cytochrome *c* molecules and transfers them to the final electron acceptor oxygen, which is ultimately reduced to two molecules of water. Coupled to this oxygen reduction reaction, complex IV also pumps out four protons across the membrane, thereby increasing the membrane potential and proton gradient and strengthening the PMF. This latter potential energy is then utilized by ATP synthase to create ATP from ADP and Pi (Kim and Hummer, 2012).

1.3 MRC Supercomplexes

MRC complexes are organized into supramolecular structures known as supercomplexes (SCs) (Schägger, 2001). The first evidence of SCs emerged in the early 2000s when mitochondrial membrane proteins were analyzed using blue native polyacrylamide gel electrophoresis (BN-PAGE) (Schägger and Pfeiffer, 2000). Although the main function of SCs is not fully elucidated, it has been suggested that SCs play an important role in enhancing MRC activity via allowing for more efficient electron transfer through the MRC. This could lead to a reduced electron leakage and consequently reduce the mitochondrial ROS production (Maranzana et al., 2013). Additionally, SCs may be also involved in stabilizing the structural integrity of individual MRC complexes (Schägger et al., 2000).

MRC complexes are integrated unequally into the structural organization of SCs, particularly the major SC, respirasome, which consists of complexes I, III, and IV (Schägger and Pfeiffer, 2000). Analysis of the structural organization of SCs from bovine heart mitochondria by BN-PAGE showed that approximately 80% of complex I, 65% of complex III and 15% of complex IV

contributed toward the structural organization (Schägger and Pfeiffer, 2000). However, complex II was not identified to be involved in SCs.

Intriguingly, neurons are critically dependent upon the availability and correct functioning of the OXPHOS pathway for energy generation. However, astrocytes depend on glycolysis to meet their energy needs (Almeida et al., 2004). In fact, these two energy pathways are tightly coupled in which astrocytes shuttle lactate as the end product of glycolysis to neighboring neurons, ultimately leading to drive the OXPHOS pathway (Allaman et al., 2011). However, the structural organization of the MRC between neurons and astrocytes are still not fully understood. A study by (Lopez-Fabuel et al., 2016) has demonstrated that MRC complex I was predominantly assembled into SCs in neurons. In contrast to neurons, the abundance of free complex I was found to be higher in astrocytes. This study also showed that the rate of mitochondrial ROS production in astrocytes was higher than in neurons.

1.4 ATP Synthase [EC 3.6.3.14]

The ATP synthase, also known as (FoF1-ATPase; mitochondrial ATPase and Complex V) is the final step enzyme in the OXPHOS pathway. It acts as a rotary molecular motor, consisting of two membrane-spanning domains: Fo and F1. The hydrophobic domain, Fo is a proton pore which is embedded in the inner mitochondrial membrane. It contains a proton channel allowing protons to flow toward F1. The letter O (written as a subscript letter "o") of Fo denotes sensitivity to oligomycin, an ATP synthase inhibitor which blocks the proton channel of Fo (Gautheron, 1984). The hydrophilic domain of ATP synthase, F1, was first extracted and purified by (Racker, 1976). This domain

which projects into the mitochondrial matrix, can subsequently hydrolyze ATP to ADP and Pi and is thus known as F1-ATPase (Gautheron, 1984).

The mechanism of how ATP synthase generates ATP from ADP and Pi was first proposed by Paul Boyer and John Walker, resulting in the award of the Nobel Prize (Osellame et al., 2012). Boyer developed the binding change or rotary-catalysis mechanism which proposed that ATP synthesis is dependent on a conformational changes in ATP synthase created by rotation of the (γ) subunit in F1 (Boyer, 1975).

The major function of ATP synthase is to create ATP from ADP and Pi. This occurs following rotation of the (γ) subunit in the F1 domain (Walker and Dickson, 2006). The potential energy is harnessed by the ATP synthase, as the protons, driven by the PMF, rotates the ring of the c-subunit of the Fo domain. The c-ring is tightly attached to the (γ) subunit in the F1 domain (the asymmetric central stalk) causing it to rotate within the (α_3 and β_3) subunits of F1 (Cox et al., 1984). This subsequently cause the three catalytic nucleotide binding sites on the solubilized F1 domain to go through a sequence of conformational changes that ultimately lead to ATP synthesis (Jonckheere et al., 2012). In the catalytic binding sites which are located in each of the (β_3) subunit and interface with an adjacent (α) subunit, describes the mechanism of how ATP synthesis and hydrolysis can occur. During ATP synthesis, each site switches cooperatively through conformation changes which in turn lead to the reaction between bound ADP and Pi to form ATP. In the same pathway, ATP hydrolysis can proceed but this occurs in reverse mode (Adachi et al., 2007). These switches are primarily caused by rotation of the (γ) subunit in the F1 domain. The central stalk is prevented by a peripheral stalk that join

the ($\alpha\beta_3$) subunits to the (a) subunit of F_0 during catalysis. Mechanically, ATP synthase can therefore be divided into two components, including rotor (c-ring, γ , δ , ϵ) and stator ($\alpha\beta_3$, a, b, d, F6, OSCP) (Figure 7) (Devenish et al., 2008).

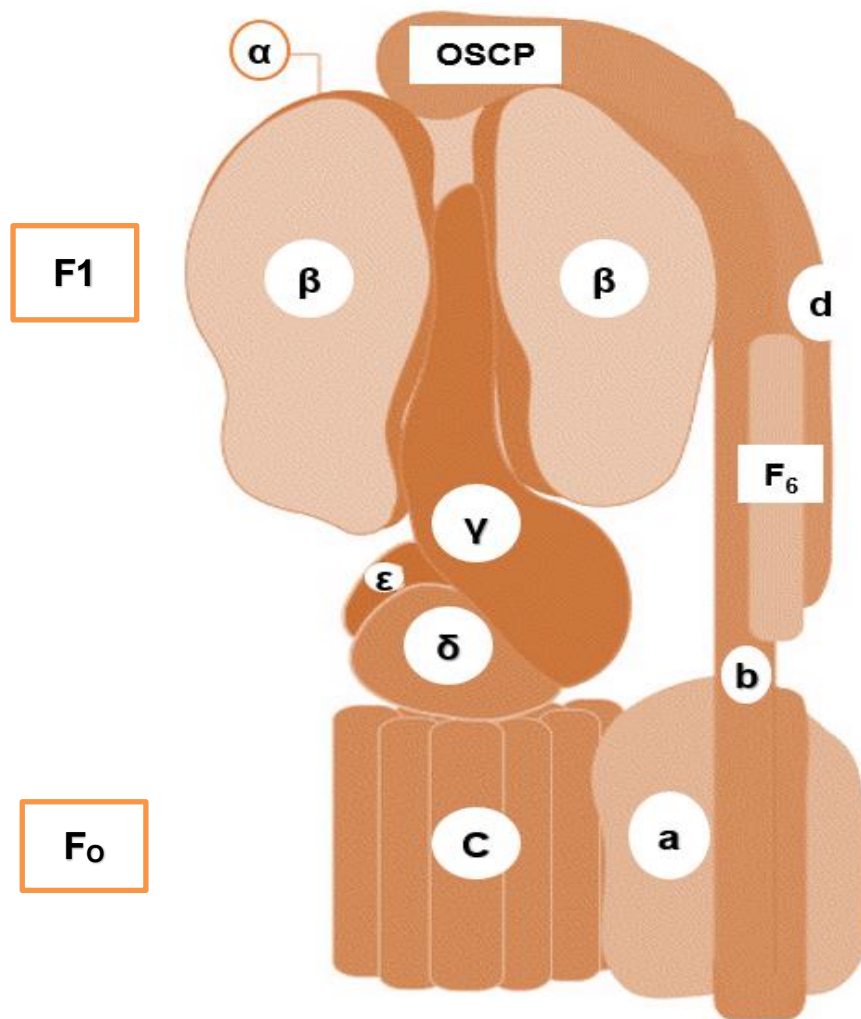


Figure 7 Illustrates the subunit organisation in ATP synthase. It consists of two membrane-spanning domains: F_o and F_1 . The catalytic domain, F_1 is made of (α , β) subunits and the three central stalk (γ , δ and ϵ) subunits. The hydrophobic domain, F_o is a proton pore domain which is made of (c-ring) subunit, (a) subunit, and the peripheral stalk (b, d, F_6 and OSCP) subunits. The rotor component is made of the c-ring subunit and central stalk (γ , δ , and ϵ) subunits. The remainder of the subunits is the stator component. Figure was adapted from (Walker and Dickson, 2006).

1.5 Citrate Synthase [EC 2.3.3.1]

Citrate synthase (CS) is an enzyme found in nearly all living cells. It plays a significant role as a pacemaker enzyme in the hub of the metabolic pathway of aerobic organisms, the tricarboxylic acid (TCA) cycle, also known as citric acid cycle (CAC) or the Krebs cycle (Figure 8). Unlike glycolysis which occurs in the cytoplasm, the TCA cycle along with OXPHOS occur in the mitochondria. The overall TCA cycle completely oxidizes acetic acid, (originating as acetyl coenzyme A (acetyl CoA) from glucose, fatty acid, and amino acid catabolism (Wakil and Abu-Elheiga, 2009) to two molecules of carbon dioxide, three NADH, one FADH, one Guanosine-5'-triphosphate (GTP) and three hydrogen ions.

CS is the first enzymatic step in the TCA cycle which catalysing the condensation reaction of oxaloacetate (OAA) with acetyl CoA to form citric acid. In eukaryotic cells, CS is located in the mitochondrial matrix. However, it is encoded by nDNA rather than mtDNA which is translated in the cytoplasm and then transported into the mitochondrial matrix (Wiegand and Remington, 1986). Therefore, it is commonly used as matrix enzyme marker as well as a mitochondria enrichment marker.

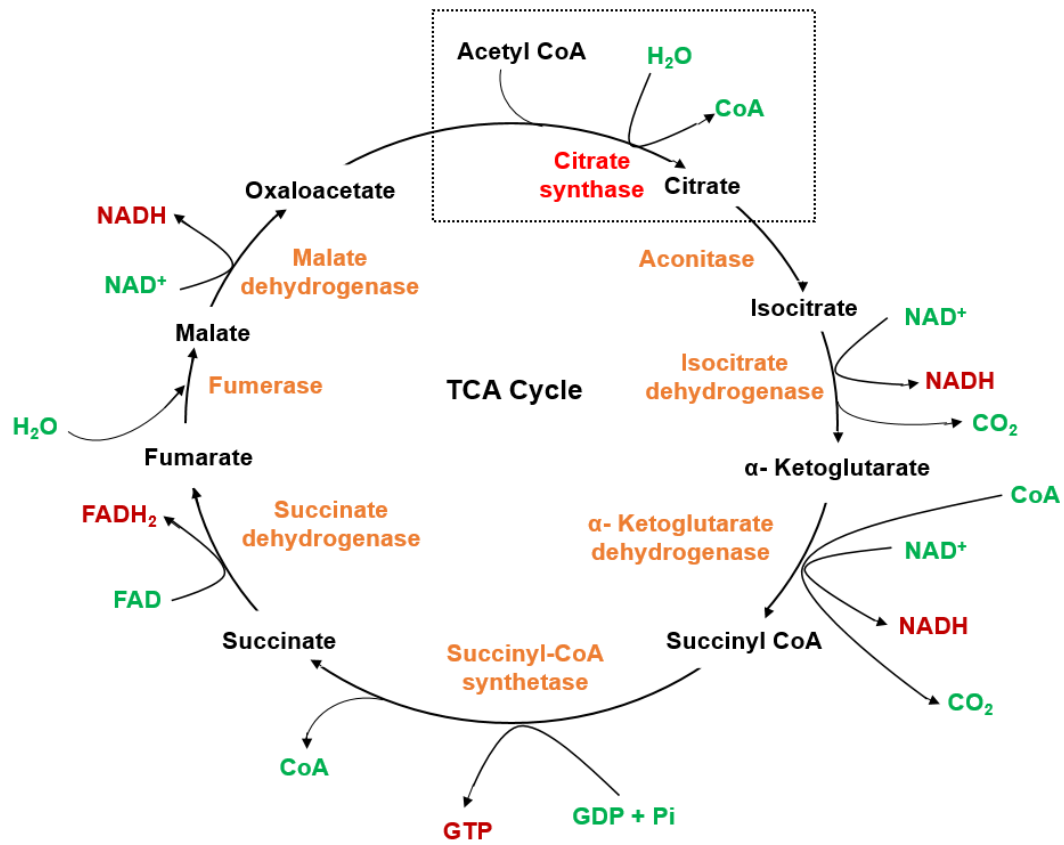


Figure 8 Schematic illustration of the TCA cycle.

1.6 Oxidative Stress

Free radicals can be chemically defined as any species containing one or more unpaired electron occurring in their atom or molecular orbitals (Halliwell and Gutteridge, 2007). Oxygen is an essential element for living cells which has the ability to be generated *in vivo*, producing potentially damaging oxygen-derived species, known as reactive oxygen species (ROS). Under physiological conditions, the levels of ROS are balanced and controlled by a range of defence mechanisms, known as antioxidants. However, under pathophysiological conditions such as seen in many neurodegenerative disorders, increased ROS formation, or a reduction in antioxidant capacity, or even both simultaneously may occur. This condition known as oxidative stress, was described by Helmut Sies in the mid-1980s as an unbalance between free radicals and antioxidants in favour of free radicals, thereby leading to cellular damage (Sies, 1985). High energy demanding organs such as the brain are highly vulnerable to oxidative stress due to its high metabolic rate associated with low antioxidants content (Cobley et al., 2018).

As shown in (Table 1), instances of oxygen-derived ROS include, superoxide ($O_2^{\cdot-}$), hydrogen peroxide (H_2O_2), the hydroxyl radical (OH^{\cdot}), singlet oxygen (1O_2) and hypochloric acid (HOCL). In addition to ROS, reactive nitrogen species (RNS), is a collective term describing nitrogen-derived species such as nitric oxide (NO^{\cdot}), nitrous acid (HNO_2), peroxyxynitrite ($OONO^-$) and peroxyxynitrous acid ($ONOOH$) (Lien et al., 2008). Thus, human cells have evolved an array of enzymatic and non-enzymatic antioxidant defence mechanisms to help protect themselves from the harmful effects of ROS or RNS (Table 2).

Table 1 List of key reactive species generated during metabolism

Reactive oxygen species (ROS)	
$O_2^{\cdot-}$	Superoxide
H_2O_2	Hydrogen peroxide
HO^{\cdot}	Hydroxyl radical
HOCL	Hypochloric acid
1O_2	Singlet oxygen
Reactive nitrogen species (RNS)	
NO^{\cdot}	Nitric oxide
HNO_2	Nitrous acid
$OONO^-$	Peroxynitrite
$ONOOH$	Peroxynitrous acid

Table 2 List of key enzymatic and non-enzymatic antioxidant defence

Enzymatic antioxidants
Superoxide dismutase (SOD)
Glutathione peroxidase (GP _x)
Non-enzymatic antioxidants
Vitamin C (Ascorbic acid)
Vitamin E (α-tocopherol)
Coenzyme Q ₁₀ (Ubiquinol)
Reduced glutathione (GSH)
α-lipoic acid (ALA)
carotenoids (β-carotene)

1.7 Mitochondria are a Major Site of ROS Production and Target of ROS-mediated Dysfunction

It is thought that the formation of ROS is a dominant component produced during the generation of ATP utilizing molecular oxygen. Under normal conditions, approximately 1 % of total oxygen utilized by the MRC is converted to ROS, although under pathological conditions this may increase dramatically (Starkov, 2008). Mitochondrial ROS, particularly $O_2^{\cdot -}$ is mostly generated either in the matrix from MRC complex I or both in the intermembrane space and matrix from MRC complex III, indicating that steady state of $O_2^{\cdot -}$ has potentially higher level in the matrix than other organelle compartments (Cadenas and Davies, 2000).

$O_2^{\cdot -}$ is rapidly removed by conversion to H_2O_2 either by a manganese-dependent superoxide dismutase (MnSOD) or a copper, zinc-dependent superoxide dismutase (Cu, ZnSOD), and then ultimately reduced to water by GPx utilizing the active and reduced GSH as a cofactor (Turrens, 2003; Birben et al., 2012) (Figure 9) (Table 2). A large number of biomolecules have over the years been recognised as potent antioxidants. GSH itself, besides being a cofactor for the enzymatic antioxidant GPx, also serves as non-enzymatic antioxidant by directly removing free radicals as well as other oxidative agents (Birben et al., 2012). Similarly, other non-enzymatic antioxidants known to act as potent free radical scavengers include ascorbate (vitamin C) (Bunker, 1992), α -tocopherol (vitamin E) (White et al., 1997), coenzyme Q (ubiquinol-10) (Duberley et al., 2014), α -lipoic acid (ALA) (Smith

et al., 2004), and carotenoids (β -carotene) (Fiedor and Burda, 2014) (Table 2).

It is the uncontrolled or overproduction of ROS (oxidative stress) or RNS (nitrosative stress) which can potentially cause damage to cellular molecules, including DNA, proteins and lipids (Jacobson et al., 2005). Furthermore, it is thought that accumulation of these reactive species, resulting in oxidative stress could lead to damage to the MRC and this in turn may be a major contributing factor in the pathophysiology of several inherited and acquired mitochondrial disorders (Hayashi and Cortopassi, 2015; Stewart and Heales, 2003).

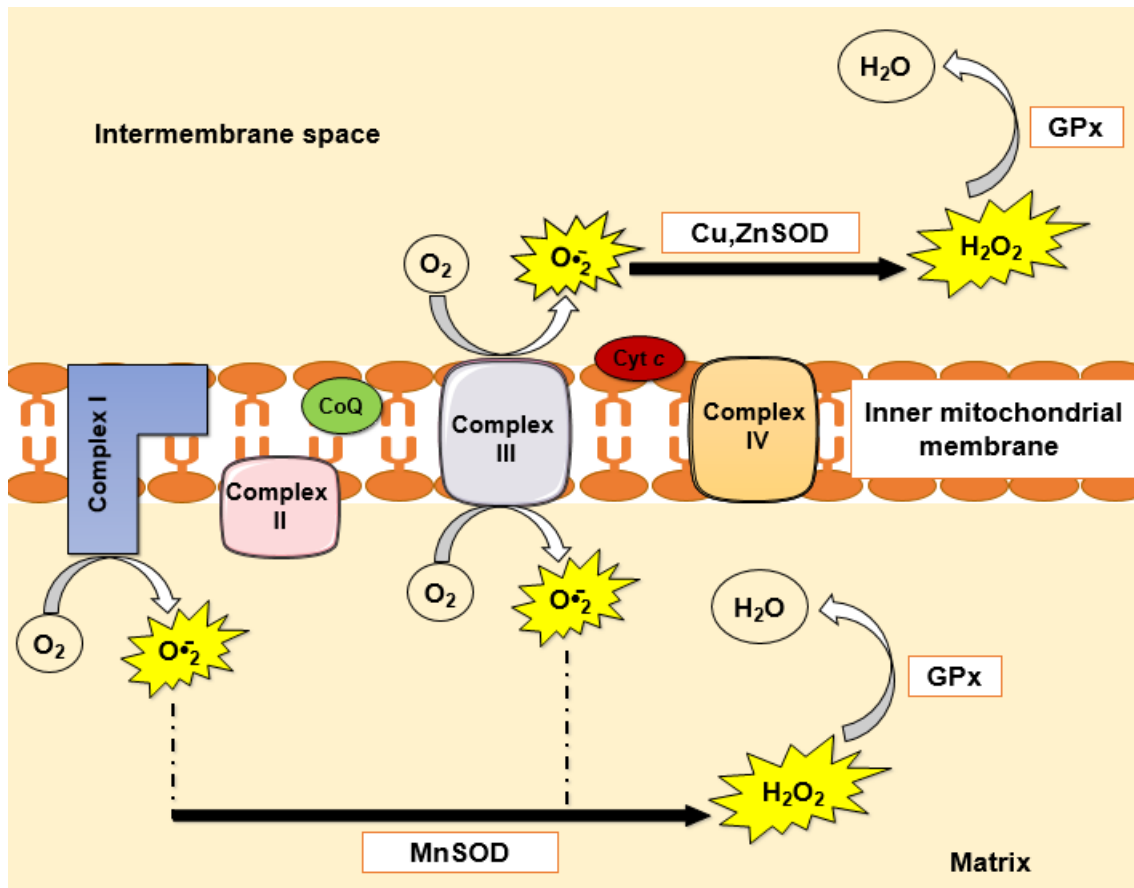


Figure 9 A schematic underlies the pathway of mitochondrial free radical generation and their enzymatic antioxidant defences. The mitochondrial O_2^- is subsequently converted to H_2O_2 either by MnSOD or Cu, ZnSOD, and then ultimately reduced to H_2O by GPx. Figure was adapted from (Al Shahrani et al., 2017).

1.8 Mitochondrial Targets of Oxidative Stress and Association with Inherited Disorders and PD

Mitochondria, as well as being a source of ROS, are susceptible to oxidative stress induced damage with a number of key biological molecules being the target of oxidative damage by radical species, including membrane phospholipids, MRC complexes, mtDNA, and proteins. As a consequence, a deficit in cellular ATP status may occur along with increased electron leak and

partial reduction of oxygen. This in turn may lead to a further increase in the generation of more ROS. Oxidative injury to certain mitochondrial biomolecules has been associated with, and implicated in the mechanism of a number of diseases. A number of which are described herein.

1.8.1 Mitochondrial DNA

Mitochondria have their own genomic system. The human mitochondrial genome contains 16,569 bp of DNA, which is primarily located in the mitochondrial matrix. Mitochondrial DNA or (mtDNA) is circular, double-strand DNA (dsDNA). It has 37 genes, which encodes (13) polypeptides, involved in the MRC or OXPHOS pathway. Of the remainder, (22) code for transfer RNA (tRNA), and a further (2) for ribosomal RNA (rRNA) (Wallace, 2005). Mitochondrial DNA (mtDNA) is solely maternally inherited, meaning that the only the mother is capable of passaging on mtDNA to her offspring (Giles et al., 1980). Therefore, disorders resulting from mtDNA mutations are inherited as a maternal trait. Each individual cell contains several thousand copies of mtDNA (Miller et al., 2003). When all copies are typically identical, the condition is known as homoplasmy. By contrast, when there are two or more genotypes of mtDNA in individual cells (wild-type and mutant), the condition is known as heteroplasmy. Within the heteroplasmic group, clinical manifestations are only detectable once the pathogenic mutation within the mtDNA exceeds a specific threshold level (Stewart and Chinnery, 2015). Inherited mitochondrial disorders are generally believed to be one of the most common inborn error metabolism with a birth prevalence of about 1:5000 (Hargreaves et al., 2016). Based on present data, mitochondrial disorders as the result of mtDNA mutation are estimated to be 1:8000 (Chinnery et al.,

2000). Furthermore, it is rare in children and accounts for less than 10 % of all mitochondrial disorders affecting children (Lamont et al., 1998). At least 200 pathogenic point mutations affecting the mtDNA-encoded MRC I, III, IV as well as tRNAs have recently been reported (Gillis and Sokol, 2003). Furthermore, patients with mitochondrial mtDNA mutations commonly develop a spectrum of clinical symptoms (Deborah et al., 2013). In comparison with nuclear-DNA (nDNA), mtDNA is particularly vulnerable to oxidative stress since it lacks protective histones, has limited of repair mechanisms as well as the major component of intracellular ROS source, the MRC (Sykora et al., 2012; Cline, 2012). Therefore, mtDNA has a potentially higher mutation rate by approximately 10- to 20- fold than nDNA (Chappel, 2013). A hypothesis, known as “mitochondrial catastrophe”, proposed that accumulation of mtDNA insults results in a deficit in MRC activity, which in turn, leads to produce further ROS, and eventually cell death (Leeuwenburgh and Hiona, 2008). This notion also yields an insightful explanation that oxidative stress might be considered as a cause rather than a consequence for the mtDNA disorders.

1.8.1.1 Leber’s Hereditary Optic Neuropathy

Leber’s hereditary optic neuropathy (LHON) (OMIM 540000) is an excellent example of inherited mtDNA disorder. In most cases, it is caused by three mtDNA point mutations involved in MRC complex I subunits (Huoponen et al., 1991). Vision loss is the main clinical features for patients with LHON disorders (Sadun et al., 2011). The involvement of oxidative stress in the mechanism of LHON disorder is well documented (Battisti et al., 2004; Lin et al., 2012). It is worth noting that mitochondrial complex I is one of the major

producer of O_2^- , which has a significant effect in such cases if not all of LHON condition (Howell, 1998). The reduction in MRC complex I activity and its subsequent accumulation which in turn, enhances the cell death via apoptosis (Kirches, 2011). A recent study demonstrated an increase in free radicals formation as well as a reduction in antioxidant levels, compared to control group in blood from patients with LHON disorder (Wang et al., 2008). In addition to an increased O_2^- production as the result of a reduction in MRC complex I activity, increase in protein oxidation, and lipid peroxidation have been detected in mutant mt-ND6 subunit of complex I. Nevertheless, in this study, the antioxidant activity of both MnSOD and GPx were not changed, suggesting that the mutation threshold might not have reached a significant level (Gonzalo et al., 2005). Additionally, an increased level of the HO^* , and lipid peroxy radicals along with an increase in the activity of both SOD forms were also demonstrated (Luo et al., 1997). Consistent with this, increased levels of chemical ROS markers have also been observed in LHON- mutant neuronal cells (Wong et al., 2002). Furthermore, the marker of oxidative DNA damage, 8-OHdG, has been shown to be elevated in white blood cells of LHON patients (Yen et al., 2004). In addition to endogenous production of ROS, exogenous ROS sources such as tobacco smoke has been linked to the onset LHON disorder (Sadun et al., 2004).

1.8.1.2 Myoclonic Epilepsy with Ragged Red Fibers

Myoclonic epilepsy with ragged red fibers (MERRF) (OMIM 545000) syndrome, is an inherited mitochondrial encephalopathy, caused by the mtDNA A8344G mutation in the tRNA (Lys) gene (Shoffner et al., 1999), affecting roughly 90 % of all MERRF cases (Shoffner and Wallace, 1992).

Myoclonus is one of the common clinical features of this syndrome. Other clinical features seen in patients with MERRF are: muscle weakness, hearing loss, cardiomyopathy, and dementia (Shoffner et al., 1999). The pathological mechanism involved however is still unknown. Nevertheless, the role of oxidative stress in the pathomechanism of MERRF has been documented (Wu et al., 1990). The dysfunction of the MRC, most predominately complex I and IV, followed by increased ROS levels has been reported in cultured fibroblasts from patients with MERRF (Mata et al., 2012). Immunohistochemical studies also revealed a selective reduction in mtDNA-encoded MRC subunits in brain tissues obtained from MERRF patients (Sparaco et al., 1995; Lombes et al., 1989). A study using hybrids carrying the A8344G mutant mtDNA revealed significantly increased ROS level together with elevated ROS-scavenger levels, implying that oxidative stress can be considered to play a crucial role in the pathophysiology of MERRF (Szczepanowski et al., 2012).

1.8.2 Mitochondrial Cardiolipin

Cardiolipin (CL) is an exclusive phospholipid component of IMM in eukaryotes where oxidative phosphorylation takes place and constitutes approximately 25% of the total lipid contents in mitochondria (Pope et al., 2008). Having a distinctive dimeric structure, CL consists of four acyl side chains within two negative charged carriers (Figure 10) (Huotkooper et al., 2006).

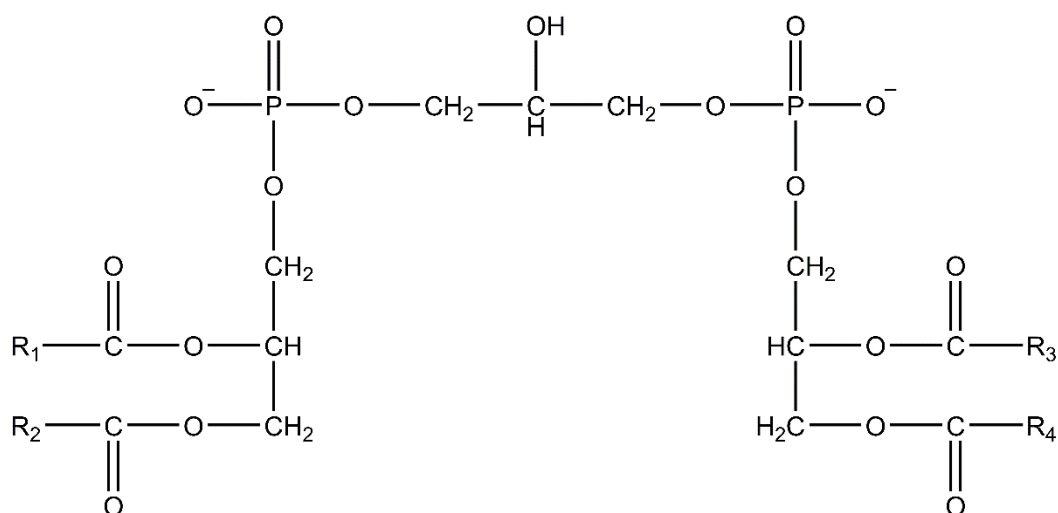


Figure 10 The chemical structure of CL.

In mammalian mitochondria, CL is synthesized from phosphatidic acid through a series of enzymatic reactions which are comparable to other phospholipid pathways. However, the final reaction which is catalysed by CL synthase is distinctive (Schlame and Greenberg, 2000). In addition to its structure and biosynthesis being unique, CL plays a crucial role in aspects of maintaining the functional properties of the mitochondrial components (Schlame and Greenberg, 2009). It has been shown that the mitochondrial enzyme complexes require CL binding for enhancing their enzymatic function (Paradies et al., 2014). Variable numbers of CL molecules integrated into MRC complexes have also been identified (Bazán et al., 2013). It is believed that the CL molecular interaction with all individual respiratory complex are paramount for their assembly into supercomplexes (Pfeiffer et al., 2003). For instance, destabilization of respiratory supercomplexes has been demonstrated as the result of a mutation in the tafazzin (*TAZ*) gene, highlighting the significant of this gene product for CL remodelling

(Houtkooper et al., 2009; McKenzie et al., 2006). In addition to the CL functions in the OXPHOS machinery, CL is also thought to play a key role in mitochondria-mediated apoptosis (Ott et al., 2007). The release of cytochrome *c* from mitochondrial intermembrane space is a key feature in the apoptosis pathway. In the inner mitochondrial membrane, cytochrome *c* is mainly bound to CL, serving as an electron carrier between respiratory chain complex III and complex IV (Tuominen et al., 2002). Upon its release, cytochrome *c* dissociates from CL-binding. Since cytochrome *c* is tightly bound to CL, it has been proposed that ROS may contribute to weaken the interaction between CL and cytochrome *c*, thereby stimulating the release of cytochrome *c* from mitochondria (Petrosillo et al., 2001). The hypothesis involved in the peroxidation of CL by ROS was demonstrated by the recent study in which ROS depleted CL content, which was subsequently followed by a reduction in cytochrome *c* oxidase activity (Petrosillo et al., 2013). In addition to ROS, calcium release may also be triggered by the detachment of cytochrome *c* from CL due to a weakening of the electrostatic interaction between them (Petrosillo et al., 2004). As CL performs a unique role in the mitochondrial compartment, it is not surprising that oxidative stress has been a significant contributor to altered CL metabolism, and mitochondrial dysfunction leading to primary metabolic disorders, mainly Barth syndrome (Chen et al., 2008).

1.8.2.1 Barth Syndrome

Barth syndrome (BTHS) (OMIM 302060) is a rare X-linked genetic disorder, characterized by cardiomyopathy, neutropenia, skeletal weakness, and growth disorders (Barth et al., 1983). It is mainly caused by a mutation in the *TAZ* gene, which encodes a putative enzyme acyltransferase that is

enzymatically responsible for CL remodelling (Barth et al., 2004). The lack of a functional enzyme consequently leads to defect in the trafficking of fatty acids, meaning that monolysocardiolipin (MLCL) is unable to recycle to mature CL (Baile et al., 2014). Based on the well-defined models of BTHS in human and yeast, results have demonstrated a reduction in CL level, and the acyl chain composition of the remaining CL, which in turn lead to mitochondrial dysfunction (Chicco and Sparagna, 2007). Furthermore, the intermediary product MLCL has shown to be raised, suggesting the important link between the *TAZ* gene and CL remodelling (Valianpour et al., 2005). Indeed, BTHS has been earlier described as mitochondrial disorder since BTHS patients can manifest symptoms consistent with known mitochondrial disorders (Jefferies, 2013).

The biochemical findings following MRC enzyme studies in 1983 by Barth together with other groups have provided the evidence of MRC deficiency (Barth et al., 1999). However, individual studies have given different results, suggesting the possibility that primary MRC defect may result in a secondary loss of other MRC activities (Hargreaves et al., 2007). Notably, loss of CL content has been associated with mtDNA instability (Martinez et al., 2015). This may suggest another possible mechanism that the dysfunctional MRC encoded by mtDNA may be the consequence of oxidative damage since the mtDNA structurally lacks protective histones (Alexeyev et al., 2013). Increased ROS levels have evidently been implicated in the *TAZ* mutation seen in cardiomyopathy which is hallmark clinical feature of BTHS syndrome (Saric et al., 2016). It is worth stressing that CL is a predisposed target for oxidative damage for the following reasons: (1) CL has a naturally high

unsaturated content, which is easily attacked by oxidative agents. (2) It is involved in MRC structure, a major intracellular source for ROS production, particularly the superoxide radical. (3) In addition to CL peroxidation, calcium-mediated detachment of cytochrome *c* from CL is induced which generates further ROS levels and results in apoptotic cell death.

1.8.3 Mitochondrial Aconitase

Aconitase [EC 4.2.1.3] is a multi-domain enzyme, which catalyses the second step of the TCA cycle in the isomerization of citrate to isocitrate. It contains of iron-sulphur [Fe-S] cluster, and comes in two different forms: an active [4Fe-4S]²⁺ and an inactive [3Fe-4S]¹⁺ cluster (Beinert and Kennedy, 1993). The active [4Fe-4S]²⁺ form of aconitase is extremely vulnerable to oxidation by O₂⁻, which subsequently converts it to the inactive [3Fe-4S]¹⁺ form. This oxidation reaction is accompanied by the release of a ferrous ion, which subsequently contributes to the generation of an OH[•] via the Fenton reaction (Vasquez-Vivar et al., 2000). As a result of this potential reaction, oxidative injury to mtDNA, lipids, and proteins may occur (Houten et al., 2006). Since the aconitase enzyme is susceptible to direct attack by free radicals, it has been recognized as an oxidative stress marker in mitochondria, suggesting that this enzyme functions as mitochondrial redox sensor (Gardner and Fridovich, 1991).

Aconitase comes in two isoenzyme forms in mammalian cells: the mitochondrial aconitase (m-aconitase), and cytosolic aconitase (c-aconitase). While the m-aconitase is a part of the TCA cycle, c-aconitase is recognized as iron-responsive protein-1 (IRP1), which performs a dual function in the

regulation of iron homeostasis through binding to iron-responsive elements (IREs), and controlling cellular iron levels (Beinert and Kennedy, 1993). Despite the m-aconitase being identical in function (with 25% sequence homology identity) to that of c-aconitase, it is clearly not recognized to have role as an IRP (Haile et al., 1992). However, the brain is highly dependent on m-aconitase activity (Liang et al., 2000) and is regulated by a 5'IRE in its mRNA (Kim et al., 1996). As a consequence of inactivation m-aconitase; neurons could be highly subject to free radical attack and subsequent iron overload, resulting in dramatic accumulation in oxidative stress (Stankiewics, and Brass, 2009). As a central role of TCA cycle in mitochondrial ATP pathway, dysfunction of aconitase may consequently lead to an impairment of TCA cycle capacity, a deficit in MRC activity, and decline in ATP production, which in turn, could lead to subsequent accumulate of ROS levels, and resulting oxidative damage (Figure 11) (Fariss et al., 2005). Collectively, it is well-known that mitochondrial dysfunction, and iron metabolism impairment, inducing oxidative stress has been implicated in various neurodegenerative disorders.

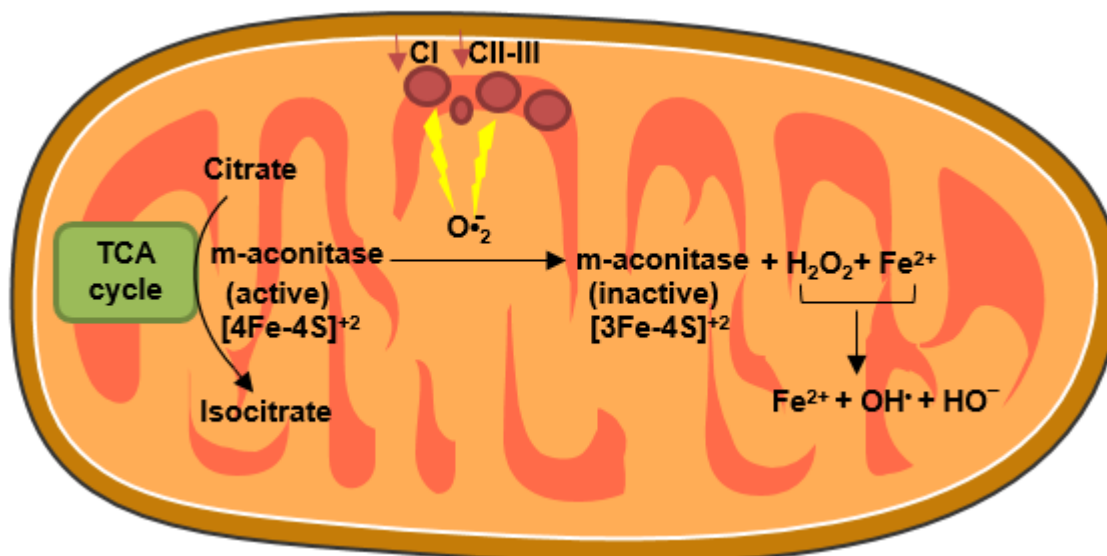


Figure 11 A potential mechanism of oxidation inactivation of m-aconitase by mitochondrial $O_2^{\cdot-}$. This oxidation reaction is accompanied by the release of a ferrous ion, which subsequently contributes to the generation of OH^{\cdot} via Fenton reaction. This scenario could consequently lead to an impairment of TCA cycle capacity, a deficit in MRC activity, and decline in ATP production, which in turn, could lead to further oxidative damage. Figure was adapted (Fariss et al., 2005).

1.8.3.1 Friedreich Ataxia

Friedreich ataxia (FRDA) (OMIM 229300), is a progressive neurodegenerative disorder with an autosomal recessive mode of inheritance, affecting roughly 1:50,000 live births (Rotig et al., 1997). In addition to neuronal injury in the dorsal root ganglia (DRG) and sensory peripheral nerves, FRDA patients also manifest with non-neurological symptoms including diabetes, cardiomegaly, and muscle weakness (Koeppen, 2011). FRDA is caused by GAA expansion in the *frataxin* gene, the product of which is predominantly located in mitochondria (Campuzano et al., 1996). The exact role of the frataxin protein

is not yet fully understood. However, it has been proposed to play crucial roles primarily in regulating iron machinery and functioning as a mitochondrial Fe-S cluster chaperone (Babcock et al., 1997; Gerber et al., 2003). In this regard, increased iron capacity, and the loss of activity of mitochondrial Fe-S cluster-containing enzymes has been evidently observed in FRDA patients, suggesting the paramount function of frataxin in iron metabolism (Rotig et al., 1997; Abeti et al., 2016; Kaplan et al., 1999). In addition to its well-established role in iron metabolism, frataxin can protect against iron-mediated oxidative stress (Bresgen and Eckl, 2015). In a previous study, exposure of fibroblast obtained from patients with FRDA to ferrous ions and H₂O₂ reduced the viability of the cells in patients (Wong et al., 1999). The most direct evidence of the critical function of frataxin in protecting against oxidative stress comes from the observation of combined reduction in activity of nuclear factor-erythroid 2 related factor 2 (Nrf2) and glutathione levels in the YG8R mouse model of FRDA (Yuxi et al., 2013). In contrast, an increased resistance to oxidative stress induced by overexpression of mitochondrial frataxin has been reported in *Drosophila* (Runko et al., 2008). Since the discovery of the frataxin gene in 1996, dysfunction of mitochondrial Fe-S cluster-containing enzymes including complex I, III and aconitase, resulting in oxidative stress has been a major contributor in the pathophysiology of FRDA (Koenig and Mandel, 1997).

1.8.4 Parkinson Disease

Parkinson's disease (PD) is a chronic and progressive neurodegenerative disorder. It is a multifactorial and age-related disorder, affecting approximately 1%, of the general population, and almost exclusively in the aged 60 years or older (Reeve et al. 2014). As the aging population and life expectancy are projected to rapidly grow over the next few decades, the prevalence of this disorder is expected to increase to 50% by 2030 (Dorsey et al., 2007). The PD incidence rates are substantially higher for men than for women within the ratio being 3:2 (men to women ratio) (De Lau and Breteler, 2006). The late-onset sporadic (idiopathic) form accounts for 90% of all PD cases, while the remaining is familial (Mendelian) form. Once approximately 70- 80 % of dopaminergic neurons depletion occurs (Bezard et al., 2001; McNamara and Durso, 2006), PD patients clinically present with motor symptoms, including bradykinesia, tremor, rigidity and often postural instability. In addition to motor symptoms, patients with PD may present with non-motor symptoms, such as depression, sleep disturbances, anxiety, and constipation (Kalia and Lang, 2015). The cardinal pathological hallmarks of Parkinsonism include selective cell death of dopaminergic neurons in the pars compacta of the substantia nigra (SN) and the presence of α -synuclein-positive intraneuronal cytoplasmic inclusions, known as Lewy bodies (LBs). For several decades, it was assumed that PD is likely caused by environmental factors until in 1997 when the autosomal dominant mutation in the alpha-synuclein (*SNCA*) gene was discovered (Abou-Sleiman et al., 2006). Since this discovery, at least seven other mutant genes, including, *parkin*, PTEN-induced putative kinase 1 (*PINK1*), *DJ-1*, HtrA serine peptidase 2 (*HTRA2*), leucine-rich repeat kinase 2

(*LRRK2*), ubiquitin C-terminal hydrolase-L1 (*UCHL1*) (Klein and Westenberger, 2012; Schapira, 2008), and glucosylceramidase beta (*GBA1*) which encodes the lysosomal enzyme glucocerebrosidase (GCCase) (Gegg et al., 2012), have also been identified that are linked to familial PD (Table 3) .

Gene product	Mendelian inheritance
<i>SNCA</i>	Autosomal dominant
<i>Parkin</i>	Autosomal recessive
<i>PINK1</i>	Autosomal recessive
<i>DJ-1</i>	Autosomal recessive
<i>LRRK2</i>	Autosomal dominant
<i>HTRA2</i>	Autosomal dominant
<i>UCHL1</i>	Autosomal dominant
<i>GBA 1</i>	Risk factor

1.8.4.1 Mitochondrial Dysfunction and PD

Neurons commonly consume large amounts of energy as a course of their normal biochemical and metabolic activities. Since 20% of total oxygen per approximately 2% of human’s weight is utilized by neurons, this oxygen needs to be delivered to mitochondria to produce energy in the form ATP through the MRC (Cobley et al., 2018). Consequently, any disturbance to mitochondrial

function can have potentially detrimental effects on neuron function. For several decades now, there has been a flurry of emerging evidence of mitochondrial dysfunction which has been implicated in the pathogenesis of PD. The first evidence emerged in the early 1980s when drug abusers intravenously injected with 1-methyl-4-phenyl-1,2,3,4-tetrahydropyridine (MPTP), which became metabolised to the MRC complex I inhibitor 1-methyl-4-phenylpyridinium ion (MPP⁺) via the monoamine oxidase-B (MAO-B) enzyme, where is taken up from glial into dopaminergic neurons by the dopamine transporter (DAT). This consequently induced Parkinsonism syndrome (Figure 12) (Langston et al., 1983). Similarly in animal models, rats and primates were shown to share Parkinson-like symptoms, following administration of MPTP (Blesa et al., 2012). In parallel with MPTP, a chronic low-dose infusion of rotenone to rats additionally induced similar features of Parkinson disorders including selective loss of dopaminergic neurons and aggregation of α -synuclein (Betarbet et al., 2002). Collectively, MRC complex I inhibitors have become commonly utilized to investigate the pathogenesis and therapeutic tools for PD. Further studies performed to support the role of mitochondrial dysfunctions have shown strong links to the aetiopathogenesis of PD. Studies of post-mortem PD patient brain tissue demonstrated complex I deficiency in the SN and frontal cortex (Schapira et al., 1989; Parker et al., 2008). In additions to being functionally impaired and misassembled, MRC complex I subunits are oxidatively damaged in SNs of patients with PD (Parker et al., 2008). In addition to post-mortem brain, MRC complex I deficiency was also demonstrated in peripheral tissues including platelets and skeletal muscle from individuals with PD (Schapira, 1994). In this context it seems that

a reduction of MRC complex I activity is systemic, thereby simultaneously affecting many tissues. In addition to a decrease in the activity of complex I, a reduction in complex III activity was further demonstrated in lymphocytes and platelets in patients with PD (Haas et al., 1995). Taken together, inhibition of mitochondrial respiratory complex I and III could consequently lead to excessive ROS production, oxidative stress, and subsequent depletion of ATP levels, elevated intracellular calcium levels, excitotoxicity, and ultimately enhanced dopaminergic neuronal cell death (Keane et al., 2011). Collectively, these scenarios have been associated with idiopathic PD pathogenesis (Figure 12). Additionally, PD-related genes also appear to be in part localized to mitochondria and therefore may contribute indirectly towards mitochondrial damage and oxidative stress (Figure 13) (Schapira, 2008).

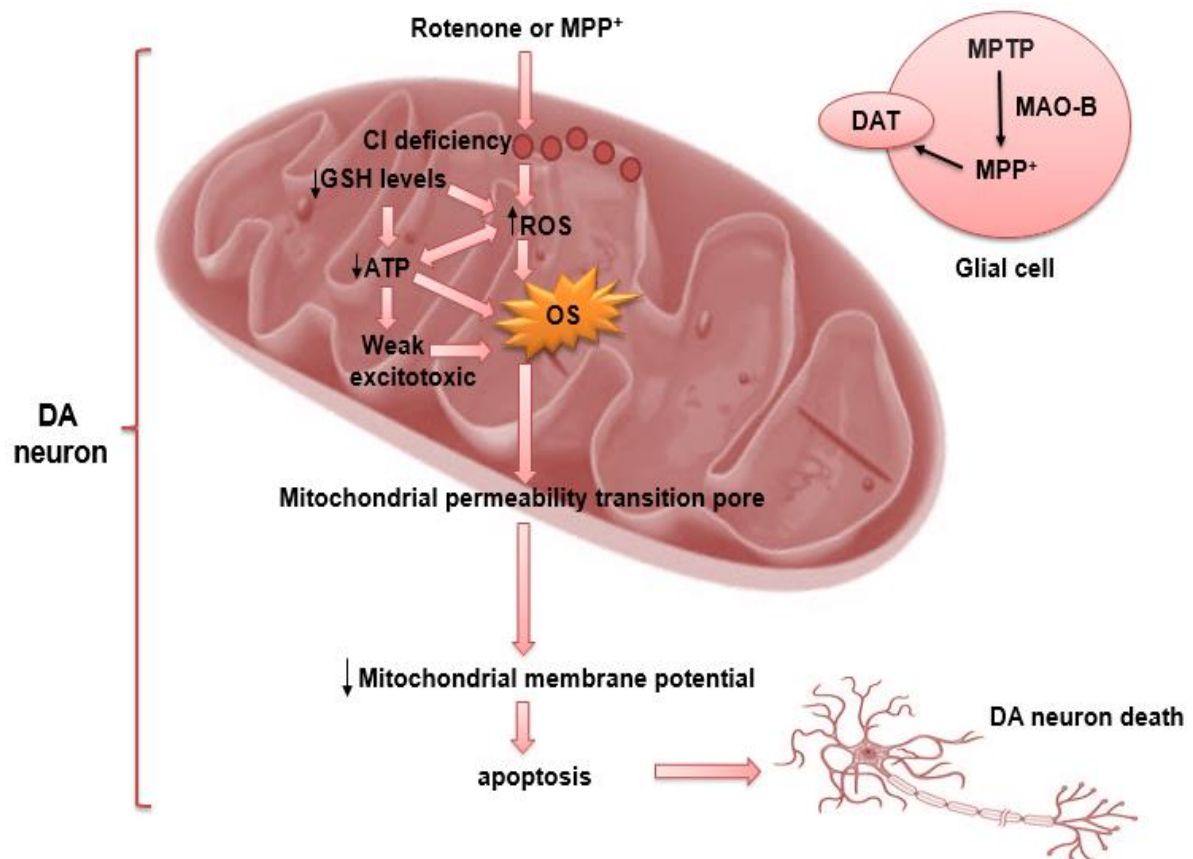


Figure 12 Schematic illustrating the potential role of mitochondrial dysfunction in the PD pathogenesis. Mitochondrial toxins, such as rotenone or MPP⁺ elicit MRC complex I inhibition, and subsequently produce ROS, reduction of the GSH status, with resulting oxidative stress. Oxidative stress consequently induces mitochondrial permeability by transiently opening a pore, which subsequently causes depolarization of the mitochondrial membrane potential. These scenarios eventually lead to neural cell death via the release of pro-apoptotic mitochondrial proteins, including cytochrome c and apoptosis-initiating factor. DA, dopamine; CI, complex I; OS, oxidative stress. Figure adapted from (Al Shahrani et al., 2017).

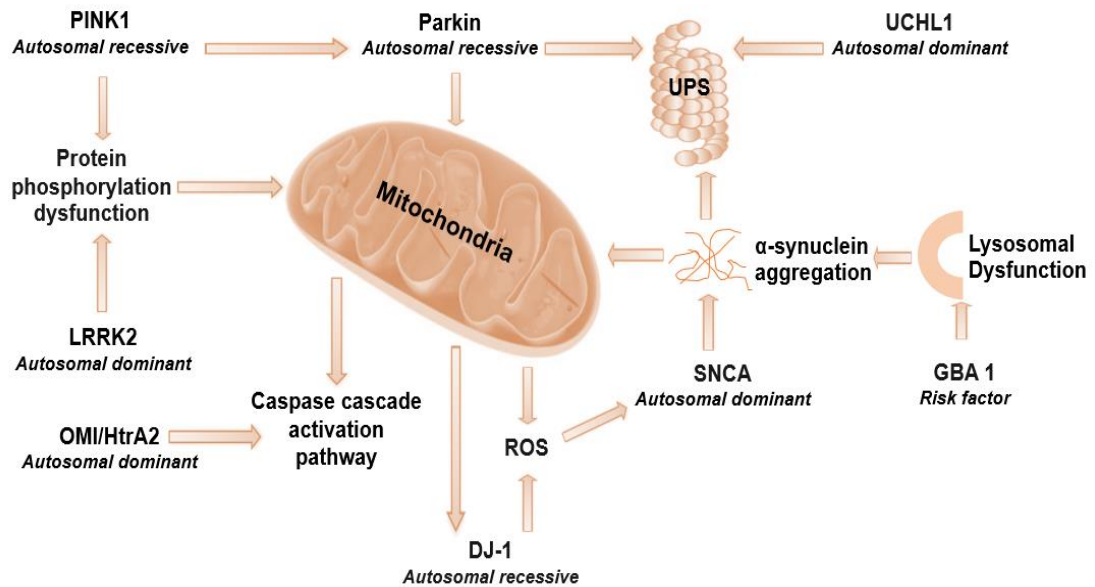


Figure 13 The potential interaction between PD-related genes and their potential impact on mitochondrial function. Mutations in mitochondrial quality control, *PINK 1* gene, which is also one of the major components of the ubiquitin proteasomal system (UPS), leads to alter in mitochondrial function and structure. Mutations in *PINK 1* in combination with mutations in *LRRK2* could also lead to a modification in protein phosphorylation, particularly in mitochondrial proteins. In addition to overload or dysfunction of protein ubiquitination, *Parkin* is downstream of *PINK1* function and may itself induce mitochondrial dysfunction. Moreover, Mutations in *UCHL1* which is encoded by ubiquitin carboxyl-terminal esterase, will also cause aberrant damage to UPS function. In addition to *GBA 1* mutation, mitochondrial dysfunction resulting in oxidative stress may also subsequently lead to an enhancement of the abnormal unfolding protein, α -synuclein. DJ-1 acts as a ROS quencher where it is located in the mitochondrial intermembrane space and matrix, thus mutations in DJ-1 may impact in its correct function. These pathological events along with mutations in *Omi/HtrA2* may consequently speed up the mitochondrial caspase cascade activation pathway. Figure was adapted from (Schapira, 2008).

Crucially, neurons are extremely vulnerable to oxidative stress for other many reasons such as : (i) their membranes are surrounded by high level of unsaturated fatty acids and phospholipids (Bazinet and Layé, 2014) (ii) coupled with insufficient amount of antioxidants capacity such as the primary defence line, GSH (Ren et al., 2017) (iii) dopamine (DA) quinones or semiquinones are continuously produced as a by-product of DA oxidative metabolism, which in turn have the capability of depleting neuronal GSH levels (Hargreaves et al., 2016) (iv) iron is considered to be the most abundant metal throughout the brain which has the capability to produce the free OH[•] radical mediated by lipid peroxidation and autoxidation of DA (Bharath et al., 2002).

Subsequent studies of Post-mortem PD patients have further showed that an increased level of malondialdehyde (MDA) can be used as an oxidative marker for lipid oxidation. In contrast, the concentration of unsaturated fatty acid was low (Dexter et al., 1989a). In addition to lipid oxidation in PD substantia nigra, markers of oxidative stress to DNA, 8-hydroxy-2' - deoxyguanosine (8-OHdG), and protein (carbonyl modifications) were also found to be elevated (Zhou et al., 2008). Antioxidants play a fundamental role in defending cells from oxidative stress. Among these antioxidants are CAT, SOD (Venkateshappa et al., 2012) GPx (Damier et al., 1993), GSH (Sian et al., 1994) and uric acid (Annamaki et al., 2007) the levels of which have all been found to be changed in PD.

1.8.4.2 The Interplay among PINK1, Parkin and DJ-1 during Mitochondrial Quality Control

A growing body of evidence has demonstrated that modified mitochondrial dynamics, turnover and function have been associated with pathological alterations in a number of neurodegenerative disorders, particularly PD (Laar and Berman, 2009). There are several mechanisms that have evolved to control and maintain mitochondrial protein integrity, including repair of dysfunctional mitochondria by fusion with healthy mitochondria and selective clearance of irreversibly dysfunctional mitochondria by the autophagy pathway (mitophagy) (Ni et al., 2015).

One of the most studied mechanisms for selective degradation of mitochondria is the activation of PINK1 and parkin-mediated mitophagy (Jin and Youle, 2012). In its full-length form, PINK1 accumulates on the OMM upon loss of mitochondrial membrane potential, which subsequently recruits parkin from the cytosol onto mitochondria (Matsuda et al., 2010). Upon activation, parkin ubiquitinates itself and other proteins on the OMM including voltage-dependent anion channel 1 (VDAC1), dynamin-related protein 1 (Drp1), mitofusin 1 and 2 (Mfn1 and 2), and TOM (Ziviani et al., 2010; Cai et al., 2012). Subsequently, ubiquitinated mitochondrial proteins are recognized by the selective autophagy adapter proteins which create double-membrane vesicles, known as autophagosomes (Johansen and Lamark, 2011). These vesicles are then fused with lysosomes to degrade the cellular organelles. Therefore, Loss-of-function mutations in PINK1 and parkin which are the most common cause of early-onset PD may lead to impair mitochondrial dynamics, thereby rendering DA neurons more susceptible to oxidative stress (Jin and

Youle, 2012). Similarly, PD-related gene mutation, DJ-1 has been shown to reduce mitochondrial membrane potential, increased mitochondrial fragmentation, autophagy and oxidative stress (McCoy and Cookson, 2011). Additionally, recent studies suggested that DJ-1 functions in a parallel pathway to PINK1 and parkin to maintain mitochondrial integrity in response to oxidative damage (Joselin et al., 2012; Hauser et al., 2017). However, whether DJ-1 functions within PINK1 and parkin-mediated mitophagy in the same pathway remains to be elucidated.

1.8.4.3 A Potential Link between Neuroinflammation and Mitochondrial Dysfunction in the Pathogenesis of PD

Chronic neuroinflammation has been implicated in the pathophysiology of PD. Studies of post-mortem PD patient brain tissue demonstrated that activation of brain glial cells and elevation in pro-inflammatory factor levels are major characteristic features of the PD brain (McGeer et al., 1988; Bartels et al., 2010). Furthermore, chronic induction of pro-inflammatory cytokines by activated microglia, a type of glial cell, results in enhanced cell death of DA neurons in the SNpc (Benner et al., 2008; Leal et al., 2013). Furthermore, mitochondrial dysfunction has been suggested to be a contributing factor in these processes (Zhou et al., 2011; Horssen et al., 2017). In fact, mitochondrial function has a potential role in pro-inflammatory signaling (López-Armada et al., 2013). In this context, alteration in mitochondrial autophagy in organismal aging has been shown to promote inflammation and cell death, suggesting that impaired autophagy may contribute to pathogenesis of aging-related disorders (Green et al., 2011). Similarly, some of pro-inflammatory factors may also interfere with mitochondrial function

(Horsssen et al., 2017). For instance, in activated microphages, high levels of free NO radical produced by inducible nitric oxide synthase (iNOS), has been demonstrated to inhibit reversibly MRC complex IV and enhance free radical generation (Brown and Cooper, 1994; Cleeter et al., 1994). Both of these pathological mechanisms may enhance mitochondrial ROS production which in turn promotes a vicious inflammatory cycle (Zorov et al., 2014). Thus, strategies aimed at alleviating mitochondrial oxidative stress within mitochondria may hold a promising therapeutic interventions in inflammation and PD.

1.8.4.4 Iron and Mitochondrial Dysfunction: Cross-Talk in PD

Amongst all transition metals, iron is considered to be the most abundant metal in the brain, predominately in the basal ganglia (Moos et al., 2007). It significantly contributes to the proper functioning of neurotransmitters, myelination, and mitochondria (Winter et al., 2014; Conner et al., 1992). The brain iron metabolism is primarily regulated by transferrin and ferritin (Kerksick and Willoughby, 2005). It commonly conjugated into iron-sulphur clusters in many proteins, which have the potential ability to accept or donate electrons, particularly in the MRC pathway (Hirsch and Faucheux, 1998). The evidence for alterations in iron metabolism during neuropathology of Parkinson disease (PD) has also been extensively demonstrated (Dexter et al., 1987; 1989b; Hirsch et al., 1991). In fact, the potential mitochondrial O_2^- toxicity due to a defect in complex I activity has been widely demonstrated in PD models. Nevertheless, the exact mechanism of whether an enhanced production of O_2^- induced neuronal injury is yet to be largely elucidated. Neurotoxins such MPP⁺, which is commonly used as PD model (Abou-Sleiman et al., 2006) has been utilized to

describe the potential harmful effects of the inactivation of m-aconitase and high amount of iron content on dopaminergic neurons (Liang and Patel, 2004). In mice, this neurotoxin model-induced neurotoxicity has been linked to the inactivation of m-aconitase, increase iron content, and depletion of DA levels (Ebadi et al., 1996). It appears that excess O_2^- production is a common denominator of these cascades. Iron and iron derivatives contributes to the generation of the most active radical OH^\bullet via the Fenton reaction, which in conjunction with DA autoxidation may further enhance OS, leading to the degeneration of dopaminergic neurons (Figure 14) (Obata, 2002; Jomova and Valko, 2011; Núñez et al., 2012).

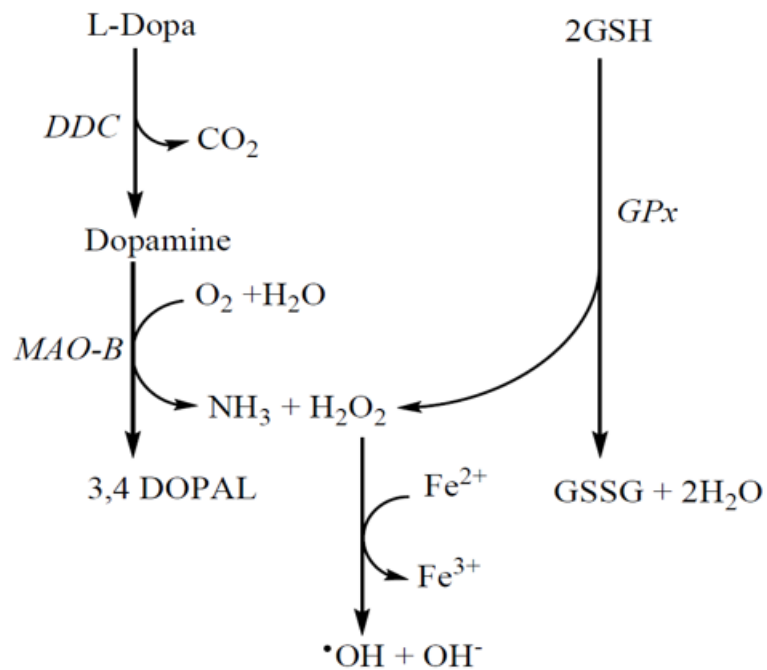


Figure 14 A potential mechanism of dopamine metabolism and OH• radical formation in the striatum of PD patients as a result of iron accumulation and decline in GSH levels. Abbreviations: DDC, dopa decarboxylase; 3,4 DOPAL, 3,4-Dihydroxyphenylacetaldehyde. Figure was taken from (Al Shahrani et al., 2017).

Post-mortem brain tissue from PD patients exhibited accumulation of iron content, which can be taken together with a reduction in the glutathione redox ratio (GSH/GSSG) as potential indicator for oxidative stress (Núñez et al., 2012; Owen and Butterfield, 2010). In glutathione-depleted (Δ gsh1) cells model, on the other hand, the mitochondrial (Fe-S) cluster wasn't affected, suggesting that m-aconitase is resistant to oxidative stress (Sipos et al., 2002). Furthermore, accumulation of iron was found to potentiate LBs formation in the substantia nigra of PD patients, supporting the link between iron-mediated oxidative stress and the degeneration of dopaminergic neurons in PD (Dias et al., 2013). To further associate such observations with the implication of iron dysregulation in PD-related aging, the level of iron was shown to be increased in parallel with age (Hagemeier et al., 2012). This finding also supports the concept of aging which is associated with mitochondrial dysfunction, and subsequently generate ROS, resulting in oxidative stress and thereby shortening life (Trifunovic, 2006). Collectively, along with iron dysregulation, these cascade of events have been suggested to be potential pathological factors contributing towards the degeneration of dopaminergic neurons in PD. As highlighted in this section, ROS-mediated oxidative damage to the mitochondrial biomolecules are intrinsically linked to the aetiology of a number of inherited mitochondrial disorders and PD (see summary in Figure 15).

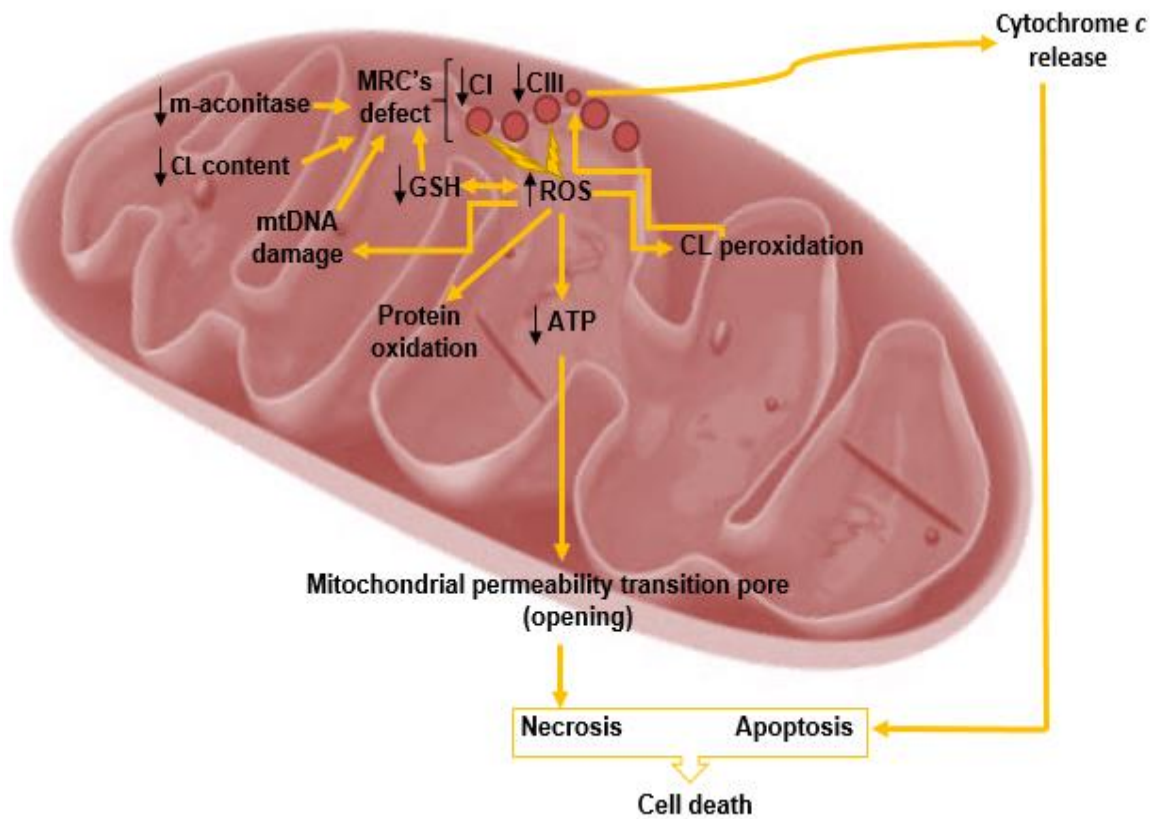


Figure 15 A summary of oxidative stress-induced mitochondrial damage is a common mechanistic link in the pathogenesis of inherited mitochondrial disorders and PD. Figure was taken from (Al Shahrani et al., 2017).

1.8.5 PD Treatments

Despite the availability of a wide range of treatment and management options for Parkinson's patients, PD is still incurable. The current therapeutic options for PD mostly focus on reducing symptoms or slowing down progression of the disorder. The main pharmacological mechanism of Parkinson's treatment relies on enhancing dopamine levels and mimicking dopamine's action (Figure 16) (Pedrosa and Timmermann, 2013). However, there is growing body of evidence reporting that PD therapies, in particular on the use of Levodopa (L-dopa), and catechol-O-methyltransferase (COMT) may induce mitochondrial dysfunction as it will be discussed in more detail in the next section.

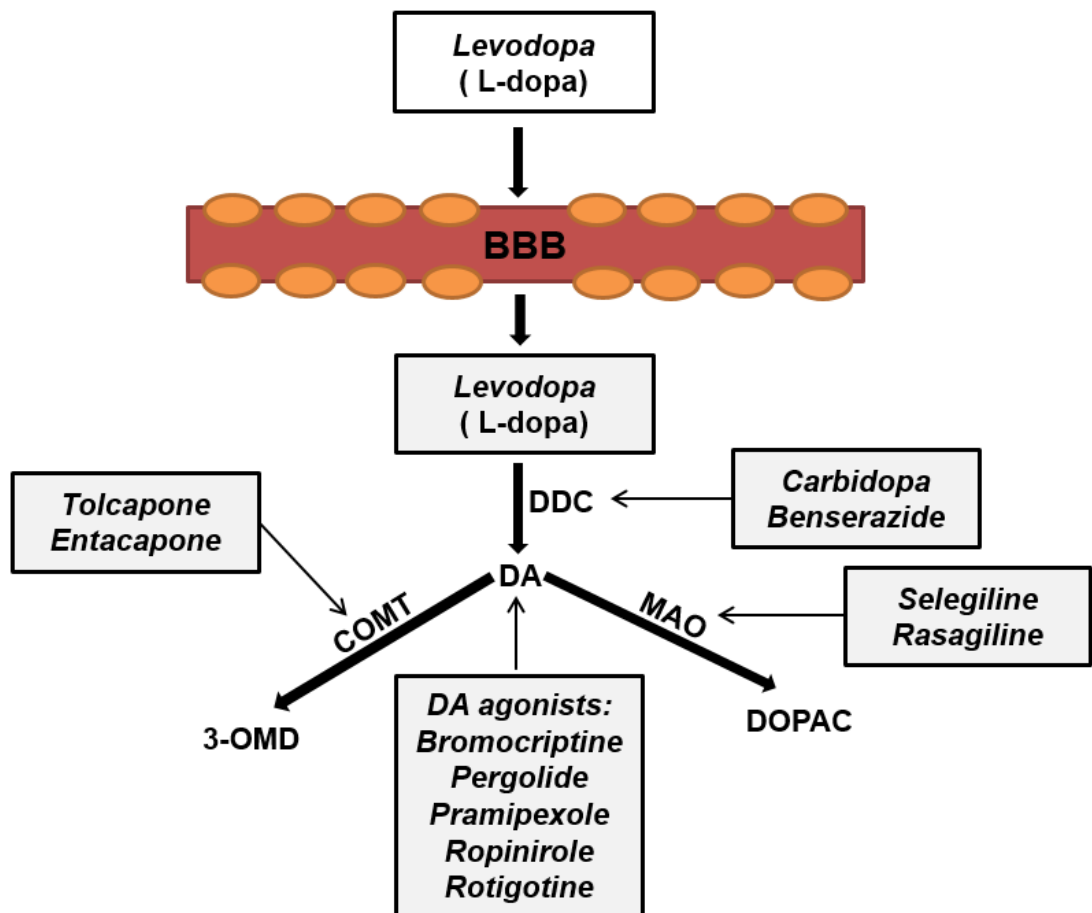


Figure 16 A schematic underlying the current treatment options for Parkinson’s patients. The dopamine (DA) precursor, L-dopa acts as a replacement therapy for DA, which has ability to cross blood brain barrier (BBB). L-dopa is combined with the inhibitor of DOPA decarboxylase (DDC), carbidopa, which improves the efficiency of oral L-dopa administration in central brain-deficient DA. Other potential strategies for maintaining and improving DA levels in PD patients is administration of L-dopa therapy with inhibitors that blocks degradation of DA, including catechol-O-methyltransferase (COMT) and monoamine oxidase-B (MAO-B) inhibitors. Another PD treatment option utilized to restore the activity of DA signaling in brain-deficient DA is the administration of a DA agonist, which typically mimics DA actions.

1. 9 Parkinson Therapies Induced MRC Toxicity

1.9.1 Levodopa (L-dopa)

A large body of evidence of mitochondrial dysfunction has been causally linked to the pathogenesis of PD (Henchcliffe and Beal, 2008). Alarming, numerous studies have also indicated that some treatments of PD may actually contribute to mitochondrial damage. (Szewczyk and Wojtczak, 2002; Neustadt and Pieczenik, 2008). These treatments may be contributing factors to mitochondrial damage through inhibition of the OXPHOS process; or production of ROS; or impairment of one of the mitochondrial enzymatic pathways (Chan et al., 2005).

From the time when Levodopa was approved in 1970 (reviewed by Hauser, 2009), it has been the first-line medication for managing PD symptoms. Levodopa or L-3,4-dihydroxyphenyl-L-alanine (L-dopa) acts as a replacement therapy for dopamine that is depleted in PD patients (Fahn, 1997). In addition to its precursor, L-dopa and other catecholamine, DA is documented as one of the various known neurotransmitters which has the potential to undergo auto-oxidization. DA quinones or semiquinones are continuously produced as a by-product of DA oxidation metabolism, which in turn have the capability of depleting neuronal GSH level by direct binding with the protein thiol groups or oxidative stress-induced GSH depletion (Bisaglia et al., 2010).

In catecholaminergic neurons, monoamine oxidase form A (MAO-A) is the preferential enzyme for the oxidation of the hydroxylated amines, serotonin and noradrenalin. However, MAO-B, which is primarily located in serotonergic neurons, has a preference for the oxidization of non-

hydroxylated amines, including benzylamine and phenylethylamine (Shih et al., 1999). In glial cells, both MAO enzymes have the capability of oxidizing DA (Glover et al., 1977). In view of the important role of GSH as a key antioxidant to protect the MRC function against ROS damage, a depletion in GSH level as the consequence of DA quinone or semiquinone exposure may lead to a secondary MRC complex deficiency (Berman and Hastings, 1999; Hargreaves et al, 2005).

Furthermore, direct exposure of isolated brain mitochondria to DA oxidation products induced mitochondrial swelling which was believed to be as the result of the opening of the mitochondrial permeability transition pore (Maharaj et al., 2005). In the brain mitochondria, the release of H₂O₂ via MAO activity was reported to damage the MRC complex activity (Moore et al., 2005). Interestingly, there is a recent indication of an involvement of L-dopa treatment in oxidative damage-induced neurotoxicity due either to its enhancement of the DA pathway or due to its reaction with iron to form the neurotoxin, 6-hydroxydopamine which is a MRC complex I inhibitor (Stansley and Yamamoto, 2013; Kurth and Adler 1998). L-dopa can also be converted to DA, mediated by serotonergic neuronal cell which can further produce ROS via its enzymatic degradation by MAO-A activity. This oxygen-derived radical can ultimately lead to serotonergic neuronal cell damage by inhibition of many cellular enzymes, including the mitochondrial complexes (Kurth and Adler 1998).

1.9.2 Catechol-O-methyltransferase (COMT)

Combining L-dopa therapy with the COMT inhibitors, entacapone and tolcapone, is one of the potential strategies to maintain and improve DA levels in PD patients (Männistö and Kaakkola, 1999). In late 1998, tolcapone was withdrawn from the EU market as consequence of three PD patients dying of fatal liver damage following administration of this drug (Borges, 2003; Nissinen et al., 1997). Considerable attention has been recently paid in investigating the mechanism responsible for (COMT) inhibitors induced liver damage. Both *in vivo* and *in vitro* studies have demonstrated that tolcapone has the potential to elicit the mitochondrial uncoupling, resulting in an ultimate depletion in cellular energy status and consequently organ damage (Haasio et al., 2002a). In contrast, entacapone has been shown to have no effect on mitochondrial membrane potential at concentrations below 100 μM , which dramatically exceeds the therapeutic peak plasma concentrations achieved by this drug (4–14 μM) (Haasio et al., 2002b). Despite extensive protein binding, both entacapone and tolcapone have potent COMT inhibitor activity, and if this is taken as a surrogate of their overall activity (Kaakkola, 2000), then serum protein binding may not influence their mitochondrial toxicity. Furthermore, the binding of a drug to serum proteins does not appear to affect its tissue concentrations (Haasio et al., 2002b).

1.10 The Role of Antioxidants in the Prevention of Oxidative Damage

Mitochondrial free radical-induced oxidative damage is a plausible pathogenic facilitator in both inherited and acquired mitochondrial disorders. Alleviation of ROS/RNS free radical-mediated oxidative stress and increased availability of ATP by antioxidants could be an effective therapeutic approach to help restore mitochondrial function, or at least to limit the progression of symptoms in a tremendous number of patients with mitochondrial dysfunction.

To limit free radical-induced oxidative stress, the human body is endowed with a variety of enzymatic and non-enzymatic antioxidant defence mechanisms. The two major antioxidants that protect the cell from ROS and RNS are GSH and coenzyme Q₁₀ (Heales et al., 2002; Duberley et al., 2014)

1.10.1 Coenzyme Q₁₀

Coenzyme Q₁₀ (CoQ₁₀) constitutes a 1,4-quinone lipophilic structure, consisting of a benzoquinone ring attached to 10 isoprene units (Figure 17). It is present in most tissues of the human body with highest amounts being found in the heart, kidney, liver and muscle. Apart from the brain and lungs, CoQ₁₀ is found predominantly in tissues in its fully reduced form, ubiquinol (Hargreaves, 2014). Due to its hydrophobic structure, CoQ₁₀ is the sole MRC component which is not anchored to the IMM. In addition to its function as an electron carrier which shuttles electrons from complexes I and II to complex III in the MRC pathway, CoQ₁₀ also serves as a free radical-scavenging antioxidant. The reduced ubiquinol form of CoQ₁₀ serves this function (Hargreaves, 2014).

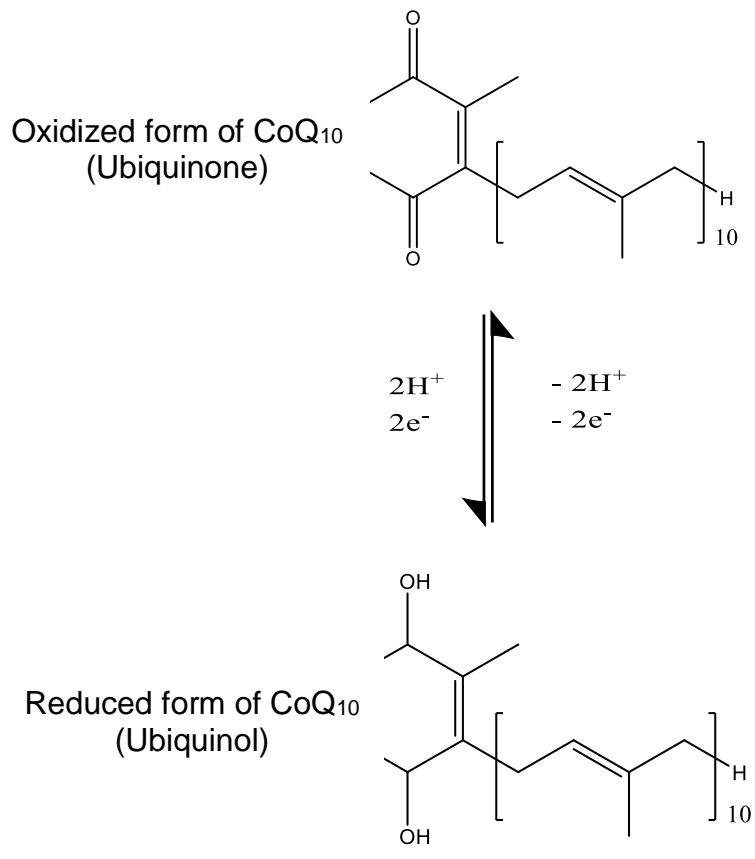
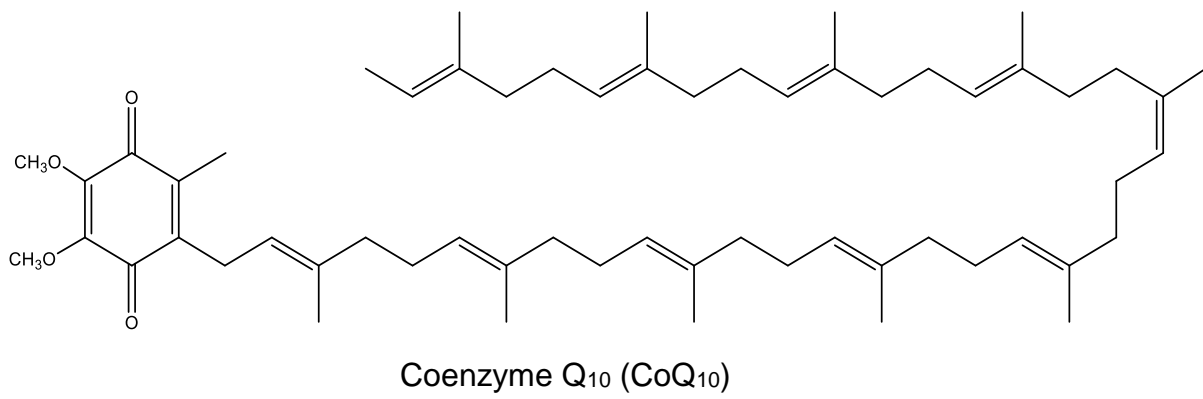


Figure 17 The chemical structure of CQ₁₀ and its two redox forms

Over the years, the clinical use of CoQ₁₀ (ubiquinone) and its analogues (quinones) have been proven to be an effective therapy for mitochondrial disorders via their capabilities to reinstate electron transfer in the MRC, increase ATP, and enhance mitochondrial antioxidant activity, which in turn, can ameliorate the harmful effects of ROS (Hargreaves, 2014).

The therapeutic potential of CoQ₁₀ in the treatment of mitochondrial disorders took the spotlight in 1985 after Ogashara and colleagues reported the sustained improvements in the clinical phenotype of patients with Kearns-Sayre syndrome (KSS is also known as inherited mitochondrial myopathy, a disorder with the onset of ophthalmoparesis before 20 years of age) following administration with CoQ₁₀ (Ogasahara et al., 1989). More recently, Maldergem also reported that CoQ₁₀ therapy was beneficial to two sisters diagnosed with Leigh's encephalopathy (Maldergem et al., 2002). Remarkably, the beneficial effects of CoQ₁₀ in two patients with KSS and hypoparathyroidism has been demonstrated to help maintain calcium levels in both patients serum, suggesting that treatment with CoQ₁₀ restored the capacity of calcitriol (the active form of vitamin D), which is located in the mitochondria of proximal tubules (Hargreaves, 2014). Some degree of sustained improvements have been noted with some patients whose clinical features can be associated with mitochondrial disorders, such as ataxia, muscle stiffness and exercise intolerance following implementation of CoQ₁₀ therapy (Hargreaves, 2014).

Despite oral CoQ₁₀ supplementation being significantly effective in patients with all forms of CoQ₁₀ deficiency, it has only been shown to be partially effective in patients who presented with neurological symptoms, suggesting

that these symptoms may only respond efficiently to high doses and long term administration of exogenous CoQ₁₀ (Quinzii et al., 2007). The efficacy of synthetic ubiquinone analogue such as idebenone, has been reported in patients with mitochondrial disorders including, LOHN, FRDA, and MELAS (Koene and Smeitink, 2011; Napolitano et al., 2000). It has also been recommended that patients with deficient levels of CoQ₁₀ should be administered with CoQ₁₀ supplementation rather than idebenone as this synthetic analogue is not a potential replacement for CoQ₁₀ in the MRC (Mancuso et al., 2012). However, in addition to its beneficial effects, idebenone may reduce MRC complex I activity, thereby affecting the mitochondrial bioenergetics function (Jaber and Polster, 2015). Therefore, further clinical studies regarding the overall benefits of idebenone need to be conducted to address this issue.

As CoQ₁₀ performs two roles, one in mitochondrial energy metabolism and the other as a free-radical scavenger, low levels of CoQ₁₀ may therefore result in the impairment of the MRC activities as well as in the accumulation of ROS levels, and thereby contribute towards the pathogenesis of PD. CoQ₁₀ deficiency associated with PD has been previously described (Shults et al., 1997; Hargreaves et al., 2008). A reduction in CoQ₁₀ level was demonstrated in the plasma (Sohmiya et al., 2004) and platelets (Götz et al., 2000) in patients with PD, thereby suggesting that systemic effects may be important. For the first time, a UK study demonstrated that CoQ₁₀ levels were lower in the brain cortex of patients with PD (Hargreaves et al., 2008). The neuroprotective role of CoQ₁₀ has also been investigated in both animal and human cell models (Kooncumchoo et al., 2006; Winkler-Stuck et al., 2004).

Using *in vitro* models of PD, CoQ₁₀ has been reported to protect dopaminergic neurons against neurotoxin-induced PD symptoms using either rotenone, paraquat or MPP⁺ (Moreira et al., 2010). Another study has shown that CoQ₁₀ treatment improved both MRC complex I and complex IV activities in skin fibroblast from PD patients (Winkler-Stuck et al., 2004).

To investigate the neuroprotective potential of CoQ₁₀ treatment in PD, 80 patients with early stage PD were randomly allocated to participate in a 16-month multicentre clinical trial (Shults et al., 2002). Results showed that participants who received high doses of CoQ₁₀ had a large improvement in their motor functions, whilst lower doses only provided mild benefits. It was therefore concluded that the beneficial effect of CoQ₁₀ treatment may contribute to a reduction in the progression of PD. However, a randomized clinical trial of two high doses of CoQ₁₀ (1200 and 2400 mg/day) was recently conducted in early stage of PD patients which failed to show any clinical benefits (Beal et al., 2014).

1.10.2 Glutathione (GSH)

The tripeptide reduced glutathione (GSH) (γ -glutamyl-L-cysteinyl-L-glycine), is an intracellular thiol-containing water soluble antioxidant (Shahripour et al., 2014). In addition to its vital antioxidant role, GSH also functions as a cofactor for other antioxidant molecules including glutathione peroxidase (GPx, EC 1.11.1.9), and thioredoxin (Trx) as well as maintaining vitamins C and E to be functionally active (Birben et al., 2012).

In the cytosol, GSH is synthesised by the action of two ATP-dependent enzymatic steps, including the rate-limiting enzyme γ -glutamylcysteine synthetase (GCS, EC 6.3.2.2), which is inhibited by a GSH feedback loop,

and GSH synthetase (GS, EC 6.3.2.3). Intracellular GSH predominately exists in the reduced form, with less than 1% of GSH existing in the oxidized form (GSSG), and a subsequent ratio of reduced to oxidized forms of approximately 100:1 (Zitka et al., 2012). The cellular redox status is maintained by reducing GSSG back to GSH by glutathione reductase (GR, EC 1.8.1.7), using NADPH as a reducing agent (Marí et al., 2013). Once the synthesis of GSH occurs, it becomes freely distributed into the endoplasmic reticulum (ER), nucleus, and mitochondria. With regards to mitochondria, GSH is transported into the mitochondrial matrix via the mitochondrial carriers, (dicarboxylate carrier, DIC) and (2-oxoglutarate carrier, OGC) both of which are located in the inner mitochondrial membrane (Figure 18) (Ribas et al., 2014).

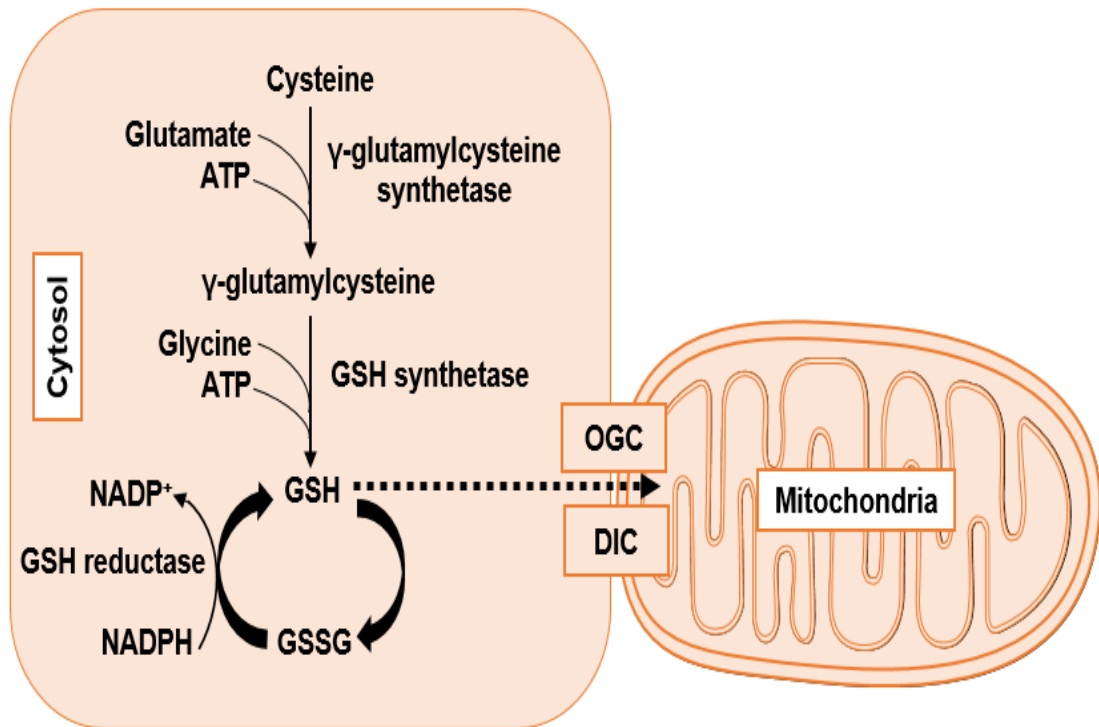


Figure 18 Illustrating the biosynthesis of GSH and its transport to mitochondria

GSH is a key antioxidant among other soluble antioxidants in the brain cells, which is present in a range of 1 to 3 mM (reviewed by Dringen, 2000). Both enzymes involved in glutathione synthesis, GCS and GS, have been found in whole brain to be lower activity, compared to kidney and liver (Sekura and Meister, 1977; Oppenheimer et al., 1979). GSH concentration in astrocytes appears to be higher than neurons both *in vivo* and *in vitro* (Rice, M.; Russo-Menna, 1998). Using cell culture experiments, several reports have shown that an elevation in neuronal GSH concentration occurs following the co-culture of neurons with astrocytes (Bolanos et al., 1996; Stewart et al., 1998; Gegg et al., 2003). Since neuronal GSH content is governed solely by

cysteine availability (Dringen et al, 1999), these increases can therefore be explained as a result of the supply of a cysteine precursor from the astrocytes to the neurons (reviewed by Dringen, 2000). In addition, there is an increasing of evidence demonstrating the ability of astrocytes to provide protection to cultured neurons from ROS induced toxicity (reviewed by Dringen, 2000), even at the level of 1 astrocyte to 20 neurons (Desagher et al., 1996). Furthermore, it has been also shown that neurones cultured alone are more vulnerable to loss of MRC activity upon exposure to nitrogen species, compared to neurones co-cultured with astrocytes (Bolanos et al., 1996). In neurones co-cultured with GSH depleted astrocytes, the GCS activity, which is the rate-limiting enzyme of GSH synthesis, was also found to be increased although there was no increase in cellular GSH levels (Gegg et al., 2005). It is evident therefore that a vital interplay exists between these distinct cell types regarding the protection of neurons from ROS induced damage as well as a dynamic metabolic interaction between them necessary to elicit and enhance GSH biosynthesis. Accumulating evidence suggest that the depletion of GSH is associated with MRC defects (Heales et al., 1995; Merad-Saidoune et al., 1999). The reduction of MRC complex I activity, followed by a depletion in GSH level has been earlier reported (Jha et al., 2000). Additionally, data from our group have recently shown that GSH levels were significantly decreased in skeletal muscle from patients with MRC defects, compared to control subjects (Hargreaves et al., 2005). Furthermore, patients with multiple MRC defects exhibited marked reduction in GSH levels. These findings suggest that oxidative stress and compromised energy status may contribute to the pathophysiology of MRC disorders. In neurodegenerative

disorders, particularly PD, it is believed that GSH depletion could be an early pathological event in PD pathogenesis prior to any significant impairment of MRC complex I and iron homeostasis occurring (Jenner et al., 1992). With regards to the latter, it is uncertain whether this depletion occurs as a result of decreased energy status (required for GSH biosynthesis) or due to elevated ROS levels. Therefore, the replenishment of cellular GSH could hold promise as a therapeutic candidate for patients with mitochondrial disorders.

The GSH ethyl ester (GEE) derivative of GSH has been subcutaneously administered to improve GSH status in rat brain. Nevertheless, the increased level of GSH in brain was only evident post-administration directly to the left cerebral ventricle (Zeevalk et al., 2007). Additionally, following co-administration with the neurotoxin MPP+, GEE has been observed to partially protect DA neurons against the neurotoxic actions of MPP+ (Zeevalk et al., 2007). However, full protection was noted only after pre-treating with GEE. As cysteine is a major component in GSH, it hinders GSH passage to across the blood brain barrier (BBB). Thus, the modified N-acetyl cysteine (NAC) form, has been effectively utilized due to its increased ability to penetrate the BBB (Farr et al., 2003). As such, this thiol antioxidant has also been demonstrated to restore GSH level thereby alleviating the free radicals-induced oxidative damage (Kerksick and Willoughby, 2005). Encouragingly, lesions of dopaminergic tissue have exhibited reduction (30%), following administered with NAC, suggesting that NAC may have neuroprotective properties (Muñoz et al., 2004).

1.11 Oxidative Stress Biomarkers as Indicators for Mitochondria Disorders

Mitochondrial oxidative damage can indiscriminately cause injury to cellular molecules, including DNA, proteins and lipids as well as antioxidant molecules. As mentioned above, mitochondrial oxidative damage has been implicated to be a dominator factor in the development of various inherited conditions as well as more common chronic neurological disorders. Thus, biomarkers of molecular injury induced by oxidative stress, may be clinically useful in the diagnosis of inherited and/or chronic mitochondrial disorders and also help to evaluate the effectiveness of potential therapies for these disorders. The potential oxidative stress biomarkers are summarised in (Figure 19) (Frihoff et al., 2015).

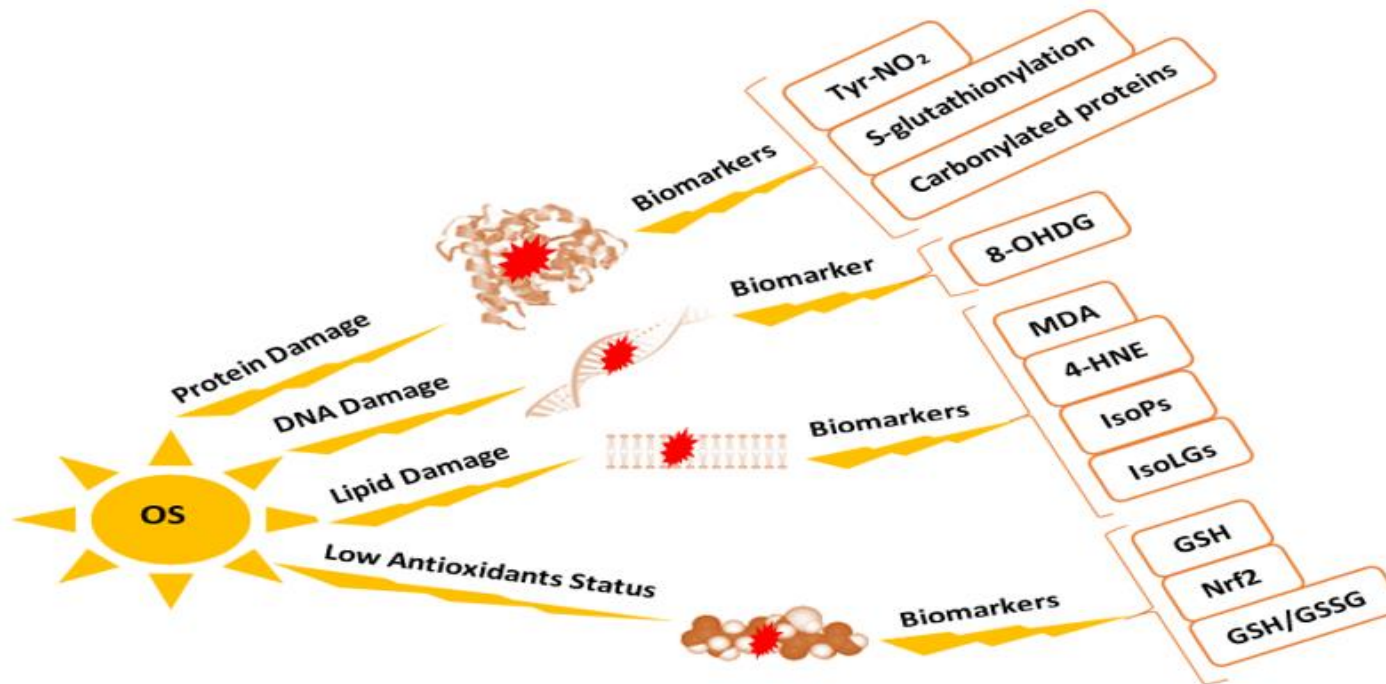


Figure 19 Highlights some of the most common oxidative stress biomarkers for cellular molecules oxidation. Tyr-NO₂, nitrotyrosine; 8-OHDG, 8-hydroxyl-deoxyguanosine; MDA, malondialdehyde; 4-HNE, 4-hydroxy-2-nonenal; IsoPs, isoprostanes; IsoLGs, isolevuglandins; GSH, reduced glutathione; Nrf2, nuclear factor (erythroid-derived 2)-like 2; GSSG, oxidized glutathione.

Aims and the Scope of this Thesis

The overall aim of this thesis was (i) to ascertain the biochemical events that occurs upon persistent loss of MRC complex I activity and its progression to other complexes, in conjunction with bioenergetic, cofactor (CoQ₁₀), and antioxidant (GSH) status. This could ultimately leads to the identification of new pathogenic mechanisms and potentially new therapeutic approaches for common neurodegenerative disorders such as PD.

Given this, an integrated approaches to assess the integrated neuronal mitochondrial function are in demand. As such, an approach in which mitochondrial oxygen consumption can be accurately evaluated using high-resolution respirometry (HHR) using the Oxygraph-2K® (O2k) instrument was developed. **Another aim was therefore (ii)** to develop and evaluate a step-wise titration protocol for the O2k instrument which will enable the assessment of integrated mitochondrial function in cultured neuronal cells under physiological condition. This will serve as an introduction to further studies which will assess mitochondrial dysfunction as well as monitoring treatments.

Furthermore, the fibroblast growth factor-21 (FGF-21) may potentially serve as a sensitive indicator for mitochondrial disorders and thereby prioritise patients for invasive muscle biopsies. **In this thesis, the focus of attention was also (iii)** to validate and evaluate the human FGF-21 sandwich ELISA as a mitochondrial biomarker assay.

CHAPTER 2

Materials and Methods

2.1 Materials

The following were purchased from Sigma Aldrich (Poole, UK):

Triton™ X-100; Trizma® base, ≥99.9%; Bovine serum albumin (BSA), ≥96%; β-Nicotinamide adenine dinucleotide, reduced disodium salt, ~98%; Coenzyme Q1 (CoQ1), ≥95%; Rotenone, ≥95%; Acetyl coenzyme A (Acetyl CoA) sodium salt ≥93%; Oxaloacetic acid ≥97%; 5,5'-Dithiobis(2-nitrobenzoic acid) (DTNB), ≥98%; Antimycin A from *Streptomyces* sp.; Cytochrome c from equine heart ≥95%; Sodium succinate dibasic hexhydrate, ≥99%; Potassium hexacyanoferrate(III), ≥99%; L-Ascorbic acid ≥98%; Carbonyl cyanide 4-(trifluoromethoxy) phenylhydrazone (FCCP) ≥98%; Oligomycin from *Streptomyces diastatochromogenes*, 1-Propanol, ≥99.9%; Sodium perchlorate, ≥ 98%; L-glutathione reduced, ≥98%

The following were purchased from Thermo Fisher Scientific (Paisley, UK):

Trypsin-EDTA (0.25%); Dulbecco's Modified Eagle Medium: Ham's F-12 nutrient mixture (DMEM/F-12) (1:1); L-glutamine; Fetal bovine serum (FBS) heat inactivated; Recovery cell culture freezing medium; Trypan blue (0.4%); Dulbecco's Modified Eagle Medium (DMEM) with low glucose (1g/L); Dimethyl sulfoxide (DMSO); MitoTracker Red CM-H2XRos.

The following were purchased from VWR International Ltd. (Lutterworth, UK):

Di-Potassium hydrogen phosphate, ≥99%; Potassium dihydrogen phosphate, 99.5-100.5%; Magnesium chloride, ≥98%; Potassium cyanide (KCN), ≥96%; Ethanol absolute, ≥99.8%; Ethylenediaminetetraacetic acid dipotassium salt

dehydrate (EDTA K+), ≥97.0%; Methanol, ≥99.8%; N-Hexane, ≥97%; Perchloric acid, 60%; Potassium hydroxide, ≥85%.

Protein Assay Reagents A and B were purchased from Bio-Rad Laboratories Ltd. (Hertfordshire, UK)

Fibroblast Growth Factor 21 ELISA Kit was purchased from 2BScientific Ltd. (Oxfordshire, UK).

2.2 Cell culture

2.2.1 Human SH-SY5Y Neuroblastoma Cell Line

The human SH-SY5Y neuroblastoma cell line was originally obtained by subcloning the SK- N- SH cell line, derived from a four-year-old female diagnosed with thoracic ganglionic tumor (Figure 20) (Biedler et al., 1973). Two distinct phenotypes are derived from the SK- N- SH cell line, including neuroblast-like cells, and epithelial-like cells. The epithelial-like cell are subsequently subcloned into SH-SY, then SH-SY5 and ultimately SH-SY5Y. Cells with epithelial-like characteristics express catecholaminergic neuronal markers, such as tyrosine hydroxylase and dopamine-β-hydroxylase (Ciccarone et al., 1989). Since the early 1980's, the human SH-SY5Y neuroblastoma cell line has been widely utilized as an *in vitro* model for PD studies as this cell line mimics dopaminergic neuronal cell death (reviewed by Yusuf et al., 2003). Furthermore, it is worthy to note that undifferentiated human SH-SY5Y neuroblastoma cells were utilized owing to their ability to survive for long periods of time in comparison to primary dopaminergic

neurons (Sherer et al., 2002; Cheung et al., 2009; Schneider et al., 2011). For instance, SH-SY5Y cells can be cultured for at least one month in the presence of the MRC complex inhibitor, rotenone at 5 nM (Sherer et al., 2002). Therefore, SH-SY5Y cells provide an experimental model for studying neurotoxicity along with a number of events implicated in the pathophysiology of PD.

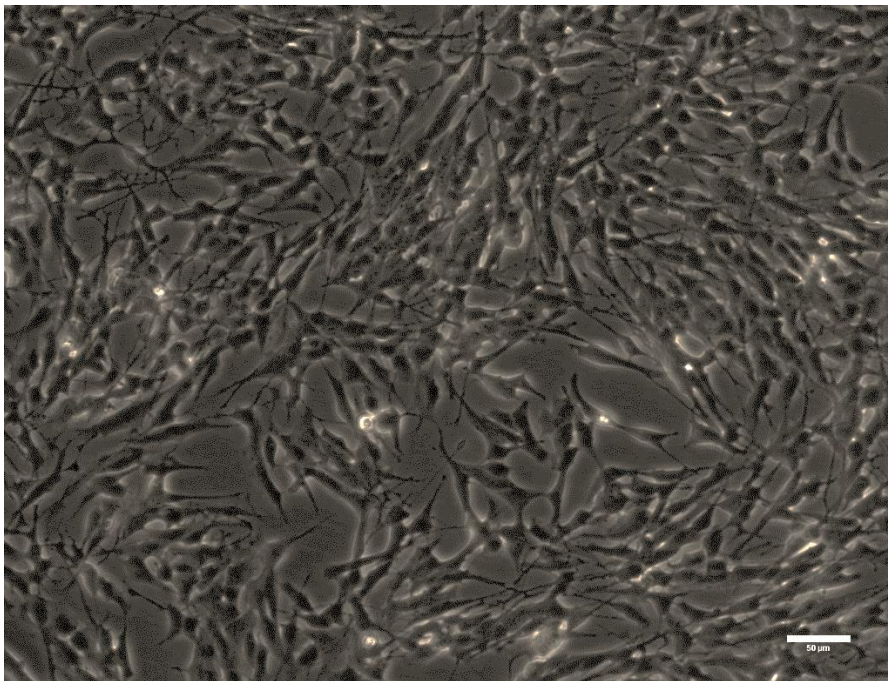


Figure 20 Microscope image of control human SH-SY5Y cells captured at 20x magnification using Olympus IX71 inverted microscope (Olympus Ltd., London, UK); scale bar: 50 μm .

2.2.2 SH-SY5Y Cell Storage and Recovery

The SH-SY5Y cell line was purchased from Sigma Aldrich (Poole, UK), and cultured and stored in accordance with the European Collection of Cell Cultures' guidelines. (Health Protection Agency, Salisbury, UK). Upon initial thawing, they were seeded at a density 1×10^4 cells/cm² in 75 cm² tissue culture flasks with a pre-warmed 1:1 mixture of Dulbecco's modified Eagle's

Medium /Ham's F-12 nutrient supplemented with 10% heat-inactivated fetal bovine serum (FBS), and 2.0 mM L-glutamine solution. Feeder cells were then grown at +37°C in 5% CO₂ and 95% air atmosphere. After 24 hours, cells were re-fed with fresh culture medium. Once cells reached the degree of confluency (80-90%), culture media was discarded and the flask washed once with Dulbecco's Phosphate Buffered Saline (DPBS) without CaCl₂ and MgCl₂. 2.0 ml of 0.25% trypsin-EDTA solution was pipetted onto the adherent cells, incubated for two minutes at 37°C and then diluted by adding 8.0 ml of fresh culture media. The supernatant was collected and centrifuged for 5 min at 500x g. The cell suspension was discarded and the cell pellet was re-suspended with freezing medium (Recovery™ Cell Culture Freezing Medium). Cells were then counted automatically by mixing 100 µl of cell suspension with 100 µl of trypan blue using a Countess Automated Cell Counter (Invitrogen Ltd). The remaining cell suspension was pipetted in 1ml aliquots in labelled cryogenic vials. Cells were stored in a freezing container (Nalgene® Mr. Frosty) at -80°C overnight and then re-located to a liquid nitrogen container for a long term storage.

2.2.3 SH-SY5Y Cell Thawing and Passaging

Cryogenic vials were removed from liquid nitrogen and thawed rapidly in a water bath at 37°C until small ice crystals dissolved. Cells were then seeded at a density 1×10^4 cells/cm² in 75 cm² tissue culture flasks in a pre-warmed 1:1 mixture of Dulbecco's modified Eagle's Medium /Ham's F-12 nutrient supplemented with 10% heat-inactivated fetal bovine serum (FBS), and 2.0 mM L-glutamine solution. Once cells reached the degree of confluency (80-90%), the culture media was discarded and the flask washed once with

Dulbecco's Phosphate Buffered Saline (DPBS) without CaCl_2 and MgCl_2 . 2.0 ml of 0.25% trypsin-EDTA solution was pipetted onto the adherent cells, incubated for two minutes at 37°C and then diluted by adding 8.0 ml of fresh culture medium. The cell suspension was collected and centrifuged for 5 minutes at $500\times g$. The supernatant was discarded and the cell pellet was re-suspended with fresh culture media. Cells were then counted by mixing 100 μl of cell suspension with 100 μl of trypan blue using a Countess Automated Cell Counter (Invitrogen Ltd). For experiments, cells of passage numbers between 20 and 24 were utilized to ensure the consistency of results.

2.2.4 SH-SY5Y Cell Harvesting for Biochemical Assays

To harvest cells for biochemical experiments, cells were firstly washed by Dulbecco's Phosphate Buffered Saline (DPBS) without CaCl_2 and MgCl_2 . They were then harvested by trypsinization, and centrifugation as described in the previous section. The supernatant was discarded and the cell pellet was re-suspended with DPBS without CaCl_2 and MgCl_2 . The resulting cell suspension then was pipetted into appropriately labelled eppendorf tubes, as shown in (Figure 21).

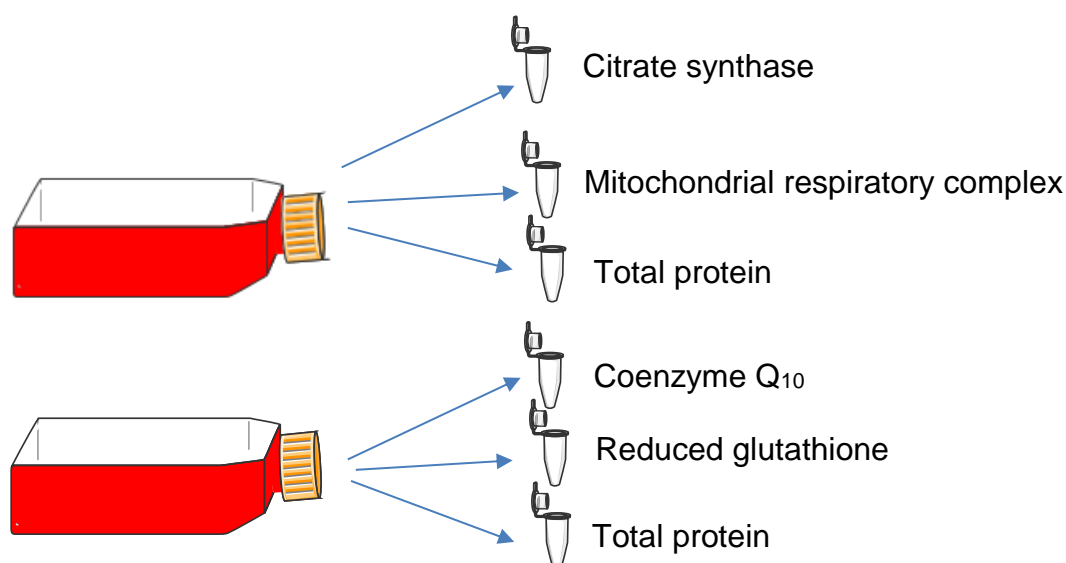


Figure 21 A schematic illustration of the preparation of SH-SY5Y cells for biochemical assays

2.2.5 Cell treatments

Stock solutions of rotenone, 100 μM was prepared in absolute ethanol, filter sterilized ($0.2 \mu\text{m}$) and stored at -20C until analysis. Cells were passaged and seeded at a density 1×10^4 cells/ cm^2 into 75 cm^2 tissue culture flasks or 6-well cell culture plates as described in (Section 2.2.3). Once cells reached the degree of confluency (80-90%), they were exposed to rotenone or absolute ethanol (vehicle control) contained in culture media for 24 and 48 hrs. A final concentration of 100 nM rotenone was chosen as pharmacological cell model based on previous studies (Sherer et al., 2003). Furthermore, our preliminary findings indicated that rotenone-treated SHSY5Y cell induced a partial (approximately 30%) reduction in MRC complex I activity after 24 hr incubation, which closely mimics the most sporadic PD cases with an approximately 15-30 % inhibition of MRC complex I (Figure 22) (Benecke et

al., 1993; Bindoff et al., 1991). Notably, the 30% inhibition of complex in rotenone-treated SHSY5Y cell had no compromised effects on cellular ATP levels. The final concentration of absolute ethanol of 0.01%, used as vehicle control, showed no effect on cell viability or any other biochemical measurement made.

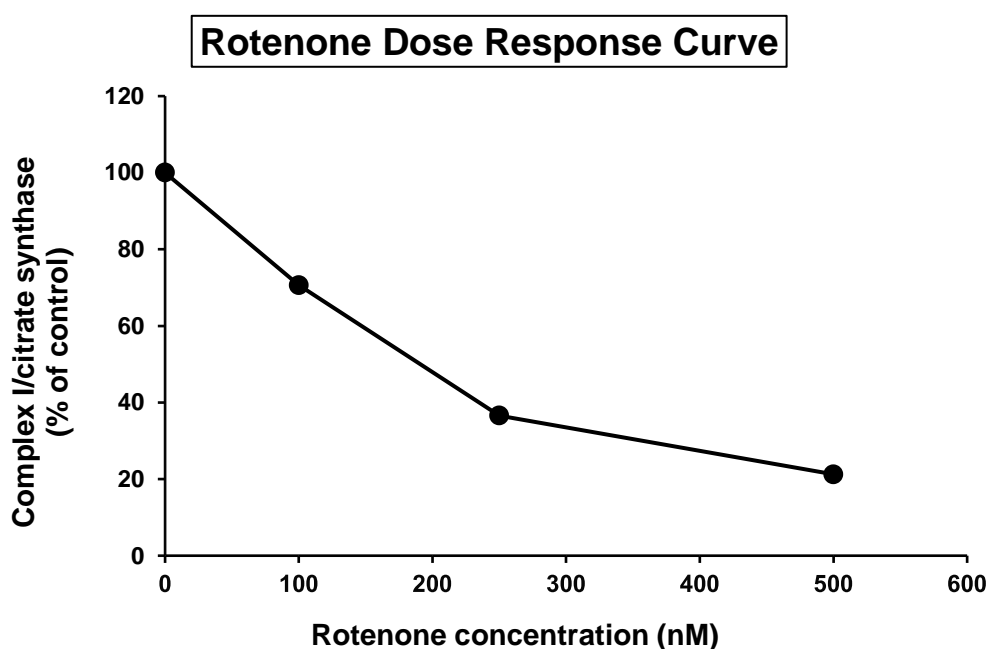


Figure 22 Dose response reduction of MRC complex I activity by rotenone. SH-SY5Y cells were exposed to 100 nM, 250 nM, and 500 nM of rotenone for 24 hr. MRC Complex I activity was determined as described in section and expressed as % activity of untreated control.

2.4 Total Protein Determination

Total protein concentration was determined according to the method of Lowry (Lowry et al., 1951). This method is primarily based on an initial Biuret reaction whereby proteins reduce copper ions (Cu^{2+} to Cu^{+}) under alkaline

conditions, followed by the reduction of Folin reagent reagent (comprised of phosphomolybdate and phosphotungstate). These reactions result in the formation of a characteristic blue colour which can be monitored spectrophotometrically at 750 nm. Briefly, all samples were appropriately diluted in Milli-Q water. Bovine serum albumin (BSA) was serially diluted in Milli Q water to obtain a 6-point standard curve, ranging from 0 to 200 μ l. To each sample and standard, 100 μ L of reagent A (alkaline copper tartrate) and 800 μ L reagent B (Folin-Ciocalteau phenol) was added. Subsequently, samples and standards were vortexed and incubated in the dark for 25 min at room temperature.

After the incubation, the absorbance of each sample and standard was measured using a spectrophotometer at 750 nm. To determine the total protein concentration in unknown samples, a standard curve was created by plotting absorbance of the standards against the respective BSA concentration and a line of best fit applied (Figure 23).

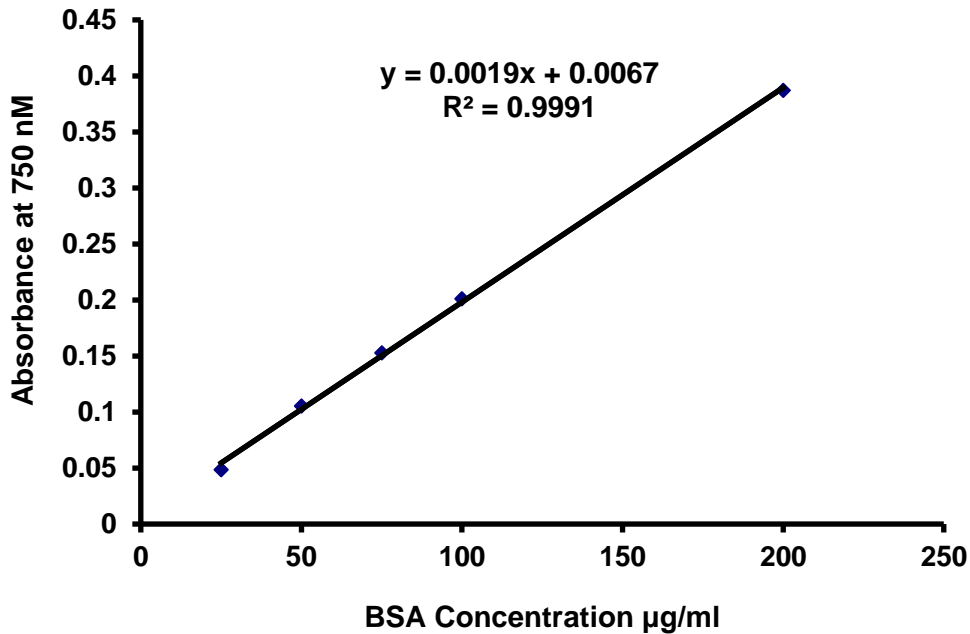


Figure 23 A typical standard curve for the Lowry assay showing the plot of BSA standard protein concentration against absorbance at 750nm.

2.5 Mitochondrial Enzymatic Assays

2.5.1 Background

A UV/Visible spectrophotometer is an instrument widely used to measure the amount of light (light intensity) absorbed by a sample at a certain wavelength. According to the Beer-Lambert law, the amount of light absorbed by a sample is directly proportional to the sample concentration. Briefly, a beam of light obtained from a light source is passed through monochromator, allowing the selection of a desirable wavelength. Subsequently, the light beam passes through the sample holder (cuvette) where a certain amount of light is absorbed by the sample. The remaining light passes out of the cuvette, where it is in turn detected by a photocell detector. The output signal obtained from

the detector is amplified and digitally displayed on the readout (Upstone, 2013). The basic components of a spectrophotometer are shown in the simple diagram in (Figure 24).

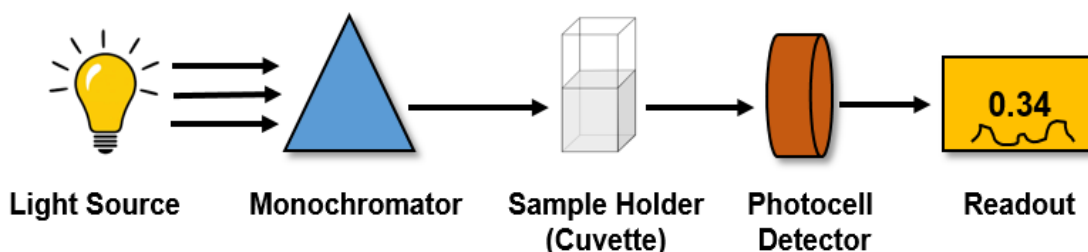


Figure 24 A simple diagram showing the basic components of a UV/Visible spectrophotometer instrument.

2.5.2 Analytical Equipment

All mitochondrial respiratory complexes (I-IV) assays as well as citrate synthase assay were carried out using an Uvikon 941 Plus spectrophotometer (Northstar Scientific, Potton, UK).

2.5.3 Analytical Procedure

All mitochondrial respiratory complexes (I-IV) assays as well as citrate synthase assay were determined at 30°C. In order to disrupt mitochondrial membranes and to ensure that substrates can easily gain access to an enzyme's active site, all sample homogenates were exposed to two freeze-thaw cycles prior to assay.

2.5.3.1 MRC Complex I [EC 1.6.5.3]

The activity of mitochondrial respiratory complex I (also known as NADH: ubiquinone oxidoreductase, NADH-CoQ reductase, or NADH dehydrogenase)

was described previously by (Ragan et al., 1987). The complex I activity relies on measuring electron shuttled from NADH to ubiquinone (CoQ₁). As the result of NADH reduction, the absorbance is determined at 340 nm in the presence or absence of the potent complex I inhibitor (Rotenone) which functionally blocks the electron transfer from NADH to CoQ₁ (Figure 25). Thus, the sensitivity to rotenone decrease in NADH was utilized to measure complex I activity.

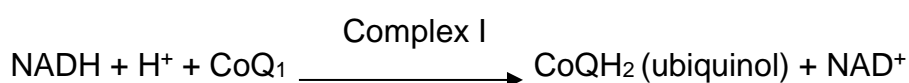


Figure 25 The reaction of MRC complex I activity. The oxidation of NADH is catalysed by complex I where electrons pass onto to ubiquinone (CoQ₁), which is then reduced to CoQH₂. Thus, Complex I activity can be measured spectrophotometrically at 340 nm as the rotenone-sensitive decrease in NADH.

Two identical cuvettes were filled with a final concentration of 2.5 mg/ml of Bovine serum albumin (BSA), 0.15 mM Nicotinamide adenine dinucleotide (NADH), 1mM potassium cyanide (KCN), 8 mM magnesium chloride in 20 mM potassium phosphate buffer (pH 7.2). 20 µl of sample was then added to each cuvette to bring the final volume of in the cuvette to 1 ml. After gently mixing, the cuvette contents were left for couple minutes to worm up at 30°C in the spectrophotometer. The reaction was initiated by the addition of 10 µl of (5mM) ubiquinone into each sample cuvette. After 5 min, 20 µl of (1mM) rotenone was added to each sample cuvette for a further 5 min measurement. The absorbance of each sample reaction was determined by subtracting the difference in absorbance before and after adding rotenone. The Beer-

Lambert law was utilized to obtain the concentration for each sample using the following equation:

$$A = \epsilon l c \quad (1)$$

By arranging the above equation (1), yielding the expression of concentration

$$c = \Delta A / \epsilon l \quad (2)$$

Where (ΔA) is the specific differences in absorbance, (ϵ) is the extinction coefficient of NADH ($6.81 \times 10^3 \text{ M}^{-1} \text{ cm}^{-1}$), (l) the length of the light path (1cm) and (c) represents the concentration of sample (mole/ml). All obtained results were expressed as a ratio to CS to compensate for mitochondrial enrichment in the tissue or cell samples. To further validate the assay, the linearity of MRC complex I activity was determined at various known protein content as shown in (Figure 26).

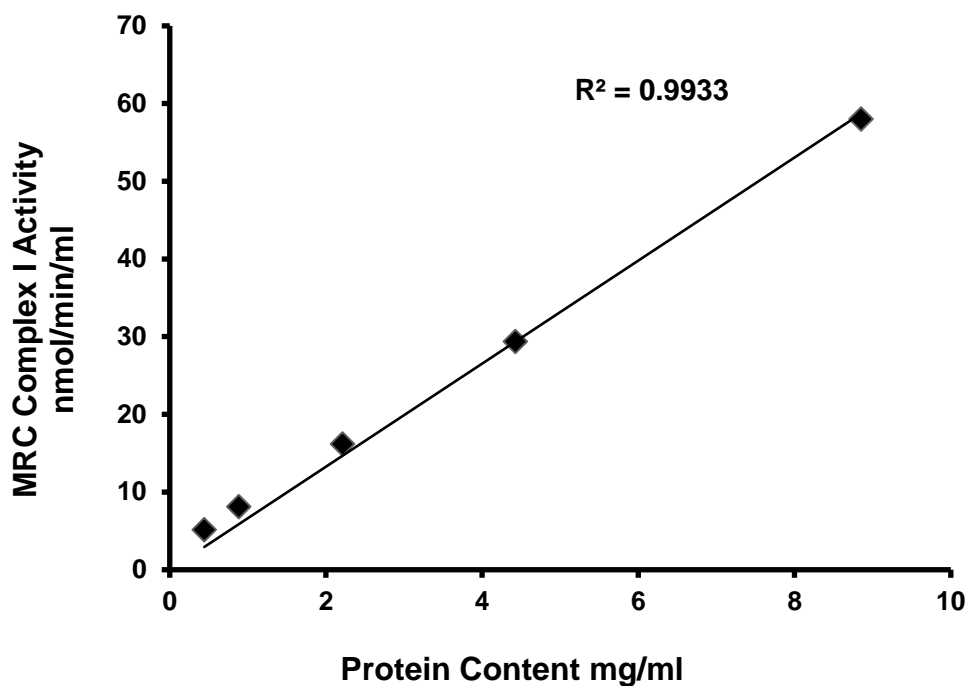


Figure 26 The standard curve of the MRC complex I activity (nmol/min/ml) plots against protein content (mg/ml). By serial dilution of a homogenized SH-SY5Y sample, containing known protein content, the MRC complex I activity appeared to be highly linear ($r^2=0.9933$) ranging from (0.5–9 mg/ml) of protein content.

2.5.3.2 MRC Complex II [EC 1.3.5.1]

The activity of mitochondrial respiratory complex II (also referred to as succinate dehydrogenase or succinate-CoQ reductase) was analyzed based on the method of (Birch-Machin et al., 1994). In complex II, the reduction of fumarate to succinate delivers further electrons to CoQ₁, which is in turn is reduced to CoQH₂. Subsequently, 2,6-dichlorophenolindophenol (DCPIP) is reduced by CoQH₂. The complex II activity is assayed as succinate-dependent 2-thenoyltrifluoroacetone (TTFA) sensitive decrease in DCPIP at

600 nm (Figure 27). TTFA is a potent CoQ₁ analogue inhibitor which prevents CoQ₁ bound to the quinone-binding site at complex II.

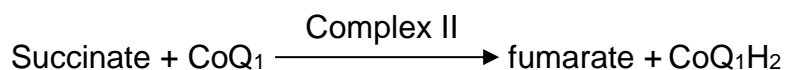


Figure 27 The reaction of MRC complex II activity. The oxidation of succinate to fumarate reaction is catalysed by complex II followed by the reduction of CoQ₁ to CoQH₂. The complex II activity is measured as a succinate-TTFA sensitive reduction in DCPIP at 600 nm.

Two identical cuvettes were filled with a final concentration of 1mM of potassium cyanide (KCN), 100 µM of ethylene diamine tetra acetic acid dipotassium salt (EDTA), 120 µM of 2,6-dichlorophenolindophenol (DCPIP), 20 mM of succinate, 10 µM of rotenone, and 1mM of thenoyltrifluoroacetone (TTFA) (only for reference cuvettes) in a 100 mM potassium phosphate buffer (pH 7.4), followed by 320, and 330 µl of distilled water into the sample and reference cuvettes respectively. 20 µl of sample was then added to each cuvette to bring the final volume of cuvette to 1 ml. After gently mixing, the cuvette contents were left for couple minutes to worm up at 30°C in the spectrophotometer. The reaction was initiated by the addition of 10 µl of (5mM) into the sample cuvette. After 6 min, 10 µl of (1mM) TTFA was added into the sample cuvettes and the absorbance followed for a further 7 min. The absorbance of each sample was determined by subtracting the difference in absorbance prior to and after adding TTFA. The rearrangement of Beer-Lambert law was utilized to obtain the concentration for each sample as described in (Equation 2; Section 2.5.3.1). The extinction coefficient of reduced DCPIP is (19.1x 10³ M⁻¹ cm⁻¹). All obtained results were expressed

as a ratio to CS to compensate for mitochondrial enrichment in the tissue or cell samples. To further validate the assay, the linearity of MRC complex II activity was determined at various known protein content as shown in (Figure 28).

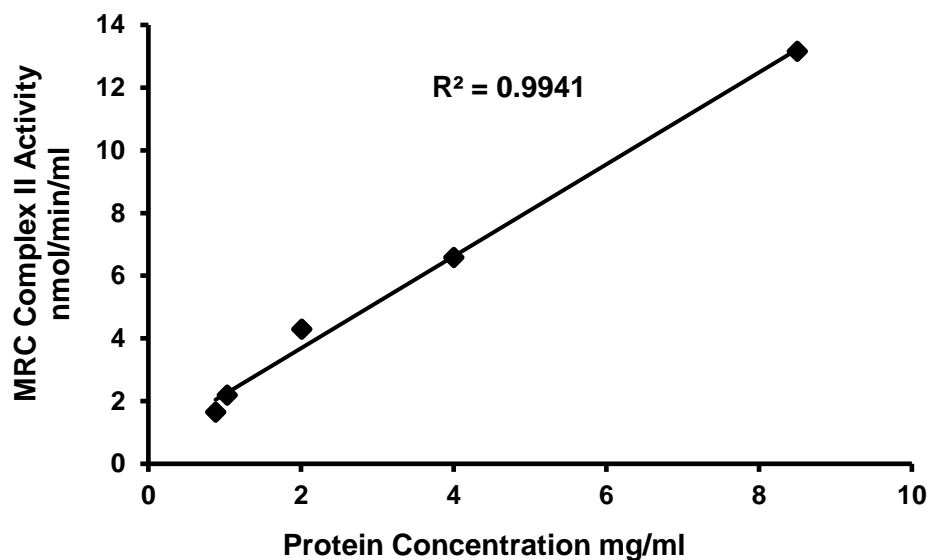


Figure 28 The standard curve of the MRC complex II activity (nmol/min/ml) plots against protein content (mg/ml). By serial dilution of a homogenized SH-SY5Y sample, containing known protein content, the MRC complex II activity appeared to be linear ($r^2=0.9941$) ranging from (1.0–8.5 mg/ml) of protein content.

2.5.3.3 MRC Complex II-III

The activity of mitochondrial respiratory complex II-III (Succinate dehydrogenase cytochrome *c* reductase) was performed according to the method of (King, 1967). This assay measures the transfer electrons during the oxidation of succinate, catalyzed by succinate-CoQ reductase (complex II) through CoQ₁₀ to complex III (also called cytochrome *bc1* complex, or CoQH₂-cytochrome *c* reductase). The reduction of cytochrome *c* (cyt *c*) is subsequently catalyzed by complex III. Therefore, the complex II-III activity is assayed as succinate-dependent antimycin A (AA) sensitive reduction of cyt *c* at 550nm (Figure 29). AA is a potent inhibitor, which acts to block electron transfer from cytochrome *b* (cyt *b*) to cyt *c* at complex III as the result of it improperly binding to the CoQ cycle.

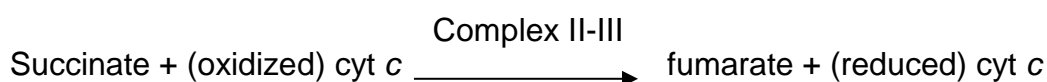


Figure 29 The reaction of MRC complex II-III activity. The electrons release from the oxidation of succinate to fumarate, catalysed by complex II, results in the electrons shuttling from CoQH₂ to reduce cyt *c* catalysed by complex III. Thus, Complex II-III activity can be measured spectrophotometrically at 550 nm as a succinate-dependent AA sensitive reduction of cyt *c*.

two identical cuvettes were filled with a final concentration of 1mM potassium cyanide (KCN), 300 μ M ethylene diamine tetra acetic acid dipotassium salt (EDTA), 100 μ M cyt *c* in a 166 mM potassium phosphate buffer (pH 7.4), followed by 185, 225 μ l of Milli-Q water into sample and reference cuvettes respectively. 20 μ l of sample was then added to each cuvette to bring the final

volume in the cuvette to 1 ml. After gently mixing, the cuvette contents were left for couple minutes to warm up at 30°C in spectrophotometer. The reaction was initiated by the addition of 40 µl of (0.5M) succinate was added into sample cuvettes. After 5 min, 10 µl of (1mM) AA to the sample cuvettes and the absorbance monitored for a further 5 min. The absorbance for each sample was determined by subtracting the difference in absorbance before and after adding AA. The rearrangement of Beer- Lambert law was utilized to obtain the concentration for each sample as described (Equation 2; Section 2.5.3.1). The extinction coefficient of reduced reduced is *cyt c* ($19.2 \times 10^3 \text{ M}^{-1} \text{ cm}^{-1}$). All obtained results were expressed as a ratio to CS to compensate for mitochondrial enrichment in the tissue or cell samples. To further validate the assay, the linearity of MRC complex II-III activity was determined at various known protein content as shown in (Figure 30).

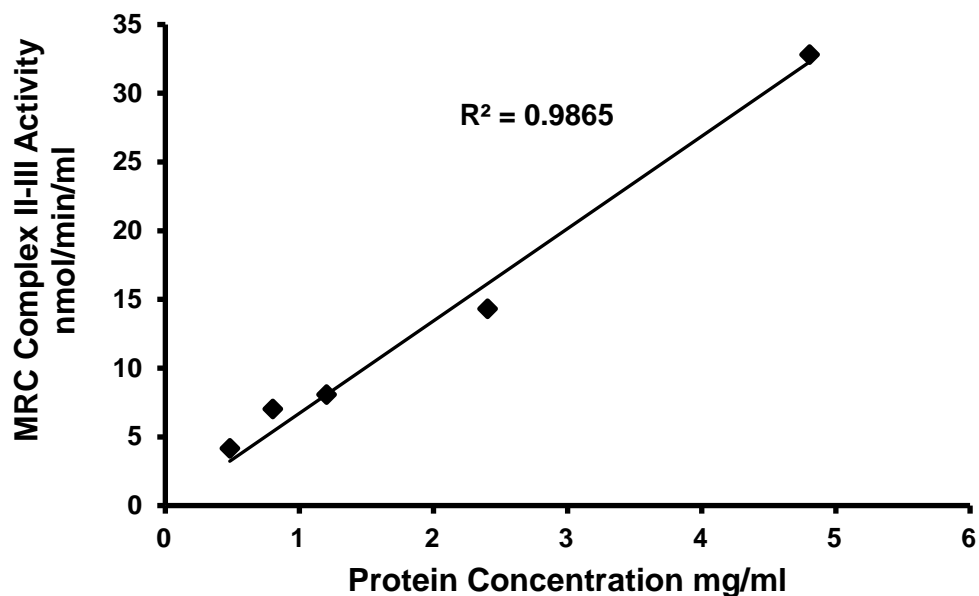


Figure 30 The standard curve of the MRC complex II-III activity (nmol/min/ml) plots against protein concentration (mg/ml). By serial dilution of a homogenized SH-SY5Y sample, containing known protein concentration, the MRC complex I activity appeared to be linear ($r^2=0.9865$) ranging from (0.5–4.8 mg/ml) of protein content.

2.5.3.4 MRC Complex IV [EC 1.9.3.1]

The activity of mitochondrial respiratory complex IV (cytochrome *c* oxidase) is the last terminal enzyme complex in the respiratory chain series in which electrons from the oxidation of reduced cyt *c* is shuttled to an oxygen (O_2) molecule to generate two molecules of water (H_2O). The activity of complex IV was analyzed according to the method of (Wharton and Tzagoloff, 1967) method by following the oxidation of reduced cyt *c* at 550 nm (Figure 31).

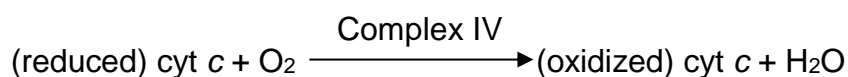


Figure 31 The reaction of MRC complex IV. Along with H₂O production, cytochrome c oxidase catalyzes the oxidation of reduced cyt c in a reaction, which is monitored spectrophotometrically at 550 nm.

Prior to the assay, the oxidized form of cyt c was initially reduced by adding a few crystals of vitamin C in Milli-Q water, and noting the colour of the solution subsequently turning from a dark red to a pale pink colour. To remove excess vitamin C from the reduced cyt c preparation, a PD-10 desalting gel filtration column, equilibrated within 0.01 M of potassium phosphate buffer (pH 7.0), was utilized to separate the reduced cyt c from vitamin C. In order to obtain the concentration of the reduced cyt c, 950 µl of Milli-Q water and 50 µl of prepared reduced cyt c were added to identical cuvettes (labelled as sample and reference). After gently mixing, the spectrophotometer was adjusted to autozero against the reference cuvette at 550nm. The absorbance of reduced cyt c was then measured after 10 µl of ferricyanide was dispensed into reference cuvette. The concentration of reduced cyt c (mole/ml) was determined, according to the arrangement of the Beer Lambert law as described (Equation 2; Section 2.5.3.1).

To perform the assay, two identical cuvettes were filled with a final concentration of 50 µM of reduced cyt c in 0.01 M of potassium phosphate buffer (pH 7.0). 10 µl of ferricyanide was then dispensed into the reference cuvette. Once 20 µl of sample was added into sample cuvettes, the absorbance of the sample was recorded at 1 min intervals for 3 min. Unlike the activity of complex I, II, and II-III whose activities are defined as an initial rate, the activity of complex VI, however, is defined as a first-order rate

constant (k), thus all obtained results were expressed as (k/ml) once divided by CS activity. To further validate the assay, the linearity of MRC complex IV activity was determined at various known protein content as shown in (Figure 32).

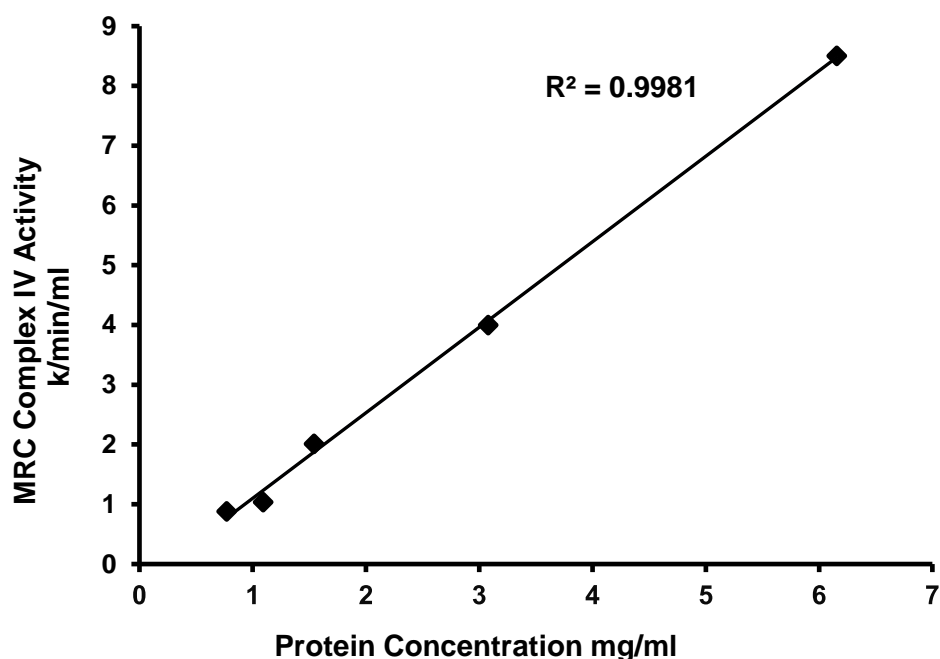


Figure 32 The standard curve of the MRC complex IV activity ($k/min/ml$) plots against protein content (mg/ml). By serial dilution of a homogenized SH-SY5Y sample, containing known protein content, the MRC complex IV activity appeared to be linear ($r^2=0.9981$) ranging from (8.5–6.0 mg/ml) of protein content.

2.5.3.5 Citrate Synthase [EC 2.3.3.1]

Citrate synthase (CS) is the first enzymatic step in the tricarboxylic acid cycle (TCA cycle) which catalyses the condensation of oxaloacetate (OAA) and acetyl coenzyme A (acetyl CoA) in a reaction to form citric acid. Since it is

located in mitochondrial matrix, it has been utilized as a matrix enzyme marker as well as a marker for mitochondrial-enrichment. The activity of citrate synthase is assayed by the reaction of free sulfhydryl group (CoA•SH) with 5,5-dithio-bis-(2-nitrobenzoic acid) (DTNB) and can be monitored spectrophotometrically at 412 nm (Figure 33).

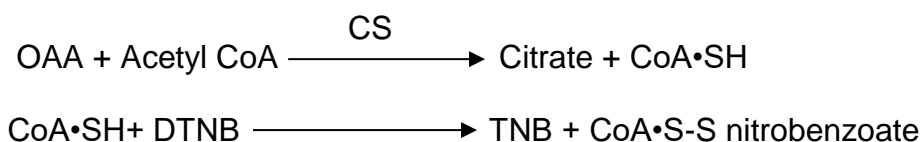


Figure 33 The reaction of CS activity. The production of CoA•SH as result of the reaction between acetyl CoA and OAA, catalysed by CS reacts with TNB to yield a yellow colour. This colour development can be monitored spectrophotometrically at 412 nm.

As performed previously by (Shepherd and Garland, 1969), two identical cuvettes were filled with a final concentration of 100 µM acetyl-coenzyme A (acetyl CoA), 200 µM 5,5-dithio-bis-(2-nitrobenzoic acid) (DTNB) in 100mM Tris–HCl buffer (pH 8.0) containing 0.1% (v/v) Triton X-100. 20 µl of sample was then added to each cuvette to bring the final volume in the cuvette to 1 ml. After gently mixing, the cuvette contents were left for couple minutes to warm up at 30°C in spectrophotometer. The reaction was initiated by the addition of 10 µl of (20 mM) of oxaloacetate to each sample cuvette. The rearrangement of the Beer- Lambert law was utilized to obtain the concentration for each sample as described in (Equation 2; Section 2.5.3.1). The extinction coefficient of DNTB is (13.6 x 10³ M⁻¹ cm⁻¹). All obtained results were expressed as (nmol/min/mg protein). To further validate the assay, the

linearity of CS activity was determined at various known protein content as shown in (Figure 34).

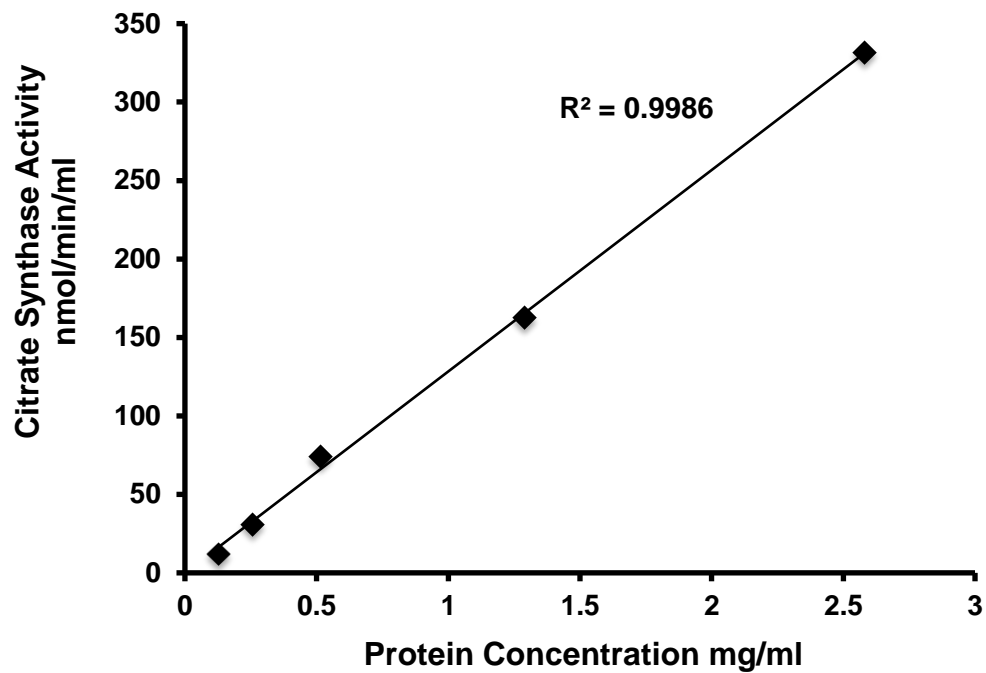


Figure 34 The standard curve of CS activity (nmol/min/ml) plots against protein content (mg/ml). By serial dilution of a homogenized SH-SY5Y sample, containing known protein content, CS activity appeared to be highly linear ($r^2=0.9986$) ranging from (0–2.5 mg/ml) of protein content.

2.6 High Performance Liquid Chromatography (HPLC)

2.6.1 Background

Chromatography is an analytical chemistry technique which is commonly used to separate mixtures of analytes in samples into their individual components based on their physiochemical properties. This is carried out by involving a mobile phase (gas or liquid) and stationary phase (solid or liquid) in which the mobile phase containing the analyte mixture passes down through the stationary phase at different speeds due to the interaction of sample components with the stationary phase (Bird, 1989).

High performance liquid chromatography (HPLC) has commonly become the most powerful liquid chromatography technique over the years. The main components of a HPLC system are shown in the simple diagram in (Figure 35). HPLC is primarily based on the principle of analyte interaction with the stationary phase at high pressure as it is pumped in a liquid solvent (mobile phase) containing a mixture of analyte sample through a column filled with silica-gel particles, generally containing a covalently attached functional group (stationary phase) (Skoog et al., 1998). Consequently, HPLC is also referred as high pressure liquid chromatography. Depending upon the interaction of the sample components with stationary phase, the analyte sample is then separated and detected as each analyte elutes from the column at different characteristic retention times. Furthermore, specific identification of each analyte can be confirmed by various detection methods, including electrochemical (EC), ultraviolet (UV) and fluorescence (FL) detectors, the

signals from which can be integrated to allow quantitation (Zhong and Hee, 2007).

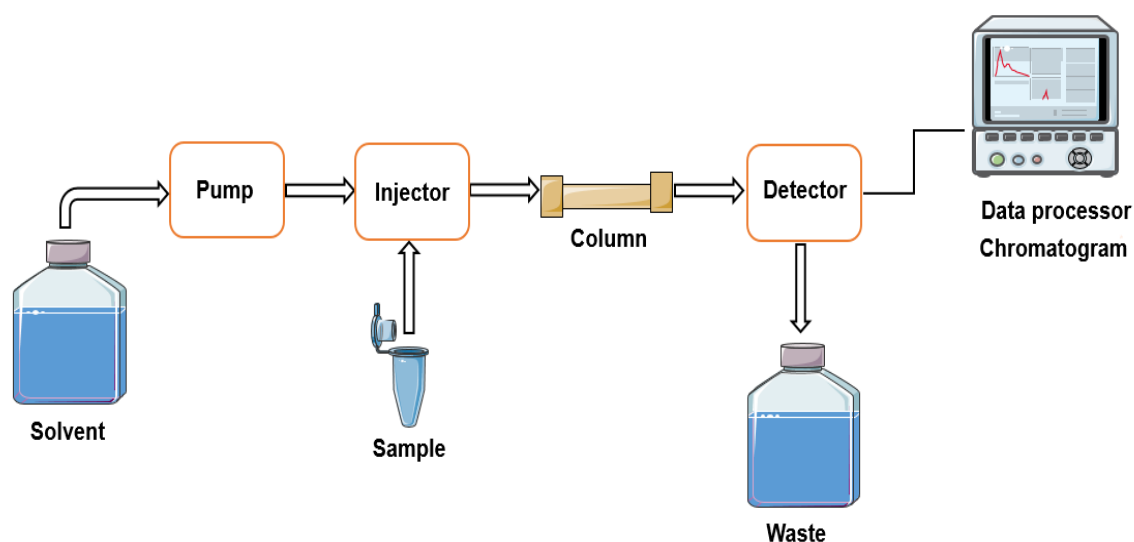


Figure 35 A simple diagram showing the basic components of a HPLC system

2.6.2 Measurement of Cellular Energy Charge (EC)

Analysis of adenine nucleotides by HPLC coupled to fluorescence detection provides a highly sensitive method capable of simultaneously detecting and quantitating levels of ATP, ADP and AMP in the nmole to pmole range (Bhatt et al., 2012). Furthermore, as well as its enhanced detection limits, fluorescence has the distinct advantage over UV detection in that it can provide a higher level of specificity of detection by utilizing specific excitation and emission maxima of the chromophores being analysed. Nevertheless, UV absorption at 254 nm has been commonly used for the detection of adenine nucleotides (Contreras-Sanz et al., 2012).

Since adenine nucleotides do not exhibit any natural auto-fluorescence, they must first be derivatized prior to HPLC separation and detection. To accomplish this, the adenine ring structure can be modified using chloroacetaldehyde to form a link between the 1st nitrogen of the purine ring and the amino group nitrogen on the 6th carbon of the purine ring to result in the formation of highly fluorescent N⁶-etheno derivatives (Figure 36) (Bhatt et al., 2012).

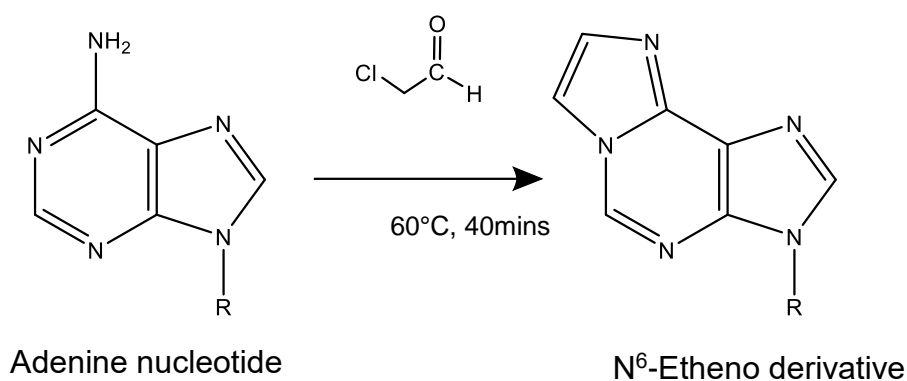


Figure 36 The reaction of chloroacetaldehyde with adenine forming N⁶-etheno derivatives.

Nevertheless, care must be taken during the derivatization procedure due to the labile nature of the high energy phosphate links in adenine nucleotides, as if not controlled carefully, can lead to various degrees of hydrolysis of the adenine nucleotides and thereby result in an under estimation of their true content (Kawamoto et al., 1998). With the ability to accurately measure cellular levels of ATP, ADP and AMP, the adenylate energy charge (AEC), also known as energy charge (EC) of the cell can be readily estimated, according to the following equation, proposed by (Atkinson, 1968):

$$\text{AEC} = \frac{[\text{ATP}] + 0.5[\text{ADP}]}{[\text{ATP}] + [\text{ADP}] + [\text{AMP}]}$$

Thus, the AEC is a tightly regulated process in living cells and is preserved within a relatively narrow ranges of 0.8 -0.9. This subsequently reflects a higher cellular level of ATP relative to ADP and AMP and a hence an energetically favourable state.

2.6.2.1 Analytical Equipment

HPLC determination of etheno-adenine nucleotides was carried out using the following equipment: PU-1580 intelligent pumps (Jasco); AS-950 intelligent autosampler (Jasco); DG-1580-53 in-line mobile phase degasser (Jasco); EZChrome Elite data capture and analysis software (Jasco); FP-920 Intelligent Fluorescence Detector (Jasco).

2.6.2.2 Analytical Procedure

Etheno-adenine nucleotides were determined using a C18 reverse phase HPLC analysis coupled to fluorescence detection at excitation/emission spectra pairs of 290/415 nm. This determination was performed according to the pervious method of (Bhatt et al., 2012) and recently developed and validated by Dr. Michael Orford and Dr. Simon Eaton.

At flow rate of 0.8mL/min, the separation was achieved using a C18 reversed phase column (Techsphere ODS 4.6 × 150 mm, 3 μm, 100 Å) (HPLC Technology, Welwyn Garden City, UK) maintained at room temperature with two mobile phase buffers: buffer A (0.2 M KH₂PO₄, pH 5.0), and buffer B (0.2 M KH₂PO₄/ 10% acetonitrile , pH 5.0). Each analyte was eluted off the column with a linear gradient from 0% buffer B to 100 % buffer B over 31 min, followed by an additional increase in buffer B to 100 % over a further 5 min as described by the following (Table 4):

Table 4 HPLC mobile phase buffers (A and B) gradient profile utilized for the elution of adenine nucleotides from the HPLC column

Time (min)	Buffer A (%)	Buffer B (%)
0	100	0
31	0	100
36	0	100
37	100	0

2.6.2.3 Cell treatment and Extraction

SH-SY5Y Cells were seeded in a 6-well cell culture plates at density (1×10^4 cells/cm²) as described in (Section 2.2.3) and were treated with rotenone for 24 and 48 hrs after reaching confluence as described in (Section 2.2.5). Upon completion of the rotenone treatment, culture medium was discarded and the 6-well cell culture plates were washed once with 1 ml of DPBS. To extract the adenine nucleotides from the cells, 0.5 ml ice cold 1.0 M perchloric acid was pipetted into each well, followed by scraping off the adherent cells. In new Eppendorf tubes, 250µl of the scraped cells was neutralized with 200µl 0.5M KHCO₃ in 1M KOH. The precipitated proteins and potassium perchlorate produced were removed by centrifugation at 13.000x g for 5 min and the clear supernatants collected into new Eppendorf tube and stored at -20°C until derivatization.

2.6.2.4 Adenine Nucleotides Derivatization

100 µl of 1.0 M sodium acetate (pH 4.5) and freshly prepared of 20 µl of 4M chloroacetaldehyde were mixed with glass vials containing 100 µl of cell-extracted adenine nucleotides. The glass vials were vortexed and then heated at 60°C for 40 min. After the incubation, the glass vials were directly placed on

ice for 5 min to cool and halt the reaction. Subsequently, 20 μ l of the cooled derivatized sample was then injected for HPLC analysis.

2.6.2.5 Data Analysis

Data were captured and analyzed using EZChrome Elite software. Peaks corresponding to the retention times for ATP, ADP and AMP were integrated and peak areas obtained (Figure 37) were used to calculate AEC using the equation described above.

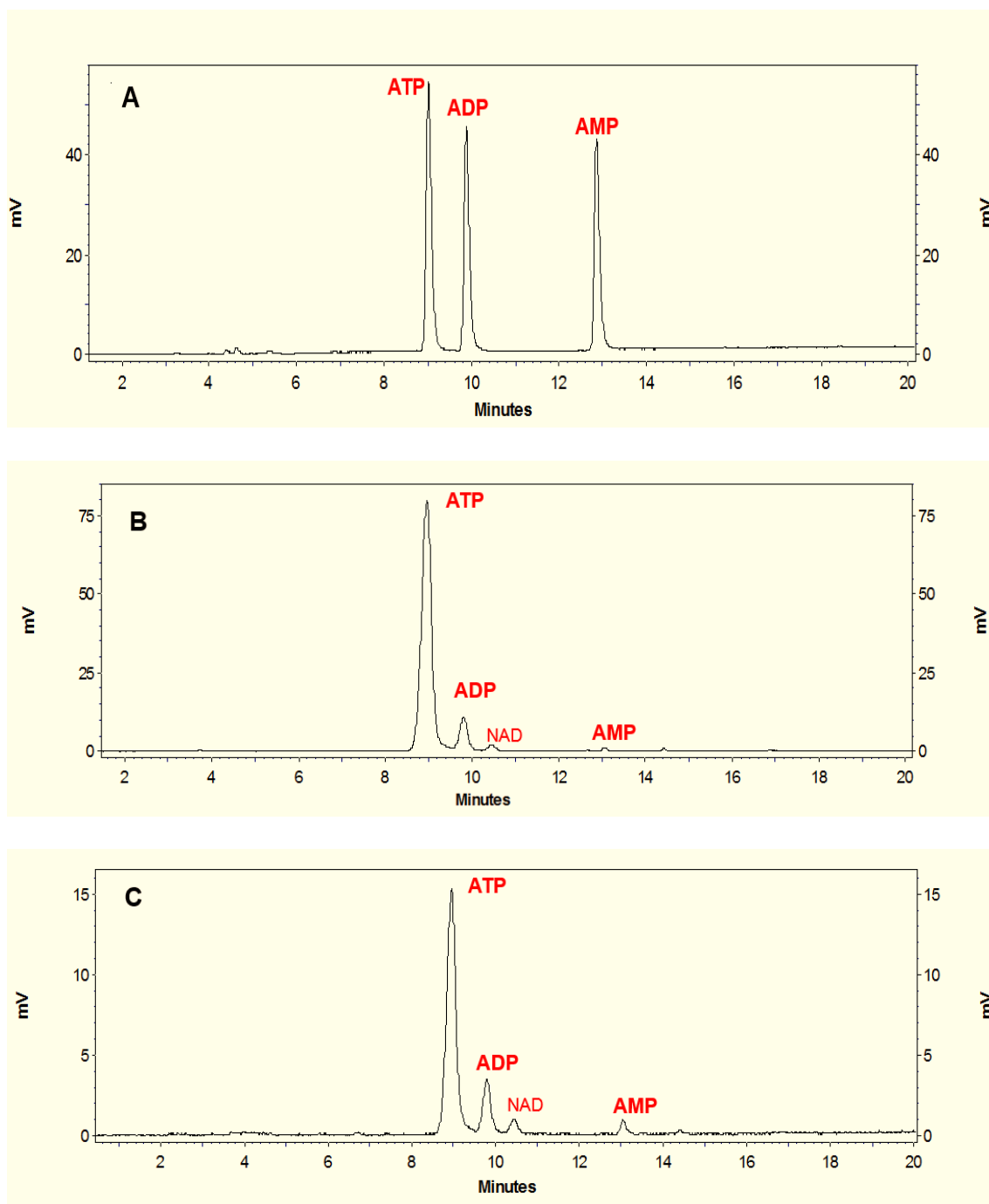


Figure 37 Representative Chromatogram of adenine nucleotides. (A) standard; **(B)** control of SH-SY5Y cells; and **(C)** SH-SY5Y cells treated with 100nM of rotenone for 48 hr. Retention times (RTs) for ATP, ADP, and AMP, were 8.99 min; 9.88 min; and 13.04 min, respectively. Note: the presence of NAD detected in cell preparation identified at 10.60 min. Abbreviations are: ATP, adenosine triphosphate; ADP, adenosine diphosphate; AMP, adenosine monophosphate; NAD, nicotinamide adenine dinucleotide.

2.6.3 Measurement of Coenzyme Q10

High performance liquid chromatography (HPLC) coupled to dual-wavelength ultraviolet detection ranging from 240 and 345 nm, offers robustness and sensitivity to determine the coenzyme Q₁₀ (CoQ₁₀) levels in samples (Orozco et al., 2007). Basically, it measures the amount of monochromatic light absorbed by a sample at a certain wavelength and relates the magnitude of the absorbance to the concentration of the analyte in the eluent passing through a flow cell contained within the instrument (Swartz, 2010).

2.6.3.1 Analytical Equipment

HPLC determination of CoQ₁₀ level was carried out using the following equipment: PU-980 intelligent pump (Jasco); AS-950 intelligent autosampler (Jasco); AZUR data capture and analysis software (Kromatek, Great Dunmow, UK); PG-975-50 UV/VIS detector (Jasco).

2.6.3.2 Analytical Procedure

CoQ₁₀ levels were quantified using a C18 reverse phase HPLC analysis coupled to UV detection at 275 nm. This analysis was performed according to the previous method of (Duncan et al., 2005). At flow rate of 0.7mL/min, the separation was achieved using a mobile phase of containing 7gm of sodium perchlorate to mixture of ethanol; methanol and perchloric acid (700:300:1.2). Initially, 30 µl of 2.0 µM internal Standard (IS) was added to 150 µl of sample prior to the extraction of CoQ₁₀, in order to account for analyte loss during sample preparation. Naturally occurring ubiquinones such as, CoQ₉, have been previously used as IS. However, such naturally occurring ubiquinones

may be present in sample due to contamination from dietary sources and may interfere with the analysis. To prevent this problem, Dipropoxy-CoQ₁₀ has therefore been suggested as a good alternative IS since this exhibits similar physiochemical characteristics to CoQ₁₀.

Before the extraction, samples were exposed to two freeze/thaw cycles, followed by vigorous mixing on a vortex to efficiently disrupt the cell membrane. CoQ₁₀ was then extracted with 700 µl of 5:2 (v/v) hexane/ ethanol, followed by centrifugation at 14.000 g for 3 min at room temperature. The upper hexane layer was then collected and stored on ice. The lower aqueous layer was further re-extracted and the combined upper hexane layers were then evaporated to dryness using a rotary vacuum evaporator. Once evaporated, samples were then re-suspended in 300 µl of ethanol prior to filtering using a 4-SF-02 1 polyvinyl (PV) and HPLC analysis.

For the calibration, a 2.0 µM sample of working standard for each CoQ₁₀ and Dipropoxy-CoQ₁₀ was injected. 50 µl of sample was injected and separated by isocratic elution using reverse phase chromatography at room temperature on a C18 reversed phase column (Techsphere ODS 4.6 × 250 mm, 5 µm, 100 Å) (HPLC Technology, Welwyn Garden City, UK). CoQ₁₀ levels were quantified with an online UV detector at 275 nm (Figure 38).

2.6.3.3 Data Analysis

CoQ₁₀ data was captured and analyzed using AZUR software (Kromatek, Great Dunmow, UK) and calculated using the following equation:

$$\text{CoQ}_{10} \text{ concentration (pmol/ml)} = (\text{Sample peak height} / \text{Internal standard peak height}) \times \text{Internal standard concentration (}\mu\text{M)}$$

All obtained results were expressed as pmol/mg protein.

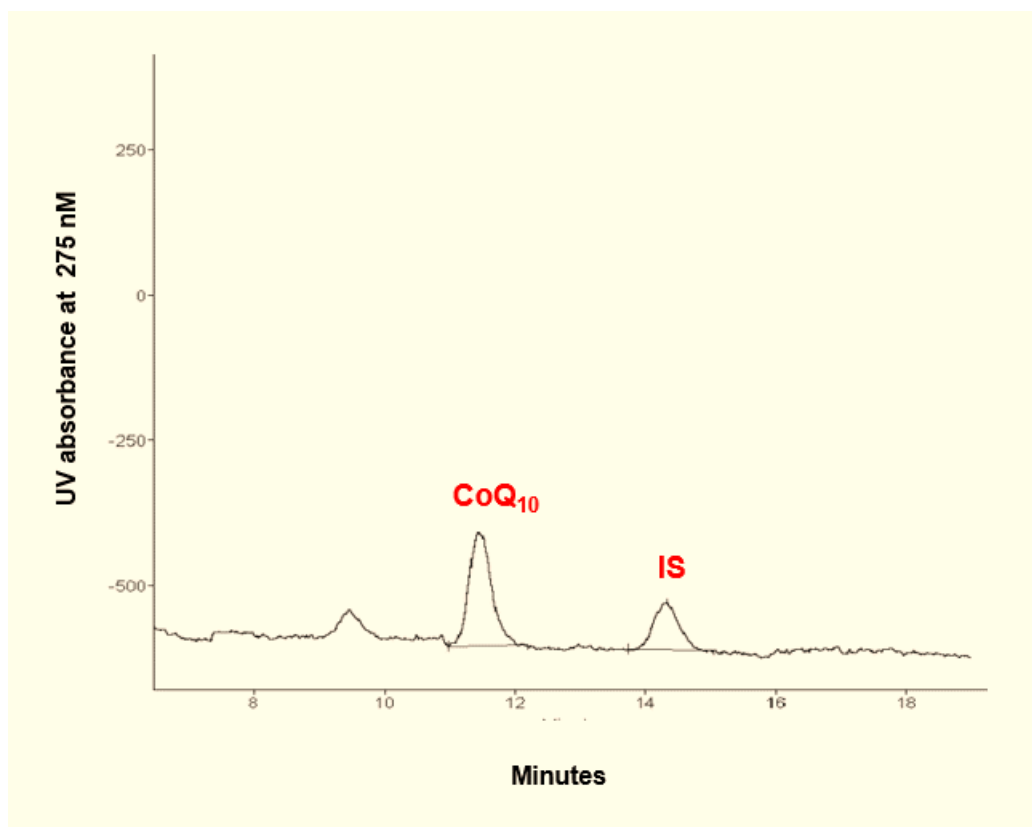


Figure 38 Representative chromatogram of CoQ₁₀ in control SH-SY5Y cells and internal standard (IS) with RT at 11.4 and 14.3 min, respectively.

2.6.4 Measurement of Reduced Glutathione (GSH)

High performance liquid chromatography (HPLC) coupled to electrochemical detection (ECD) is a very selective and sensitive analytical method commonly used to detect and quantify a wide range of electroactive analytes (Nagatsu and Kojima, 1988). It also has the additional practical advantage over many alternative detection methods such as UV or fluorescence in that samples do not require derivatization prior to analysis (Yap et al., 2010). It relies on the ability of the analytes to become either oxidized or reduced as they interact with the surface of the electrode as they pass through the ECD cell, and in

doing so either donate or accept electrons which subsequently generate an electrical current capable of being integrated and amplified. In general, samples are first injected into the HPLC system and separated on the basis of their differing polarities using reverse phase chromatography (Štulík and Pacáková, 1981). They are subsequently carried through the detector in the mobile phase as they elute from the column where they subsequently undergo the necessary redox reaction in order to generate a quantifiable signal. Furthermore, the signal generated is directly proportional to analyte concentration allowing accurate and reproducible quantitation over a wide concentration range.

2.6.4.1 Analytical Equipment

HPLC determination of GSH was carried out using the following equipment: PU-1580 intelligent HPLC pump (Jasco UK Ltd., Great Dunmow, UK); AS-2055 Plus autosampler (Jasco); mobile phase was degassed utilizing DG-980-50 inline degasser (Jasco); Coulochem™ III electrochemical detector (ESA); 5010 analytical cell (ESA); AZUR data capture and analysis software (Kromatek, Great Dunmow, UK).

2.6.4.2 Analytical Procedure

GSH was measured using reversed-phase high performance liquid chromatography (HPLC) with electrochemical detection as described previously by (Riederer et al., 1989). Separation was achieved using a C18 reversed phase column (Techsphere ODS 4.6 × 250 mm, 5 μm, 100 Å) (HPLC Technology, Welwyn Garden City, UK) maintained at room temperature with 15mM o-phosphoric acid as the mobile phase at a flow rate of 0.5ml/min.

In order to disrupt cellular membranes, samples were exposed to three freeze-thaw cycles prior to assay, and then diluted within 15mM o-phosphoric acid. Subsequently, samples were incubated on ice for 10 min and then centrifuged for 5 min at 15000x *g* at 5°C. A 50 µl aliquot of the supernatant was injected. To ensure the analytes were being oxidized at low oxidation potential, the screening electrode (E1) was set held at +50mV. For GSH detection, the optimal electrode (E2) potential was determined via voltammogram. Thus, the oxidation peak potential of 5µM GSH standard was monitored between a range of detector electrode potentials (+200mV to +600mV) (Figure 39). The maximum oxidation peak potential was found at 550 mV, and this was therefore subsequently used for GSH determination. For quantification, GSH peak area was determined for 5µM GSH dissolved in 15mM o-phosphoric acid (Figures 40 and 41). The peak area of GSH in samples was then used to calculate GSH concentration in comparison to this external GSH standard.

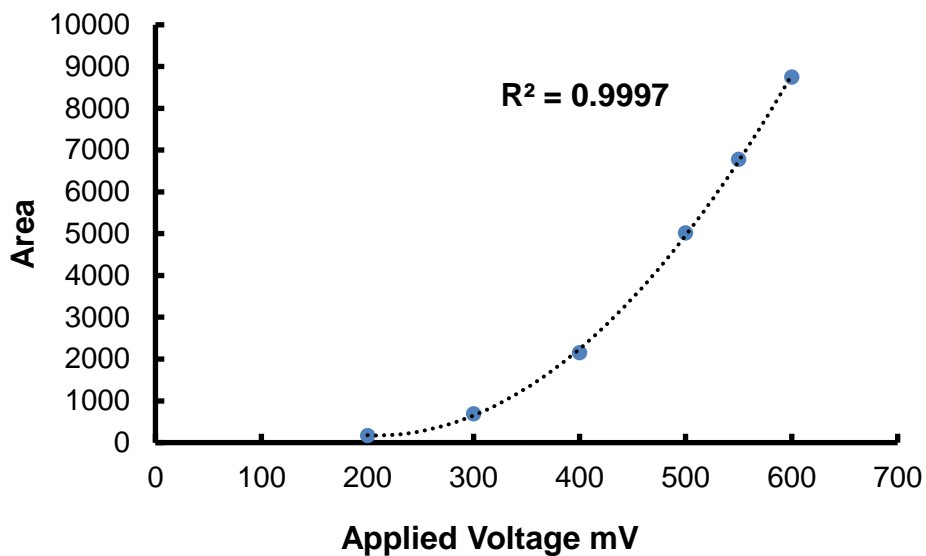


Figure 39 The oxidation peak potential of 5 μ M GSH standard from +200 to +600 mV was monitored via voltammogram.

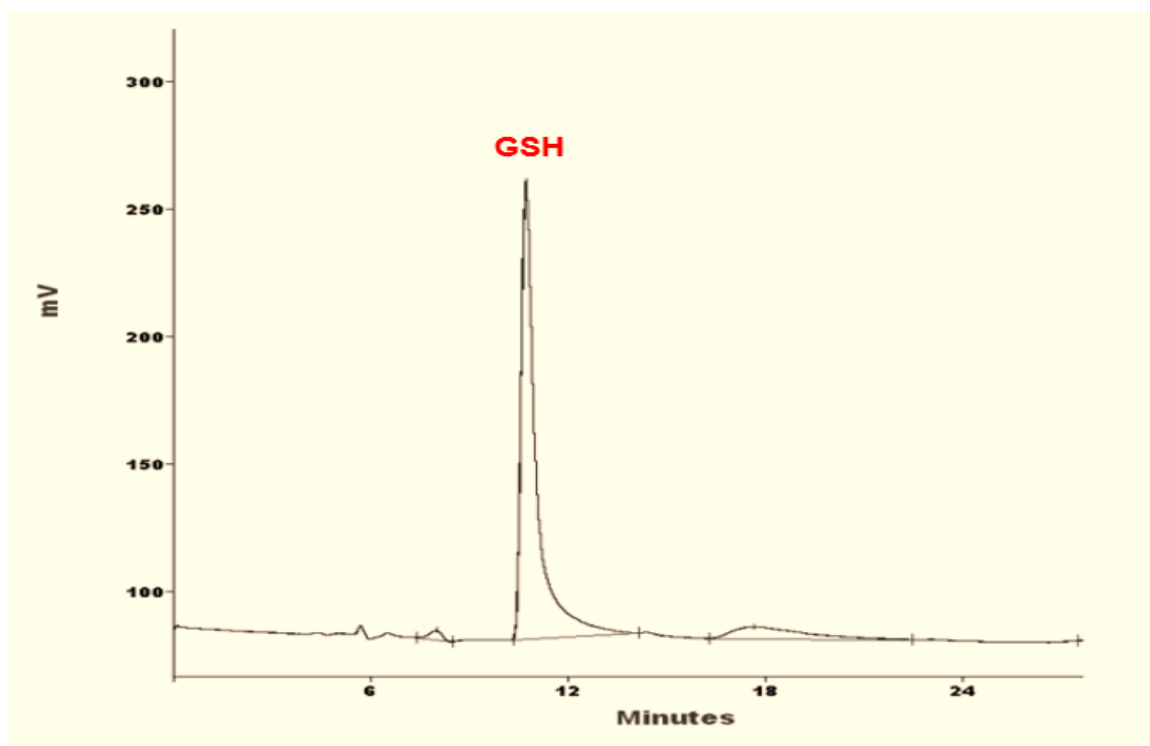


Figure 40 Representative chromatogram of the external GSH standard (5 μ M) with RT at 10.7 min.

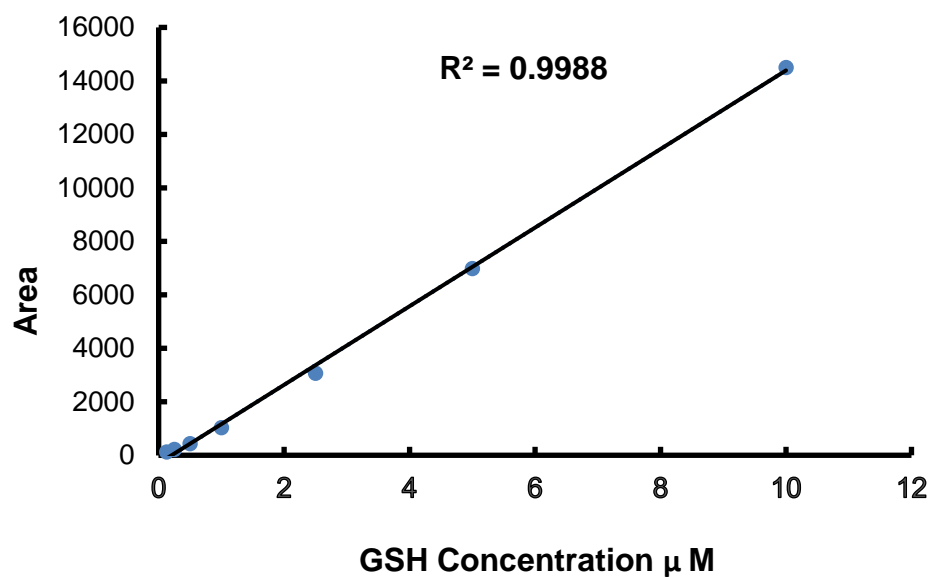


Figure 41 The standard curve of the external GSH standard (μM) plots against peak area. By serial dilution of external GSH standard in 15mM *o*-phosphoric acid, which appeared to be highly linear ($r^2=0.9986$).

2.6.3.4 Data Analysis

GSH data was captured and analyzed using AZUR software (Kromatek, Great Dunmow, UK) and calculated using the following equation:

GSH Concentration (μM) = (sample peak area / external standard peak area) x external standard concentration (μM) x sample dilution

All obtained results were expressed as nmol/mg protein.

2.7 Statistical Analysis

All statistical analyses were performed using Graphpad Prism 4 software (Graphpad Software Inc. San Diego, CA, USA) unless otherwise stated. The D'Agostino-Pearson omnibus test was performed to assess whether data are normally distributed. Results expressed as ratios (i.e MRC complex activities ratio to citrate synthase) were transformed using arcsin square root to yield normal distribution values before the statistical performance (Gegg et al., 2003). All results obtained were expressed as mean \pm standard error of the mean (SEM). Unpaired student's *t*-test was performed for statistical two-group comparison, while one-way ANOVA (analysis of variance), followed by Tukey's *post-hoc* test was performed for statistical multiple-group (usually ≥ 3) comparison. In all cases $p < 0.05$ was considered to be statistically significant.

CHAPTER 3

Evaluation of Mitochondrial Enzyme Complex Activities in Post-Mortem Brain Tissue from Patients with Parkinson's Disease

3.1 Background

Parkinson's disease (PD) is a chronic and progressive neurodegenerative disorder. It is a multifactorial and age-related, affecting approximately 1%, of the general population, and almost exclusively in the age 60 years or older (Reeve et al. 2014). The late-onset sporadic (idiopathic) form accounts for 90% of all PD cases, while the remaining is familial (Mendelian) form (Kroemer and Blomgren, 2007). Once approximately 70- 80 % of dopaminergic neurons depletion occurs (Bezard et al., 2001; McNamara and Durso, 2006), PD patients clinically present with motor symptoms, including bradykinesia, tremor, rigidity and often postural instability (reviewed by Al Shahrani et al., 2017). In addition to motor symptoms, patients with PD may present with non-motor symptoms, such as depression, sleep disturbances, anxiety, and constipation (Kalia and Lang, 2015). The cardinal pathological hallmarks of Parkinsonism include selective cell death of dopaminergic neurons in the substantia nigra pars compacta (SNpc) and the presence of α -synuclein-positive intraneuronal cytoplasmic inclusions, known as Lewy bodies (LBs) (Winklhofer and Haass, 2010).

Although there has been considerable effort to elucidate the mechanism related to the neuropathology of PD, the precise underlying mechanism of dopaminergic PD is still not yet entirely understood. However, there is now increasing evidence that altered mitochondrial function, resulting in oxidative stress and depletion in ATP level, has been causally linked to dopaminergic PD pathogenesis (Schapira, 2008; Winklhofer and Haass, 2010). The most compelling evidence for altered mitochondrial function, and in particular that of MRC complex I, has been observed in post-mortem brains, as well as other

tissues of PD patients (Schapira, 1994). Furthermore, a deficit in MRC complex I activity has been appeared to be systematic, affecting multiple tissues (Schapira, 2008). Additionally, as a consequence of suppressed electron flux via MRC complex I, mitochondrial ROS may be dramatically exaggerated, resulting in oxidative injury or stress to major cell biomolecules including mtDNA, protein, and lipid (reviewed by Al Shahrani et al., 2017). The loss of the tripeptide thiol GSH, the key antioxidant in the brain, has been reported in early-stage PD post-mortem brain, preceding even MRC complex I deficiency (Jenner et al., 1992). In addition to mitochondrial dysfunction, substantial evidence for neuropathological role of α -synuclein in the PD pathogenesis has been demonstrated (Wills et al., 2010; Devi et al. 2008; and Sharon et al., 2003).

The presynaptic nerve terminal protein, α -synuclein, is an abundantly found in neurons and to a lesser extent in glial cells (Kim et al., 2014). It consists of 140 amino acids-encoded by the *α -synuclein (SNCA)* gene in human (Breydo et al., 2003). It was shown in 1997 to be a major constituent of spherical-like LBs and strand-like Lewy neurites (LNs) in the brainstem of both sporadic PD and dementia with LBs (DLBs) patients (Polymeropoulos et al., 1997; Norris and Giasson, 2005). In addition to synaptic α -synuclein protein, LBs which predominantly develop in neurons (Brück et al., 2015), are also composed of neurofilaments, and ubiquitin (Giráldez-Pérez et al., 2014). In the cytosol, a native α -synuclein exists as an unfolded monomer, but it undergoes a conformational change to a folded α -helical secondary structure in the presence of lipid membranes, forming dimers and oligomers (Chandra et al., 2003). Thus, a conformational change from an α -helical to a beta sheet

configuration in α -synuclein is crucial to their accumulation into LBs (Chandra et al., 2003). It has been suggested that posttranslational modification of α -synuclein, including phosphorylation, ubiquitination and nitration, has been implicated in the process of α -synuclein aggregation (Kim et al., 2014).

Aggregation of α -synuclein intracellularly has recently emerged as new insights into the neuropathological diagnosis and progression of sporadic PD. For a long time, it was assumed that aggregation of α -synuclein induced neurotoxic effects and mediated neuronal cell death (Masliah et al., 2000). For instance, at the cellular level, the aggregation of α -synuclein was previously found to be neurotoxic by inhibiting the activity of the neuronal survival protein, myocyte enhancer factor 2D (MEF2D) (Chu et al., 2011). However, the accumulation of these protein inclusions could be elicited as a compensatory protective response against proteolytic stress, as recent findings reported (Hashimoto et al., 2002 and McNaught et al., 2003).

Braak and his colleagues (Braak et al., 2003) proposed a dual-hit hypothesis that the pathological sporadic PD process initiates once a neurotropic pathogen transmits to the brainstem via gastrointestinal (GI) tract, suggesting that non-motor features may precede the brain-deficient DA. Their claim was further reinforced by the presence of abnormal α -synuclein aggregation in the enteric nervous system (ENS) and olfactory system which selectively spread within the CNS via the vagus nerve (Hawkes et al., 2007). Braak, therefore, proposed a six-staging model for PD progression based on LBs pathology spreading. Each stage is characterized and associated with pathological condition in certain neurological structures. In a cross-sectional study, the staging system of Braak was performed on brain autopsy examinations of 168

patients incidentally and clinically diagnosed with sporadic PD. In stage 1 and 2, the aggregated α -synuclein in the form LNs, are more pronounced than LBs which the disorder initiates in the anterior olfactory structures, medulla oblongata and pontine tegmentum. In addition to neurological lesions observed in stage 1 and 2, stages 3 to 4 are characterized by additional lesions in the midbrain (substantia nigra), basal prosencephalon and mesocortex. The motor symptoms probably manifest during this stage. In stage 5 and 6, the lesions entirely invaded the neocortex region, by which at this stage the disorder becomes an extremely severe illness.

3.2 Aims

There is now considerable evidence that implicates the loss of the enzymatic activity of MRC complexes in the pathophysiology of PD. However, it is still currently uncertain whether altered respiration is an early event in the pathophysiology of PD, or a late consequence of cellular stress induced by protein aggregation and neuronal death. Therefore, this chapter aims to

- (i) Further investigate MRC activity in PD post-mortem brain, and
- (ii) Compare brain regions that are pathologically affected with LB formation and neuronal loss to regions that are unaffected. This may identify whether alterations in MRC activity occur prior to significant neuronal cell death in PD.

3.3 Methods

3.3.1 Brain samples

Human post-mortem flash frozen brain tissues were gratefully obtained from Queen Square Brain Bank for Neurological Disorders (QSBB) at the UCL Institute of Neurology.

3.3.2 PD brain cases and control groups

Putamen (moderate pathology), parahippocampus and temporal cortex (mild pathology), frontal cortex, and parietal cortex (no pathology) were punch dissected from human post-mortem flash frozen tissue in 4-6 neurologically normal controls and 4-6 Parkinson's disease Braak stage 3/4 cases. These cases were matched for age, gender and post-mortem delay, as presented in (Table 5). The severity of disease (mild or moderate) was based upon relative Lewy Body Pathology, i.e. number of aggregates. This was assessed by a neuropathologist at QSBB.

3.3.3 Brain Tissue Homogenization

Flash-frozen brain tissue homogenates were prepared, according to method of (Heales et al. 1995). By using a glass-glass homogenizer, brain tissues (10–50 mg) were homogenised 1:9 (w/v) in ice-cold homogenization Buffer, containing 320 mM, 1 mM EDTA, 10 mM Trizma-base. Prior to MRC complex activities, the homogenates were aliquoted and stored at -70°C .

3.3.4 Mitochondrial Enzymatic Assays

MRC complex I, II-III, IV, II and CS activities in each brain tissue homogenate were spectrophotometrically determined at 30°C as described in (Section 2.6)

3.3.5 Statistical Analysis

Statistical analysis was carried out as described in (Section 2.7)

Table 5 Demographic data of the post-mortem PD cases used in this study

**Pathologically Unaffected
(A)**

Frontal Control	PMD (hrs)	Gender M/F	Age at death (Year)
1	11	M	77
2	12	M	65
3	6	M	73
4	5	M	81
5	5	F	79
6	6	F	67
Mean ± SEM (n=6)	7.5 ± 1.2	4M:2F	73.6 ± 2.6

Frontal PD	PMD (hrs)	Gender M/F	Age at death (Year)
1	4.5	F	70
2	16.5	F	88
3	9.33	M	68
4	13.17	F	82
5	5	F	86
6	3.5	F	79
Mean ± SEM (n=6)	8.6 ± 2.1	1M:5F	78.8 ± 3.3

Parietal Control	PMD (hrs)	Gender M/F	Age at death (Year)
1	11	M	77
2	17	M	72
3	6	M	73
4	5	M	81
5	5	F	79
6	6	M	76
Mean ± SEM (n=6)	8.3 ± 2.0	5M:1F	76.3 ± 1.4

Parietal PD	PMD (hrs)	Gender M/F	Age at death (Year)
1	4.5	F	70
2	16.5	F	88
3	9.33	M	68
4	13.17	F	82
5	5	F	86
6	3.5	F	79
Mean ± SEM (n=6)	8.6 ± 2.15	1M:5F	78.8 ± 3.3

**Mild Pathology
(B)**

Parahippocampus Control	PMD (hrs)	Gender M/F	Age at death (Year)
1	5	F	72
2	4	M	63
3	6	M	73
4	5	M	81
5	5	F	79
Mean ± SEM (n=5)	5.0 ± 0.31	3M:2F	73.60 ± 3.1

Parahippocampus PD	PMD (hrs)	Gender M/F	Age at death (Year)
1	4.5	F	70
2	5.75	M	73
3	7.3	M	87
4	13.17	F	82
5	5	F	86
Mean ± SEM (n=5)	7.14 ± 1.5	2M:3F	79.60 ± 3.4

Temporal Cortex Control	PMD (hrs)	Gender M/F	Age at death (Year)
1	6	M	73
2	5	F	79
3	5	M	81
4	6	F	76
5	5	F	72
6	4	M	63
Mean ± SEM	5.1 ± 0.30	3M:3F	74.0 ± 2.6

Temporal Cortex PD	PMD (hrs)	Gender M/F	Age at death (Year)
1	4.5	F	70
2	16.5	F	88
3	9.33	M	68
4	13.17	F	82
5	5	F	86
6	6.55	M	73
Mean ± SEM	9.1 ± 2.0	2M:4F	77.8 ± 3.5

**Moderate Pathology
(C)**

Putamen Control	PMD (hrs)	Gender M/F	Age (Year)
1	11	M	77
2	5	M	61
3	6	M	73
4	6	M	76
5	5	F	79
6	5	M	67
Mean ± SEM (n=6)	6.3 ± 1.0	5M:1F	72.17 ± 2.8

Putamen PD	PMD (hrs)	Gender M/F	Age (Year)
1	4.5	F	70
2	16.5	F	88
3	9.33	M	68
4	13.17	F	82
5	5	F	86
6	5.75	M	73
Mean ± SEM (n=6)	9.04 ± 2.0	2M:4F	77.83 ± 3.5

Results represent as mean ± SEM of (n = 5-6) per post-mortem brain samples. Statistical analysis was carried out using unpaired student's *t*-test. There was no significant difference in age, gender or PMD between control and PD patients. Abbreviations are: PD, Parkinson's disease; PMD, post-mortem delay; hrs, hours; M, male; F; female.

3.4 Results

The enzymatic studies showed that multiple mtDNA-encoded MRC activities were significantly reduced (MRC complex I (63 %): $p < 0.0005$, complex II+III (74 %): $p < 0.005$, and complex IV (33%): $p < 0.05$) in the most moderately affected region, the putamen, compared to brain age-matched controls (Figure 42-44). Mildly affected regions, the parahippocampus and temporal cortex both exhibited a significant reduction only in MRC complex I activity (40%: $p < 0.05$ and 26%: $p < 0.005$, respectively), while pathologically unaffected regions (frontal and parietal cortices) had no significant loss of MRC activity, compared to brain age-matched controls (Figure 42-44). Interestingly, MRC complex II activity, which is entirely nuclear encoded appears to be preserved, in contrast to MRC complex I, III and IV (Figure 45). The results of MRC I, II–III and IV activities in PD post-mortem brain regions with different pathological severity are summarised in (Table 6).

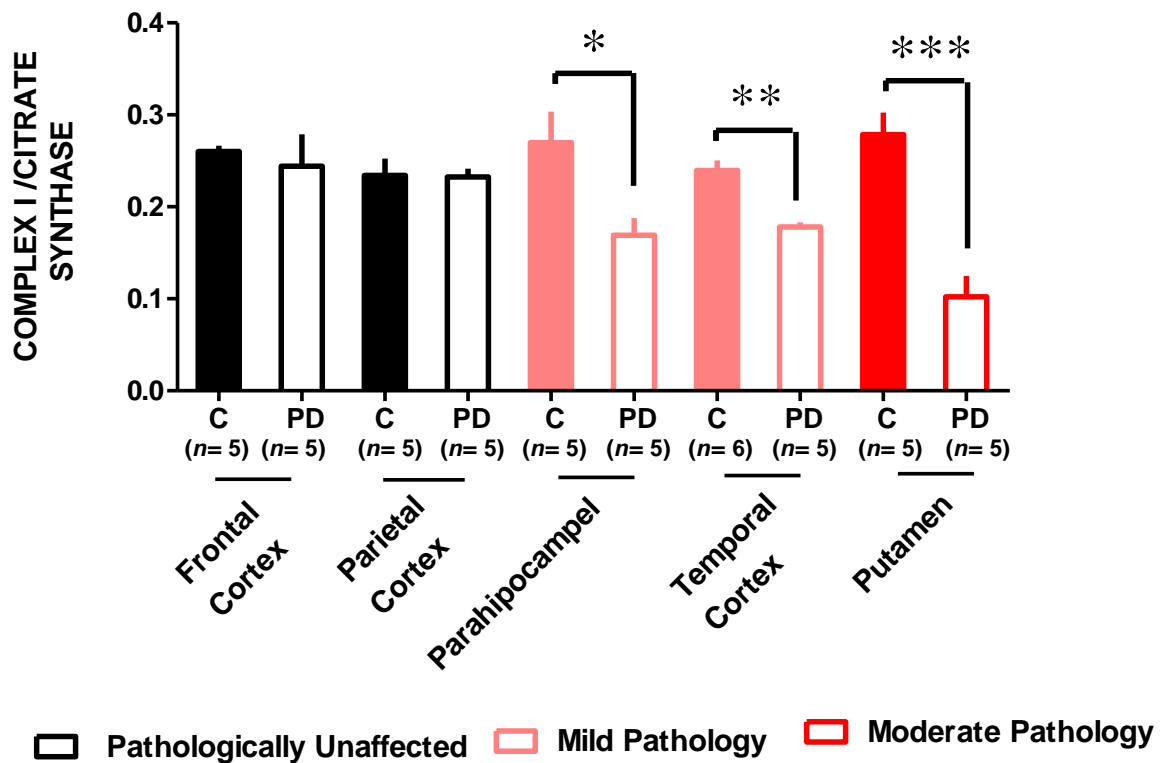


Figure 42 MRC complex I activity in post-mortem brain regions of control (C) and the Parkinson's disease (PD) with different pathological severity. Error bars indicate SEM for ($n = 5-6$) per post-mortem brain samples; statistical analysis was carried out using unpaired student's t -test; significant differences: $*p < 0.05$, $**p < 0.005$, $***p < 0.0005$.

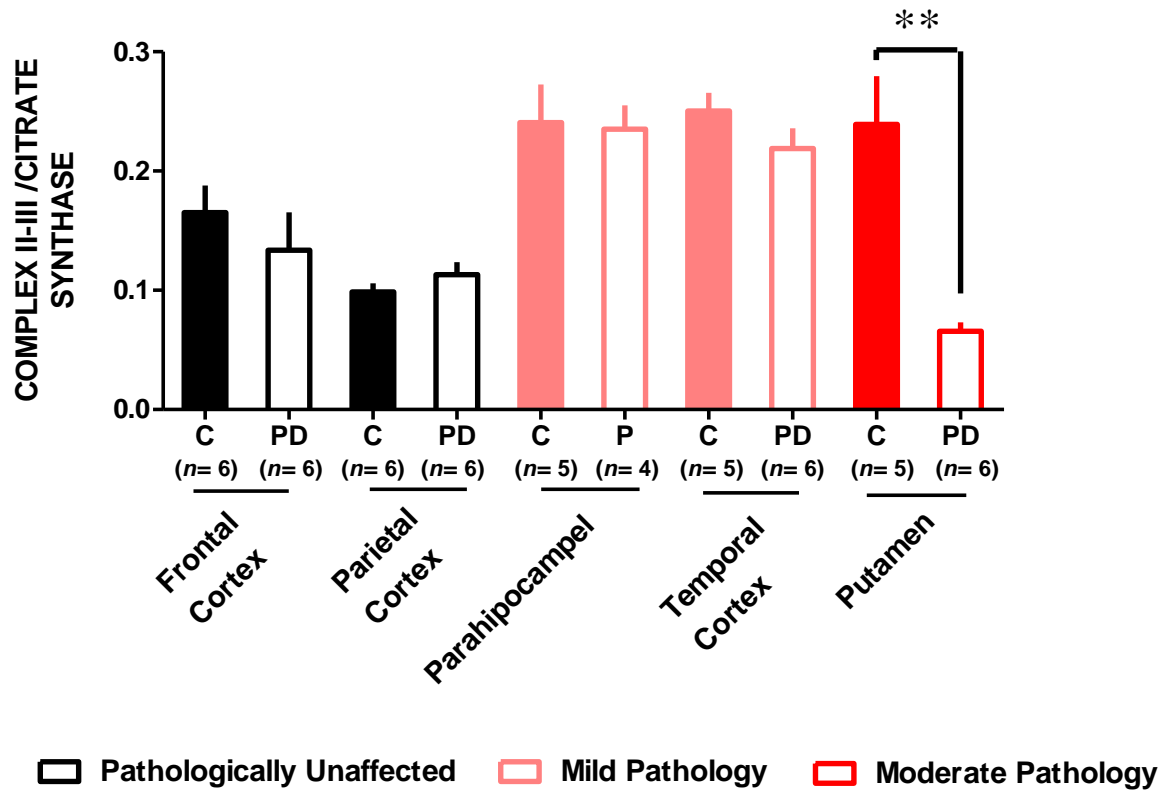


Figure 43 MRC complex II-III activity in post-mortem brain regions of control (C) and the Parkinson's disease (PD) with different pathological severity. Error bars indicate SEM of ($n= 4-6$) per post-mortem brain samples; statistical analysis was carried out using unpaired student's t -test; significant differences: $**p < 0.005$.

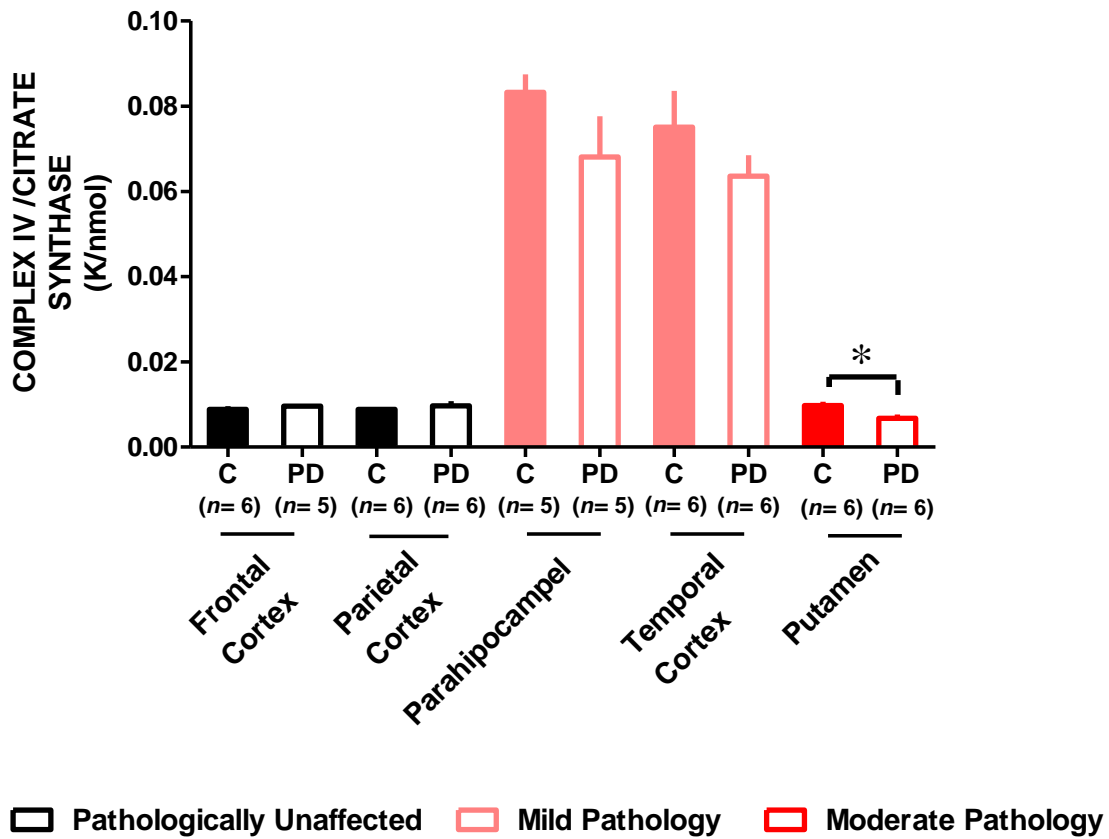


Figure 44 MRC complex IV activity in post-mortem brain regions of control (C) and the Parkinson's disease (PD) with different pathological severity. Error bars indicate SEM of ($n = 5-6$) per post-mortem brain samples; statistical analysis was carried out using unpaired student's t -test; significant differences: $*p < 0.05$.

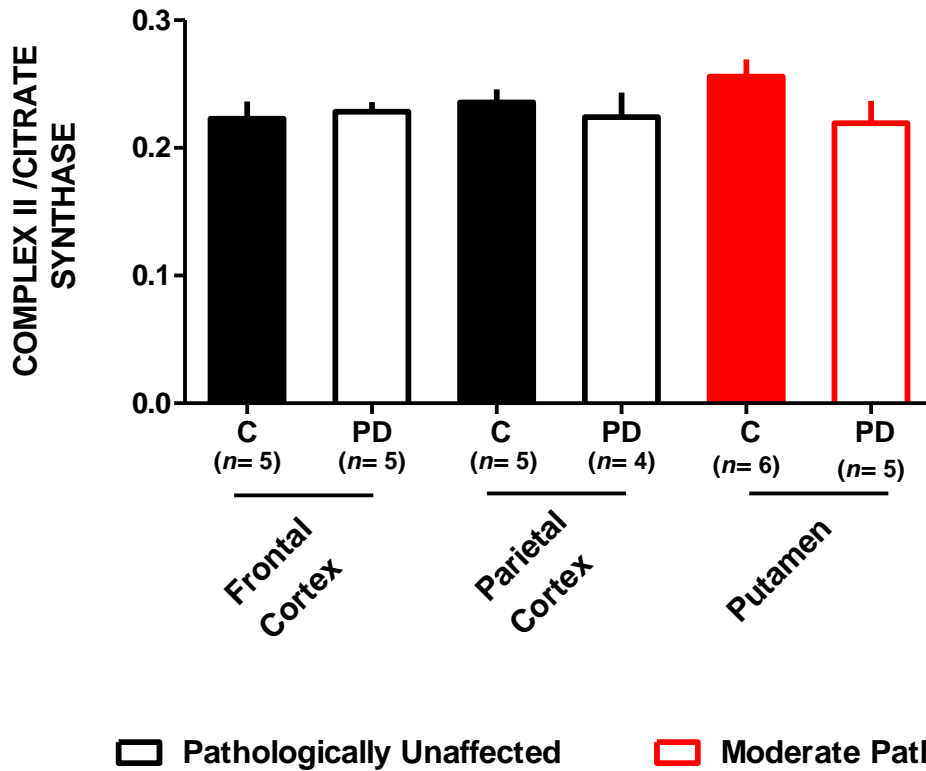


Figure 45 MRC complex II activity in post-mortem brain regions of control (C) and the Parkinson's disease (PD) with different pathological severity. Error bars indicate SEM for ($n= 4-6$) per post-mortem brain samples; statistical analysis was carried out using unpaired student's *t*-test; there is no significant difference.

Table 6 MRC complex I, II-III and IV activities are expressed as a ratio to CS activity in post-mortem brain regions of control (C) and the Parkinson's disease (PD) with different pathological severity.

MRC Activity	The PD post-mortem brain with different pathological severity									
	Frontal Cortex		Parietal Cortex		Parahippocampus		Temporal Cortex		Putamen	
	C	PD	C	PD	C	PD	C	PD	C	PD
Complex I	0.26±0.006 (n=5)	0.24±0.03 (n=5)	0.23±0.01 (n=5)	0.23±0.008 (n=5)	0.27±0.03 (n=5)	0.16±0.018* (n=5)	0.23±0.01 (n=6)	0.17±0.005** (n=5)	0.27±0.02 (n=5)	0.10±0.02*** (n=5)
Complex II-III	0.16±0.02 (n=6)	0.13±0.03 (n=6)	0.10±0.007 (n=6)	0.11±0.010 (n=6)	0.24±0.03 (n=5)	0.23±0.01 (n=4)	0.25±0.015 (n=5)	0.21±0.017 (n=6)	0.23±0.04 (n=5)	0.06±0.007** (n=6)
Complex IV (k/nmol)	0.008±0.0007 (n=6)	0.0096±0.0005 (n=5)	0.008±0.0005 (n=6)	0.0096±0.001 (n=6)	0.08±0.004 (n=5)	0.06±0.009 (n=5)	0.07±0.008 (n=6)	0.06±0.004 (n=6)	0.009±0.0008 (n=6)	0.006±0.0008* (n=6)
Complex II	0.22±0.013 (n=5)	0.22±0.007 (n=5)	0.23±0.010 (n=5)	0.22±0.019 (n=4)	-	-	-	-	0.25±0.013 (n=6)	0.21±0.017 (n=5)

Pathologically Unaffected
 Mild Pathology
 Moderate Pathology

Results represent as mean ± SEM of (n= 4-6) per post-mortem brain samples.

*denotes a statistically significant decrease, compared to control value (*p < 0.05, **p < 0.005, ***p < 0.0005).

3.5 Discussion

The reduction of MRC activity in multiple tissues of PD patients has been extensively demonstrated. Many studies have focused on the MRC activity in post-mortem human brain tissues of PD such as the substantia nigra (Schapira et al., 1989), the frontal lobe and the striatum (Mizuno et al., 1990). However, these biochemical findings following MRC enzyme studies are somewhat conflicting most likely due to aetiologically heterogeneity in the brain tissues of PD subjects or a variety of methodological issues that have been employed in these studies (Schapira, 2008). Therefore, this present study contributes differently from other studies as to the ongoing investigations about MRC activity in PD post-mortem brain based on pathological severity. Our enzymatic results show the evidence of the reduction of MRC complex I in both pathologically mild, parahippocampus and temporal cortex (40% and 26% reduction, respectively) and progressive reduction as seen in pathologically moderated (63% inhibition) brain region, putamen, in contrast to unaffected brain region which were not significantly affected. This implies that MRC complex I deficiency is seemingly a common pathophysiological event in neurodegeneration of PD and it is directly associated with pathological PD severity. It was thought that the mitochondrial complex I activity is exclusively reduced in SN of PD rather than other brain regions (Greenamyre et al., 1999). However, the MRC complex I impairment occurring in mildly affected regions, the parahippocampus, temporal cortex along with recent detection in frontal cortex of PD patient (Parker et al., 2008), support the proposal that the reduction of MRC complex I activity is not only

specific to the substantia nigra region but also could occur in other affected brain regions.

Interestingly, the findings of the present study have demonstrated that the activity of multiple mitochondrial complexes I (63% inhibition), II-III (74% inhibition) and IV (33 % inhibition) were significantly reduced in the most moderately affected region, the putamen, which is the largest dopamine-depleted region in substantia nigra of PD (Bernheimer et al., 1973), raising the possibility that these complexes are particularly susceptible to perturbed process occurring in PD. Similarly with brain tissues, multiple mitochondrial complexes I, II-III and IV were also shown to be markedly reduced in multiple tissues, including, platelets, lymphocytes, and lesser detected in skeletal muscle obtained from PD patients (Schapira, 1994; Mizuno et al. 1989; Parker et al. 1989; Shoffner et al. 1991; Bindoff et al. 1991), which supports the concept that the multiple MRC dysfunction is not only involved in neuron tissue of PD patients. The main mechanism of multiple mtDNA encoded complexes impairments seen in PD is not fully understood. Nevertheless, it has been hypothesized that multiple MRC dysfunction results from the main therapy for PD patients (L-dopa) due to its oxidative stress, however, earlier study (Haas et al., 1995) revealed an inhibition in both MRC complex I and II-III activities in platelets of untreated PD patients. Considerable evidence exists suggesting a role for mtDNA defects in dopaminergic neurodegeneration of PD pathogenesis (Kirches, 2009). Many studies have reported that somatic mtDNA deletions dramatically accumulated in various tissues with age, and further accumulation was observed in the SN of PD patient (Lin et al. 1995). Unlike nDNA, mtDNA is particularly susceptible to

oxidative damage since it lacks protective histones, has limited repair mechanisms as well as sharing its location in the cellular compartment known to be the major sources of ROS production, MRC complex I and complex III (reviewed by Al Shahrani et al., 2017). This is also supported by the observation of an increased level of DNA oxidation product, 8-hydroxydeoxyguanosine (8-OHdG) in human brain tissues of PD (Alam et al., 1997). Intriguingly, loss of mitochondrial phospholipid CL content has been linked to mtDNA instability (Al Shahrani et al., 2017), suggesting another possible mechanism that the dysfunctional MRC encoded by mtDNA may be the consequence of oxidative damage, although there is no compelling evidence, showing alterations in brain CL content of PD patients (Yan and Kang, 2012). Our findings also reveal that there were no significant differences in the activity of complex II between PD and control, suggesting that the exclusively nDNA-encoded complex II is less likely to be associated with PD as it is less sensitive to oxidative-induced MRC damage (Figure 45). Strikingly, a recent study was investigated in PD neurons by (Muller et al. 2013) showing that there was a positive correlation between the accumulation of mtDNA deletions and LB aggregates, but no association between LB aggregates and MRC dysfunction. With regards to the latter, however, our present findings show a relationship between MRC dysfunction and LB pathology. In addition, it has been suggested that primary MRC deficiency may lead to a secondary loss of other MRC activities. This latter has been earlier assessed in human astrocytoma cells by (Hargreaves et al. 2007) where a KCN induced MRC complex IV defect resulted in a secondary loss of MRC complex II-III activity, yet the exact mechanism remains an elusive. Notably, the reduction in the

combined activity of complex II-III might result in decrease CoQ₁₀ levels or complex III activity. Furthermore, the enzymatic results of the present study have also noted that the activity control of MRC complex I, II and IV were comparable in contrast to complex II-III activity which was found to be different (Table 6).

One question still unanswered is whether the activity of multiple mitochondrial respiratory complex I, II+III and IV deficiencies are potential causes or a secondary consequence of oxidative stress induced by LBs aggregate or cell death. The compelling evidence of this issue requires further study.

3.6 Conclusion

In conclusion, the results demonstrate that impaired MRC complex I function occurs in regions with both moderate and mild pathology in PD brain, in contrast to unaffected brain region. Additionally, moderate affected brain region shows multiple MRC deficiencies. However, MRC complex II shows to be preserved. Taken the aforementioned findings together with our own findings from PD patients, suggests that the impairment of MRC activity may be a common event in PD pathogenesis. Clearly, further experiments will be necessary to investigate whether the multiple complexes defect observed in moderate affected brain region, putamen is the result of the brain region itself or the duration of disorder. This will be further explored in the next chapter.

CHAPTER 4

Development of a Neuronal Cell model to Investigate Mitochondrial Respiratory Chain Dysfunction in Parkinson's Disease

4.1 Background

MRC complex I deficiency is one of the most common apparent MRC disorder and is associated with various clinical features, ranging from lethal neonatal disorders to adult-onset neurodegenerative disorders such as Parkinson's Disease (PD) (Fassone, and Rahman, 2012). With regards to PD, the most compelling evidence for altered mitochondrial function, and in particular that of MRC complex I, has been observed in post-mortem brains, as well as other tissues of PD patients (Schapira, 2008). In additions to being functionally impaired and misassembled, MRC complex I subunits are oxidatively damaged in SNs of patients with PD (Keeney et al., 2006).

As was demonstrated in the previous chapter, multiple mitochondrial complexes I, II-III and IV were shown to be markedly reduced in moderate affected brain region, putamen. The exact underlying mechanism of a multiple complex defect is not fully understood. However, the possibility arises that impairment of complex I results in secondary oxidative damage to the other complexes. While it is very challenging and complicated to study the biochemical events of chronic MRC complex I deficiency promoted secondary damage to other complexes in brain tissues of PD patients, *in vitro* mitochondrial inhibitors, particularly MRC complex I inhibitors have been widely utilized to replicate particularly the mitochondrial events in PD pathogenesis.

Over the last decade, the development of an experimental model for neurodegenerative disorders has been challenging due to its complexity until the early 1980s once drug abusers intravenously injected with chemical toxin, 1-methyl-4-phenyl-1,2,3,4-tetrahydropyridine (MPTP), producing active MRC

complex I inhibitor 1-methyl-4-phenylpyridinium ion (MPP⁺) via monoamine oxidase B (MAO-B) enzyme, which is actively accumulated in mitochondria and consequently induced Parkinsonism syndrome (Langston et al., 1983). Later on, several epidemiologic studies have reported that pesticide exposure such as rotenone is more likely to increase the risk for PD (Le Couteur et al., 1999). A common biochemical feature which is an inhibition of MRC complex I activity has been observed within individual who have been exposed to some pesticides such paraquat (PQ), and rotenone, developing Parkinson-like symptoms (Betarbet et al., 2002). Since then, PD among neurological disorders has become the first disorder to be mimicked.

As a widely utilized as a pesticide in USA, mitochondrial toxin-MRC complex I inhibitor, rotenone has been commonly used as a pharmacological model to elucidated PD pathogenesis and gain insights into the plausible interactions of environmental and genetic factors, leading to dopaminergic cell death (Schapira, 2008). Being a potent and specific MRC complex I inhibition and generator of oxidative stress, it is particularly damaging to highly vulnerable to dopaminergic neurons, compared to other mitochondrial inhibitors such as 3-nitropropionic acid and malonate (MRC complex II inhibitors) (Haddad and Nakamura, 2015). Even though, there is no evidence showing that rotenone caused nigrostriatal cell death and inclusions bodies in human (Bové et al., 2005) it has been reported in rodents that following administration with low doses of rotenone over 1 month induced pathological features of PD, including selective loss of dopaminergic neurons and aggregation of α -synuclein (Betarbet et al., 2002). In addition to these pathological features, chronic exposure to rotenone revealed evidence of increased oxidative

damage. This is supported by the observation of an increased oxidation levels of DNA and proteins as well as reduced levels of reduced glutathione (GSH) suggesting that oxidative stress might be a pathogenic factor associated with neurodegeneration of PD (Betarbet et al., 2002 and Sherer et al., 2002).

4.2 Aims

Based on the observation that multiple complexes deficiencies were noted in the post-mortem PD brains detailed in the previous chapter, this chapter aims to gain insight into the mechanism underlying the multiple MRC complexes impairment. As a cellular and pharmacological model system mimicking complex I deficiency in post-mortem PD brain, we employed dopaminergic neuroblastoma SH-SY5Y cells to study the effect of rotenone induced MRC complex I deficiency upon the activity of the other complexes. In this particular study, we will evaluate the biochemical parameters upon rotenone treatment. These include:

- i) The enzymatic activity of mitochondrial respiratory chain (MRC) to investigate the loss of the activity of MRC complex I and its progression to other complexes
- ii) The cellular energy charge (EC) to gain more insight into the mechanism of how MRC complex I inhibition affects bioenergetics status over time.
- iii) The intracellular coenzyme Q₁₀ (CoQ₁₀) levels to ascertain whether the reduction in the combined activity of complex II-III a result of a decrease in CoQ₁₀ levels or complex III activity since the MRC

complex II-III activity is dependent upon the endogenous CoQ₁₀ availability.

- iv) The antioxidant reduced glutathione (GSH) status since it has a fundamental cellular redox function as a key antioxidant and has a potential as an earliest indicator for oxidative stress.

4.3 Methods

4.3.1 Cell Culture

SH-SY5Y cells were cultured as described in (Section 2.2) and were treated with 100 nM of rotenone for 24 and 48 hrs after reaching confluence as described in (Section 2.2.5).

4.3.2 Total Protein Concentration

Total protein concentration in SH-SY5Y cells was determined according to Lowry method as described in (Section 2.4)

4.3.3 Mitochondrial Enzymatic Assays

MRC complexes (I-IV) activities as well as CS activity in SH-SY5Y cells were determined spectrophotometrically at 30°C as described in (Section 2.5)

4.3.4 Measurement of Cellular Energy Charge

Since all biochemical processes in living cells are strictly coupled and tied to ATP, ADP and AMP levels, the energy charge (EC), also known adenylate energy charge (AEC), has been utilized as a metabolic regulatory indicator to determine the bioenergetics status in living cell as described previously in (Section 2.6.2) . Thus, energy charge in SH-SY5Y cells was determined using

a C18 reverse phase HPLC analysis coupled to fluorescence as described in (Section 2.6.2.2-2.6.2.5).

4.3.5 Measurement of Coenzyme Q₁₀

CoQ₁₀ level in SH-SY5Y cells was determined using a C18 reverse phase HPLC analysis coupled to UV detection at 275 nm as described in (Section 2.6.3)

4.3.6 Measurement of Reduced Glutathione (GSH)

GSH status in SH-SY5Y cells was determined using a C18 reverse phase HPLC analysis coupled to ECD as described in (Section 2.6.4).

4.3.7 Statistical Analysis

Statistical analysis was carried out as described in (Section 2.7)

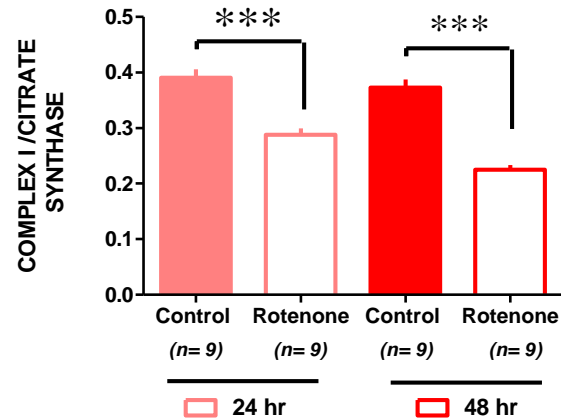
4.4 Results

4.4.1 Mitochondrial Enzymatic Assays

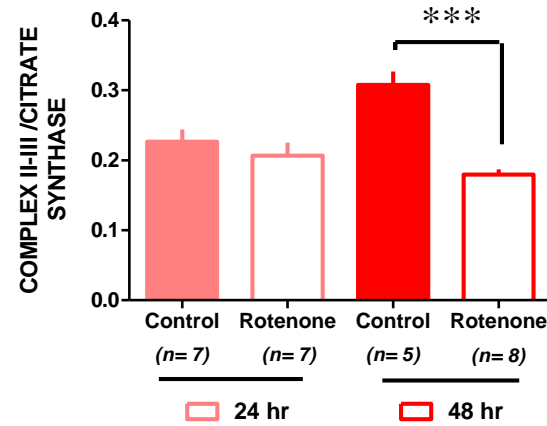
To mimic PD induced MRC complex I deficiency, a model of MRC complex I deficiency was first assessed in neuronal-like SH-SY5Y cells by co-incubating cells with rotenone, an inhibitor of MRC complex I. At a final concentration of 100 nm, rotenone induced a 30% significant inhibition of MRC complex I activity following 24 & 48 hrs of rotenone treatment ($p < 0.0005$), compared to control cells incubated with ethanol vehicle alone (Figure 46-A). Following 48 hr of rotenone treatment, the enzymatic studies indicated a significant inhibition in multiple mitochondrial complexes including, complex I ($p < 0.0005$), II-III (40 %) ($p < 0.0005$), and IV (30 %) ($p < 0.0005$), compared to the controls (Figure 46). However, there was no significant effects on both complex II-III and IV following 24 hr of rotenone treatment (Figure 46-B and C). Remarkably, the activity of MRC complex II which is entirely nuclear DNA encoded activity appeared to be preserved (Figure 46-D), in contrast to complex I, III & IV which are encoded by both nuclear and mtDNA. As shown in (Figure 64-B, C and D), a significant increase between controls measured at 24 and 48 hrs was noted in complex II-III ($p < 0.05$), complex IV ($p < 0.0005$) and complex II ($p < 0.05$). The results of MRC I, II-III and IV activities in rotenone-treated cells for 24 and 48 hrs are summarized in (Table 7).

As MRC complexes results were expressed as a ratio to CS activity to compensate for mitochondrial enrichment in the sample, the mitochondria-enriched marker was exhibited to be comparable following rotenone-treated cells for 24 and 48 hrs (Figure 47).

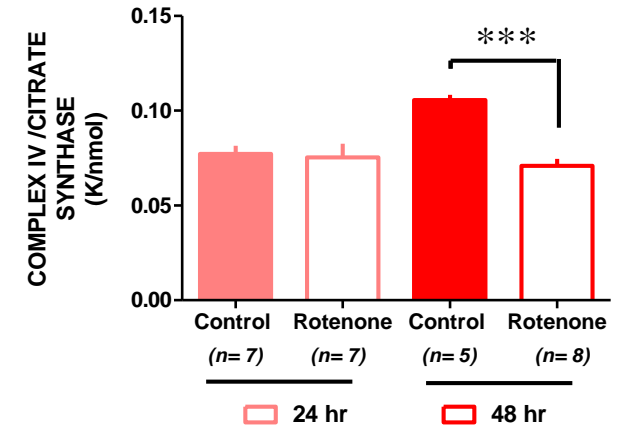
A)



B)



C)



D)

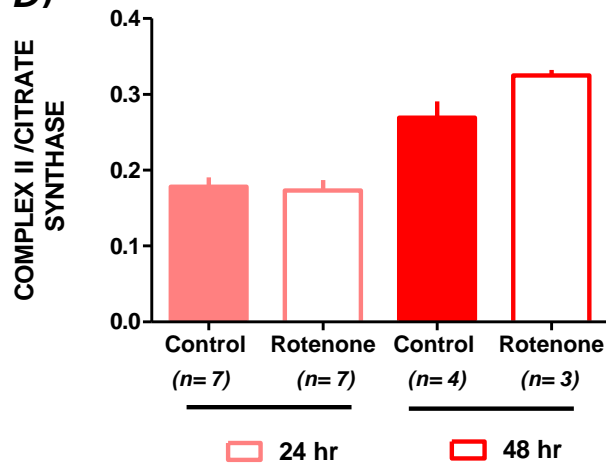


Figure 46 MRC complexes activities are expressed as a ratio to CS activity in SHSY5Y cells treated with 100 nM of rotenone for 24 and 48 hrs. **A.** MRC complex I activity **B.** MRC complex II-III activity **C.** MRC complex IV activity **D.** MRC complex II. Error bars indicate SEM of (n= 3-9) of independent experiments; statistical analysis was carried out using unpaired student's t-test; significant differences: * $p < 0.05$; ** $p < 0.005$; *** $p < 0.0005$.

Table 7 MRC complex I, II-III and IV activities are expressed as a ratio to CS activity in SHSY5Y cells treated with 100 nM of rotenone

MRC Activity	24 hr		48 hr	
	Control	Rotenone-treated SH-SY5Y Cells	Control	Rotenone-treated SH-SY5Y Cells
Complex I	0.40 ± 0.01 (n= 9)	0.28 ± 0.01*** (n= 9)	0.37 ± 0.01 (n= 9)	0.23 ± 0.01*** (n= 9)
Complex II-III	0.22 ± 0.01 (n= 7)	0.20 ± 0.01 (n= 7)	0.30 ± 0.02 (n= 5)	0.17 ± 0.01*** (n= 8)
Complex IV (k/nmol)	0.074 ± 0.004 (n= 7)	0.075 ± 0.007 (n= 7)	0.10 ± 0.002 (n= 5)	0.075 ± 0.005*** (n= 8)
Complex II	0.17 ± 0.01 (n= 7)	0.17 ± 0.01 (n= 7)	0.27 ± 0.02 (n= 4)	0.32 ± 0.007 (n= 3)

Results represent as mean ± SEM of (n= 3-9) of independent experiments.

***denotes a statistically significant decrease, compared to control value (**p < 0.0005).

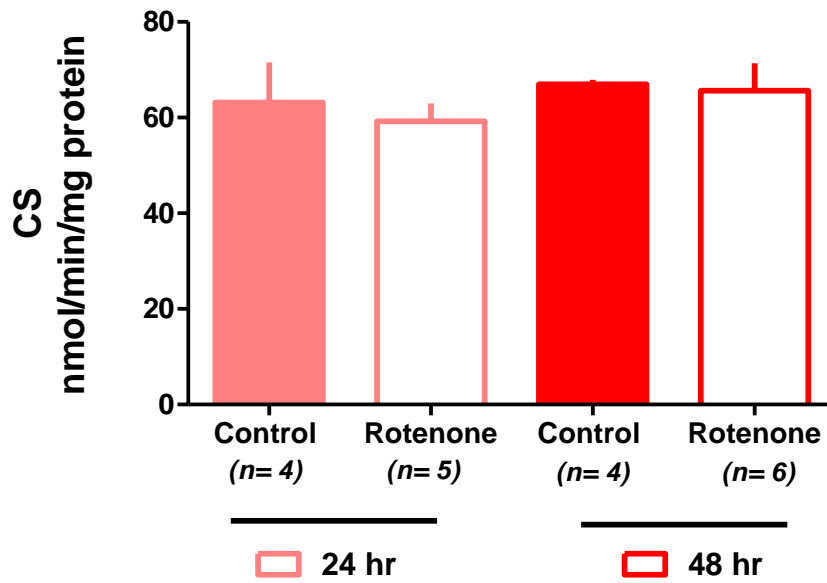


Figure 47 CS activity in SH-SY5Y cells treated with 100 nM of rotenone for 24 and 48 hrs. Error bars indicate SEM of ($n= 4-10$) of independent experiments; statistical analysis was carried out using unpaired student's t -test; significant differences: $**p<0.005$.

4.4.2 Measurement of Cellular Energy Charge

To gain more insight into the mechanism of how MRC complex I inhibition affects bioenergetics status over time, we assessed adenosine nucleotides, the levels of which are very tightly regulated under normal physiological conditions. Although there was no significant effect of rotenone on the adenylate energy charge at 24 hr, it was significantly decreased after 48 hr ($p < 0.0005$) (Figure 48- A), compared to control cells. As would be expected a decrease levels in ATP ($p < 0.0005$) (Figure 48- B), were observed with parallel increases in ADP ($p < 0.0005$) (Figure 48- C), ATP/ADP ratio ($p < 0.0005$) (Figure 48- D), and AMP ($p < 0.005$) (Figure 48- E).

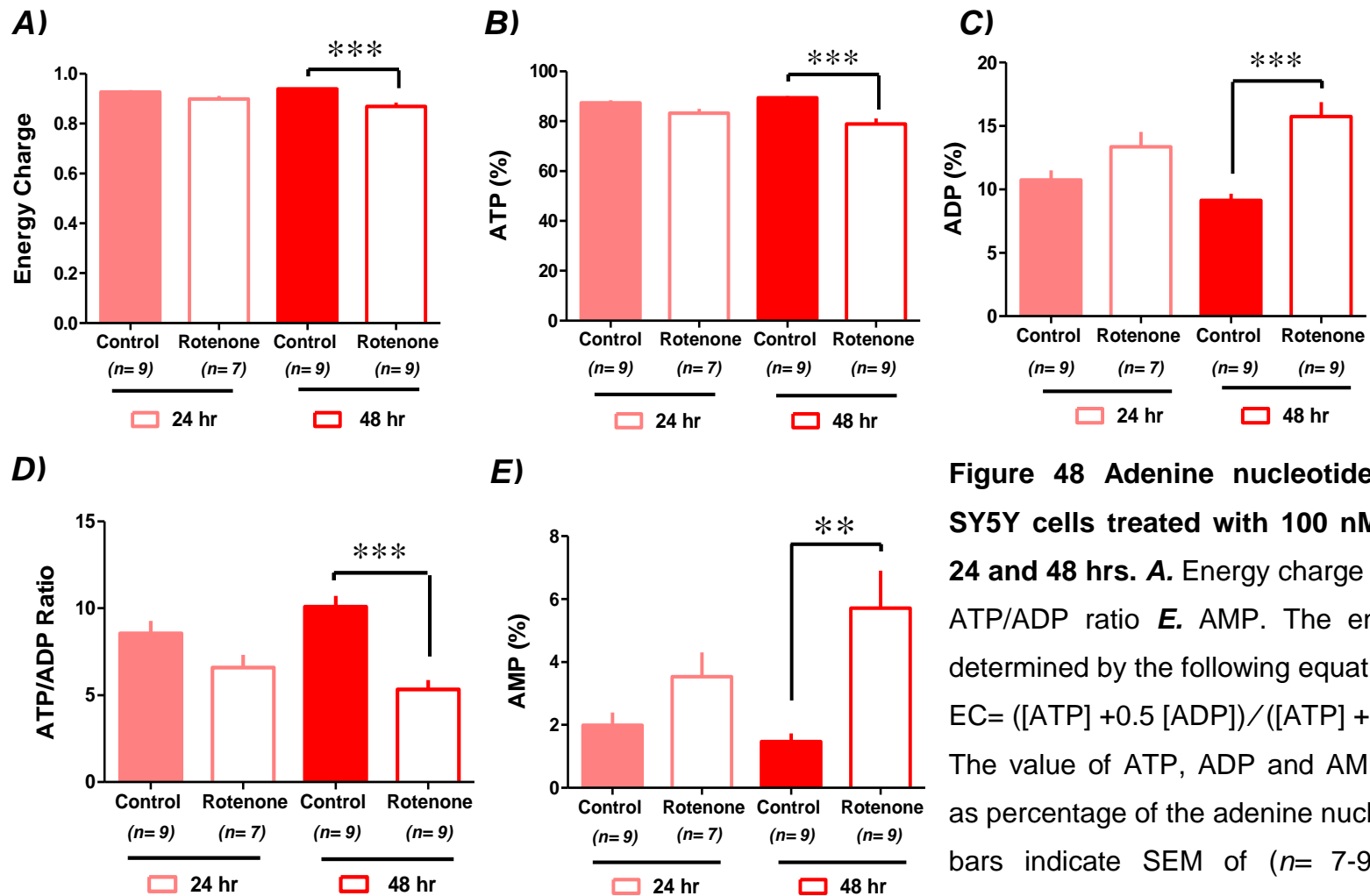


Figure 48 Adenine nucleotides status in SH-SY5Y cells treated with 100 nM of rotenone for 24 and 48 hrs. A. Energy charge B. ATP C. ADP D. ATP/ADP ratio E. AMP. The energy charge was determined by the following equation: $EC = ([ATP] + 0.5 [ADP]) / ([ATP] + [ADP] + [AMP])$. The value of ATP, ADP and AMP were expressed as percentage of the adenine nucleotide pools. Error bars indicate SEM of ($n = 7-9$) of independent experiments; statistical analysis was carried out using unpaired student's *t*-test; significant differences: ** $p < 0.005$, * $p < 0.0005$.**

4.4.3 Measurement of Coenzyme Q₁₀

Since the MRC complex II-III activity is dependent upon the endogenous CoQ₁₀ availability (Hargreaves, 2003), we assessed the intercellular CQ₁₀ level in SH-SY5Y cells after exposure to rotenone for 24 and 48 hrs. Although there was no significant change of rotenone on the intercellular CQ₁₀ level at 24 hr, it was significantly increased (80 %) after 48 hr ($p < 0.0005$) when expressed on a protein baseline (pmol/mg) (Figure 49). However, no significant change was observed once CQ₁₀ levels were expressed as a ratio to CS activity (Figure 50).

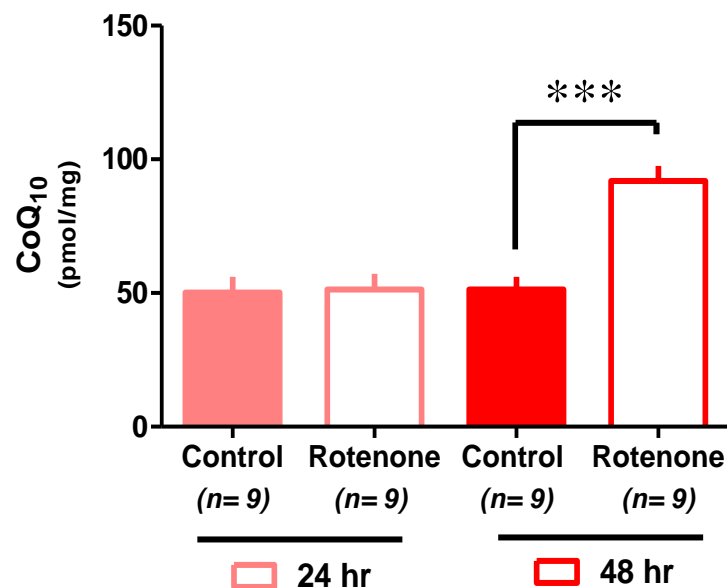


Figure 49 CoQ₁₀ level in SH-SY5Y cells treated with 100 nM of rotenone for 24 and 48 hrs. Error bars indicate SEM of ($n = 9$) of independent experiments; statistical analysis was carried out using unpaired student's t -test; significant differences: *** $p < 0.0005$.

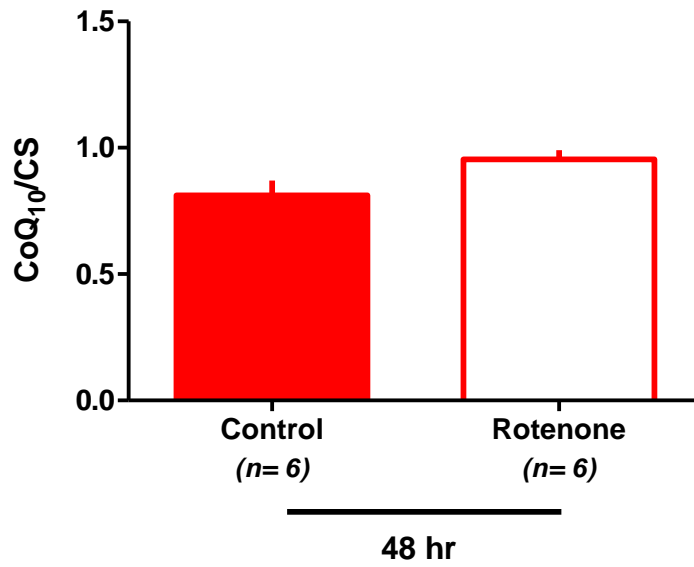


Figure 50 CoQ₁₀ level is expressed as a ratio to CS activity in SHSY5Y cells treated with 100 nM of rotenone for 48 hr. Error bars indicate SEM of ($n = 6$) of independent experiments; statistical analysis was carried out using unpaired student's *t*-test; there was no statistical differences

4.4.4 Measurement of Reduced Glutathione (GSH)

Being a key antioxidant among other soluble antioxidants in the brain, depletion in GSH status is also considered to be an early indicator of oxidative stress (Jha et al., 2000). Hence, we measured the intracellular status of GSH in rotenone-treated SH-SY5Y cells for 24 and 48 hrs. Following 24 hr rotenone treatment, the intracellular GSH status was significantly upregulated (up to 30 %) ($p < 0.005$) compared to the control cells, whereas it was found to be significantly depleted by (23%) ($p < 0.05$) after 48 hr of exposure SH-SY5Y cells to rotenone (Figure 51).

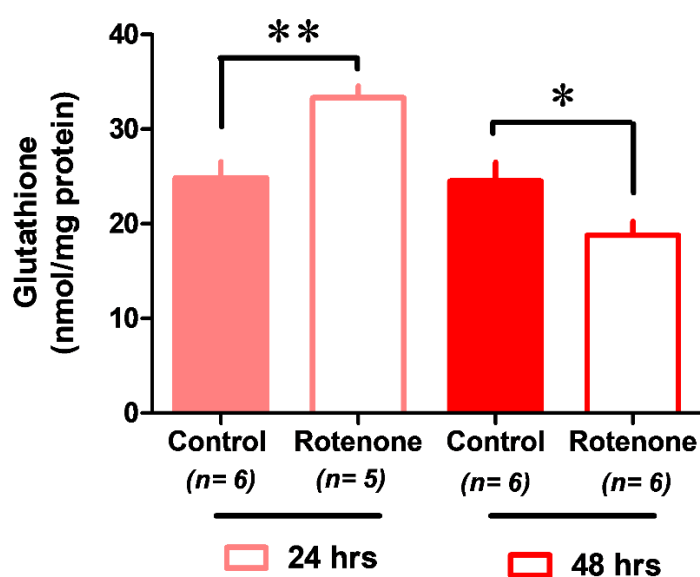


Figure 51 GSH status in SH-SY5Y cells treated with 100 nM of rotenone for 24 and 48 hrs. Error bars indicate SEM of ($n = 5-6$) of independent experiments; statistical analysis was carried out using unpaired student's t -test; significant differences: * $p < 0.05$, ** $p < 0.005$.

4.5 Discussion

The MRC complex I deficiency causing oxidative stress has a potential implication in patients with PD. In addition to the observation in the post-mortem PD brains detailed in the previous chapter, it has been also shown in some cases that multiple respiratory chain complex deficiencies have been associated with complex I deficiency of inherited mitochondrial disorders. The exact underlying mechanism of a multiple complex defect is not yet fully elucidated. However, it has been hypothesized that impairment of MRC complex I results in secondary oxidative damage to the other complexes. To investigate this hypothesis, a model of MRC complex I deficiency was assessed in neuron-like SH-SY5Y cells by treating cells with rotenone, an inhibitor of MRC complex I. Exposure of SH-SY5Y cells to 100 nM of rotenone for 24 and 48 hrs decreased cell viability by 30% and 50 % respectively, when compared to the control. At this concentration, rotenone induced a 30% inhibition of MRC complex I activity ($p < 0.0005$) following 24 & 48 hrs of rotenone treatment, a level of inhibition which has been frequent reported with idiopathic PD patients. Additionally, the level of inhibition of MRC complex I in this model was insufficient to compromise bioenergetics status as shown in (Figure 45). Furthermore, evidence from our laboratory also showed that partial MRC complex I inhibition using 100 nM of rotenone may enhance mitochondrial ROS production (Aylett et al., 2013), suggesting that rotenone-induced neuronal cell death could be as the result of oxidative damage rather than a deficit in ATP level.

It is of note that a mild increase between controls measured at 24 and 48 hrs is apparent in complex II-III, IV, and II although assays of control and

treatment samples were always performed in parallel on the same day with the same batch of reagents (Figure 46). There are a number of possible explanations for this such as slight variation in assay conditions, or increase in cell number, emphasising the absolute need for an appropriate matched control. Furthermore, it is worthy to emphasise that SH-SY5Y cell line is cancerous in origin which may consequently affect its proliferation rate, viability, metabolic and genetic properties (Xicoy et al., 2017). This could further explain the variations between controls measured at 24 and 48 hrs.

The enzymatic results of the present study have also indicated that multiple mtDNA-encoded MRC activities including MRC complex I (30% inhibition), II-III (40% inhibition) and IV (30 % inhibition) were significantly reduced after prolonged exposure of neuronal cells to rotenone for 48 hrs (Figure 46), while MRC complex II which is entirely nuclear DNA encoded activity appeared to be unaffected. These findings suggest that an increase in ROS production resulting in oxidative stress could be a possible mechanism since mtDNA is particularly susceptible to oxidative damage, unlike nDNA. As MRC complex I is the major site of ROS production within mitochondria and is also encoded by seven mtDNA genes, in comparison to other mitochondrial complexes, it therefore has a proportionally high susceptibility to oxidative damage.

Furthermore, the present study has also showed the evidence for alterations in the adenine nucleotide pool (ATP+ADP+AMP) together with energy charge status after 48 hr of exposure SH-SY5Y cells to rotenone (Figure 47). Consequently, increased the adenine nucleotides is also accompanied by increased level of ATP/ADP ratio. This suggests that prolonged exposure of

neurons to rotenone may lead to compromise bioenergetics status. Furthermore, the 5' AMP-activated protein kinase (AMPK) may be stimulated which consequently leads to enhanced glycolysis by phosphorylating Phosphofructokinase-2 (PFK-2) (Wu and Wei, 2012).

GSH has a fundamental cellular redox function as a key antioxidant and has a potential as an earliest indicator for oxidative stress. Subsequent studies reported that the loss of GSH in substantia nigra pars compacta (SNpc) of PD patients has been detected at the earliest stage of PD-related pathology, even preceding a decreased in MRC complex I activity (Bharath et al., 2002). In accord with the above study, depletion of GSH status has been demonstrated to lead to MRC complex I inhibition and compromised energy levels in a dopaminergic PC12 cell lines (Jha et al., 2000). Thus, we assessed the neuronal GSH status in rotenone- treated cells, which was found to be significantly increased up to (30%) following 24 hr rotenone treatment (Figure 50), indicating that may reflect an upregulation in the synthesis of GSH in order to cope with increased oxidative stress. Similar observation was also reported by (Zhu et al. 2007 and Duberley et al., 2014). The plausible cause associated with the upregulation of neuronal GSH status in a partially inhibited MRC I model is not fully understood. However, the possible explanation of this upregulation may be as the result of the activation of the antioxidant response element signalling pathway, nuclear factor-erythroid 2 related factor 2 (Nrf-2), which is an important regulatory factor to enhance gene expression of cellular antioxidant enzymes such as GSH biosynthesis (Harvey et al., 2009). Interestingly, cells treated with rotenone for 48 hr were found to be significantly decreased in GSH status (Figure 51), with a concomitant

depletion in ATP level ($p < 0.0005$) (Figure 48), supporting the hypothesis that oxidative stress may contribute to the pathophysiology of multiple MRC deficiencies. As GSH biosynthesis is an ATP-dependent mechanism, the OXPHOS pathway supplies the ATP for two- enzymatic steps involved in GSH biosynthesis which in turn resists the capacity of oxidative stress by neutralize free radicals. Accumulating evidence suggest that the loss of GSH is associated with MRC defects. Thus, profound defect in OXPHOS complexes-producing ATP may indirectly lead to reduced GSH biosynthesis resulting in increased oxidative stress which consequently leads to neuronal cell death.

A deficiency in intracellular CoQ₁₀ level has been reported in PD (Hargreaves et al., 2008). Furthermore, since the MRC complex II-III activity is dependent upon the endogenous CoQ₁₀ availability, the reduction in the combined activity of MRC complex II-III may have resulted from a decrease in either CoQ₁₀ status or MRC complex III activity. Therefore, we assessed the level of endogenous CoQ₁₀ in neuronal cells following exposure to rotenone. Despite the reduction in MRC complex II-III activity following 48 hr rotenone treatment, there was a significant increase ($p < 0.0005$) in neuronal CoQ₁₀ level. Although CoQ₁₀ status was found to increase when expressed on a protein baseline (pmol/mg), when expressed as a ratio to CS, the CoQ₁₀/CS was found to be comparable to the control. Therefore, this increase in CoQ₁₀ status may reflect an increase in mitochondrial enrichment of the cell. However, more research into the precise cause of this finding is still necessary before obtaining a definitive answer. Taken together, these findings suggested that an alteration in neuronal CoQ₁₀ status is unlikely to be

responsible for the inhibition of MRC complex II- III activity associated with the exposure of neuronal cells to rotenone for 48 hr or post-mortem PD brain. This suggestion is further supported by the study of iNOS-expressing astrocytes, showing that there was no a significant change in CoQ₁₀ level, despite the reduction of MRC complex II-III activity (Heales et al., 1999).

4.6 Conclusion

Exposure of SH-SY5Y cells to 100 nM of rotenone induced an approximate (30%) significant inhibition of MRC complex I after 24 and 48 hrs. At 24 hr no effect could be recorded in the other complexes. However at 48 hr, significant inhibition of complex II-III (40%) and complex IV (30%) activity was noted. Additionally, bioenergetics and GSH status were compromised. It is interesting to note that the activity of MRC complex II which is entirely encoded by nDNA appeared to be preserved in contrast to MRC complex I, III, and IV which are encoded by both mtDNA and nDNA. This cell-based model, therefore, provides us insights into the underlying mechanism of multiple MRC complexes deficiencies associated with persistent MRC complex I deficiency in which could be exploited further for potential therapeutic interventions aimed at attenuating oxidative stress-induced multiple MRC complexes deficiencies.

CHAPTER 5

Evaluation of the Efficacy of Antioxidants on Mitochondrial Respiratory Chain Dysfunction in a Neuronal Cell Model

5.1 Background

Mitochondrial respiratory chain (MRC) complex I activity is considered to be the rate-limiting step of the overall MRC activity and oxidative phosphorylation pathways, and it is particularly susceptible to reactive oxygen species (ROS)-mediated oxidative stress (Sharma et al., 2009). Furthermore, a defect in MRC complex I activity is regarded as one of the major contributing factor to several inherited and age-related mitochondrial disorders such as Parkinson's disease (PD) (see the chapter 1). Despite substantial efforts over the last decades aiming to identify the underlying mechanism responsible for the impairment of mitochondrial complex I activity, there is still currently no effective treatment available to restore or delay the progression of mitochondrial complex I defect. Based on recent studies focusing on the underlying mechanism of mitochondrial dysfunction, it has become clear that oxidative stress is a pathogenic factor in the aetiology of both inherited and acquired mitochondrial disorders associated with MRC complex I defect (see the chapter 1).

As was reviewed in the Chapter 1, to cope with increased free radicals produced as by-products of aerobic respiration, the human body is endowed with a number of enzymatic and non-enzymatic defence molecules, collectively known as antioxidants, which both protect the cellular biomolecules from the deleterious effects of free radical species. However, any loss in antioxidant status may lead to the accumulation of free radicals and resulting oxidative damage. Therefore, strategies to suppress oxidative damage and enhance mitochondrial function by antioxidants may hold a promising therapeutic intervention for patients with oxidative stress-associated

mitochondrial disorders (reviewed by Al Shahrani et al., 2017). Amongst the potential antioxidants available are ascorbate (vitamin C), α -tocopherol (vitamin E), and glutathione (GSH), which are the most commonly used antioxidants demonstrated to have their protective effects by alleviating oxidative stress (Yai and Herb, 2007).

5.1.1 Ascorbic Acid (Vitamin C)

Vitamin C, particularly the reduced form, ascorbic acid (AA) or L-ascorbic acid, is one of the water-soluble free radicals scavenger in the circulation (Yai and Herb, 2007). However, vitamin C is a “double-edge sword” which can also acts as prooxidant, particularly in the presence of redox-active metal ions such as Fe^{+3} and Cu^{2+} (Carr and Frei, 1999). Additionally, vitamin C also acts as an essential cofactor in the biosynthesis of collagen, carnitine, and neurotransmitters (Chambial et al., 2013). This water soluble vitamin cannot be endogenously synthesised by human due to the deficiency of gulonolactone oxidase, an essential enzyme for AA biosynthesis (Chambial et al., 2013). Thus, it is required to obtain from food or dietary supplements to ensure appropriate amounts of this vitamin are available for biochemical metabolism and protection.

Vitamin C is absorbed from the small intestine and has the ability to cross the plasma membrane in its oxidized form (dehydroascorbic acid, DHA) via glucose transporters. Once within cells, DHA is immediately reduced to generate AA, which then in turn is available to functionally attenuate any free radical-induced oxidative damage (Yai and Herb, 2007). Among all human tissues, the highest concentration of AA is located in the brain with concentrations in the range of 2-10 mM (Harrison and May, 2008). It is taken

up by the brain via the sodium-dependent vitamin C transporter 2 (SVCT2) which consequently leads to an accumulation of AA within neuronal cells against a plasma concentration gradient (Harrison and May, 2008).

Vitamin C is also a potent reducing agent, which is capable of neutralizing free radicals by donating high-energy electrons. Once acting as antioxidant, vitamin C is converted into oxidized form and subsequently regenerated back into AA by glutathione-dependent dehydroascorbate reductase (DHA reductase), thereby enabling it to release further electrons (Rose and Bode, 1992). In addition to being a potent radical-scavenging antioxidant in the circulatory system and cells, vitamin C also synergistically participates in recycling vitamin E back into an active form (α -tocopherol) by reducing tocopheroxyl radicals, thus enabling it to indirectly protect cellular membranes and other hydrophobic compartments from peroxidation (Figure 52) (Traber and Stevens, 2011). Additionally, vitamin C is independently maintained in a reduced form (AA) by the action of the thiol-containing antioxidant, reduced glutathione (GSH) (Figure 52) (Forman et al., 2008).

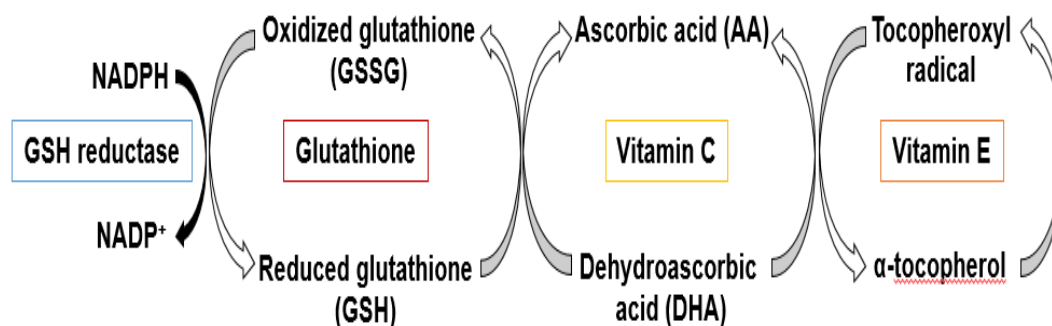


Figure 52 Vitamin C acts as a powerful antioxidant alone or synergistically with other free radical antioxidants, such as GSH and α -tocopherol.

5.1.2 α -Tocopherol and its Analogue

Vitamin E, in the form of α -tocopherol is a lipid-soluble antioxidant found in biological membranes. Lipid peroxidation is considered to be one of major consequences of free radical damage that occurs in most cellular membranes (Traber and Stevens, 2011). This peroxidation occurs in three steps: initiation, propagation, and termination. Under physiological condition, α -tocopherol acts as a chain breaking antioxidant, which inhibits the propagation of autoxidation of unsaturated lipids reaction (Burton et al., 1983). This occurs once α -tocopherol transfers its a phenolic hydrogen (H^+) to the lipid peroxy radical ($LOO\bullet$) and converts it to a lipid hydroperoxide ($LOOH$). The tocopheroxyl radical which is produced during this reaction, is relatively stable and thereby insufficient to be able to initiate the lipid peroxidation again (Figure 53) (Esterbauer et al., 1991).

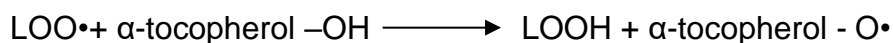


Figure 53 The reaction which α -tocopherol terminates lipid peroxidation reaction by scavenging the chain-carrying $LOO\bullet$

Several α -tocopherol analogues have also been shown to exert a potential antioxidant effects against oxidative damage mediated by lipid oxidation. Amongst the α -tocopherol analogues is Trolox (6-hydroxy-2,5,7,8-tetramethylchroman-2-carboxylic acid). Since it lacks the phytyl side chain, Trolox shows some advantages as a water-soluble antioxidant. Thus, it is able to incorporate easily into the lipid membrane without any solvent extraction and co-evaporation processes (Lúcio et al., 2009). Furthermore, although they

are structurally different, α -tocopherol and Trolox share similar redox potential (Lúcio et al., 2009). With regards to the phenolic OH-group, the chemical reactivity of α -tocopherol and Trolox are comparable (Naguib, 1998). Therefore, they are functionally involved in lipid radicals scavenging.

5.1.3 Reduced Glutathione and its Analogue

As was pointed out in details in the chapter 1, the tripeptide reduced glutathione (GSH) (γ -glutamyl-L-cysteinyl-L-glycine), is an intracellular thiol-containing water soluble antioxidant (Shahripour et al., 2014). In addition to its vital antioxidant role, GSH also functions as a cofactor for other antioxidant molecules including glutathione peroxidase (GPx, EC 1.11.1.9), and thioredoxin (Trx) as well as maintaining vitamins C and E to be functionally active (Birben et al., 2012).

As cysteine is a major component in GSH, it hinders GSH passage to cross the blood brain barrier (BBB). Thus, the modified N-acetyl cysteine (NAC) form, have been effectively utilized due to its increased ability to penetrate BBB (Farr et al., 2003). As such, this thiol antioxidant has also demonstrated to restore GSH level thereby alleviating the free radicals-induced oxidative damage (Kerksick and Willoughby, 2005). NAC is an acetylated cysteine residue and precursor of GSH which exerts a profound protective effect on cells against oxidative stress mainly by increasing the availability of intercellular glutathione (Shahripour et al., 2014). The sulfur-containing amino acid, cysteine is the rate-limiting substrate for GSH biosynthesis which is taken up by cells through the alanine-serine-cysteine (ASC) transporter. However, NAC is unique due to its ability to effectively

deliver cysteine into the cell without the ubiquitous ASC transport system (Sen, 1997). Upon entering the cell, the membrane-permeable cysteine precursor, NAC rapidly releases cysteine via a hydrolysis reaction, which can then serve as a precursor for GSH biosynthesis (Figure 54). The structures and functions of the antioxidants ascorbate, Trolox and NAC are summarised in (Table 8).

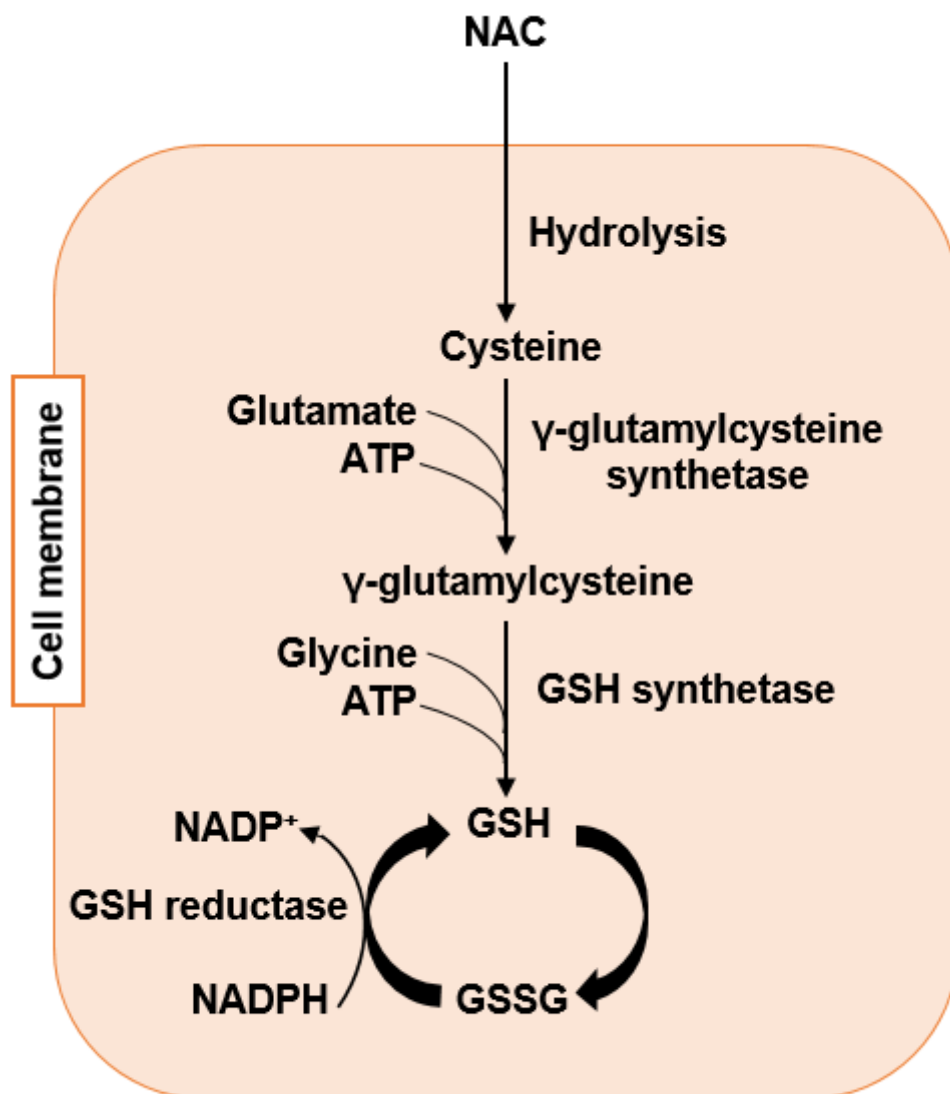
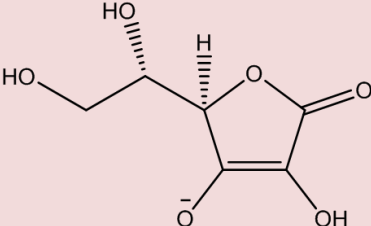
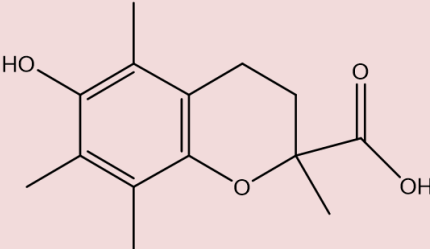
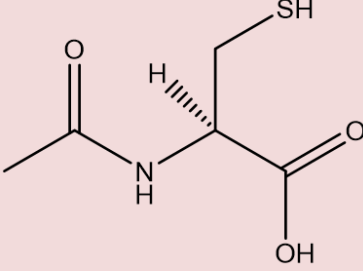


Figure 54 The potential mechanism of the membrane-permeable cysteine precursor, N-acetylcysteine (NAC).

Table 8 The structure and function of antioxidants ascorbate, Trolox and NAC

Antioxidant	Structure	Function
Ascorbate		<p>A potent radical-scavenging antioxidant in the circulatory system in addition to its connections to antioxidants such as vitamin E and GSH</p>
Trolox		<p>α-tocopherol analogue which is a cell-permeable antioxidant that breaks the lipid peroxidation chain reactions in biological membranes</p>
N-acetylcysteine		<p>GSH analogue acts as free radical scavenger by increasing the intracellular GSH status</p>

5.2 Aims

Our previous laboratory work have demonstrated that exposure SH-SY5Y cells to 100 nM of rotenone enhanced the mitochondrial ROS production (Aylett et al., 2013) Furthermore, the neuronal cell model detailed in chapter 4 provides us with insight into the underlying mechanism of multiple MRC complexes deficiencies which could be exploited for early therapeutic interventions aimed at attenuating defects in MRC complex I and its progression to other complexes. Therefore, the aim of this chapter is to build upon our previous works to evaluate and compare the effectiveness of ascorbate, Trolox and NAC at limiting/reversing multiple MRC complexes as consequence of rotenone treatment.

5.3 Methods

5.3.1 Cell Culture

SH-SY5Y cells were cultured as described in (Section 2.2) and were treated with 100 nM of rotenone for 24 and 48 hrs after reaching confluence as described in (Section 2.2.5).

5.3.2 Antioxidant Treatment

The antioxidant treatment concentrations of ascorbate, Trolox and NAC were appropriately chosen for screening based on their efficacious non-toxic effects as detailed in previous studies (Covarrubias-Pinto et al, 2015; Heales et al., 1994; Monti et al., 2016).

On the day of the experiment, stock solution of the sodium salt of ascorbic acid (ascobate; 10 mM), α -tocopherol analogue (Trolox; 5 mM), and the

glutathione analogue N-acetylcysteine (NAC; 10 mM), and were freshly prepared in sterile culture medium and filter sterilized (0.22µM). SH-SY5Y cells were cultured as described in Section 2.2.4. After reaching confluence, they were incubated with NAC, Trolox, and vitamin C at final concentrations of 500 µM, 500 µM and 1mM, respectively for 24 hrs after being pre-incubated without (antioxidant controls) or with 100 nm of rotenone previously for 24 hrs. Additionally, untreated and rotenone-treated SH-SY5Y cells were cultured for 48 hrs as appropriate controls. See (Figure 55) for further illustration of the experimental design described above.

5.3.3 Mitochondrial Enzymatic Assays

MRC complexes (I-IV) activities as well as CS activity in SH-SY5Y cells were determined spectrophotometrically at 30°C as described in (Section 2.5).

5.3.4 Statistical Analysis

Statistical analysis was carried out as described in (Section 2.7).

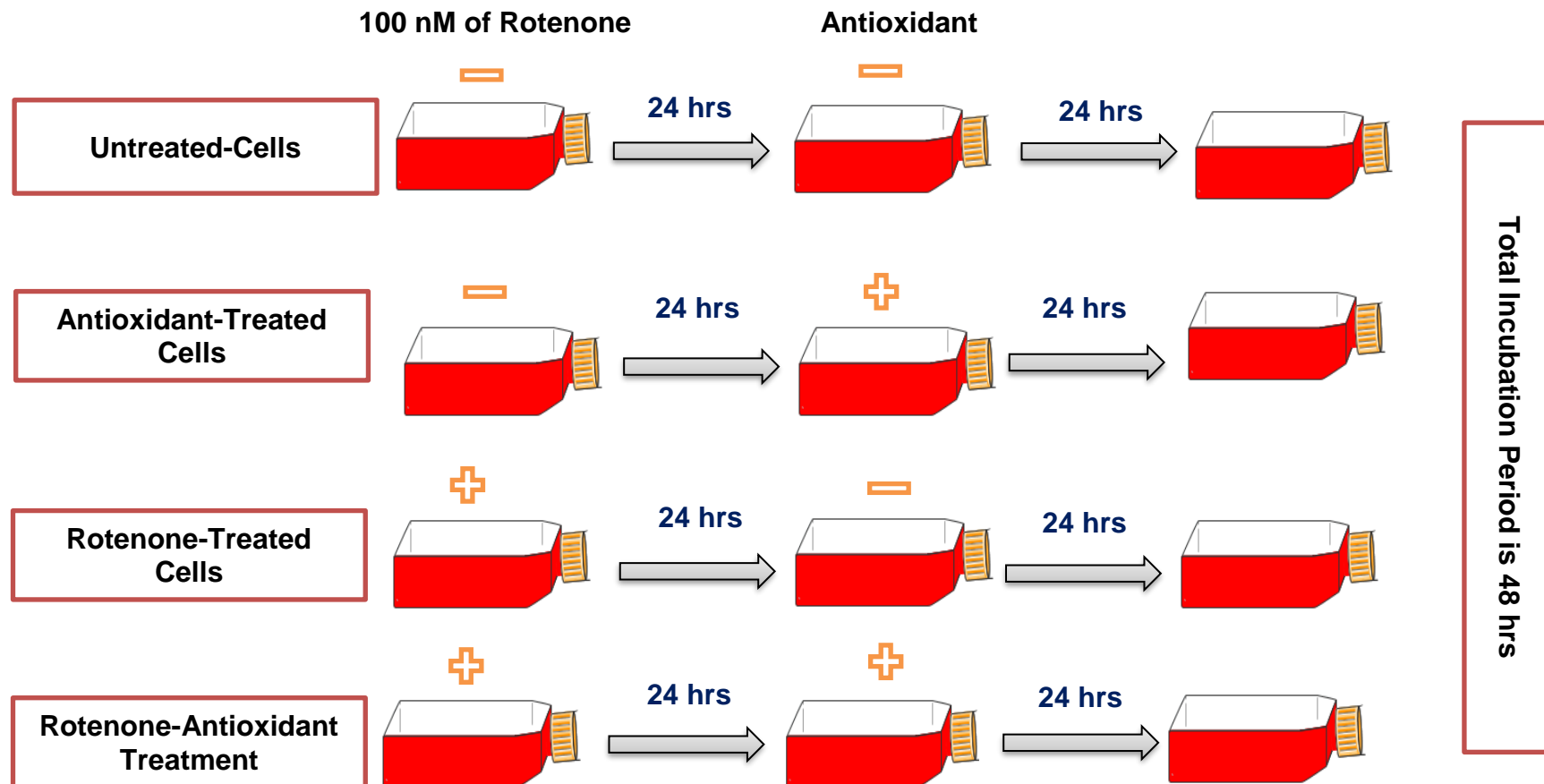


Figure 55 Schematic underlying the experimental design for rotenone and antioxidants treatment

5.4 Results

5.4.1 Evaluation of the Protective Effects of Ascorbate on MRC Complex I, II-III and IV Activity

SH-SY5Y cells were treated for 24 hr with (1.0 mM) ascorbate, after being exposed to rotenone for 24 hr. At the concentration tested, ascorbate was able to completely restore MRC complex I activity from approximately (60% to 100 %) of control cells ($p < 0.05$) (Figure 56-A). In addition to its potential effect to restore the defective MRC complex I activity, ascorbate treatment was similarly able to restore both MRC complex II-III activity to 100% of control cells ($p < 0.005$) as well as MRC complex IV to (~100%) of control cells ($p < 0.005$) (Figure 56-B and C).

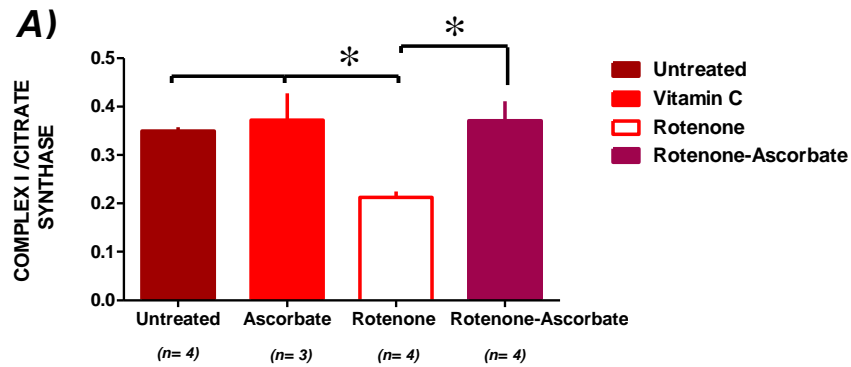
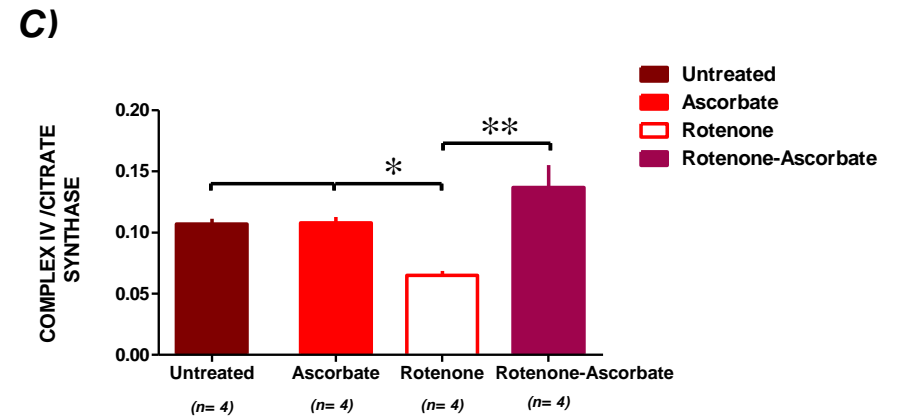
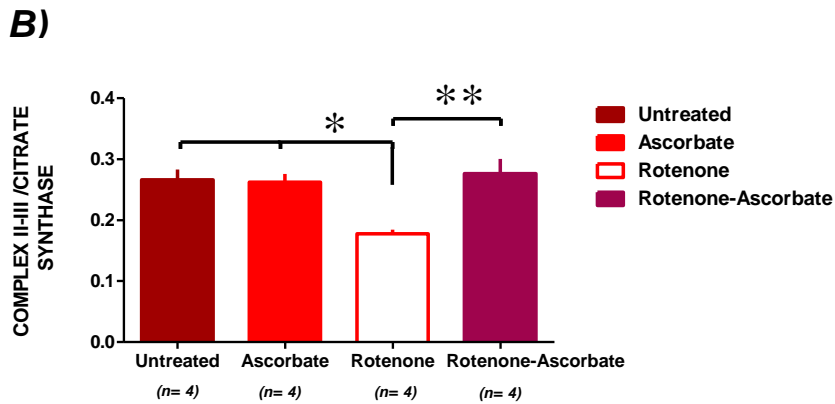


Figure 56 Effect of ascorbate (1.0 mM; 24 hr) on MRC complex I, II-III and IV activity after 24 hr exposure of SH-SY5Y cells to rotenone. Error bars indicate SEM of (n= 3-4) independent experiments; statistical analysis was carried out using one-way ANOVA followed by Tukey's *post hoc* test; significant differences: * $p < 0.05$; ** $p < 0.005$.



5.4.2 Evaluation of the Protective Effects of Trolox on MRC Complex I, II-III and IV Activity

SH-SY5Y cells were treated for 24 hr with (500 μ M) Trolox after being pre-exposed to rotenone for 24 hr. As compared with rotenone-treated cells for 48 hr, Trolox treatment was able to significantly increase MRC complex I activity by approximately (14 %) ($p < 0.05$) (Figure 57-A), but was unable to exert effect to the same order of magnitude to that of ascorbate. Although its effect didn't exhibit any significant improvement at restoring MRC II-III activity, Trolox was able to significantly increase MRC IV complex activity back to approximately 100% of control cells ($p < 0.0005$) (Figure 57-B and C).

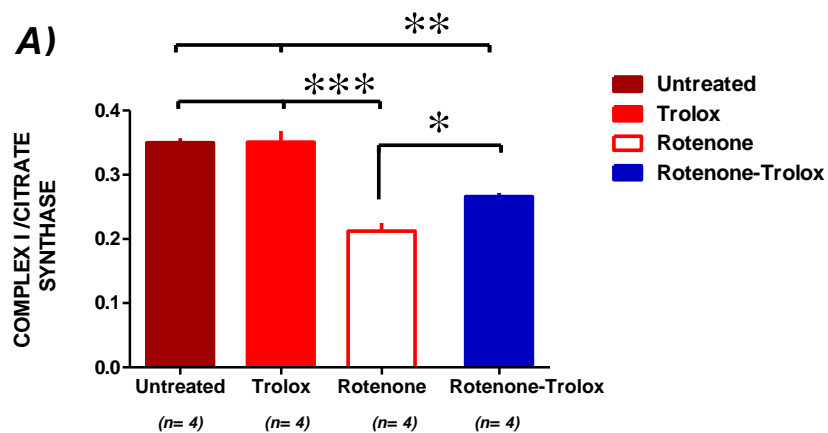
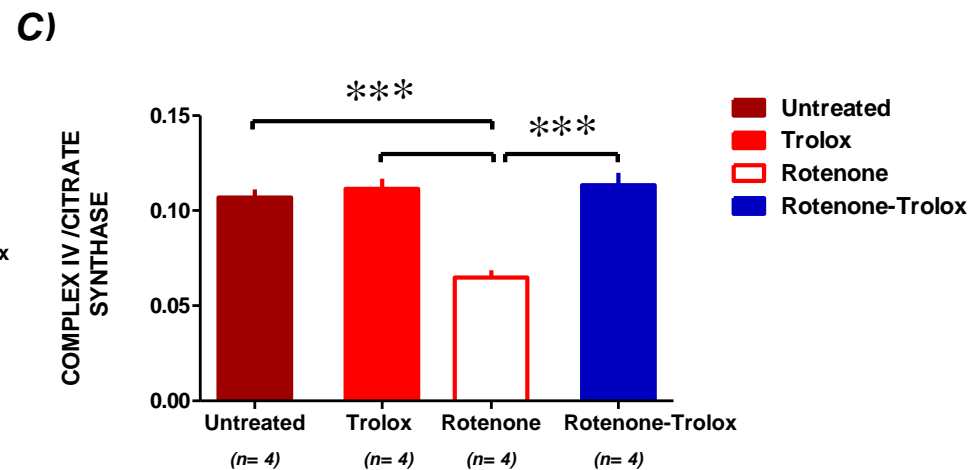
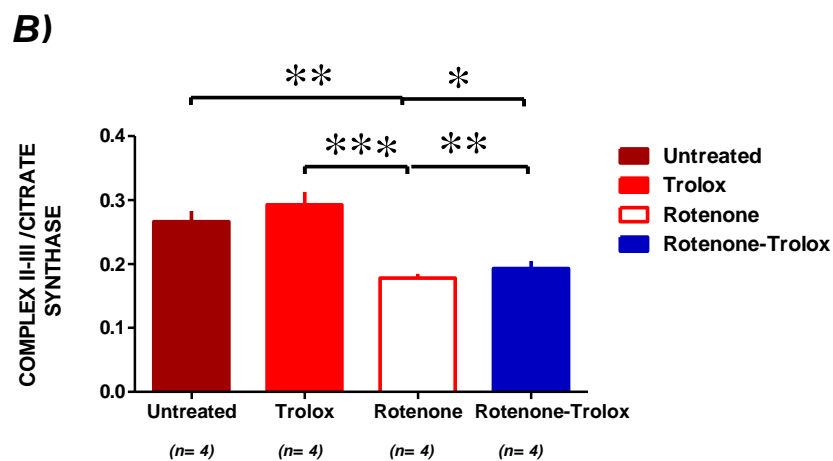


Figure 57 Effect of Trolox (500 μ M; 24 hr) on MRC complex I, II-III, and IV activity after 24 hr exposure of SH-SY5Y cells to rotenone. Error bars indicate SEM of ($n= 4$) independent experiments; statistical analysis was carried out using one-way ANOVA followed by Tukey's *post hoc* test; significant differences: * $p<0.05$; ** $p<0.005$; *** $p<0.0005$.



5.4.3 Evaluation of the Protective Effects of NAC on MRC Complex I, II-III and IV Activity

Following NAC treatment, a (20 %) increase above the rotenone effect was noted for MRC complex I activity, but this finding did not reach statistical significance (Figure 58-A). Although its antioxidant effects didn't exhibit any significant improvement at restoring MRC II-III activity (Figure 58-B), NAC showed a significant restoration of MRC IV complex activity to approximately 100% of control cells ($p < 0.0005$) (Figure 58-C). The protective effects of ascorbate, Trolox and NAC on MRC activity are summarised in (Table 9).

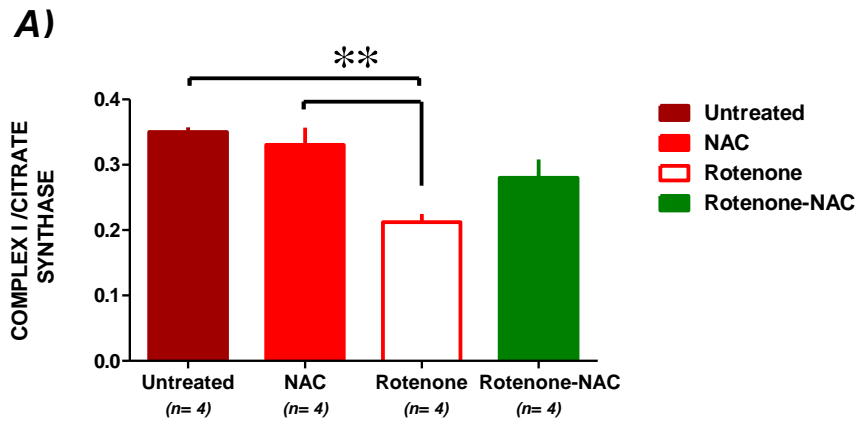


Figure 58 Effect of NAC (500 μ M; 24 hr) on MRC complex I, II-III and IV activity after 24 hr exposure of SH-SY5Y cells to rotenone. Error bars indicate SEM of ($n= 4$) independent experiments; statistical analysis was carried out using one-way ANOVA followed by Tukey's *post hoc* test; significant differences: * $p<0.05$; ** $p<0.005$.

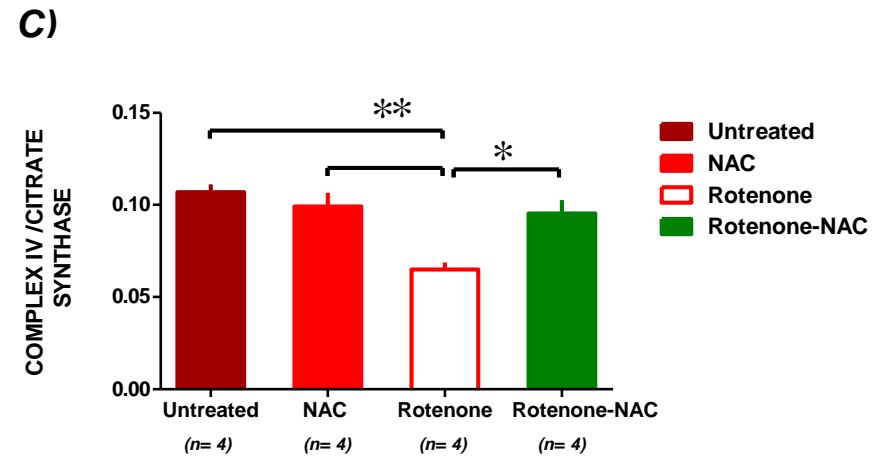
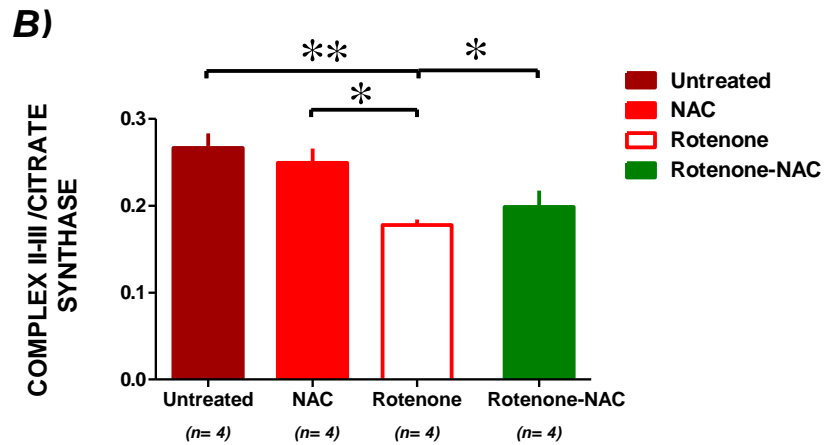


Table 9 The protective effects of ascorbate, Trolox and NAC on MRC activity in rotenone-treated cells

MRC Activity* (%)	Rotenone	Rotenone-Ascorbate	Rotenone-Trolox	Rotenone-NAC
Complex I	60	100	74.3 (↑14.3%)	80 (↑20.0%)
Complex II-III	64.6	100	72.2 (↑7.6%)	72.2 (↑7.6%)
Complex IV	58.2	100	100	100

- The activities were expressed as a percent % of control cells.
- Numbers in brackets represent the increase in activity (%) due to the presence of the antioxidants.

5.5 Discussion

Despite significant advances that have been made towards the diagnosis and characterization of mitochondrial disorders, appropriate treatment still remains an obstacle. Numerous therapeutic strategies have been proposed and evaluated over the years with limited outcome. One therapeutic strategy that may hold promise is to suppress oxidative damage and improve mitochondrial function by the use of antioxidant molecules. With regards to PD, data obtained from clinical trials failed to show any significant effects using antioxidants such as coenzyme Q₁₀, vitamin E, and creatine. However, it has been reported that at the time of PD diagnosis, the majority of dopaminergic neurons have been already lost (Bernheimer et al., 1973). Consequently, any antioxidant interventions at this stage would be unable to prevent the subsequent neuron death. This therefore suggests that antioxidant intervention at early stage of PD would be needed to halt or slow down the neurodegenerative process. Taken together, we aimed in this present study to evaluate and compare the effects of the early intervention of three antioxidants which have different structure and mechanisms of action, including ascorbate, Trolox and NAC on MRC activity, employing a MRC complex I deficient neuron model that has been previously described in chapter 4.

In this screening study, SH-SY5Y cells treated with the above antioxidants at the levels utilized in this study for 24 hrs failed to show any toxicity when compared with untreated cells (Figure 56-58). The reduced form of vitamin C, ascorbate, is one of the most popular used supplements due to its potent

antioxidant activity. The ability of ascorbate to enhance mitochondrial function has been demonstrated (Mandl et al., 2009).

The results of the present study have demonstrated that this hydrophilic antioxidant fully restores the lowered activity of MRC complex I seen in cells treated with rotenone. In a similar fashion, ascorbate was efficiently able to restore MRC complex II-III and IV activities to 100% of control cells ($p < 0.005$). These findings corroborate the ideas of (Li et al., 2003), who showed that rotenone-mediated apoptosis via increasing mitochondrial ROS levels was almost fully blocked by ascorbate treatment, suggesting that ascorbate exerts its anti-apoptotic effect via its ability to alleviate ROS accumulation. However, whether this protective effect of ascorbate on complex I is due to its antioxidant properties or its action on blocking the action of rotenone are still elusive although likely to be a combination of both mechanism. It is apparent however that the complete restoration of complex II-III and complex IV which are unaffected by rotenone directly could be explained by an antioxidant effect. Therefore, these results need to be interpreted with caution and further work needed to fully elucidate the precise mechanism(s) of action.

In accordance with the present results, previous studies also have demonstrated that ascorbate administration has protective effects on fibroblasts from patients with Leigh syndrome caused by MRC complex I deficiency (Saada, 2011). Additionally, oxidative stress-mediated cell death was attenuated in fibroblasts of CoQ₁₀-deficient patients harbouring mutations in QoQ₂ after ascorbate administration (López et al., 2010). In fibroblasts of patients with defects in multiple MRC complexes, ascorbate treatment significantly enhanced ATP levels, coinciding with a reduction of ROS

production (Soiferman et al, 2014), suggesting that ascorbate acts as electron donor to MRC complex IV activity in addition to its antioxidant properties. Our enzymatic findings together with these above findings suggest that ascorbate treatment might therefore provide a therapeutic option for mitochondrial patients associated with oxidative stress. However, its beneficial effects cannot be extrapolated to all mitochondrial patients.

The water-soluble α -tocopherol analogue, Trolox, is an antioxidant involved in scavenging lipid peroxide radicals. The potential effects of Trolox in augmenting mitochondrial dysfunction have been previously reported (Blanchet et al., 2015). Thus, we have also studied the effects of Trolox on the enzymatic activity of MRC complexes in the complex I-deficient neuron model. SH-SY5Y cells treated with Trolox for 24 hrs were found to have significantly enhanced MRC complex I activity by (14 %) ($p < 0.05$) (Figure 57-A), but was unable to exert a same effect level as ascorbate does. In contrast to the MRC complex I finding, however, no significant evidence of Trolox effect was observed on MRC complex II-III activity. Since a progressive inhibition of MRC complex II-III was observed in the previous chapter, among other MRC complexes, it seems possible that this result in part be due to the concentration of Trolox tested not being sufficient enough to attenuate MRC complex II-III deficiency. Therefore, further work is required to determine the non-cytotoxic dose-dependent effect of Trolox.

In addition to its potential effect to recover the defective MRC complex I enzymatic activity in rotenone-treated SH-SY5Y cells, the enzymatic results demonstrated that a significant restoration of MRC IV complex activity to (100%) of control cells upon treatment with Trolox. The findings observed in

this study are in agreement with those of the previous studies that have examined the effect of Trolox on MRC activity. For instance, our laboratory have demonstrated that Trolox markedly protects MRC complex IV against endogenous NO-induced damage in astrocytes (Heales et al., 1994). Furthermore, chronic administration of Trolox significantly enhanced the activity of fully assembled MRC complex I in both healthy and patient fibroblasts from a complex I nuclear gene defect (Distelmaier et al., 2009a). This was accompanied by a restoration of mitochondrial membrane potential and calcium homeostasis associated with complex I deficiency (Distelmaier et al., 2009b). In PD models, Trolox markedly enhanced MRC complex I activity in both PINK1- and DJ-1-deficiency in dopaminergic neuronal cells (Shim et al., 2011). In the same study, Trolox was also found to enhance the activity of MRC complex IV in PINK1- deficient but not in the DJ-1-deficient neuronal cells. Taken together, these results suggest that Trolox may provide a potential therapeutic intervention in patients with defects in MRC complex I or IV activity.

The thiol antioxidant, NAC is the precursor of L-cysteine which in turn, enhances the intercellular glutathione status. The potential effects of NAC as an oxygen free radical scavenger has been extensively studied particularly in age-related mitochondrial disorders (Shahripour et al., 2014). We further investigated the protective effects of NAC on MRC enzymatic activity in SH-SY5Y cells exposed to rotenone for 48 hrs. As shown in (Figure 58-A), pre-treatment with antioxidant NAC for 24 hr increased MRC complex I by 20 % as compared to cells treated with rotenone alone for 48 hrs, but this increase was no statistically significant. Similarly to the effects observed with Trolox,

there was no significant effect on MRC complex II-III after NAC treatment. The weak impact of this thiol antioxidant on MRC complex II-III activity may be due to insufficient concentration utilized in this study such that it was not efficient enough to restore the activity of complex II-III. Another possible explanation is that there is a low bioavailability of NAC that limits its therapeutic usefulness as pointed out in the previous studies (Hara et al., 2017). Thus, administration of NAC over a long period of time at low concentrations could be an alternative therapeutic strategy, which could be used to optimize its protective effects (Ohnishi et al., 2014). Similarly to the effects of ascorbate and Trolox, the results of this study also showed that NAC significantly enhanced the activity of MRC complex IV activity. These findings are in agreement with previous findings that showed an increase in the activities of MRC complexes I, and IV in age-related mitochondrial disorders models (Miquel et al., 1995; Cocco et al., 2005; Kamboj and Sandhir, 2011).

5.6 Conclusion

From the results of this screening study it is possible to conclude that ascorbate evoked a complete restoration of multiple MRC activity in rotenone-treated SH-SY5Y cells. However, it is unlikely that this effect can be solely attributed to an antioxidant effect and as such, multiple mechanisms are likely to be responsible. Furthermore, the antioxidant effects of Trolox and NAC enhanced the activity of both complex I and IV, but not II-III. Taken together, ascorbate appears to be more effective than Trolox and NAC in alleviating MRC complexes defects caused by rotenone treatment. Due to its efficacy at multiple sites, it could be hypothesised that ascorbate may therefore provide

an adjunctive therapeutic intervention for patients with mitochondrial complexes defect when used in combination with other medication to slow down mitochondrial damage caused by oxidative stress. However, ROS threshold should also be considered as a parameter when selecting the appropriate antioxidant for patients with mitochondrial disorders associated with oxidative stress (reviewed by Al Shahrani et al., 2017).

CHAPTER 6

Mitochondrial Cellular Respiration Measurement Using High Resolution Respirometry

6.1 Background

The energy utilised from the passage of electrons the down mitochondrial respiratory chain (MRC) is utilised to pump protons from the mitochondrial matrix into the inner mitochondrial membrane space creating a proton motive gradient which is then harnessed to drive ATP synthesis from inorganic phosphate and ADP in process collectively known as oxidative phosphorylation (OXPHOS) (Figure 59) (Smith et al., 2012). Although the details concerning the conservation of this ATP production in cellular respiration is still controversial, the chemiosmotic coupling hypothesis is widely accepted as the plausible mechanism for the energy transfer (Menéndez, 1996). This hypothesis was first postulated by the British biochemist, Peter Mitchell who suggested that the hydrogen ions (H⁺) facilitated by electron transfer are pumped out of the basic and negatively charged mitochondrial matrix into the acidic and positively charged intermembrane space through the MRC complexes particularly I, III, and IV. This then results in the creation of the proton-motive force (PMF) (also known as chemiosmotic potential) which is harnessed by mitochondrial ATPase enzyme, complex V, to phosphorylate ADP and inorganic phosphate to ATP (Mitchell, 1961).

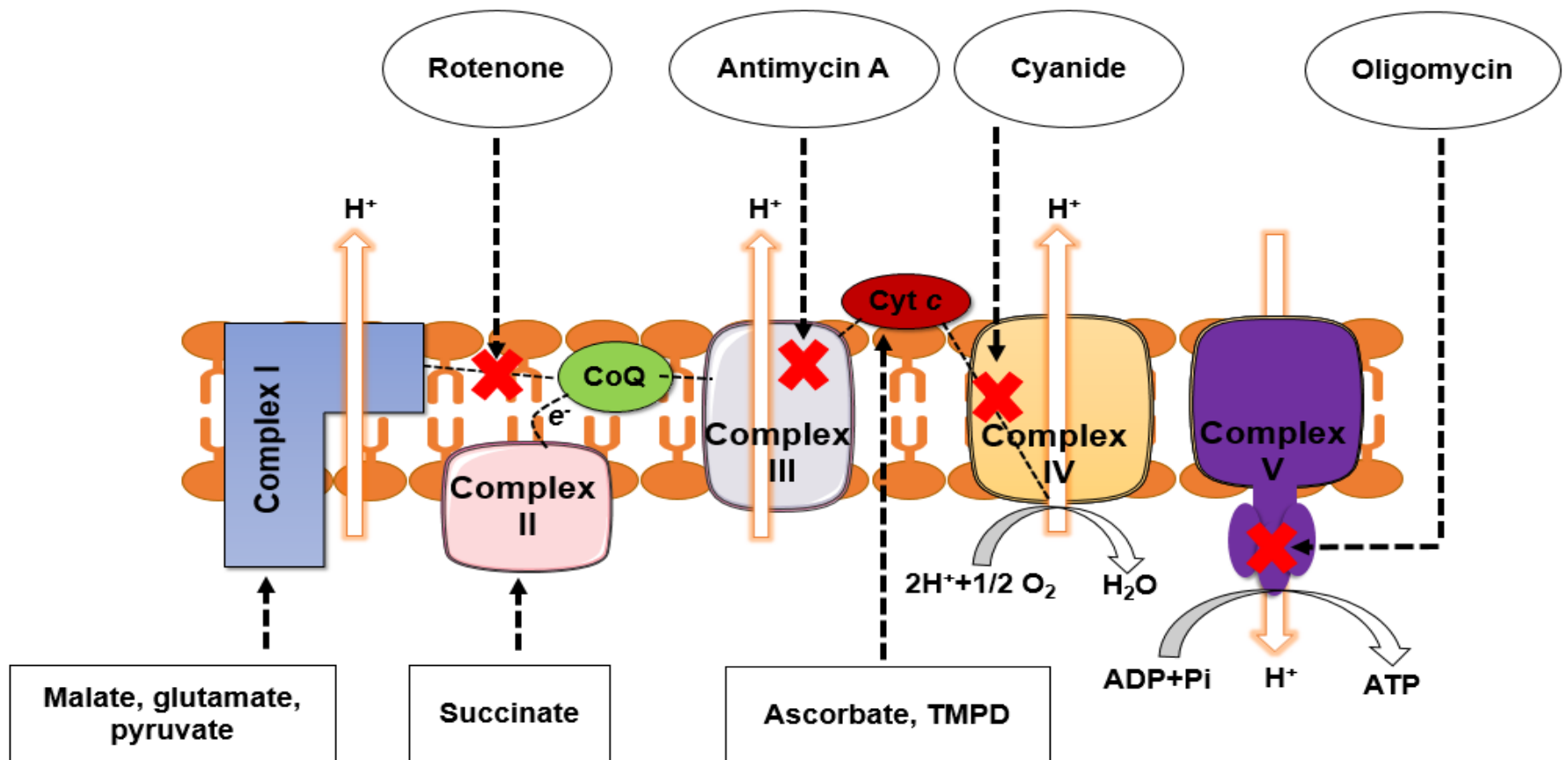


Figure 59 The schematic diagram outlines the MRC and OXPHOS pathways with substrates (electron donors) shown in rectangular box and inhibitors in circular box. CoQ, coenzyme Q; Cyt c, cytochrome c; TMPD, N,N,N',N'-tetramethyl-p-phenylenediamine.

The major site of ATP synthesis is the inner mitochondrial membrane which harbours a series of multi-subunit enzymes known as the MRC complexes. As mentioned above, these complexes utilize the energy conserved in electron passage to make ATP from ADP and inorganic phosphate. The transference of a pair of electrons through the MRC complexes releases redox energy which is sufficient to generate 3 ATP molecules. For instance, the donation of a pair of electrons from one molecule of NADH which are ultimately accepted by molecular oxygen creating a molecule of water, generates 3 ATP molecules (Gautheron, 1984). Thus, the ratio between oxidation and phosphorylation, recognized as (P:O) ratio, is 3:1. Furthermore, the passage of electrons from FADH₂ to oxygen generates 2 ATP molecules, thus the P:O ratio, is 2:1 (Gautheron, 1984). However, these P/O ratios of oxidative phosphorylation have been modified over years to 2.4 and 1.5 respectively, due to possibly proton leakage across the membrane (Hinkle, 2005).

The chemiosmotic coupling hypothesis was further supported by experiments that utilized uncoupling which dissociated ATP synthesis and other energy-dependent membrane functions from the process of electron transference in the MRC (Hopfer et al., 1968). Therefore, in the presence of uncoupling agents, electron transport in the MRC continues, but ATP is no longer produced. Furthermore, the rate of electron transport which is evaluated by the rate of oxygen consumption, is also stimulated in the presence uncoupling agents (Lechner et al., 1970).

Isolation mitochondrial from cultured cells or animal tissues retain the ability to carry out electron transport (Schägger, 2002). Currently, the process can be

manipulated by adding exogenous substrates that donate electrons to the MRC at different levels, or by the use of uncoupling agents as well as inhibitors of the MRC enzymes (Barrientos et al., 2009). Since the final step of MRC is the reduction oxygen molecule to water, the rate of the electron transport in isolated mitochondria can be feasibly monitored by the polarographic technique which is generally used to measure the oxygen consumption rate. The latter technique will be discussed in more detail in this section.

6.1.1 Mitochondrial Respiration States

Chance and Williams introduced the polarographic technique to assess the rate of MRC activity (Chance and Williams, 1956). They defined the respiratory states according to the order of substrate(s) additions evaluated in the isolated mitochondrial experiments. In a Subsequent study, Nicholls and Ferguson modified those definitions, providing an alternative sequence of substrate additions in their mitochondrial studies (Nicholls and Ferguson, 2002). Accordingly, the initial mitochondrial respiratory (State 1) refers to the rate of oxygen consumption in mitochondria in the absence of any addition of exogenous substrates or inhibitors. In (State 2), the O₂ consumption rate is increased following the addition of exogenous substrate(s) which can also can reflect the rate of basal proton conductance (i.e., leak) in the absence of ADP. The (State 3) refers to the stimulated respiratory rate following the addition of a small amount of ADP. State 3 can be terminated by the addition of the ATP synthase (complex V) inhibitor, oligomycin. State 3 respiration returns to State 4 once all the ADP has been phosphorylated to ATP (Figure 60). Furthermore, the respiratory control ratio (RCR) which is defined as `state

3/state 4, is often utilized as a parameter to indicate the coupling between respiration and phosphorylation. The amount of ATP synthesized per molecule of oxygen consumed by mitochondria, known as P/O ratio, is also another parameter to evaluate the integrity of mitochondria function. This can be calculated by measuring the decrease in oxygen concentration after the addition of a known amount of ADP.

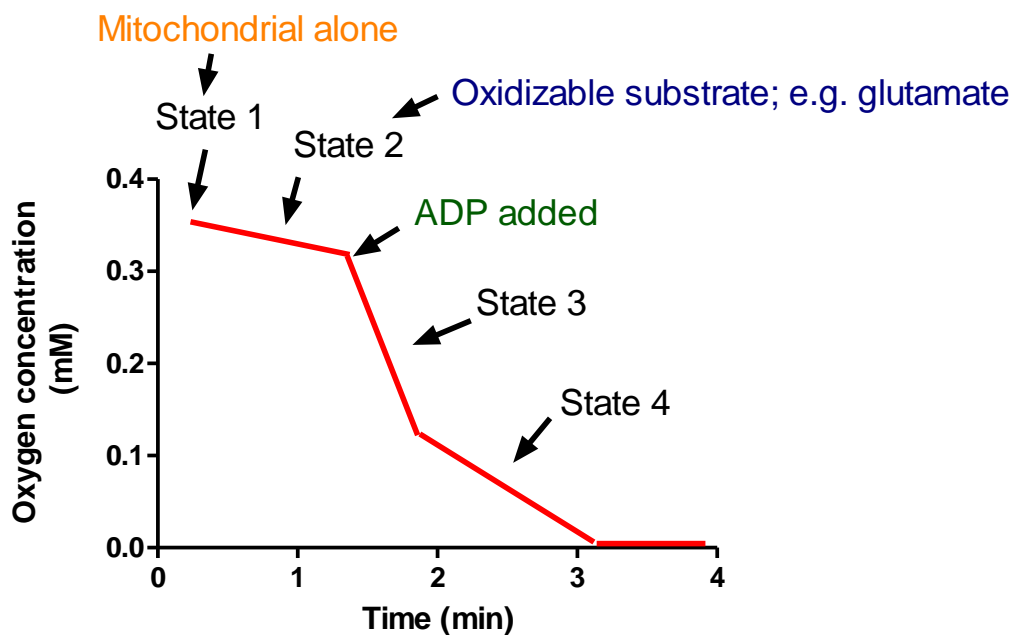


Figure 60 An experimental example of polarographic oxygen consumption showing mitochondrial respiration states upon addition of substrates.

Several exogenous substrates (electron donors) can experimentally be applied to initiate electron flow from the different enzyme complexes within the MRC of isolated mitochondria (Figure 59). This allows the rate of oxygen consumption to be assessed in the different regions of the MRC, allowing the identification of possible impairment of electron transfer within the chain. For instance, NADH-generating substrates including pyruvate, malate and

glutamate feed electrons indirectly into MRC at the level of complex I. Furthermore, FADH₂-generating substrates such as succinate feed electrons directly into the MRC at the level of complex II. Additionally, ascorbate and N,N,N',N'-tetramethyl-p-phenylenediamine (TMPD) also act as respiratory substrates, donating electrons directly to complex IV via cytochrome c. Moreover, mitochondrial respiratory rate can also be investigated using MRC enzyme complex inhibitors, such as rotenone and antimycin A (Figure 59). Following the addition of the inhibitor, exogenous substrates that act proximal to the inhibited enzyme complex can then be added to initiate electron flow in the MRC. For instance, if NADH is added to a suspension of isolated mitochondria, electron transference proceeds with the concomitant consumption of oxygen. If, however, the MRC complex I inhibitor, rotenone is added to this suspension, electron flow is terminated which ultimately leads to cessation of oxygen consumption. However, if succinate is then added to the rotenone treated mitochondrial suspension, the complex I inhibition created by rotenone is by-passed and electron transport and oxygen consumption will be initiated again. Some common substrates, inhibitors, and uncouplers of the MRC complexes are listed in (Table 10).

Table 10 The most commonly used substrates, inhibitors, and uncouplers of MRC function.

Name	Classification	Place of action
<i>Rotenone</i>	Inhibitor	MRC Complex I
<i>Malate</i>	Substrate	
<i>Glutamate</i>	Substrate	
<i>Pyruvate</i>	Substrate	
<i>Succinate</i>	Substrate	MRC Complex II
<i>Antimycin A</i>	Inhibitor	MRC Complex III
<i>Cyanide</i>	Inhibitor	MRC Complex IV
<i>Ascorbate</i>	Substrate	
<i>TMPD</i>	Substrate	
<i>Oligomycin</i>	Inhibitor	MRC Complex V
<i>FCCP</i>	uncoupler	Mitochondrial membrane

6.1.2 The Measurement of Mitochondrial Respiration

The rate of electron transference to molecular oxygen as a result of the oxidative phosphorylation (OXPHOS) pathway can be assayed polarographically using a Clark oxygen electrode. The Clark electrode was named after Dr. Leland Clark after its inventor in the mid-1960s (Severinghaus and Astrup, 1986). It typically consists of a platinum cathode and a silver or silver/silver chloride anode (Ag/AgCl), which are separated by a potassium chloride (KCl) solution. The two-half cells are separated from assay medium by a teflon membrane. As oxygen molecules move freely

across the membrane, they are electrically reduced as a result of a constant voltage (usually -0.6 V) applied between the electrodes, according to the following equation:



This reduction subsequently creates an electrical current which is proportional to the amount of oxygen in the solution. Thus, the rate of oxygen consumption in a biological sample can therefore be estimated by calibrating a known oxygen concentration to a particular voltage of electricity (Figure 61) (Lanza et al., 2009).

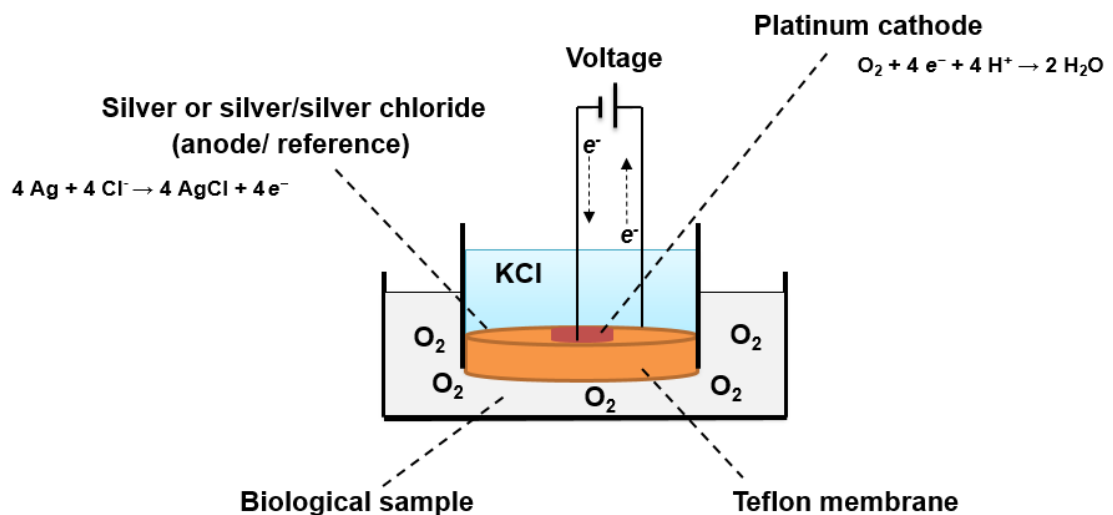


Figure 61 A schematic representation of Clark amperometric sensor for determining dissolved O₂ in biological sample.

There are a number of analytical techniques which are available for the evaluation of mitochondrial function. These include the enzymatic MRC complex assays, bioenergetics status, blue native polyacrylamide gel

electrophoresis, oxygen-derived radical assays, and ATP synthesis assays (Brand et al., 2011). Nevertheless, these analyses are destructive to biological samples, and do not provide an estimate of the activity of the MRC at the physiological level (Martin et al., 2012). As opposed to these analyses, assessing mitochondrial respiration by polarography reflects the integrity of mitochondria, which yields a dynamic evaluation of metabolic rates simultaneously in mammalian cells (Lanza et al., 2009). Furthermore, mitochondrial respiration provides an integrated bridge between the enzyme complexes and metabolic pathways, in contrast to evaluating activities of isolated or linked MRC complex enzymes (Pesta and Gnaiger, 2012). To date, the evaluation of integrated mitochondrial function has commonly relied upon the conventional Clark-type oxygen electrode. Although the Clark-type oxygen electrode is still less expensive and a widely accessible tool for the assessment mitochondrial respiration, it nevertheless has notable limitations and there are concerns in regards to its signal stability, resolution and background noise (Martin et al., 2012). To this end, a variety of technologically advanced Clark electrode systems were developed utilizing numerous other materials and configurations. One such system in which mitochondrial oxygen consumption can be accurately evaluated using high-resolution respirometry (HHR) is the Oxygraph-2K[®] (O2k, Oroboros[®] instruments. Innsbruck. Austria) (Figure 62).

Since its development in the mid-1990s, the O2k instrument has been utilized for the assessment of mitochondrial respiration (Gnaiger et al., 1995). Several features distinguish O2k from the traditional Clark-type oxygen electrode. For example, O2k consists of two-parallel and independent glass

chambers equipped with polarographic oxygen sensors (POS) which have the ability to assess both oxygen concentration (nmol/ml) and oxygen flux rate [pmol/(s*ml)] within each chamber in real time (Gnaiger, 2008). In addition to requiring only small quantities of biological sample, the oxygen concentration in each chamber can be kept constant throughout an experiment or until the functional stability of the sample is impaired. Thus, it enables further substrates, or uncouplers, or inhibitors to be applied. Furthermore, the limit for oxygen flux rate detection in the O2k is 1.0 [pmol/(s*ml)], and the limit of detection of oxygen concentration is less than 0.05 μ M (Gnaiger, 2008). The O2k, therefore, provides a direct and convenient way to evaluate integrated mitochondrial function.

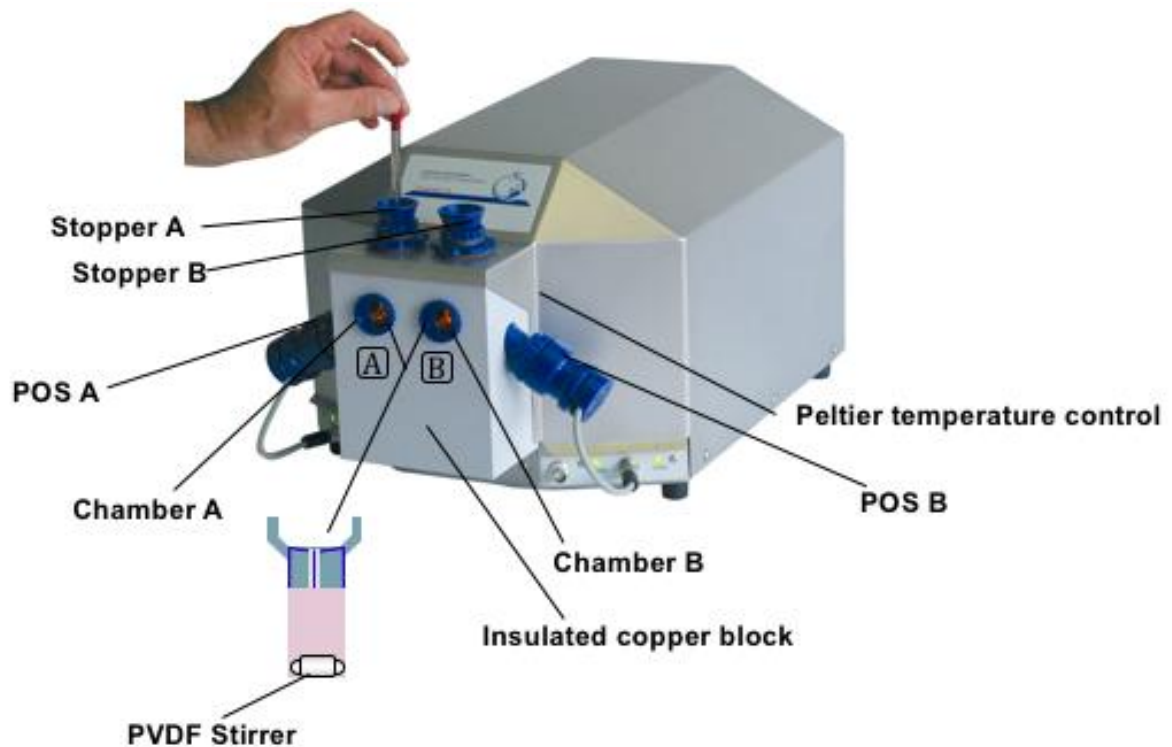


Figure 62 The Oxygraph-2K[®] (O2k) for high-resolution respirometry (HRR) instrument. The Oxygraph respiratory system is appropriately designed as two-parallel and independent glass chambers. The volume capacity of each glass chamber is 2 ml. The chambers feature a large inner diameter (16 mm), thereby yielding an effective space for sensors and light conductor. Along with two glass chambers, Peltier temperature control are placed into mineral-insulated copper block where the temperature in the range of 2–50 °C is electronically maintained. In addition to titanium stopper, oxygen level of mitochondria is simultaneously monitored by polarographic oxygen sensors (POS) with a large (2-mm diameter) cathode, (POS is defined as electrochemical sensor that measures dissolved oxygen in biological sample) which are inserted into each glass chamber. To minimize fluid current which is exposed by cathode, POS is inserted into each glass chamber in an angular position allowing optimal stirring. In order to account for artefacts as a result of oxygen diffusion, the electromagnetic polyetheretherketone (PEEK) stirrer bars are applied as an alternative to conventional Teflon (polytetrafluoroethylene, PTFE) stirrers. The image was adapted from (Gnaiger, 2008).

6.1.3 The Assessment of Integrated Mitochondrial Function in Cultured Cells

The loss of the enzymatic MRC activity is intimately associated with age-related disorders (see chapter 1). However, progress toward understanding of these disorders has been hampered by methodologies employed to evaluate the integrated mitochondrial function of the biological samples studied. Therefore, the ability to evaluate oxygen consumption rate in cultured cells is a decisive step forward for better elucidating the underlying mechanism of cellular heterogeneity in these disorders thus ultimately leading to the development of novel therapeutic strategies.

The measurement of mitochondrial oxygen consumption to study various aspects of neuronal mitochondrial function has been previously reported (Lesage et al., 2016; Zanellati et al., 2015; Cronin-Furman et al., 2013; Nakamura et al., 2011). An early study using isolated mitochondria from primary neuron and astrocyte cultures has highlighted the vulnerability of this neural cell to mitochondrial energy impairment (Almeida and Medina, 1997), providing a further evidence for the utility of oxygen consumption rate determination in neuronal mitochondrial studies. However, mitochondrial respiratory rates evaluated in intact cultured cells vary in comparison to rates measured in isolated mitochondria (Gnaiger, 2008). For instance, the ADP-stimulated rate (state 3) is not possible to evaluate in cultured cells since the cell membrane is not permeable to ADP. Recently, O₂k titration protocol was developed by applying mitochondrial inhibitors and uncouplers to measure the respiration rate in intact cultured cells such as SH-SY5Y neuroblastoma cells (Geoghegan et al., 2017; Boyle et al., 2012). Therefore, the development

and evaluation of this protocol using O2k instrument could provide us an effective way to assess the integrity of mitochondrial function in cultured SH-SY5Y cells.

6.2 Aim

The aim of this chapter was to develop a step-wise titration protocol for the O2k instrument which will enable the assessment of integrated mitochondrial function in cultured SH-SY5Y cells suspensions. This will serve as an introduction to further studies which will assess mitochondrial dysfunction using the cell-based model as previously described in chapter 4.

6.3 Methods

6.3.1 Cell culture

SH-SY5Y cells were passaged as describes in (Section 2.2.3). Once cells reached the desired degree of confluency (80-90%), culture medium was discarded and the flask washed once with Dulbecco's Phosphate Buffered Saline (DPBS) without Ca^{2+} and Mg^{2+} . 2 ml of 0.25% trypsin-EDTA solution was pipetted onto the adherent cells and incubated for two minutes at 37°C and then diluted by adding 8 ml of fresh culture medium to deactivate the trypsin. The cell suspension was collected and centrifuged for 5 minutes at 500x *g*. The supernatant was discarded and the cell pellet was re-suspended at a density of 3×10^6 cells/ml in 6 ml of pre-warmed of Dulbecco's modified Eagle's Medium (DMEM) supplemented with 1,000 mg/L D-glucose, L-glutamine, 25 mM HEPES buffer, and 110 mg/L sodium pyruvate (Thermo Fisher Scientific). Cells were then counted automatically by mixing 20 μl of cell suspension with 20 μl of trypan blue using a Countess Automated Cell

Counter (Invitrogen Ltd). The remaining cell suspension was utilized for high resolution respirometry experiment.

6.3.2 Mitochondrial Cellular Respiration Measurement

Respiratory rate of neuronal cells was assessed by applying a phosphorylation or coupling control protocol, as described by (Gnaiger, 2008) with some modifications. This protocol simply evaluated the mitochondrial respiration rate of a cultured SH-SY5Y cells suspension, and included the following determinations:

- 1) Mitochondrial basal respiration,
- 2) Uncoupled respiratory capacity, and
- 3) Non-mitochondrial respiration

Furthermore, the main advantage of applying this protocol was that all inhibitors and the uncouplers utilized in this protocol were freely permeable via the cell membrane; and hence do not require cell membrane permeabilization prior to initiate the experiment.

6.3.3 Analytical Protocol

At temperature of 37°C and stirring speed of 750 r.p.m, the two identical glass chambers were filled with 2.2 ml of cell suspension at the density of 3×10^6 cells/ml (see above section) after calibrating of oxygen concentration with the POS at air saturation, corresponding to the oxygen solubility factor (F_M , accounts for the effect of the dissolved salt ions on oxygen solubility relative to pure water) of (0.89) for culture media (Gnaiger, 2008). Further details regarding the oxygen calibration is shown below in (Figure 63).

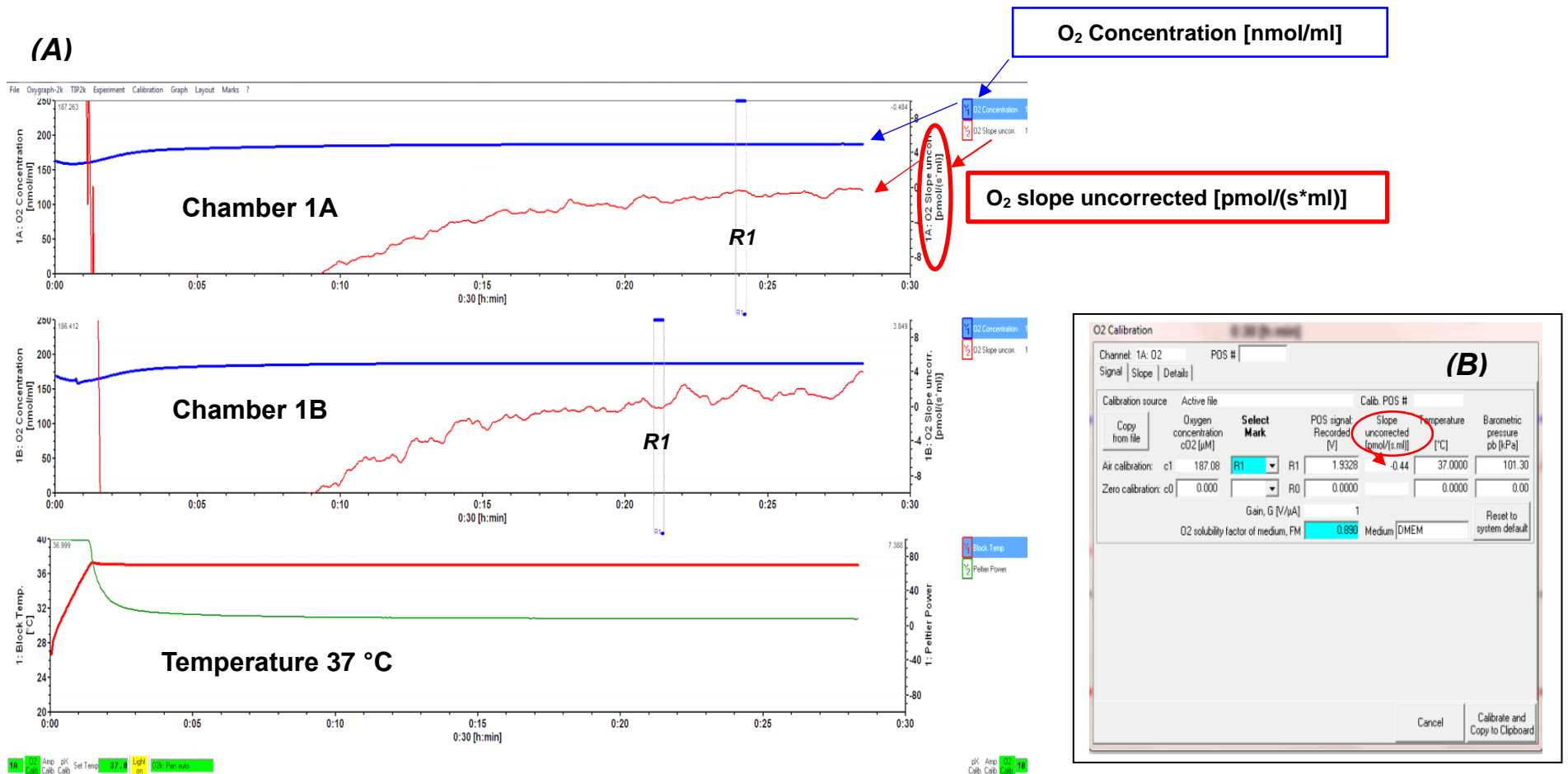


Figure 63 Illustrate (A) the calibrating of oxygen concentration in two chambers (1A and 1B) at air saturation (R1), constant temperature (37 °C), and stirrer speeds of 750 rpm in culture media. The slope uncorrected value for R1 should be within (± 1.0) [pmol/(s*ml)] as shown in circular box (B).

The mitochondrial respiration rates in SH-SY5Y suspension was manually performed by stepwise titration using a Hamilton microliter syringes (Hamilton, Reno, Nevada, USA) as the following:

1. The basal respiration rate (routine respiration; $[R]$) state which reflects the only physiological substrate conditions present in the culture media, was initially monitored after a 10 minutes period as shown (Figure 64).

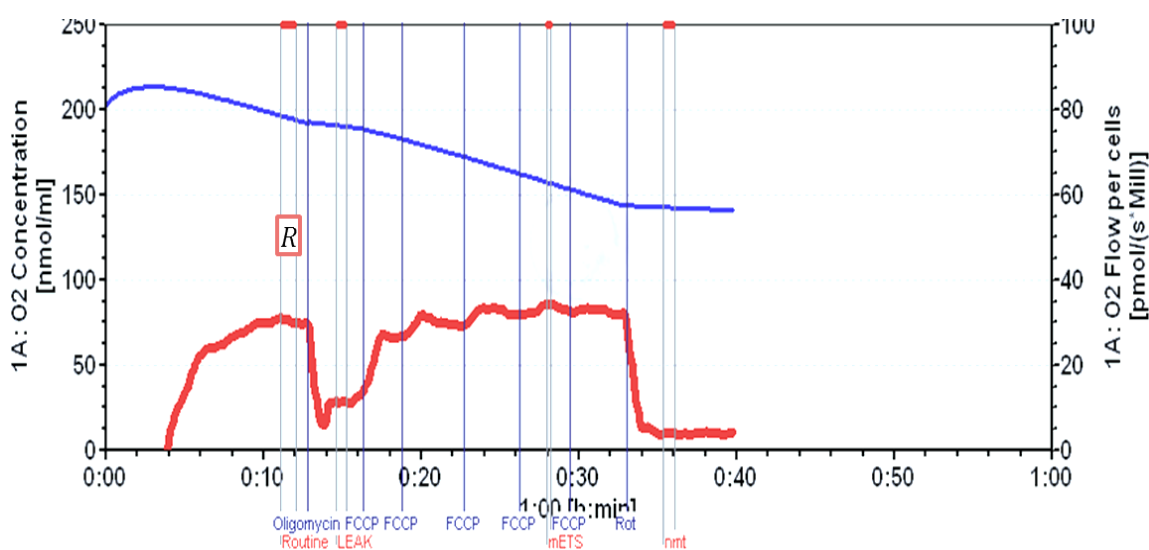


Figure 64 The routine respiration; $[R]$ state was evaluated after a 10 minutes period under SH-SY5Y cell media. Oxygen concentration (nmol/ml) in the chamber is indicated as (blue plot; left Y-axis) and oxygen flow rate is calculated as the negative time derivative obtained from the measured of oxygen concentration and normalized to number of SH-SY5Y cells [pmol/(s*Mill)] (red plot; right Y-axis).

2. After addition of the final concentration of 2 $\mu\text{g/ml}$ of oligomycin (complex V inhibitor or ATP synthase inhibitor), leak respiration [L] state was consequently induced which was consequently caused by the compensation for the proton leak after the blockage of complex V by oligomycin (Figure 65).

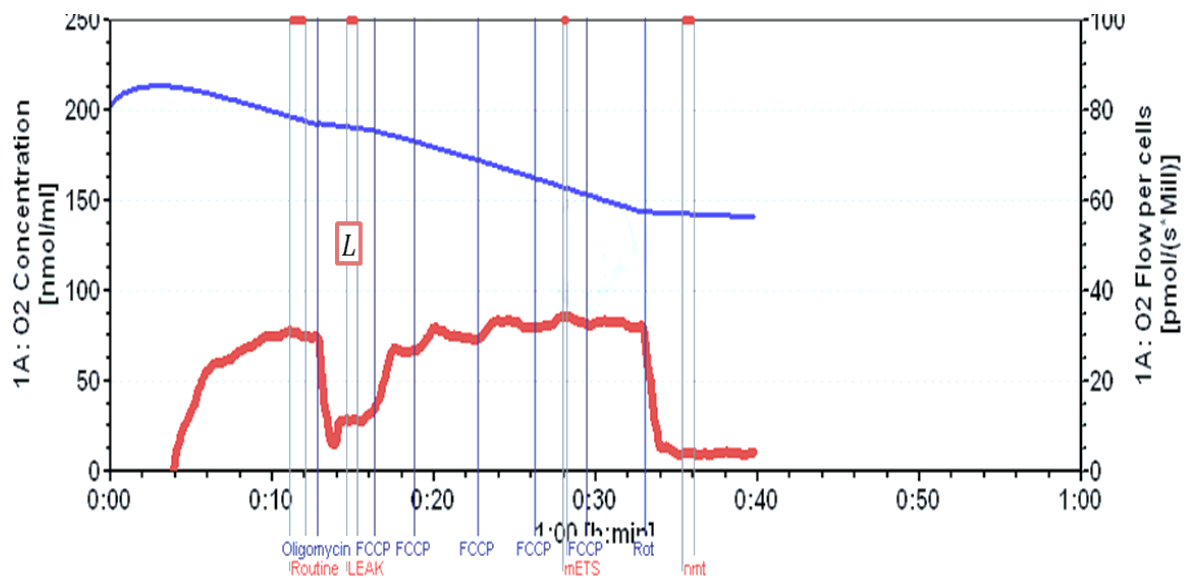


Figure 65 The leak respiration [L] state was consequently induced after inhibiting complex V. Oxygen concentration (nmol/ml) in the chamber is indicated as (blue plot; left Y-axis) and oxygen flow rate is calculated as the negative time derivative obtained from the measured of oxygen concentration and normalized to number of SH-SY5Y cells [pmol/(s*Mill)] (red plot; right Y-axis).

3. The maximal of electron transfer rate (ETS; [E]) state at non-coupled respiration of SH-SY5Y cells was achieved by a careful stepwise 0.5 μM titration of the uncoupler, carbonyl cyanide-(trifluoromethoxy) phenylhydrazone (FCCP) as shown below in (Figure 66).

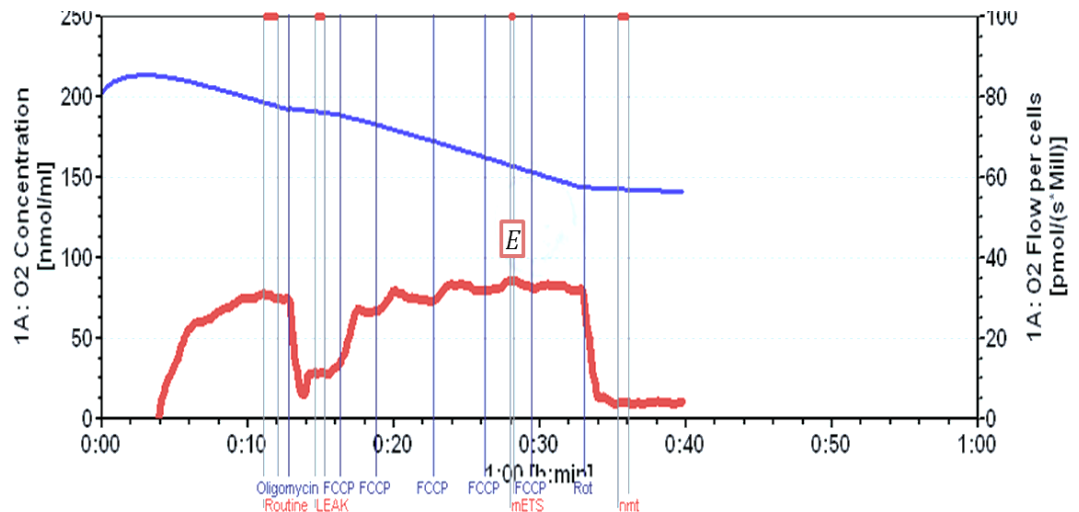


Figure 66 The uncoupler FCCP enhanced respiration rate, which reflects the maximal of electron transfer system (ETS; [E]) state. Oxygen concentration (nmol/ml) in the chamber is indicated as (blue plot; left Y-axis) and oxygen flow rate is calculated as the negative time derivative obtained from the measured of oxygen concentration and normalized to number of SH-SY5Y cells [pmol/(s*Mill)] (red plot; right Y-axis).

4. Non-mitochondrial respiration, also termed as residual oxygen consumption (ROX) was ultimately induced by adding 0.5 μM of rotenone (complex I inhibitor) (Figure 67).

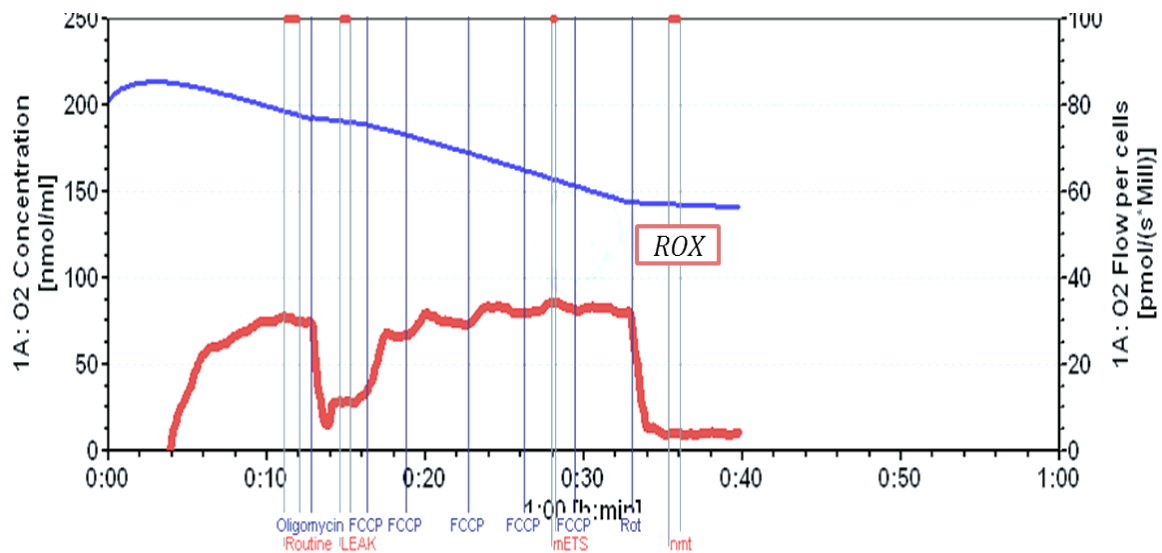


Figure 67 Rotenone blocks the mitochondrial respiration and induced residual oxygen consumption (ROX) state after inhibits MRC complex I. Oxygen concentration (nmol/ml) in the chamber is indicated as (blue plot; left Y-axis) and oxygen flow rate is calculated as the negative time derivative obtained from the measured of oxygen concentration and normalized to number of SH-SY5Y cells [pmol/(s*Mill)] (red plot; right Y-axis).

5. The endogenous respiratory rates were evaluated for each mitochondrial state as an average value of the oxygen flux rate [pmol/(s*Mill)]. In order to minimize the alterations in the volume of the cell suspension loaded into electrode chambers, endogenous respiration rates were eventually normalized to the number of cells [pmol/(s*Mill)]. All mitochondrial states; *R*, *L* and *E* values were corrected to *ROX*. The (Figure 68) below summarise all the above information regarding mitochondrial respiration states in the cultured SH-SY5Y cells suspension.

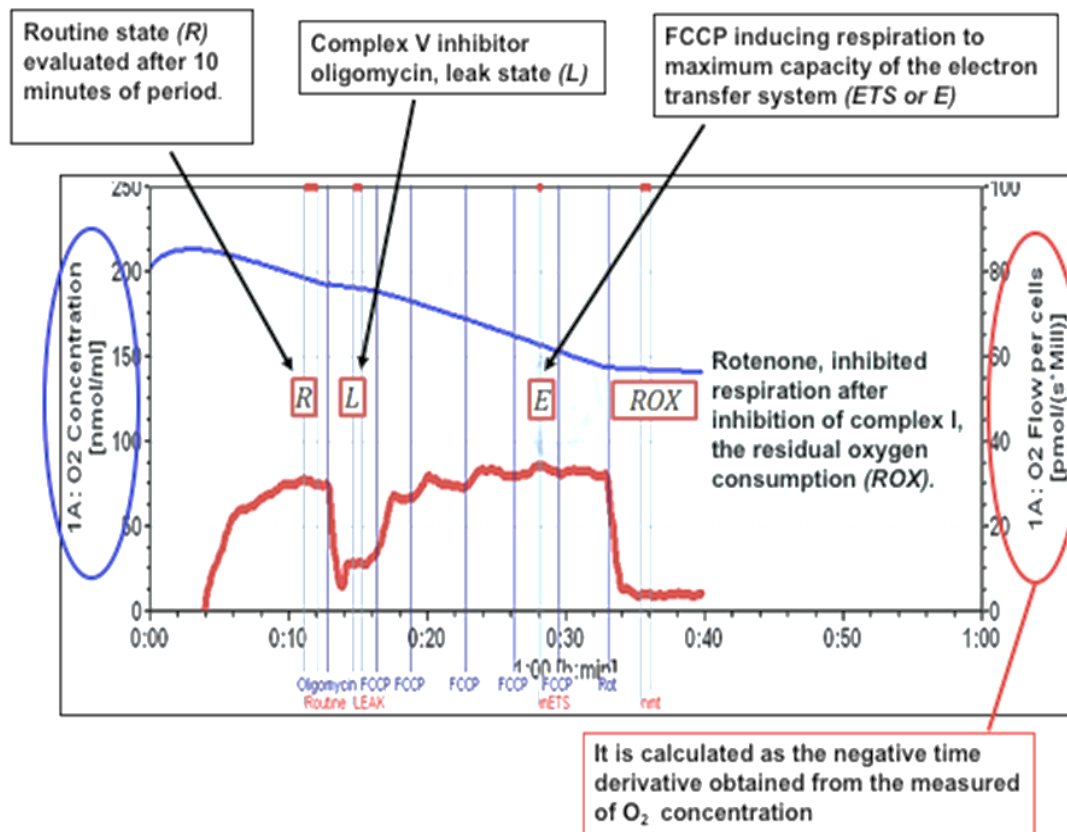


Figure 68 Representative oxygraph traces of oxygen consumptions in SH-SY5Y cells Oxygen concentration (nmol/ml) in the chamber is indicated as (blue plot; left Y-axis) and oxygen flow rate is calculated as the negative time derivative obtained from the measured of oxygen concentration and normalized to number of SH-SY5Y cells [pmol/(s*Mill)] (red plot; right Y-axis). Under physiological substrate conditions (no additives), routine state (R) was evaluated after a 10 minutes period. Vertical lines are events for step-wise titration of complex V inhibitor oligomycin, reducing cellular routine respiration to uncoupled respiration, leak state (L); FCCP inducing respiration to maximum capacity of the electron transport system (ETS or E), and inhibition by complex I inhibitor rotenone, measuring the non-mitochondrial respiration, known as the residual oxygen consumption (ROX).

6.3.4 Data Analysis

Oxygen concentration and oxygen flux were continuously recorded on line by DatLab the DatLab 5 software (Oroboros Instruments, Innsbruck, Austria).

6.4 Results

Oxygen consumption rates in SH-SY5Y cells was investigated using a high resolution respirometry (O2k). In a single analysis paradigm and after the oxygen flow was normalized to the number of SH-SY5Y cells, the routine respiration rate (**R**) was initially obtained with no added substrates or inhibitors and respiratory flux in **R** state was 30.2 [pmol/(s*Mill)] (Figure 69). Following the addition of oligomycin (MRC complex V inhibitor) which induced an immediate inhibition of respiration, the Leak respiration (**L**) was found to be 33% of **R** (Figure 69). To obtain the maximal capacity of the electron transfer system (**ETS**) a step-by-step titration with the uncoupler, FCCP was applied and the induced maximum uncoupled respiratory rate was found to be 39.2 [pmol/(s*Mill)] (Figure 69). The Residual oxygen consumption (**ROX**) was obtained following the inhibition of MRC complex I by the addition rotenone. This **ROX** was found to be 10 % of **R** respiration, but 34 and ~ 7 % of rates **L** and **ETS**, respectively (Figure 69). We subsequently corrected the obtained mitochondrial respiration rates (**R**, **L**, and **ETS**) to the **ROX** (Figure 70). The results of the determinations of the mitochondrial respiratory rates in the SH-SY5Y cells are summarized in (Table 11).

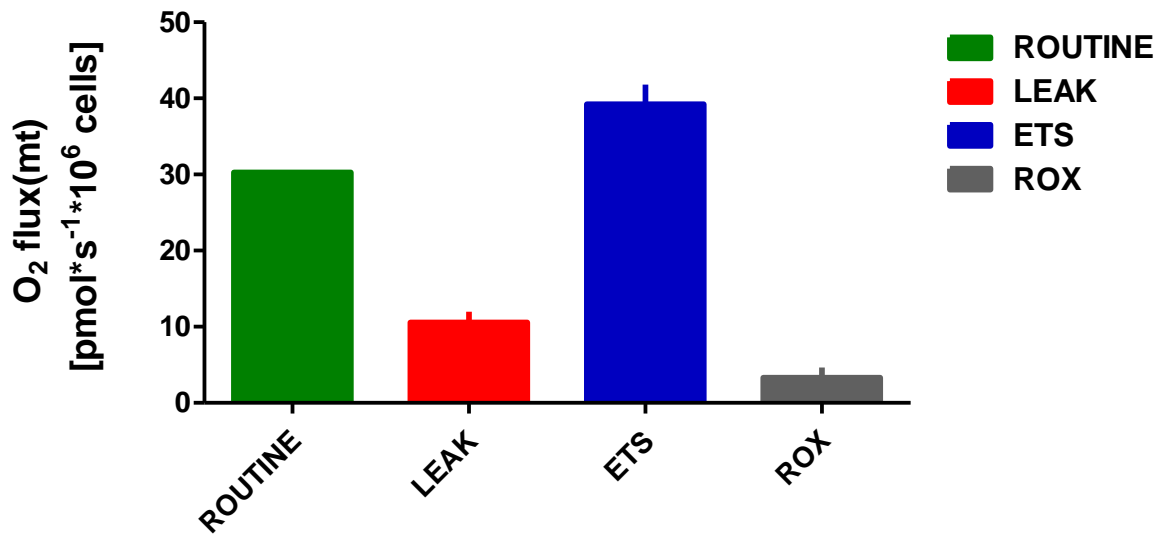


Figure 69 Mitochondrial respiration rates in cultured SH-SY5Y cells. Results represent as mean \pm SEM of ($n=3$) independent experiments.

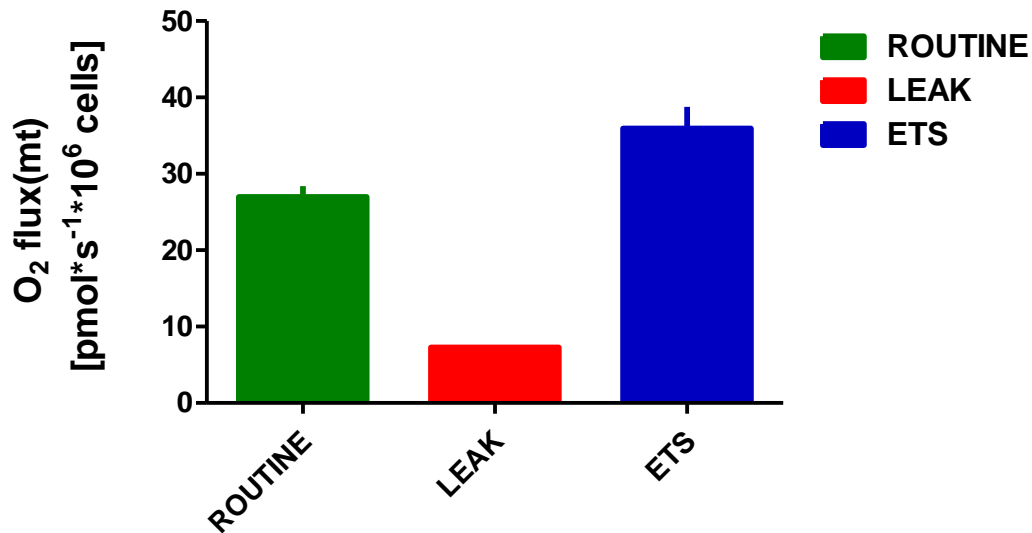


Figure 70 Mitochondrial respiration states in cultured SH-SY5Y cells after corrected to residual oxygen consumption (ROX). Results represent as mean \pm SEM of ($n=3$) of independent experiments.

Table 11 Mitochondrial respiratory rates in cultured SH-SY5Y cells

	Addition	O₂ flow (pmol/s* million cells)
Routine (R)	No	30.2 ± 0.1
Leak (L)	Oligomycin	10.5 ± 1.3
ETS (E)	FCCP	39.2 ± 2.5
Residual oxygen Consumption (ROX)	Rotenone	3.3 ± 1.3
R-ROX	-	27.0 ± 1.4
L-ROX	-	7.2 ± 0.08
E-ROX	-	36.0 ± 2.8

- Results represent as mean ± SEM of (n= 3) of independent experiments.

6.5 Discussion

Oxygen molecules play a crucial role in producing cellular energy via the MRC and the oxidative phosphorylation pathways. Therefore, one of the main purposes of this chapter was to extend our methodology regarding the determination of mitochondrial oxygen consumption rates and to evaluate a step-wise titration protocol for the assessment of integrated mitochondrial function in cultured SH-SY5Y cells.

Although studies measuring individual MRC complex enzyme activity can provide a wealth of information, it should be noted that optimised assays operates under V_{max} (the maximum rate of a reaction) which may not necessarily occur under physiological conditions. Therefore, in this study, highly advanced oxygen consumption measurements utilising small amounts of cells provides an effective tool to assess the integrity of mitochondrial function in SH-SY5Y cells. By successfully applying a step-wise titration protocol including MRC complex inhibitors and uncouplers, we had the

opportunity to evaluate the mitochondrial basal respiration, uncoupled respiratory capacity as well as non-mitochondrial respiration. In the absence of substrates and inhibitors, routine (**R**) respiration of SH-SY5Y cells was assessed and found to be steady. ATP synthesis in neuronal-like cells was blocked by adding complex V inhibitor and subsequently induced a noticeable proton leak of about 33% of routine respiratory rate. Following a step-wise serial titration of FCCP, our results demonstrated a maximum uncoupled respiration (**ETS**) at the respiration flux of 39.2 [pmol/(s*Mill)]. This result suggested that a high level of proton leak was dissipating the mitochondrial proton gradient. Our finding also demonstrated that non-mitochondrial respiration (**ROX**) detected after the complete inhibition of complex I activity by rotenone addition (10 % of **R** respiration, but 34 and ~ 7 % of states **L** and **ETS**, respectively), made little contribution to total respiratory rate. Few comparable findings are published on cultured SH-SY5Y cells. The results of the present study agree with those reported by (Boyle et al., 2012). For instance, they found that **ROX** state was approximately 7% of **ETS**. Taken together, this assay provides a standardized protocol for the assessment of integrated mitochondrial function in cell-culture-based model systems. A specific advantage of studying cultured cells is that the quantification of mitochondrial respiration under physiological state (Routine, **R**) in response to mitochondrial inhibitors or respiratory stimulators, avoids many of the potential artefacts associated with isolated mitochondrial or cell permeabilization such as alterations possibly in mitochondrial morphology (Jang and Javadov, 2018). The use of cultured cell studies also provides insights into the underlying mechanism(s) of mitochondrial disorders. However, it is not

possible to determine maximum OXPHOS capacity in cultured cells since ADP is not freely permeable via the cell membrane (Gnaiger, 2008). Furthermore, the accurate assessment of the activity of the MRC may not be possible in cultured cells because several substrates are also not freely permeable via the cell membrane (Gnaiger, 2008). Thus, cultured cells require further step which is either isolation of mitochondria, or partially permeabilized cell membrane using saponin or digitonin and optimal incubation conditions (Saks et al., 1998; Kuznetsov et al., 2004).

6.6 Conclusion

The use of the O2K instrument together with step-wise protocol has enabled us to gain information regarding the integrated mitochondrial function in cultured SH-SY5Y cells under physiological condition. In this study, we had the opportunity to evaluate the mitochondrial respiratory rate of cultured SH-SY5Y cells suspension, including the mitochondrial basal respiration, uncoupled respiratory capacity, and non-mitochondrial respiration. Based on these promising results, further studies will be undertaken in which this protocol will be utilised to study the rotenone-induced multiple mitochondrial complexes deficiencies as described in chapter 4. Furthermore, the isolation of intact functional mitochondria from SH-SY5Y cells based on the method of (Almeida and Medina, 1997) to investigate the overall oxidative phosphorylation (OXPHOS) system could be usefully explored in further work.

CHAPTER 7

Development of an Accurate and Robust Assay for Fibroblast Growth Factor-21

7.1 Background

Mitochondrial disorders are generally thought to be one of the most common inborn errors of metabolism (IEM) with a minimum birth prevalence of approximately 1:5000, affecting heterogeneously multiple organs and tissues at any age (Hargreaves et al., 2016). Disturbances to the mitochondrial energy machinery, oxidative phosphorylation (OXPHOS) pathway, are commonly referred to as mitochondrial disorders, and can be caused by defects in genes of either the mtDNA or nDNA genes that encode the OXPHOS complexes (Zeviani and Di Donato, 2004)

A multidisciplinary laboratory analysis is required to evaluate patients with suspected mitochondrial disorders in which biochemical analysis is often the initial not non-invasive parameter to be evaluated. For instance, elevated levels of lactic acid in serum, CSF or urine can be a useful biochemical diagnostic indicator of mitochondrial diseases. However, some patients with mitochondrial disease including mitochondrial DNA polymerase gamma (POLG)-associated diseases, Leigh disease, Leber Hereditary Optic Neuropathy (LHON) and Kearns-Sayre syndrome, may show either normal or only mildly altered levels of lactate and pyruvate (Triepels et al., 1999). Elevated plasma pyruvate may additionally result from the impairment of pyruvate metabolic enzymes (Patel et al., 2012). Moreover, these biochemical parameters may be elevated as the result of physiological conditions such as improper specimen collection or inadequate handling. For example, paediatric patients whose samples require prolonged time to acquire during sample collection by venepuncture results in increased level of lactate (Haas et al., 2008). For this reason, evaluation of lactate or pyruvate should

therefore be used with an element of caution since normal levels are not always able to confidently rule out mitochondrial diseases. Consistent with this, the lactate: pyruvate ratio is another biochemical parameter used to help diagnose mitochondrial diseases, since it reflects the cellular redox status (NADH: NAD⁺), i.e. a decrease in the cellular redox status results in an increase in the lactate: pyruvate ratio and vice versa (Debray et al., 2007). Notably, the plasma lactate: pyruvate ratio always appears to be elevated in encephalomyopathy disorders (Haas et al., 2008). Additionally, the elevation of the lactate: pyruvate ratio may be secondary to severe liver failure (Feldman et al., 2017).

Elevated alanine could also be used as a biochemical indicator, since it reflects an accumulation in pyruvate levels. However, an increased plasma alanine level could be secondary to other metabolic disorders such as impairment of the pyruvate metabolic enzymes, pyruvate dehydrogenase (PDH) or pyruvate carboxylase (PC) (Haas et al., 2008). Furthermore, quantitative urinary organic acids such as TCA cycle intermediates and 3-Methylglutaconic acid may be particularly elevated in patients with certain mitochondrial disorders (Barshop, 2004; Gibson, 1999). Together with acylcarnitine profiling, plasma free carnitine analysis may be useful in detecting fatty acid oxidation defects (Haas et al., 2008). Similar to other biochemical parameters which lack specificity, the elevation of creatine kinase (CK), which is released as the result of muscle damage, may often occur in patients with myopathic forms of mtDNA depletion syndrome (Suomalainen, 2013). The recent suggested biochemical biomarkers for mitochondrial disease are summarized in (Table 12). It is worthy to emphasise that normal

values for biochemical biomarkers don't necessarily rule out the mitochondrial diseases.

To date, there is still no first-line non-invasive diagnostic test available for mitochondrial disorders, and as such, a wide range of biochemical surrogates are required to make a definitive diagnosis. However, the starvation hormone, fibroblast growth factor-21 (FGF-21) has been recently proposed as a potential biomarker for mitochondrial disorders (Suomalainen et al., 2011), although a thorough evaluation of its usefulness and careful validation of analytical methods are required before it can be used extensively in the clinical setting.

Table 12 Non-invasive biochemical parameters for evaluating mitochondrial disorders (MDs)

	Biomarker	Sample type	Finding in MDs	Differential diagnosis	Reference(s)
Amino Acids	Lactate	Plasma/CSF/ Urine	↑ or N	Liver failure, drug toxicity, errors in collection and handling sample	(Haas et al., 2008)
	Pyruvate	Plasma/CSF/ Urine	↑ or N	Impairment of pyruvate metabolic enzymes, errors in collection and handling	
	Lactate /Pyruvate ratio	Plasma/CSF	↑ or N	Impairment of pyruvate metabolic enzymes, thiamine deficiency, errors in collection and handling	
	Alanine	Plasma/CSF/ Urine	↑	Impairment of pyruvate metabolic enzymes.	
Organic acids	TCA cycle intermediates	Urine	↑	Organic acidaemias, amino acidopathies, disorders in fatty acid oxidation, glycogen storage, and urea cycle	(Suomalainen, 2011; Wortmann et al., 2012; 2013)
	3-Methylglutaconic acid	Urine	↑		
Acylcarnitine	Free carnitine	Plasma	↓	Fatty acid oxidation defects, primary carnitine deficiency, and carnitine therapy	(Haas et al., 2008)
	Acyl/Free carnitine	Plasma	↑		
Enzyme	Creatine kinase	Plasma	↑	Muscle dystrophies	(El-Bohy and Wong,2005)

N, normal; ↑ increased; ↓ decreased.

FGF-21 is recognized as a member of fibroblast growth factors family. It is a signal protein of 209 amino acids and appears to be highly conserved between species. For example, human FGF-21 shares a 75% structural identity to the mouse FGF-21 homologue (Nishimura et al., 2000). Unlike most other growth factor members, FGF-21 acts in an endocrine manner since it lacks a heparin-binding domain and is thereby released into the blood stream (Itoh et al., 2010). FGF-21 is primarily found in the liver although very low levels are additionally found in other tissues such as adipose tissue, pancreas, and skeletal muscle (Tacer et al., 2010). This potent metabolic regulator has unique metabolic actions on glucose and lipid metabolism. In addition to its effects on glucose and lipid metabolism, it also plays dominant roles in energy metabolism (Figure 71).

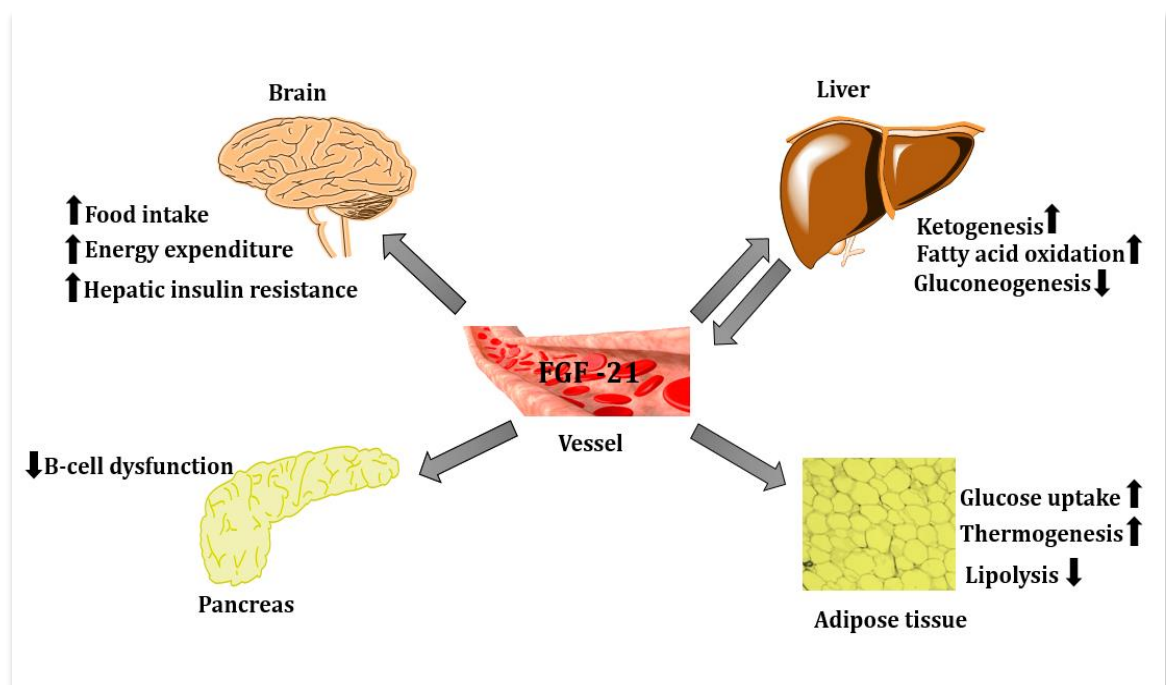


Figure 71 The potential action of FGF-21 on glucose metabolism in various organs and tissues. The figure was adapted from (Woo et al., 2013).

Notably, some metabolic actions of FGF-21 such as its ability to decrease glucose levels, body weight, triglyceride levels, cholesterol levels, and enhancing insulin resistance have been demonstrated when administered therapeutically to both diabetic and obese mouse models (Kharitonov and Adams, 2014; Woo et al., 2013; Iglesias et al., 2012). Favourable metabolic effects of FGF-21 administration on glucose levels, body weight and lipid levels have also been observed in type 2 diabetic patients (Gaich et al., 2013). Furthermore, pharmacological administration of FGF-21 showed improvements in cardiovascular risk profile biomarkers including a decrease in low-density lipoprotein (LDL) “bad-cholesterol” and an increase in high-density lipoprotein (HDL) “good-cholesterol” (Domouzoglou, et al., 2015). Many experimental studies in humans and mice have indicated that FGF-21 can function as a myokine and is induced in skeletal muscle in response to metabolic stress (Figure 72) (Itoh, 2014).

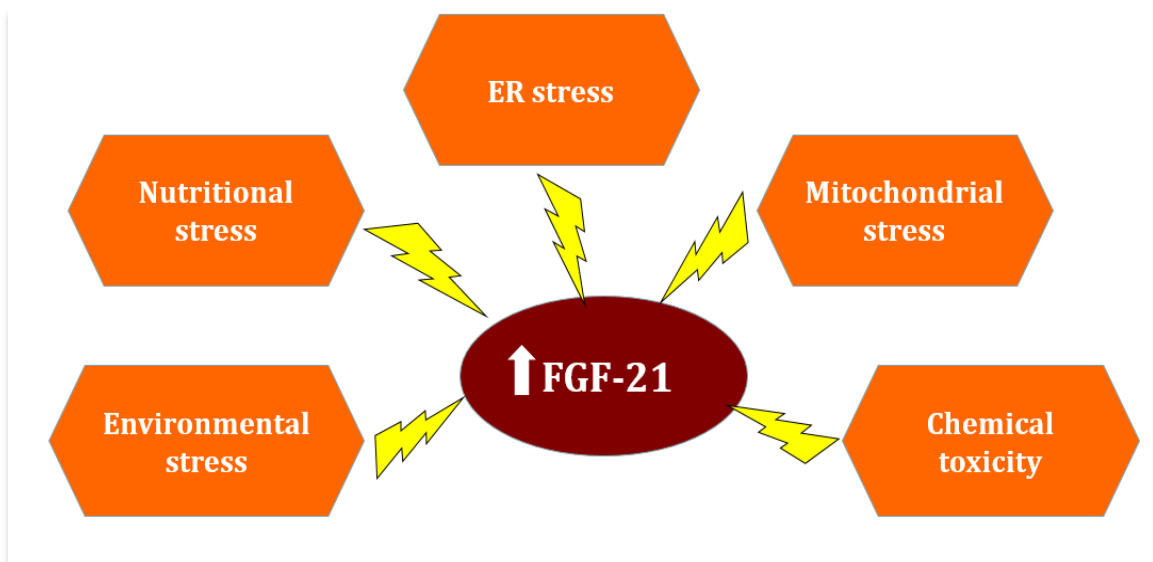


Figure 72 FGF-21 acts as a novel regulator and adaptor against physiological and pathological stress.

Consistent with this, a recent study proposed that the link between mitochondrial ROS production and the subsequent activation of activating transcription factor 2 (ATF2) in the promoter region of the *FGF21* gene through the stimulation of mitogen activated protein kinase (P38 MAPK) in myogenic cells. In this context, the myogenic factor (MyoD) appears to be needed for the induction of *FGF21* gene transcription (Figure 73) (Ribas et al., 2014).

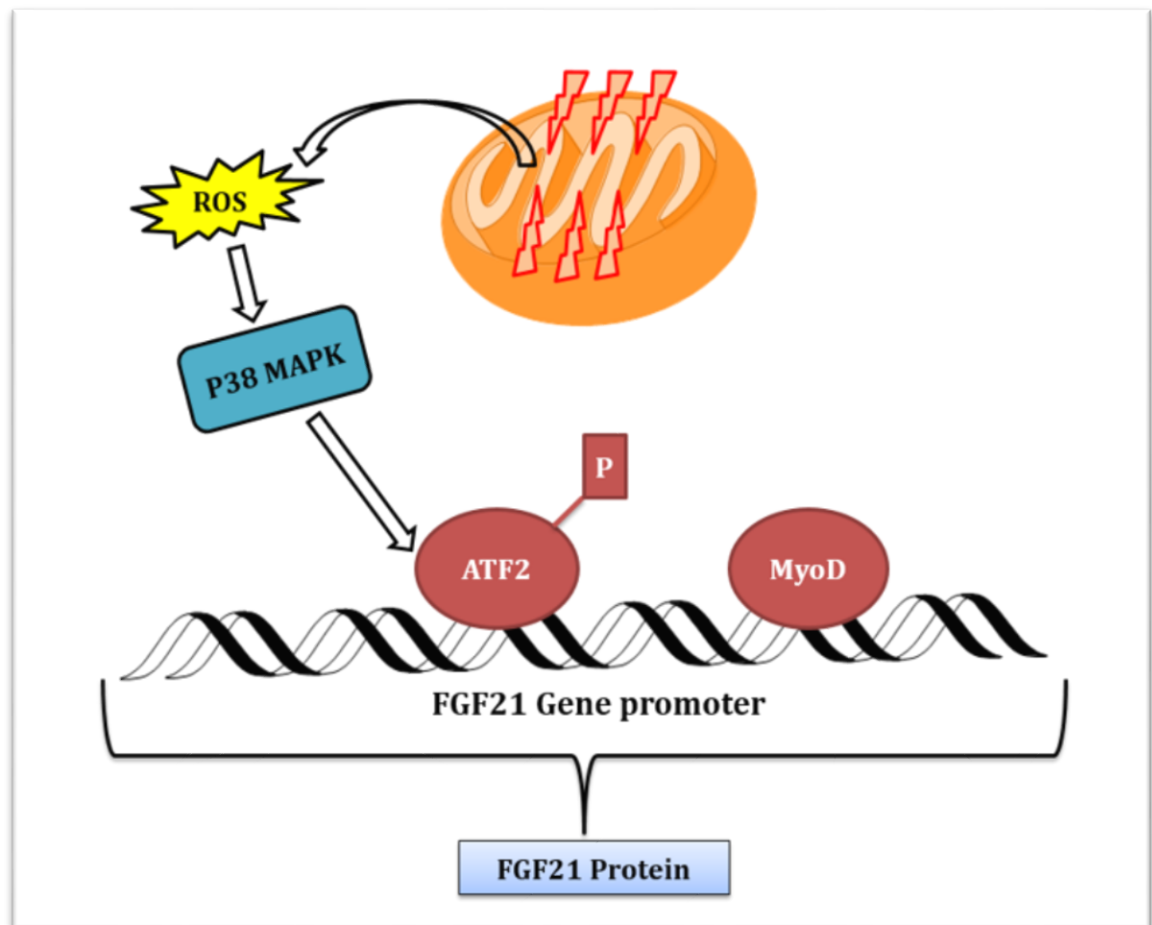


Figure 73 The putative mechanism of the induction of FGF-21 protein in response to the mitochondrial stress stimuli in muscle cells. The figure was adapted from (Ribas et al., 2014).

FGF-21 was first associated with MRC-deficient muscle after being characterized in Deletor (a mutation in TWNK encoding the Twinkle mitochondrial DNA helicase) mice-induced with mitochondrial myopathy. In this study, progressive accumulation of large-scale mtDNA deletions were observed in mice muscle along with negative and positive histochemical staining for cytochrome oxidase (COX) and succinic dehydrogenase (SDH) in muscle fibres, respectively (Suomalainen et al., 1992; Tynismaa et al., 2005; Tynismaa et al., 2010). In the fed state, increased FGF-21 levels were subsequently detected in both muscle fibers, and blood of mice with deficient MRC due to a pseudo-starvation response. Interestingly, once these mice were treated with the ketogenic diet, a reduction of FGF-21 level was accompanied by a parallel improvement in the structure and function of their mitochondria (Ahola-Erkkila et al., 2010). Subsequently, a follow on from this animal study has been translated successfully into the clinical diagnostic setting and measurement made with highly specificity and sensitivity have demonstrated increased FGF-21 levels in patients with neuromuscular disorders resulting from mitochondrial dysfunction (Suomalainen et al., 2011). Taking these findings into consideration, it can be hypothesised that FGF-21 may have the potential to be utilized as a sensitive and selective non-invasive biomarker for mitochondrial diseases.

7.2 Aims

The FGF-21 may potentially serve as a sensitive indicator for mitochondrial disorders and thereby prioritise patients for invasive muscle biopsies. As such, the main aim of this chapter is to

- (i) Validate the reliability of a commercially available FGF-21 Sandwich ELISA assay
- (ii) Apply this analytical technique to evaluate serum FGF-21 levels in paediatric and adult patients.
- (iii) Attempt quantification of FGF-21 levels in neuronal cells under conditions of rotenone induced MRC defect as described previously in chapter 4.

7.3 Methods

7.3.1 Background

The Sandwich Enzyme-Linked ImmunoSorbent Assay (ELISA) offers a highly sensitive and robust technique capable of detecting and quantitating the amount of analyte antigen in an unknown sample. The Sandwich ELISA basically relies on quantifying a particular antigen of interest between two layers of antibody pairs (capture and detection antibodies) (Figure 74) (Suleyman, 2015). It also has the practical advantage over many ELISA techniques in that it provides high affinity and specificity as two layers of antibody pairs are used to detect the target antigen (Sakamoto et al., 2018).

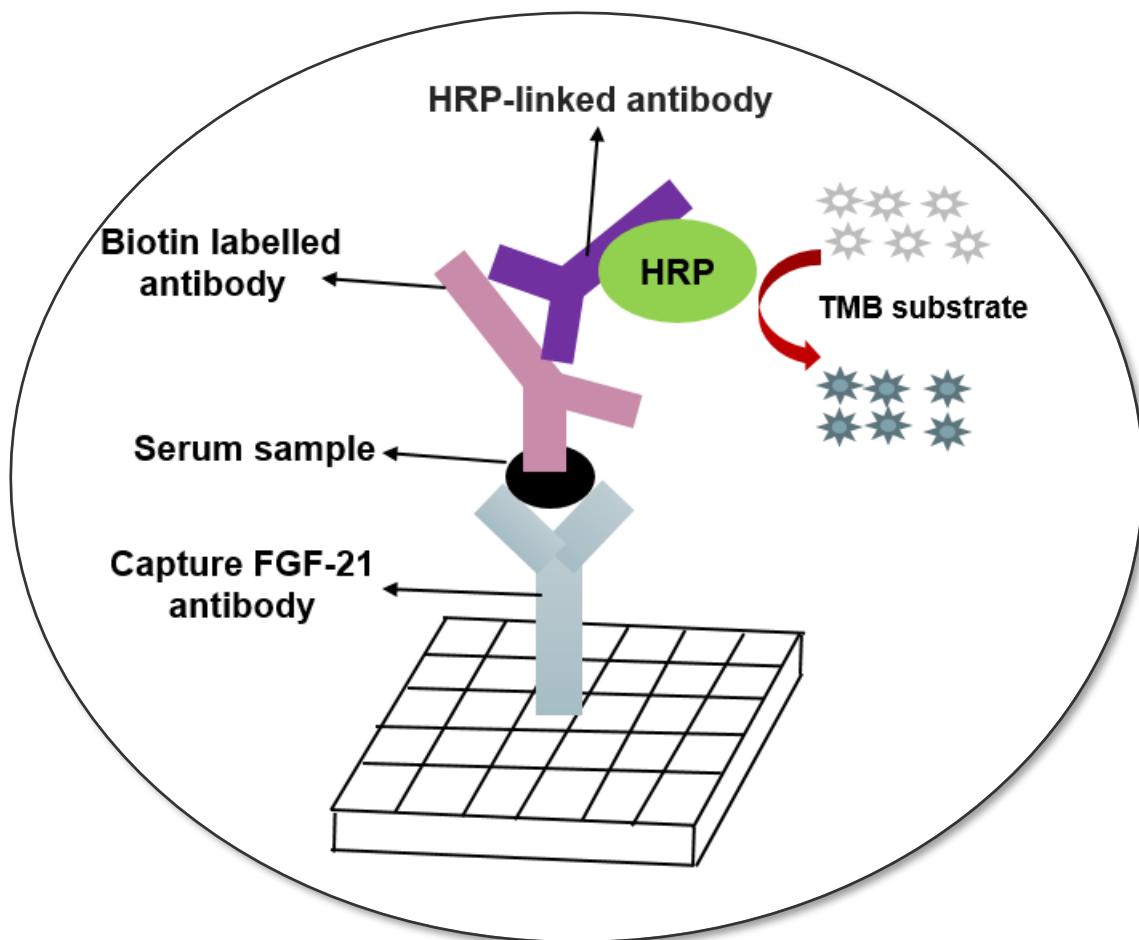


Figure 74 A typical Sandwich ELISA assay. HPR, Horseradish peroxidase; TMB, 3,3',5,5'-Tetramethylbenzidine.

7.3.2 Patient Samples

Anonymised Patient serum samples were collected from the Chemical Pathology Laboratory at Great Ormond Street Hospital for Children (London, UK) and the Neurometabolic Unit at the National Hospital for Neurology and Neurosurgery (London, UK) and stored at -80°C until assayed. Briefly, serum was separated by allowing blood to clot for 15 minutes at room temperature, followed by centrifugation at $3,000\times g$ for 15 minutes at $+4^{\circ}\text{C}$.

7.3.3 Analytical Procedure

The fibroblast growth factor-21 (FGF-21) human ELISA kit was purchased from (BioVendor, Brno, Czech Republic), and the assay was performed, according to the manufacturer's instructions. Prior to assay, ELISA reagents and serum samples were allowed to equilibrate to room temperature. In duplicate, 100 µl of known standards, quality controls, and diluted samples were added into a 96-well microtiter plate pre-coated with polyclonal anti-human FGF-21 antibody. The microtiter plate was sealed and incubated at room temperature for 1 hr on a microtiter plate shaker. Each well was then washed three times with 250 µl of washing solution. After washing, 100 µl of biotin labelled antibody was added and then incubated with coated FGF-21 for 1 hr at room temperature on a microtiter plate shaker. After the incubation time, each well was again washed three times with 250 µl of washing solution. 100 µl Streptavidin- Horseradish peroxidase (HRP) conjugate enzyme was then pipetted into the wells and incubated for 30 mins at room temperature on a microtiter plate shaker. After a final washing step, 3,3',5,5'-Tetramethylbenzidine (TMB) substrate solution was added and the plate was placed in a dark box to avoid light exposure for 15 min at room temperature. In order to stop development colour, 100 µl of stop solution was finally added. The absorbance of each well was then measured using an ELISA microplate reader (MRX TC Revelation, Dynex Technologies Limited, UK) at a 450 nm. To determine the FGF-21 concentration in the unknown samples, a standard curve was created by plotting on the y-axis against known standard amounts on the x-axis. Unknown amounts in the samples were then estimated from the line of best fit.

7.3.4 Statistical Analysis

All statistical analyses were performed using Graphpad Prism 4 software (Graphpad Software Inc. San Diego, CA, USA). All results obtained were expressed as mean \pm standard error of the mean (SEM). Non-parametric *t*-test, Mann-Whitney *U* test was performed for statistical comparison of FGF-21 levels between patients and controls. Spearman rank correlation analysis was performed to examine the relation of FGF21 levels to age and biochemical parameters. In all cases $p < 0.05$ was considered to be statistically significant.

7.4 Results

7.4.1 Validation Process

To investigate whether the FGF-21 ELISA assay is a reliable marker for mitochondrial dysfunction, we set up a validation process of the Human FGF-21 ELISA kit with a sensitivity lower limit of 7 pg/ml and specific for human (see Appendix; Section 1 and 2 for further details about validation process). In each run, the standard curve of human FGF-21 was performed and appeared to be highly linear (Typically, $r^2 = 0.9986$) (Figure 75).

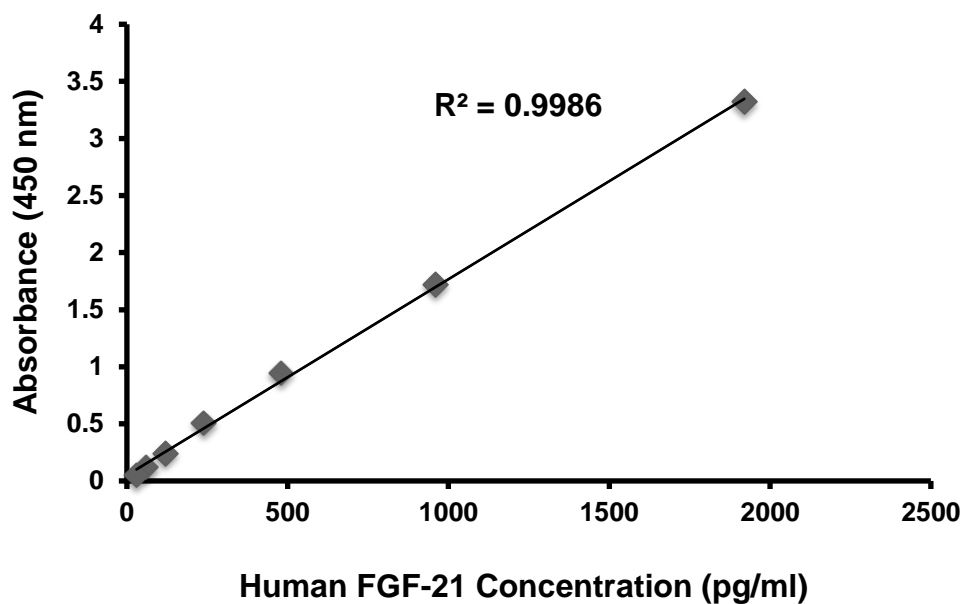


Figure 75 The standard curve for the FGF-21 ELISA assay showing the plot of FGF-21 standard concentration against absorbance at 450 nm.

The two most important aspects for any analytical method validation are precision and accuracy. The precision of an analytical method determines how closely two or more measurements are to each other, whilst accuracy determines how closely a measured value is to a true or actual value. The intra-assay and inter-assay were employed to evaluate the precision of the ELISA assay. We analysed in terms of intra-assay validation by assaying eight replicates of two serum samples of known concentration within one run. The percentage of coefficient of variance (CV %) of the intra-assay precision for the two serum samples was 3.7% and 3.6% (Table 13). Furthermore, the percentage of coefficient of variance (CV %) of inter-assay precision was 5.1% after analysis of three replicates of one pooled serum sample of known concentration in separate runs (Table 14).

Table 13 Two serum samples of known concentration were assayed on one plate to assess intra-assay precision of Human FGF-21 ELISA assay

Sample	1	2
n	8	8
Mean (pg/ml)	690.6	1402
SD (pg/ml)	25.75	51.17
CV %	3.73	3.65

Table 14 Pooled serum sample of known concentration was assayed on different plates to assess inter-assay precision of Human FGF-21 ELISA assay

Sample	1	1
n	3	3
Mean (pg/ml)	417	341.2
SD (pg/ml)	10.11	17
CV %	2.42	5.39
Average Inter- Assay Precision CV%		
5.1		

The linearity of dilution and spike recovery are the most widely used tools for the validation of analytical techniques. Thus, the linearity of dilution was evaluated by serially diluting samples with dilution buffer and showed a high linearity with correlation coefficients of 0.99 (Figure 76). With regards to the accuracy of the ELISA assay, two serum samples were spiked with known concentration of human FGF-21 and recovery values of 90% and 89% were measured (Table 15).

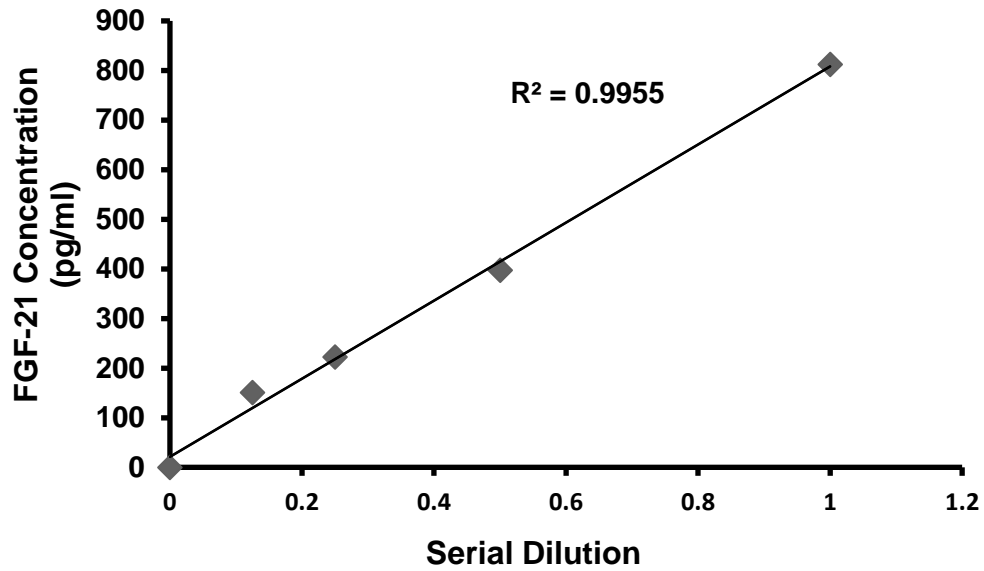


Figure 76 The standard curve for dilution of serum sample. The sample was serially diluted with dilution buffer and assayed. The FGF-21 values appeared to be highly linear ($r^2=0.9986$).

Table 15 Two serum samples were spiked with known concentration of human fibroblast growth factor (FGF-21) and assayed

Sample	Observed (pg/ml)	Expected (pg/ml)	Recovery O/E (%)
1	346.5	-	-
	887.01	986.5	90
2	417	-	-
	941.06	1057	89

We assessed serum samples from 39 paediatric patients with non-mitochondrial disorders (disease controls), and 30 paediatric patients, with the hypothesis that they may be expected to have raised FGF-21 levels. The mean of FGF-21 concentrations in disease control serum (age, gender and clinical manifestation of patients not yet identified), was 512 (SEM 71) pg/ml, (reference range: 44-1515 pg/ml), while the mean of FGF-21 concentrations in patients with suspected mitochondrial disorders (MD) was 2100 (SEM 475) pg/ml (Figure 77).

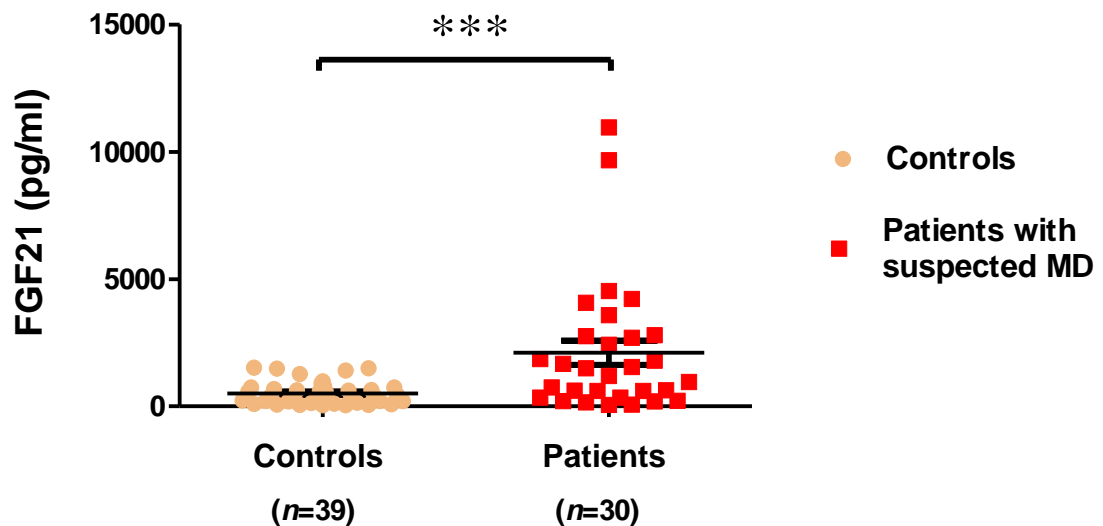


Figure 77 Serum FGF-21 levels (pg/ml) in both disease controls and patients with suspected MD. Error bars indicate SEM; statistical analysis was carried out using Mann-Whitney *U* test; significant differences: *** $p < 0.0005$.

7.4.2 The Induction of FGF21 in Mitochondrial Disorders Patients

We assessed serum levels of FGF21 in 66 paediatric patients. Of these, 63 patients had genetically confirmed mitochondrial disease and 3 patients in whom the basis of their disorder has not yet been identified. Based on their genetic mitochondrial defects, 63 paediatric patients were categorized into seven groups as shown in (Table 16). The serum FGF21 concentration was significantly increased by 7-fold in patients with mtDNA maintenance defects (3438 [SEM 948] pg/mL vs 512 [71] pg/mL; $p < 0.05$; figure 78), whereas in other genetically confirmed patients levels appeared to be slightly elevated, compared to disease controls, although this difference was not significant (Figure 78). However, patients with defects in coenzyme Q synthesis (*ADCK4*) (246 [116] pg/ml; not significant; figure 78) and riboflavin transporter (*SLC52A3*) had slightly reduced (422 [51] pg/ml; figure 78) FGF-21 levels. Furthermore, we assessed FGF21 levels in 38 adult patients (7 adults—3 with a genetic confirmed diagnosis, 2 with typical clinical diagnosis of mitochondrial disease and one dystonia patient, while the other patients haven't been identified yet (Figure 79). Patients with genetically and clinically confirmed mitochondrial diseases showed significantly higher FGF21 levels (3188 [SEM 793] pg/mL vs 512 [71] pg/mL; $p < 0.0005$; figure 80). Similarly, FGF21 was induced in a dystonia patient (>1515 pg/ml) (Figure 79). Furthermore, 27 adult patients had levels within the established reference range, whereas 5 patients were less than 44 pg/ml (Figure 79).

Table 16 Paediatric patients with genetically confirmed mitochondrial disease

Disease group	Gene defect	No. samples	No. patients	No. families
PDH deficiency	<i>PDHA1</i>	4	3	3
OXPHOS subunit & assembly factor defects	<i>MT-ND1</i>	1	1	1
	<i>MT-ND6</i>	1	1	1
	<i>NDUFV1</i>	1	1	1
	<i>BCS1L</i>	2	2	1
	<i>MT-CO1</i>	1	1	1
	<i>SURF1</i>	1	1	1
	<i>MT-ATP6</i>	1	1	1
MtDNA maintenance defects	<i>POLG</i>	3	3	3
	<i>TK2</i>	7	2	1
	<i>RRM2B</i>	1	1	1
	<i>TYMP</i>	1	1	1
Mitochondrial translation defects	<i>MT-TL1</i>	5	3	3
	<i>MT-TK</i>	1	1	1
	<i>mtDNA deletion</i>	4	3	3
	<i>MTO1</i>	1	1	1
	<i>ELAC1</i>	1	1	1
	<i>SARS2</i>	2	1	1
	<i>C12orf65</i>	1	1	1
	<i>RMND1</i>	2	1	1
	<i>LRPPRC</i>	2	2	2
	<i>PNPT1</i>	1	1	1
Coenzyme Q synthesis defects	<i>ADCK4</i>	2	2	1
	<i>IBA57</i>	1	1	1
Mitochondrial import & membrane lipid & homeostasis defects	<i>SLC25A22</i>	8	3	1
	<i>SLC25A26</i>	1	1	1
	<i>SERAC1</i>	3	2	1
	<i>AGK</i>	1	1	1
	<i>CLPP</i>	1	1	1
Riboflavin transporter disorders	<i>SLC52A3</i>	2	1	1
Total	30 genes	63	45	39

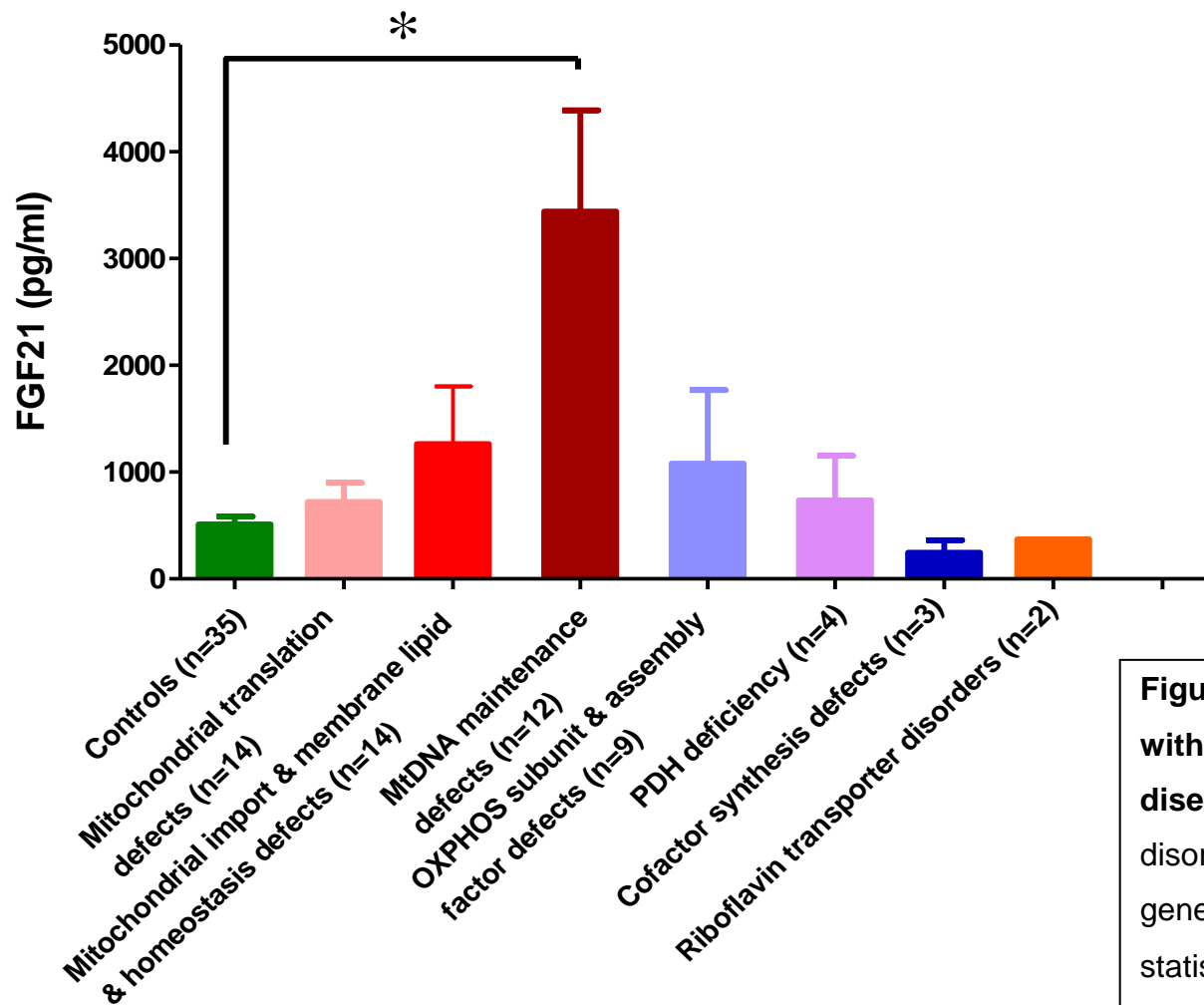


Figure 78 FGF-21 levels in paediatric patients with genetically confirmed mitochondrial disease. Results for patients with mitochondrial disorders are separated shown by particular genetic groups. Error bars indicate SEM; statistical analysis was carried out using Mann-Whitney *U* test; significant differences: * $p < 0.05$.

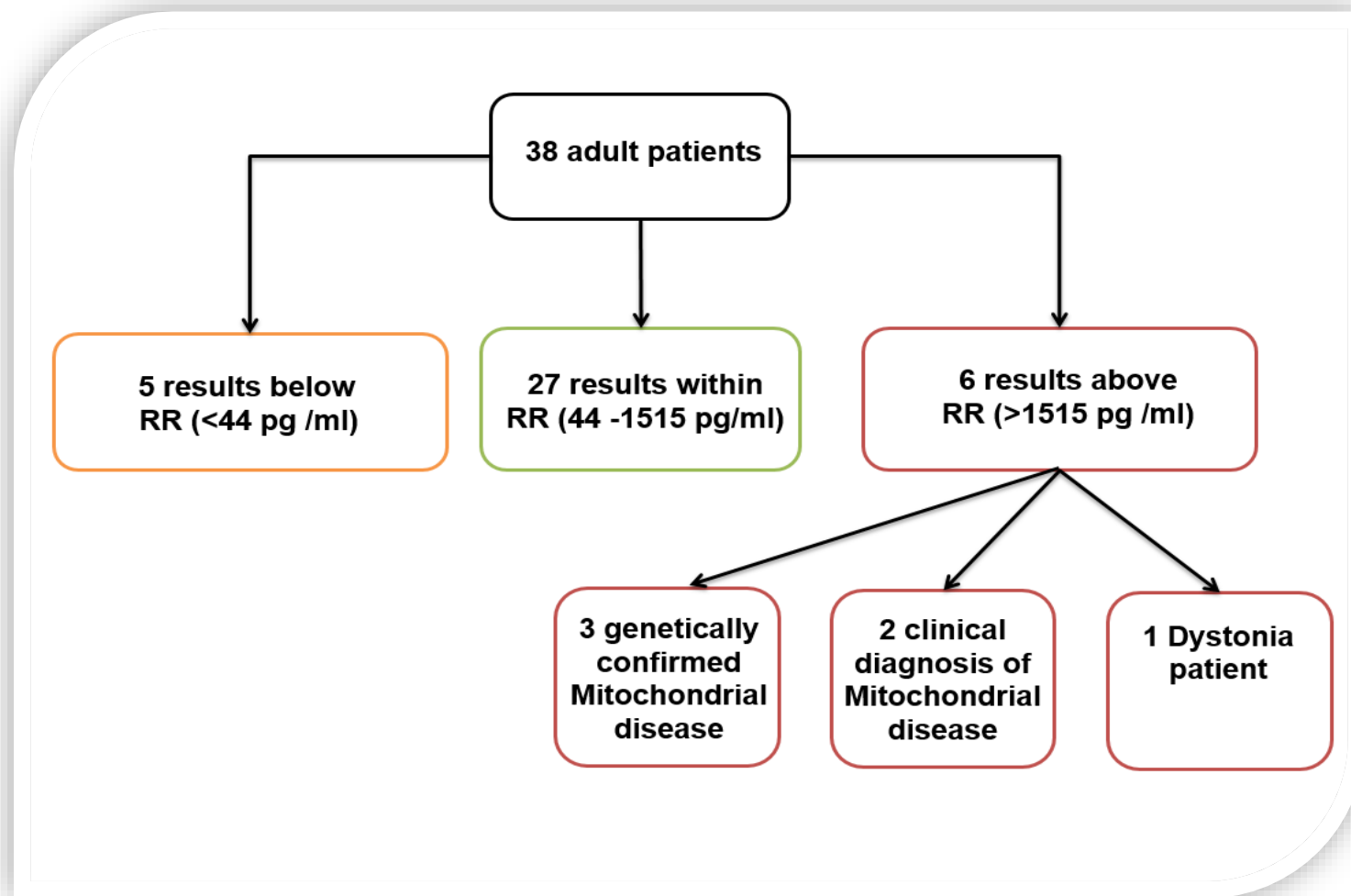


Figure 79 A Flow chart illustrates the serum level of FGF-21 in 38 adult patients. RR; reference range

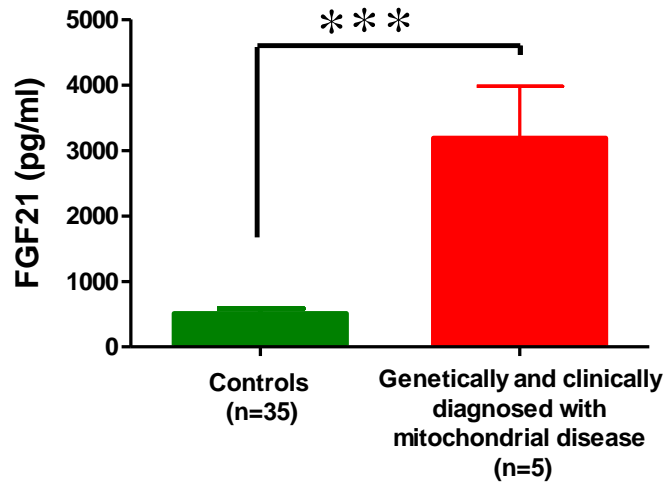


Figure 80 FGF-21 levels in adult patients genetically and clinically diagnosed with mitochondrial disease. Error bars indicate SEM; statistical analysis was carried out using Mann-Whitney *U* test; significant differences: *** $p < 0.0005$.

7.4.3 Association between FGF21 Levels and Age and Biochemical Parameters in Paediatric Patients with Genetically Confirmed Mitochondrial Disease

There was no significant correlation observed between serum FGF-21 levels and ages ($r = -0.15$, $p = 0.20$; figure 81). However, serum FGF-21 levels were shown to be significantly correlated with classical mitochondrial biomarkers, lactate ($r = 0.36$, $p < 0.005$; figure 82), and CK ($r = 0.31$, $p < 0.05$; figure 83), but no correlation was noted between FGF-21 levels and alanine ($r = -0.007$, $p = 0.095$, figure 84). Furthermore, liver function enzymes, particularly alanine aminotransferase (ALT) exhibited a significant correlation with FGF-21 levels ($r = 0.42$, $p < 0.005$; Figure 85), but not with alkaline phosphatase (ALP) ($r = 0.14$, $p = 0.32$; figure 86). Although FGF-21 levels were showed to be inversely correlated with creatinine ($r = -0.30$, $p < 0.05$; figure 87), they were not significantly correlated with urea ($r = -0.10$, $p = 0.45$; figure 88) or glucose ($r = 0.13$, $p = 0.41$; figure 89).

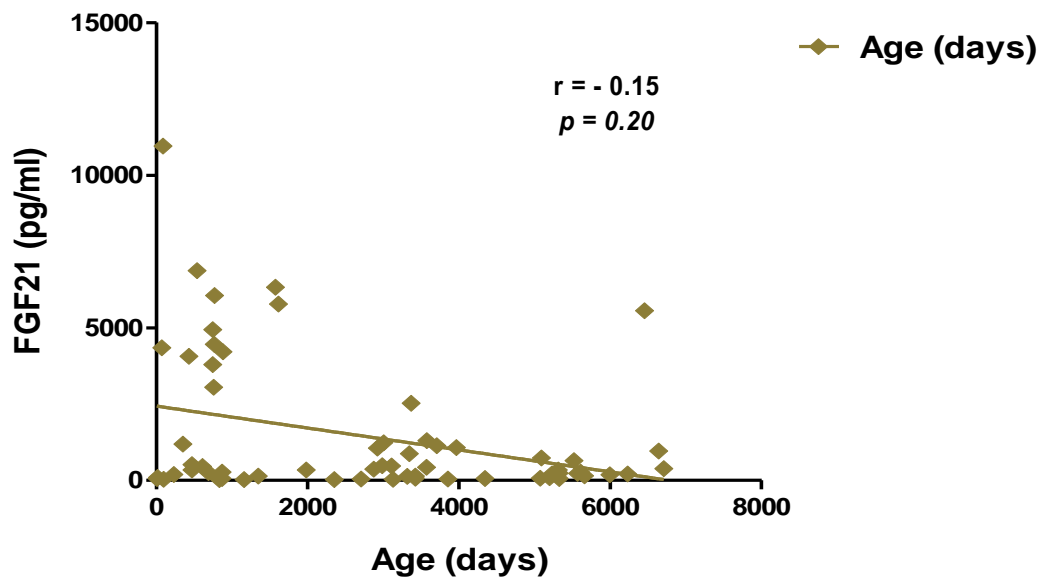


Figure 81 Correlation between serum FGF-21 levels (pg/ml) and age (days) in paediatric patients with genetically confirmed mitochondrial disease (n= 63). Ages were plotted against FGF-21 levels. Line indicates the calculated linear correlation curve. Statistical analysis was carried out using Spearman’s rank correlation coefficient (r); there is no significant correlation between ages and FGF-21 levels.

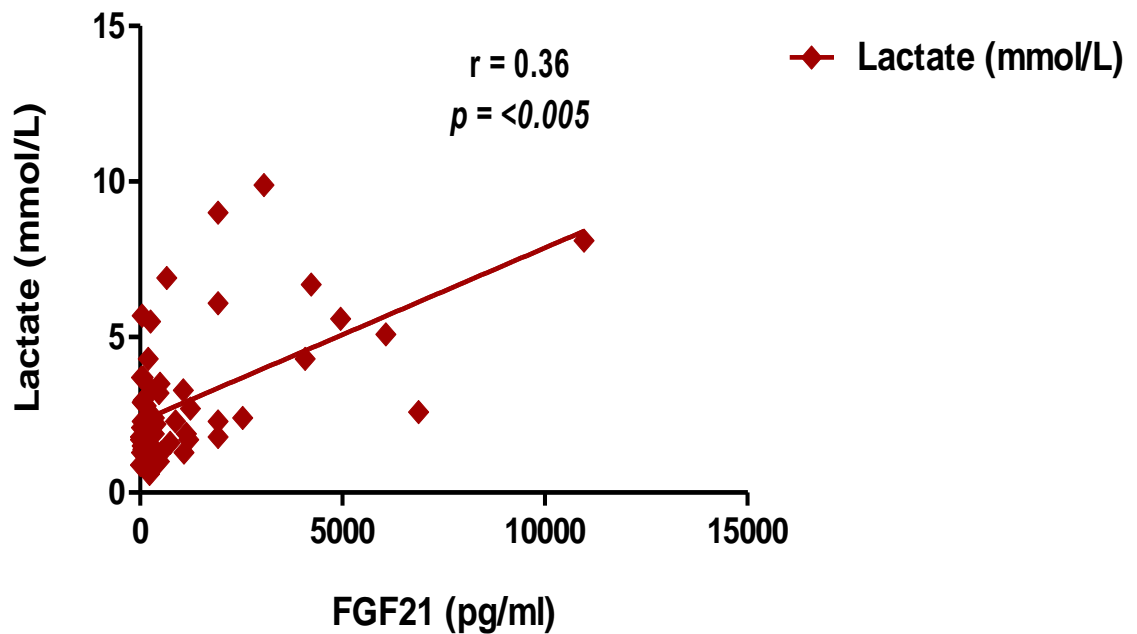


Figure 82 Correlation between serum FGF-21 levels (pg/ml) and lactate levels (mmol/L) in paediatric patients with genetically confirmed mitochondrial disease (n= 60). Serum FGF-21 levels were plotted against lactate levels. Line indicates the calculated linear correlation curve. Statistical analysis was carried out using Spearman's rank correlation coefficient (r); there is significant correlation ($p < 0.005$) between FGF-21 and lactate levels.

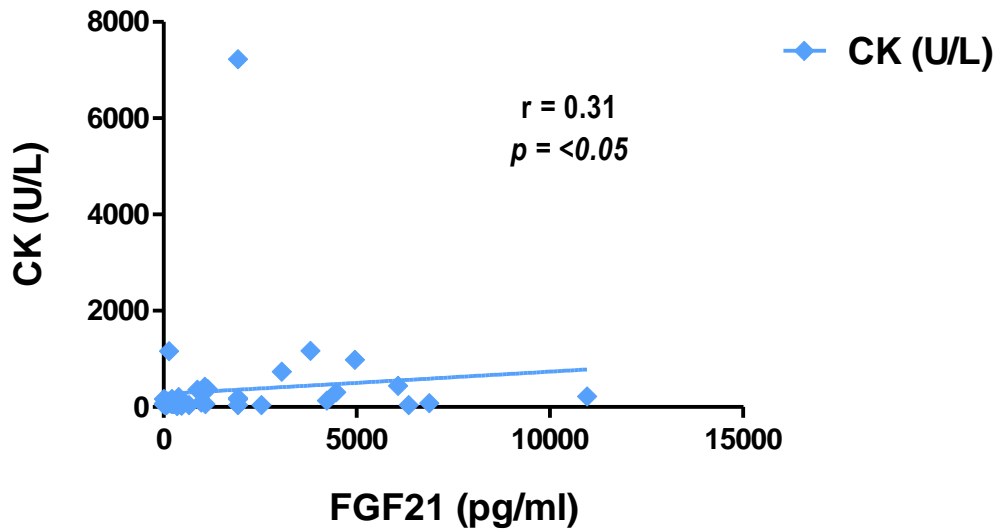


Figure 83 Correlation between serum FGF-21 levels (pg/ml) and CK levels (U/L) in paediatric patients with genetically confirmed mitochondrial disease (n= 50). Serum FGF-21 levels were plotted against CK levels. Line indicates the calculated linear correlation curve. Statistical analysis was carried out using Spearman’s rank correlation coefficient (r); there is significant correlation ($p < 0.05$) between FGF-21 and CK levels.

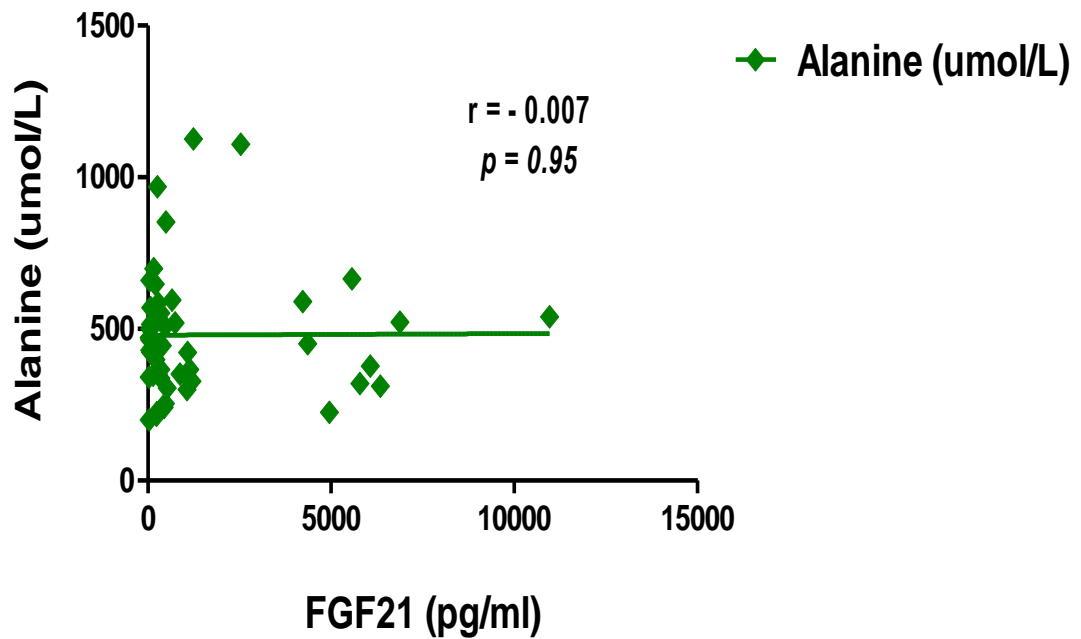


Figure 84 Correlation between serum FGF-21 levels (pg/ml) and alanine levels ($\mu\text{mol/L}$) in paediatric patients with genetically confirmed mitochondrial disease ($n= 49$). Serum FGF-21 levels were plotted against alanine levels. Line indicates the calculated linear correlation curve. Statistical analysis was carried out using Spearman's rank correlation coefficient (r); there is no significant correlation between FGF-21 and alanine levels.

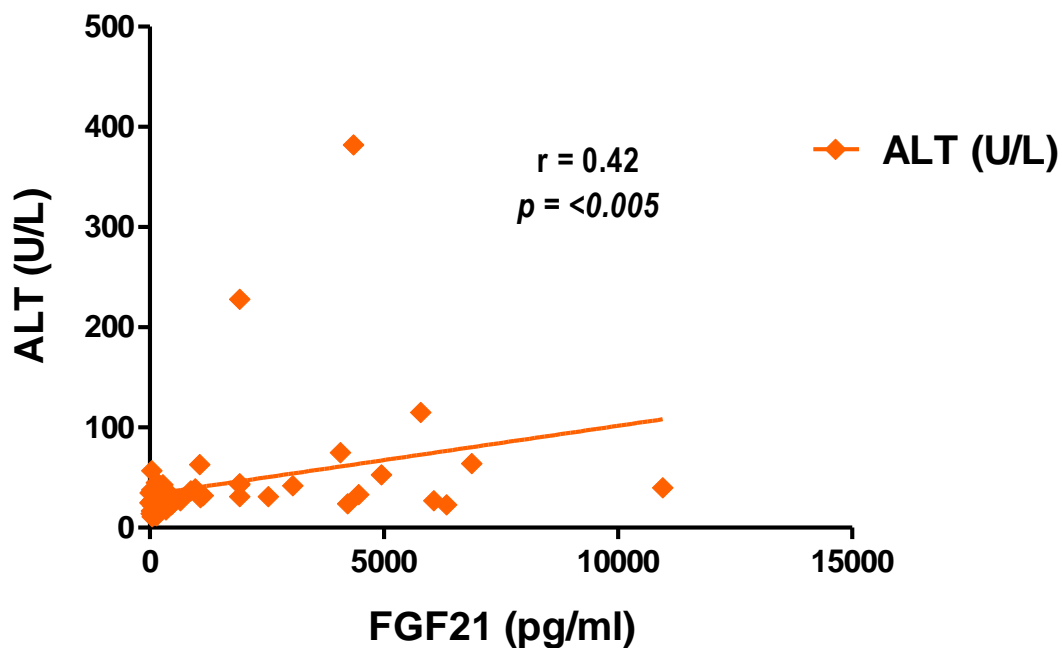


Figure 85 Correlation between serum FGF-21 levels (pg/ml) and ALT levels (U/L) in paediatric patients with genetically confirmed mitochondrial disease (n= 57). Serum FGF-21 levels were plotted against ALT levels. Line indicates the calculated linear correlation curve. Statistical analysis was carried out using Spearman’s rank correlation coefficient (r); there is significant correlation ($p < 0.005$) between FGF-21 and ALT levels.

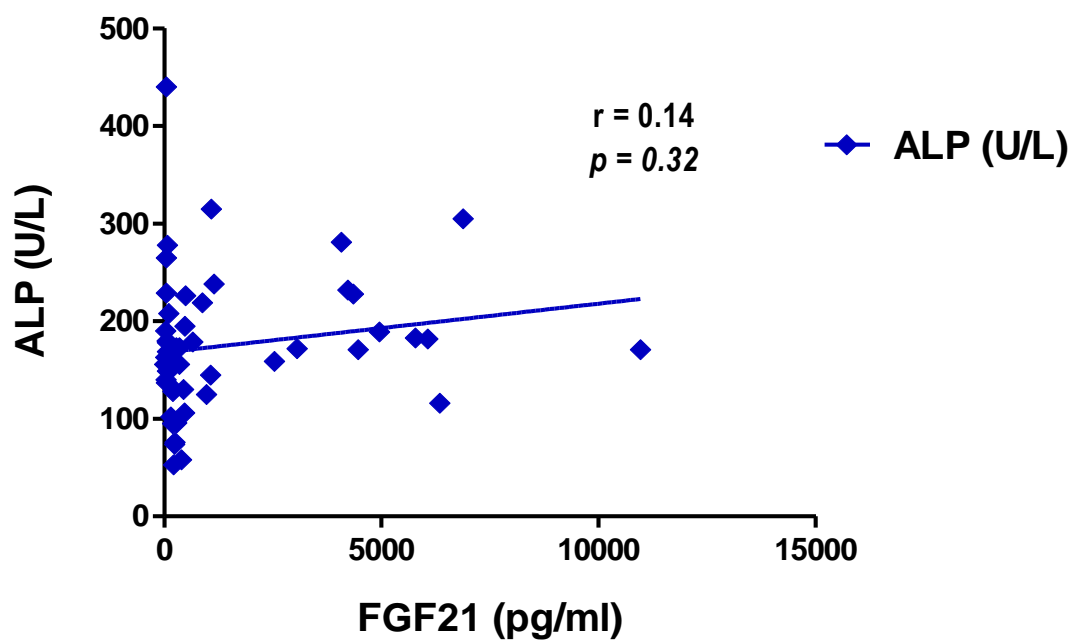


Figure 86 Correlation between serum FGF-21 levels (pg/ml) and ALP levels (U/L) in paediatric patients with genetically confirmed mitochondrial disease (n= 51). Serum FGF-21 levels were plotted against ALP levels. Line indicates the calculated linear correlation curve. Statistical analysis was carried out using Spearman’s rank correlation coefficient (r); there is no significant correlation between FGF-21 and ALP levels.

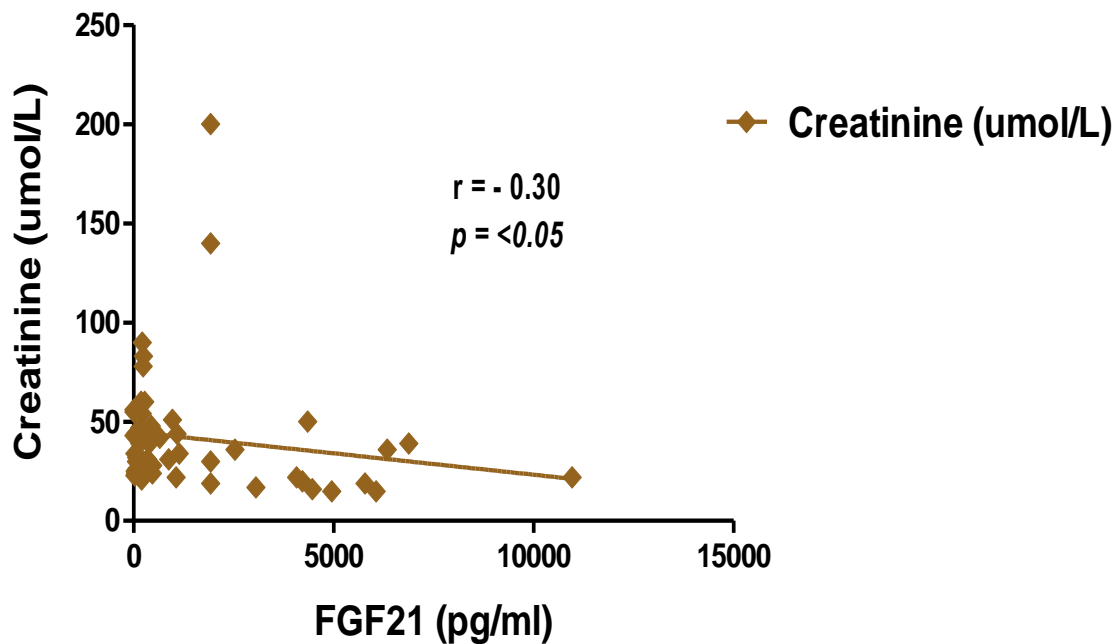


Figure 87 Correlation between serum FGF-21 levels (pg/ml) and creatinine levels ($\mu\text{mol/L}$) in paediatric patients with genetically confirmed mitochondrial disease ($n= 58$). Serum FGF-21 levels were plotted against creatinine levels. Line indicates the calculated linear correlation curve. Statistical analysis was carried out using Spearman’s rank correlation coefficient (r); there is significant correlation ($p < 0.05$) between FGF-21 and creatinine levels.

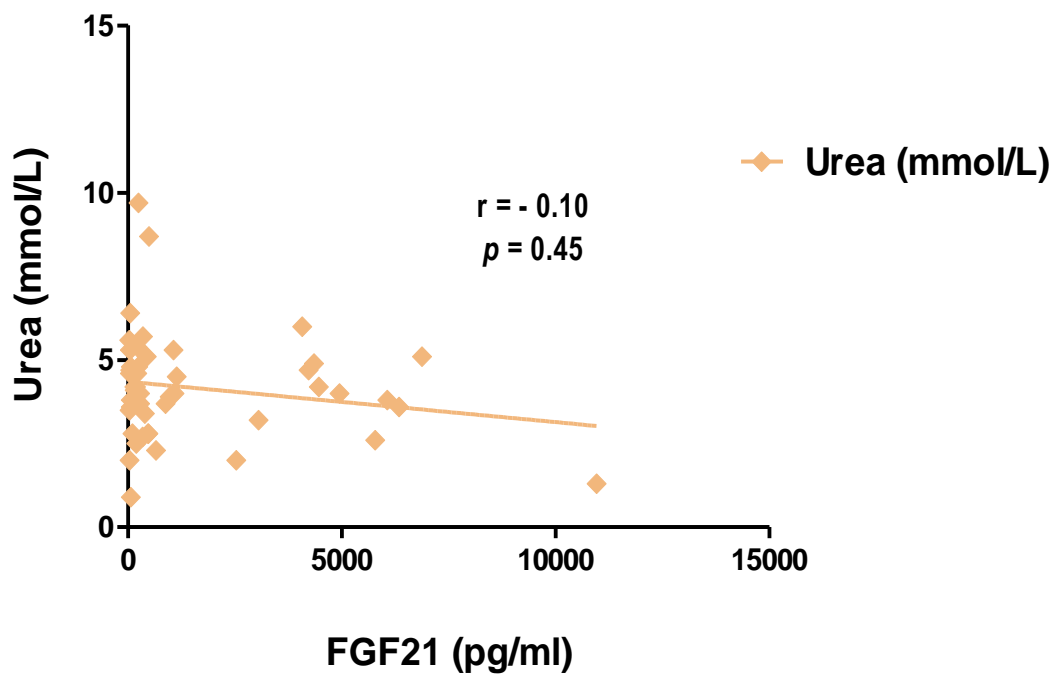


Figure 88 Correlation between serum FGF-21 levels (pg/ml) urea levels (mmol/L) in paediatric patients with genetically confirmed mitochondrial disease (n= 50). Serum FGF-21 levels were plotted against urea levels. Line indicates the calculated linear correlation curve. Statistical analysis was carried out using Spearman’s rank correlation coefficient (r); there is no significant correlation between FGF-21 and urea levels.

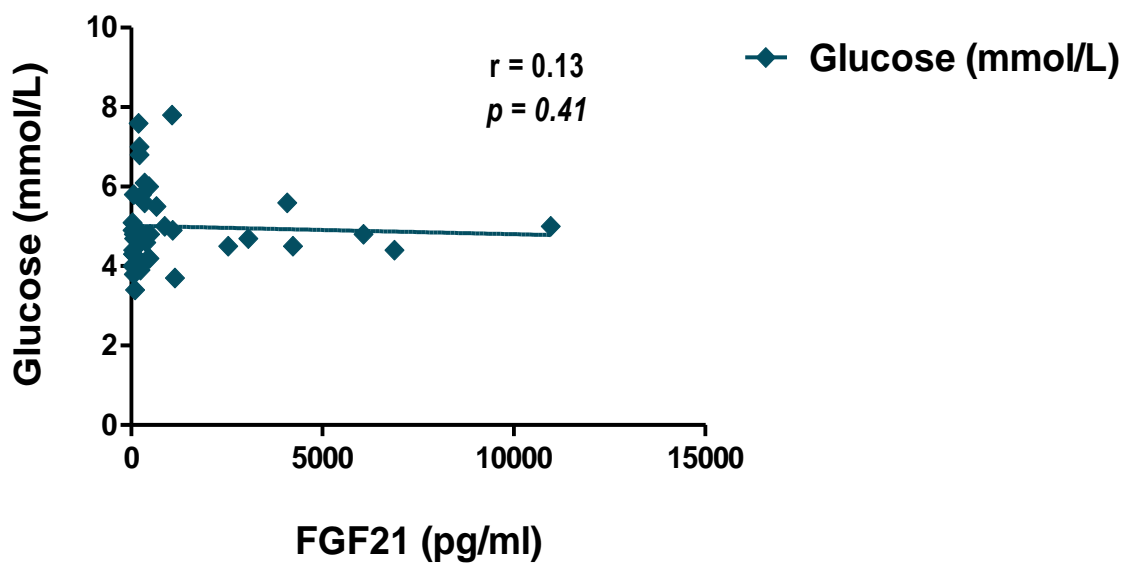


Figure 89 Correlation between serum FGF-21 levels (pg/ml) glucose levels (mmol/L) in paediatric patients with genetically confirmed mitochondrial disease ($n= 40$). Serum FGF-21 levels were plotted against glucose levels. Line indicates the calculated linear correlation curve. Statistical analysis was carried out using Spearman's rank correlation coefficient (r); there is no significant correlation between FGF-21 and glucose levels.

7.5 Discussion

Since the clinical manifestation for patients with mitochondrial disease varies considerably, mitochondrial diseases are still challenging for clinicians to obtain an accurate diagnosis. Despite there being numerous of laboratory diagnostic tests available, including biochemical assays, histological examination, and DNA genetic analysis for mitochondrial disorders, muscle biopsy remains a gold standard diagnostic tool for patients with suspected mitochondrial disorders due to the variability of sensitivity of serum biomarkers. Nevertheless, the muscle biopsy is an invasive procedure that requires both surgical technique and anesthesia.

In a retrospective diagnostic study conducted by (Suomalainen et al., 2011), it was concluded that a hormone-like cytokine, FGF-21, could serve as a potential first-line biomarker for mitochondrial diseases using a sandwich ELISA assay. A great advantage of FGF-21 as a biomarker is that as well as being a non-invasive tool, may be a more specific biomarker which can be assayed with a high degree of sensitivity, when compared to classical serum biomarkers such as lactate, pyruvate and CK.

In this thesis, the focus of attention also was to initially validate the human FGF-21 sandwich ELISA as a mitochondrial biomarker assay. Firstly, the assay appears to demonstrate high sensitivity and linearity. Following regression analysis, the standard curve of human FGF-21 showed high correlation ($r^2 = 0.9986$) with a reliable detection range of 7 to 2000 pg/ml (Figure 75). Moreover, the precision of the ELISA assay was validated and the results obtained were consistent with those reported by the manufacturer (4.0 pg/ml).

Furthermore, linearity dilution of serum sample and spike recovery were evaluated. Serial dilutions of serum sample ranged from 1:2 to 1:8 and revealed high linearity, indicating that no potential interference in the serum samples was observed. Consistent with this finding, the recovery of two spiked serum samples were estimated to be 90% and 89% and were deemed acceptable since recovery values fall in the globally accepted ranges of 80-120 % (Andreasson et al., 2015). In our ELISA validation, reference serum values obtained showed comparable values to those in a previous study (Fu et al., 2014).

To ascertain the usefulness of this analytical assay for clinical practice, we assessed 66 paediatric and 38 adult patient samples. Amongst genetically confirmed mitochondrial disease in paediatric patients, circulating FGF-21 levels were significantly higher with mtDNA maintenance defects patients ($p < 0.05$) (Figure 78), which are consistent with previous study (Lehtonen et al., 2016). In addition to mtDNA maintenance defects, it has been proposed that FGF-21 could be a signature biomarker for mitochondrial translation rather than in patients with defects either in MRC subunits or assembly factors (Lehtonen et al., 2016). However, patients with mitochondrial translation defects exhibited to be slightly elevated in the FGF21 circulation, although this difference did not appear to be significant (Figure 78). Additionally, a slight reduction in FGF-21 levels was noted in patients with defects in cofactor synthesis (ADCK4) and riboflavin transporter (SLC52A3) (Figure 78), although the significance of this finding needs to be verified in a larger number of patient samples before any significance can be tested.

In this study, we further applied the FGF-21 Sandwich ELISA assay to adult patients who had been either clinically or genetically diagnosed with mitochondrial diseases, and showed higher levels of FGF-21 in their serum ($p < 0.0005$) (Figure 80). Additionally, FGF-21 was found to be elevated in a patient with dystonia (muscle disorder), suggesting that the FGF-21 may also be induced by skeletal muscle dysfunction, thereby supporting the findings from several other previous studies (Suomalainen et al., 1992; Ribas et al., 2013 ; Itoh, 2014). Nevertheless, this finding should be interpreted with caution due to small sample size (Figure 79). FGF-21 was also found to be low in five adult patients (Figure 79), although no conclusion can be drawn regarding this finding in the absence of any confirmed diagnosis.

In addition to the variability in serum, FGF-21 levels was observed among paediatric patients with genetically confirmed mitochondrial diseases not to be correlated with age, further supporting a previous study of mitochondrial patients (Suomalainen et al., 2011). An assessment of association between classical mitochondrial biomarkers with serum FGF-21 levels showed that lactate levels were significantly correlated with FGF-21 levels (Figure 82). However, it has been noted in mitochondrial patients that slightly elevated or even normal lactate levels may be accompanied by higher levels of FGF-21 (Suomalainen et al., 2011), suggesting that lactate lacks specificity as a mitochondrial biomarker. In addition, variation in lactate levels could be due to errors in collection, sample handling or assay technique. Furthermore, CK which is an established biomarker for muscle damage, has been additionally suggested to play a role as a mitochondrial biomarker. It was shown to be significantly correlated with increased FGF-21 levels. Although it has been

suggested that alanine may also serve as a biomarker for mitochondrial disease, our results failed to demonstrate any correlation between its serum levels and that of FGF-21.

Of note, FGF-21 is expressed predominately in hepatocytes in the fasting state (So and Leung, 2016). Thus, an elevation of circulating FGF-21 levels has also been suggested as a biomarker for liver damage. It has been reported that circulating levels of FGF-21 increased significantly in patients with non-alcoholic fatty liver disease (NAFLD) (Zhu et al., 2016). Therefore, we need to gain further insight into the relationship between FGF-21 levels and liver enzymes to ascertain whether the increased FGF-21 levels result as a consequence of muscle-manifesting mitochondrial diseases or liver damage. In this study, results showed that FGF-21 levels significantly correlated with ALT, but not with ALP, indicating that elevated of serum FGF-21 levels, which also correlated well with CK, could possibly be explained as a result of muscle damage but rather than liver damage.

Previous clinical studies furthermore indicated that increased FGF-21 plasma levels were observed patients with renal dysfunction, the levels of which additionally correlated with the renal function biomarker, creatinine (Stein et al., 2009; Lin et al., 2011). However, paediatric mitochondrial patients showed a significant inverse correlation between FGF-21 levels and creatinine. Moreover, urea, another metabolite used to assess renal function test, was also shown not to be correlated with FGF-21 levels. Taken together, these findings suggested that the association between the loss of creatinine function and FGF-21 level, but not with that of urea could be possibly related to muscle conditions.

Being an effective therapeutic agent as an antidiabetic target, FGF-21 has also been suggested as a potential biomarker for obesity-related metabolic disorders (So and Leung, 2016). Several studies showed evidence of increased levels of FGF-21 in obese (Zhang et al., 2008; Fisher et al., 2010; Reinehr et al.; 2012) and diabetic (Chavez et al., 2009; Xiao et al., 2012; So et al., 2013) humans and animal models. In contrast, our findings showed that there was no evidence of any relationship between FGF21 and glucose levels in paediatric mitochondrial patients.

FGF-21 has been reported to be expressed in the brain and can be synthesised by neurons and glia cells (Johanna Mäkelä et al., 2014). Additionally, FGF21 is able to cross the blood brain barrier by simple diffusion which is further supported by detecting FGF-21 levels in human cerebrospinal fluid (Hsuchou et al., 2007; Tan et al., 2011). In SH-SY5Y cells model, FGF-21 exhibited neuroprotective effects against oxidative damage, mediated by an increased activity of the peroxisome proliferator activated receptor γ co-activator 1 α (PGC1- α) and resulted in improved of mitochondrial biogenesis and antioxidant enzymes activities (Mäkelä et al., 2014). Based on these observations, we attempted to measure FGF-21 levels in SH-SY5Y cells model. However after repeated attempts, we were unable to detect any FGF-21 signal. This could be explained by a number of possible reasons such as a lack of sensitivity of the kit to measure very low levels of the target antigen, produced by a limited number of cells in cell culture, the inability of these particular neuroblastoma cells in culture to produce FGF21 in any appreciable amount, or possibly due to a component in the culture medium interfering with

the assay. Clearly, further research will be required to optimize and develop new FGF21 assays more suited for cell culture applications.

7.6 Conclusions

Based on the results, it can be concluded that the human FGF-21 ELISA assay appears to be a reliable and reproducible method and potentially useful clinically as part of the diagnostic algorithm for the evaluation of patients with mitochondrial disorders. Although some variations were observed in FGF-21 levels among patients with mitochondrial diseases, it seems that FGF-21 has a great potential as a biomarker as well as a monitor of the progression of mitochondrial disorders. Further work should therefore be directed towards evaluating levels in a larger cohort of patients with confirmed diagnoses of mitochondrial disease.

CHAPTER 8

General Discussion, Conclusion and Further Work

8.1 Discussion

As was reviewed in the chapter 1 of this thesis, mitochondria can be thought of as the main energy supply of the living cell. Among all living cells, neurons are critically dependent upon the availability and correct functioning of mitochondria (Cobley et al., 2018). If these organelles begin to fail then the ability of the neurons to carry out their normal activity can consequently become compromised. Of note, impairment of mitochondrial function has been potentially implicated to be a contributing factor in the pathophysiology of a number of inherited disorders as well as more common neurodegenerative disorders such as Parkinson's disease (PD) (Hayashi and Cortopassi, 2015) (Stewart and Heales,2003).

Evidence is now emerging that increased generation of mitochondrial reactive oxygen or nitrogen species (ROS/RNS), resulting in oxidative damage, may cause mitochondrial damage. Although mitochondrial respiratory chain (MRC) complexes, particularly complex I and III, are major mitochondrial ROS production, MRC complexes are among the systems that can potentially be affected by oxidative damage (Bolaños and Heales, 2010). Furthermore, when this damage has occurred, a self-propagating cycle of events can ensue leading to further MRC complexes damage, ROS, and alteration of intracellular antioxidants such as reduced glutathione (GSH). This sequence of events may lead ultimately to neuronal cell death (Keane et al., 2011). Additionally, it is worth emphasising that the loss of MRC complex activity doesn't necessarily equate to a failure of the mitochondrial ATP pathway, i.e. a specific threshold of compromised activity has to be exceeded 50% inhibition before ATP synthesis is affected (Davey et al., 1998).

It has previously been demonstrated in a range of *in vitro* and *in vivo* models that increased oxidative stress, within the central nervous system (CNS) can lead to mitochondrial damage at the level of the MRC complexes (Guo et al., 2013). In view of all that has been mentioned so far, the overall aim of this thesis was therefore to ascertain the biochemical events that occurs upon persistent loss of MRC complex I activity and its progression to other complexes, in conjunction with bioenergetic, cofactor (CoQ₁₀), and antioxidant (GSH) status. This could ultimately leads to the identification of new pathogenic mechanisms and potentially new therapeutic approaches for common neurodegenerative disorders such as PD

Despite the precise mechanism associated with neurodegeneration of PD not yet having been fully elucidated, the inhibition of MRC complexes activities, particularly, the ROS- generator MRC complex I has been invoked as a potential contributor to the pathophysiology of PD. Since it was firstly demonstrated in 1989, the loss of MRC complex I activity has provided the biochemical tie between neurotoxin MPP⁺ and idiopathic Parkinsonism (Schapira et al., 1989). Subsequent studies were undertaken to elucidate the cause of MRC complex I deficiency in the aetiology of PD. As such, early studies focused on the anatomic and disease specificity of the MRC complex I deficiency in PD. Using post-mortem brain, MRC complex I deficiency has been detected in the substantia nigra (SN) (Schapira et al., 1989), the frontal lobe and the striatum (Mizuno et al., 1990) as well as in frontal cortex of PD patients (Parker et al., 2008). Furthermore, a deficit in MRC complex I activity appears to be systematic, affecting multiple tissues (Schapira, 2008). In addition to MRC damage which plays a crucial role in the pathogenesis of PD,

its closely relationship with the other pathogenic factor— the aggregation of α -synuclein— has been evidently demonstrated (Rocha et al., 2018). Nevertheless, whether the defect in MRC activity precedes the α -synuclein pathology is still less understood. **In chapter 3 of this thesis**, MRC enzyme complex activities were therefore evaluated in PD post-mortem brain with different α -synuclein pathological severity, and a number of key findings were documented, as summarised in (Table 17).

Table 17 MRC complex I, II-III and IV inhibitions in post-mortem PD brain regions with different pathological severity

<i>MRC Activity (%)</i>	<i>The PD post-mortem brain regions with different pathological severity</i>				
	<i>Frontal Cortex</i>	<i>Parietal Cortex</i>	<i>Parahippocampus</i>	<i>Temporal Cortex</i>	<i>Putamen</i>
<i>Complex I</i>	No change		40%	26%	63%
<i>Complex II-III</i>	No change		No change	No change	74%
<i>Complex IV (k/nmol)</i>	No change		No change	No change	33%
<i>Complex II</i>	No change				



Pathologically Unaffected
Mild Pathology
Moderate Pathology

- MRC complex I, II-III and IV inhibitions were expressed as a percent % of brain control

Furthermore, the most interesting result to emerge from the data is that the moderately affected brain region, the putamen, shows multiple MRC deficiencies. Similar defects have been also reported in various tissues of PD patients (Schapira, 1994; Mizuno et al., 1989; Parker et al., 1989; Shoffner et al., 1991; Bindoff et al., 1991). Furthermore, it has been also shown in some cases that multiple respiratory chain complex deficiencies have been associated with inherited mitochondrial disorders (Mayr et al., 2015). However, whether the multiple complexes defect observed in the putamen is the result of the brain region itself or the duration of the disorder is not fully understood. In order to gain insight into the mechanism associated with multiple complex defects in the putamen, **the next chapter** then utilized SH-SY5Y cells to characterize the effect of rotenone induced MRC complex I deficiency upon the activity of the other MRC complexes at 24 and 48 hrs. At the level of inhibition which has been frequent reported with idiopathic PD patients, 100 nM of rotenone partially induced MRC complex I deficiency. Furthermore, this partial inhibition did not result any significant ATP depletion. Nevertheless, it may be sufficient to increase ROS production in agreement with previous our laboratory work (Aylett et al., 2013), suggesting that rotenone-induced neuronal cell death could be as the result of oxidative damage rather than a deficit in ATP level (Sherer et al., 2003). These findings also may address the question as to whether the inhibition of MRC complex I in PD might be a consequence of neuronal cell death.

Furthermore, the enzymatic results of MRC have indicated the evidence of multiple mtDNA-encoded complexes deficiencies after 48 hrs of rotenone

treatment. Similarly to pathologically moderated brain region, putamen, the activity of MRC complex II, which is entirely encoded by nuclear DNA also appeared to be preserved. The results of MRC I, II–III and IV activities in rotenone-treated cells for 24 and 48 hrs are summarised in (Table 18).

Table 18 MRC complex I, II-III and IV inhibitions in SHSY5Y cells treated with 100 nM of rotenone for 24 and 48 hrs

<i>MRC Activity (%)</i>	<i>24 hr</i>	<i>48 hr</i>
<i>Complex I</i>	30%	
<i>Complex II-III</i>	No change	40%
<i>Complex IV (k/nmol)</i>	No change	30%
<i>Complex II</i>	No change	

MRC complex I, II-III and IV inhibitions were expressed as a percent % of control cells.

At the level of the MRC complexes, these findings observed in this chapter mirror to that seen in moderate affected brain region, putamen (**chapter 3**). There are several possible explanations for these findings which may be explained by the concept that an increase in ROS production resulting in oxidative stress could be a possible mechanism since mtDNA is particularly susceptible to oxidative damage, unlike nDNA. As MRC complex I is the major site of ROS production within mitochondria and is also encoded by seven mtDNA genes, in comparison

to other mitochondrial complexes, it therefore has a proportionally high susceptibility to oxidative damage. During this vicious cycle of damage, the accumulation of mtDNA lesions results in a deficit in MRC function, which in turn, leads to further elevation of cellular ROS level, and ultimately cell damage (reviewed by Al Shahrani et al., 2017). This is also supported by the observations in human brain tissues from PD patients where an increased level of the DNA oxidation product, 8-hydroxy-deoxyguanosine (8-OHdG) have been reported. (Alam et al., 1997). Intriguingly, impairment of mitochondrial phospholipid CL content and mitochondrial aconitase enzyme have been linked to mtDNA instability, suggesting another possible mechanism that the dysfunctional MRC encoded by mtDNA may be the consequence of oxidative damage (reviewed by Al Shahrani et al., 2017). Therefore, the crucial roles of mitochondrial CL content and aconitase enzyme in maintaining MRC function require to be investigated in this model.

Furthermore, It is interesting to note that GSH status was found to be significantly increased up to (30%) following 24 hr rotenone treatment indicating that may reflect an upregulation in the synthesis of GSH in order to cope with increased oxidative stress. Similar observation was also previously reported by (Zhu et al. 2007; Duberley et al., 2014). The plausible cause associated with the upregulation of neuronal GSH status in a partially inhibited MRC I model is not fully understood. However, the possible explanation of this upregulation may be as the result of the activation of the antioxidant response element signalling pathway, nuclear factor-erythroid 2 related factor 2 (Nrf-2), which is an important

regulatory factor to enhance gene expression of cellular antioxidant enzymes such as GSH biosynthesis (Harvey et al., 2009). However, more research into the precise cause of the upregulation of neuronal GSH status is still necessary before obtaining a definitive answer. It must also be noted that the intriguing relationship between GSG status and MRC activity. A Study by (Vásquez et al., 2001) have demonstrated that a loss of cellular GSH leads to an upregulation of the MRC complex I activity. The authors proposed that oxidative stress could lead to enhance the expression of the mitochondrial complex I enzyme.

In this chapter, the mechanism of how MRC complex deficiency affects energy charge, GSH, and CoQ₁₀ status over time was also carried out. The key findings were documented, as summarised in (Table 19). Taken together, the cell-based model provides evidence that persistent MRC complex I deficiency could lead to multiple complexes defects along with biochemical alterations in bioenergetics and GSH status (Figure 90).

Table 19 Summarised of key findings of energy charge, CoQ10 and GSH status upon exposure SH-SY5Y cells to 100 nM of rotenone for 24 and 48 hrs

Biochemical Parameter	24 hr	48 h
Energy Charge	No change	↓
GSH	↑	↓
CoQ ₁₀ Expressed as pmol/mg protein	No change	↑
CoQ ₁₀ Expressed as a ratio to CS activity	No change	No change

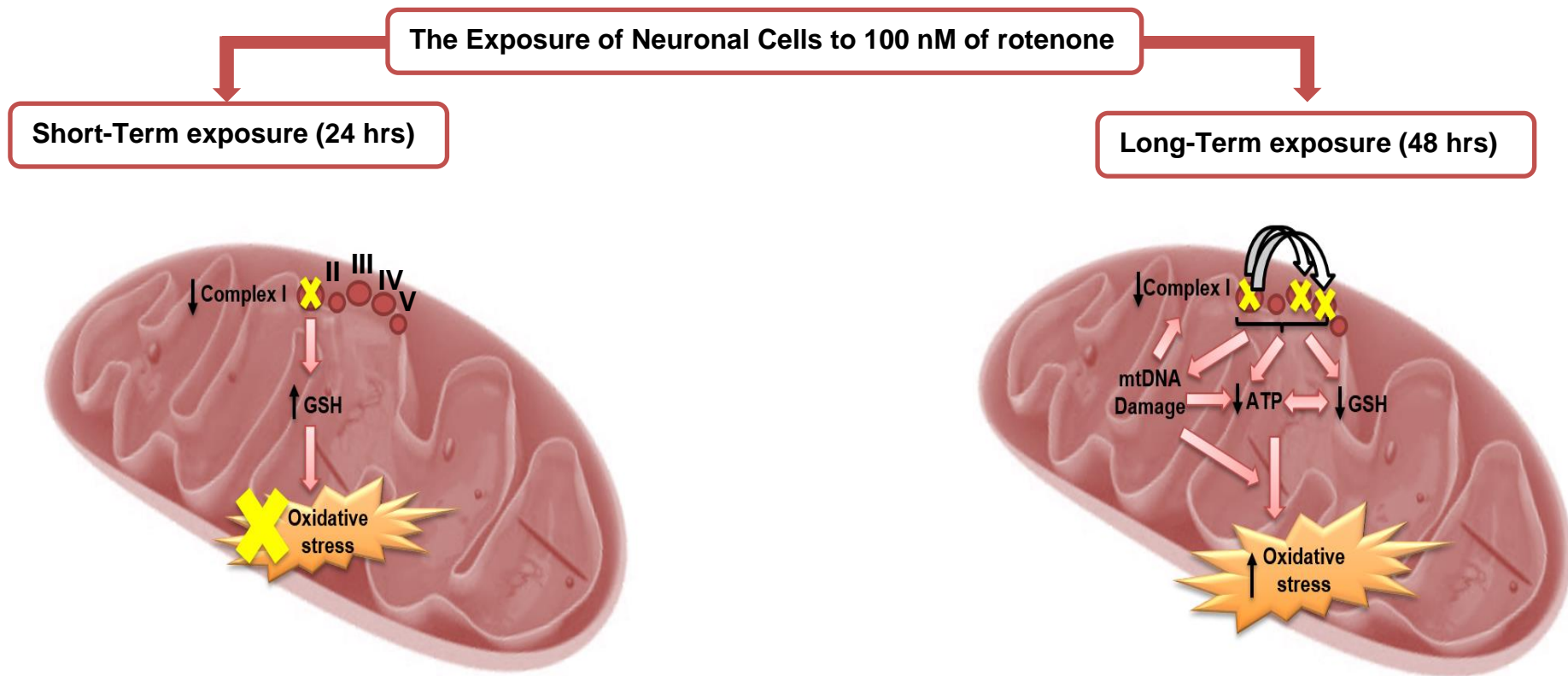


Figure 90 Summarised of the biochemical consequences associated with short and long-terms exposure to 100 nM of rotenone-induced MRC complex I deficiency. In this cell based-model, rotenone-treated (100 nM; 24-48 hrs) SH-SY5Y cells induced a significant inhibition of complex I. At 24 hrs (short-term exposure) no effect was observed on the other complexes. Moreover, the GSH status was significantly upregulated. However at 48 hrs (long-term exposure), multiple complexes defect was noted, but the activity of complex II appeared to preserved. Additionally, bioenergetics and glutathione status were compromised.

Additionally, bioenergetics and glutathione status were compromised. Despite significant advances being made towards the diagnosis and characterization of mitochondrial disorders, appropriate therapy to halt or slow the disorder progression remains an obstacle. As mentioned above, the neuronal cell model presented **in chapter 4** provides us with insight into the underlying mechanism of multiple MRC complexes deficiencies which could be exploited for potential therapeutic interventions to convey protection towards mitochondria and thereby protecting neuronal cell. A potential strategy for reversing the effects of mitochondrial damage could be through suppression of oxidative stress and improvement of mitochondrial function by the use of antioxidant molecules. Therefore, **chapter 5 of this thesis** sheds new light on the effectiveness of ascorbate, Trolox and NAC at limiting/reversing multiple MRC complexes deficiencies following 48 hrs rotenone treatment. Due to its multiple antioxidant properties, ascorbate evoked a complete restoration of multiple MRC activity in rotenone-treated SH-SY5Y cells. However, it is unlikely that this effect can be solely attributed to an antioxidant effect and as such, multiple mechanisms are likely to be responsible. However, the antioxidant effects of Trolox and NAC enhanced the activity of both MRC complex I and IV, but not II-III.

Despite the considerable scientific evidence that has accumulated to support the use of these antioxidants, many patients with either inherited or acquired mitochondrial disorders have shown variable clinical improvements when administered with these antioxidants alone (El-Hattab et al., 2017; Enns, 2014, 2017; Dias et al., 2013). Nevertheless, it could be postulated that in combination, a cocktail antioxidant therapy may effectively improve clinical

and biochemical features in patients with mitochondrial disease, particularly if they target various pathogenetic sites, to an extent not observed previously with an individual antioxidant molecule (Viscomi et al., 2015; Schapira, 2008). Recently, mitochondrial-targeted antioxidants (MTAs), such as mitoquinone (MitoQ) and mitotocopherol (MitoVitE), have become attractive therapeutic agents in the treatment of mitochondrial disease associated with oxidative stress (Smith et al., 2008; Ross et al., 2005). These well-established agents, MTAs are known to easily cross cellular membranes and attain the target of mitochondrial ROS sites, providing additional protective effects against deleterious effects of mitochondrial oxidative damage (Jin et al., 2014). Furthermore, in its various forms, the ketogenic diet (KD) has been recently proposed as a potential therapeutic therapy for mitochondrial associated with neurological disorders particularly, epilepsy (Kossoff and Hartman, 2012). The KD mechanism of action with regards to how the diet exerts its efficacy is not fully understood. However, considerable evidence exists suggesting that the KD efficacy may occur, in part, as result of stimulation of mitochondrial biogenesis. Recently, our laboratory has also revealed that decanoic acid (C10) which is a component of the medium chain triglyceride KD, enhances mitochondrial biogenesis and improves the activity of MRC complex I as well as antioxidant levels in SH-SY5Y cells (Hughes et al., 2014). Additionally, exposure of fibroblast cells derived from MRC complex I-deficient patients to C10 have showed various beneficial effects in some cases (Kanabus et al., 2016). With regards to PD, Unified Parkinson's Disease Rating Scale (UPDRS) scores improved by 43 % in five PD patients on the KD for 28 days when conducted in an uncontrolled study (Vanitallie et al., 2005). This

suggests that the KD could be helpful as possible a therapeutic approach for inherited and acquired mitochondrial disorders. However, these therapeutic approaches mentioned above need to be further conducted in double blind, randomized, placebo-controlled clinical trials with large sample size to evaluate their long-term clinical efficacy and safety as potential therapeutic treatments for mitochondrial disorders.

From the previous discussion, it is obvious that the assessment of neuronal mitochondrial function is a decisive step forward for better elucidating the underlying mechanism of PD, thus ultimately leading to the development of novel therapeutic strategies. Given this, an integrated approach to assess the integrated mitochondrial function are in demand. As such, an approach in which mitochondrial oxygen consumption can be accurately evaluated using high-resolution respirometry (HHR) using the Oxygraph-2K® (O2k) instrument was developed.

As was pointed out in the introduction to chapter 6, mitochondrial respiratory rates evaluated in intact cultured cells differ comparison to rates measured in isolated mitochondria. For instance, the ADP-stimulated rate (state 3) is not possible to evaluate in cultured cells since the cell membrane is not permeable to ADP. However, the use of the real-time O2K instrument together with a step-wise protocol by applying mitochondrial inhibitors (eg, oligomycin and rotenone) and an uncoupler (FCCP) has enabled us to gain information (i.e. oxygen consumption) regarding the integrated mitochondrial function in cultured SH-SY5Y cells (see **chapter 6**). In this chapter, we also had the opportunity to evaluate the mitochondrial respiratory rate of cultured SH-SY5Y cells, including the basal respiration, proton leak, maximum

respiration and non-mitochondrial respiration rates. The development and evaluation of this technique has set the scene to allow subsequent further work in which this protocol can be utilised to study the neuronal cell model as described previously in **chapter 4** to gain a better understanding of the changes that occur in mitochondrial function as whole as opposed to changes to the individual complexes measured in isolation. The isolation of intact functional mitochondria from SH-SY5Y cells to investigate the overall oxidative phosphorylation (OXPHOS) system could be usefully explored in further work.

To date, there is still no first-line non-invasive biomarker test available for mitochondrial disorders, and as such, a wide range of biochemical surrogates are required to make a definitive diagnosis and monitor the therapeutic interventions. However, the stress hormone, fibroblast growth factor-21 (FGF-21) has been recently proposed as a potential biomarker for mitochondrial disorders. **In chapter 7 of this thesis**, the focus of attention therefore was to initially validate the human FGF-21 sandwich ELISA as a mitochondrial biomarker assay. Overall, although some variations were observed in FGF21 levels among patients with mitochondrial diseases, it seems that FGF-21 has a potential as a biomarker as well as a monitor of the progression of mitochondrial disorders. Nevertheless, there are some principal challenges that should be considered. At present, there are many commercial ELISA kits available for quantitation of FGF-21 in serum samples such as Biovender, Abcam, Biomatik, AssayPro, and Nordic BioSite which are not validated for clinical implementation. Furthermore, studies have indicated that lot-to-lot and manufacturer-to-manufacturer variability of calibrators and reagents occur in

all currently available kits (Suomalainen, (2013). Additionally, our experience throughout the validation process showed that lot-to-lot variability exists even within the same kit (Biovender). Although all available ELISA kits ostensibly serve to quantitate FGF-21 levels, the literature indicates variation even within the reference range of healthy subjects. Thus, improving manufacturing procedures to enhance the specificity, limit of detection, monoclonal antibodies as well as the reduction of the lot to lot variability may be required to meet the high diagnostic standards.

Furthermore, several studies have found that circulating levels of FGF-21 increased also in obesity-related metabolic disorders and non-alcoholic fatty liver disease (NAFLD). In fact, these non- mitochondrial disorders are not basically associated with muscle weakness and hence could not complicate the utilization of FGF-21 as a biomarker in diagnostics of muscle-manifesting mitochondrial disorders. Additionally, patients who are associated with these metabolic syndromes are possibly a heterogeneous group, characteristically without confirmed genetic diagnosis, and thus could include patients with mitochondrial disorders (Suomalainen, 2013). Further studies in well-characterized patient materials are required for further investigation to gain knowledge, whether other physiological or pathological conditions consistently linked with increased level of FGF-21 occur. These conditions should be therefore considered as differential diagnoses, when using FGF-21 as a biomarker in lab diagnosis of mitochondrial disorders.

Although several lines of evidence suggest that FGF-21 may have the potential to be utilized in clinical practice as a sensitive non-invasive biomarker for mitochondrial diseases, muscle biopsy remains a gold

diagnostic tool. Thus, patients with high level of FGF-21 in their serum could be possibly forwarded to muscle sampling, as their muscle genetic, biochemistry, and histology is likely to be more informative for their conditions. Conversely, patients with low level of FGF-21 are less likely to have a muscle-manifesting mitochondrial disease and therefore they could be forwarded to other diagnostic tests rather than for muscle biopsy (Suomalainen, 2013).

Furthermore, the recognition that oxidative stress and mitochondrial impairment has a potential role in the pathophysiology of PD has yielded means to test the hypothesis that the stress hormone, FGF-21 and its expression in brain cells, might be useful as a surrogate biomarker for PD. In this context, we attempted to evaluate the effect of compromised neuronal mitochondrial function on FGF-21 levels utilizing SH-SY5Y cells model. Nonetheless, we were unable to detect any FGF-21 signal. The reason for this finding is not completely clear, but it is possibly due to the lack of sensitivity of the ELISA kit to measure very low levels of the target antigen or the inability of SH-SY5Y cells in culture to produce FGF21 in any appreciable amount. Thus, a reasonable approach to tackle this issue could be to optimize and develop new FGF21 assays more suited for cell culture applications.

8.2 Conclusion

This thesis has investigated the biochemical consequences of MRC complex I deficiency. Based on the observation that multiple complexes deficiencies were noted in the moderate affected brain region of PD patients, SH-SY5Y cell was therefore employed to study the effect of rotenone induced MRC complex I deficiency upon the activity of the other complexes. This cell-based model provides evidence that persistent MRC complex I deficiency may lead to secondary loss of other complexes, potentially involving loss of GSH and reduction energy charge. This model not only provides a possible approach to study the biochemical consequences of complex I deficiency in acquired adult-onset neurodegenerative disorders such as PD, but it also could be potentially applicable to study these biochemical consequences in an inherited mitochondrial disorder as well as monitoring therapeutic interventions. As such, the early intervention of three antioxidants including ascorbate, Trolox and NAC were evaluated employing this cell-based model. In this study, ascorbate appears to be more effective than Trolox and NAC in alleviating MRC complexes defects caused by rotenone treatment. Furthermore, using an O2K instrument and applying a step-wise titration protocol including the use of MRC complex inhibitors and uncouplers has enabled us to develop an approach to assess the integrated mitochondrial function in cultured SH-SY5Y cells which could also be useful for investigating mitochondrial dysfunction as well as monitoring treatments.

In order to limit the need for an invasive muscle biopsy, FGF-21 is being evaluated as a potential biomarker since it has been suggested that it may act as a useful and reliable tool for the identification and monitoring of patients

with suspected mitochondrial disorder. Although a number of promising and interesting findings have been presented in this thesis which can help provide new insights into possible mechanistic events associated with the loss of MRC complex I activity, further studies will no doubt enhance our understanding better and potentially contribute towards the development of a diagnostic biomarker as well as novel therapeutic strategies aimed at slowing down disease progression.

8.3 Further work

This thesis has raised many questions and highlighted many issues that require further investigation. Therefore, it would be interesting that further studies be carried out in the following areas:

8.3.1 Neuronal Cell Model

As was shown in the chapter 4, the earliest indicator for oxidative stress, GSH was depleted following rotenone treatment for 48 hrs with a concomitant depletion in ATP levels. With regards to the latter, it is uncertain whether this depletion occurs as a result of decreased energy status (required for GSH biosynthesis) or due to elevated ROS levels. Further experimental investigations are therefore needed to analyse the mitochondrial ROS generation in this model.

As mentioned previously (**chapter 1**), mitochondrial CL plays a crucial role in aspects of maintaining and stabilizing the functional properties of the mitochondrial complexes and their assembly into supercomplexes. Considerably more studies will need to be carried out to study the effects of CL content and supercomplexes upon MRC activity. Another possible study

of future research would be also to investigate the potential implication of mitochondrial aconitase enzyme on MRC function as was pointed out in **(chapter 1)** that the loss of mitochondrial aconitase activity has been linked to mitochondrial oxidative damage that results in reduced the MRC activity as was reviewed in chapter 1.

Furthermore, the most interesting result to emerge from the data is that multiple mtDNA encoded complexes impairments are seen in post-mortem putamen **(chapter 3)** and rotenone- treated cells at 48 hrs **(chapter 4)**. Thus, the quantification of mtDNA content would be worthwhile. Furthermore, this cell-based model used undifferentiated cell and that may not be suitable model for studying pathological events in a chronic and progressive disorder such as PD. Due to the onset of replicative senescence, undifferentiated neuronal cells cannot be cultured or even treated with neurotoxin for a sufficiently long period of time (Constantinescu et al., 2007). Therefore, neuronal differentiation to a neuronal-like state would be interesting to establish a suitable chronic neuronal cell model. Additionally further investigation into the potential involvement of glial (astrocytes) cells with regards to influencing (positively or negatively) neuronal to oxidative stress and availability of antioxidants. Furthermore, with the advent of induced pluripotent stem cells (iPSC) technologies being developed, it is now possible to accurately model α -synucleinopathies with induced pluripotent stem cells (iPSC)-derived neurons. This technique will increase our understanding regarding the underlying mechanism of PD at early stages, thus potentially leading to identify new therapeutic targets (Singh et al., 2017). Therefore, further investigation into this advanced technique would be of interest.

8.3.2 Antioxidant Treatments

We have observed that ascorbate is an effective antioxidant at restoring normal activity of multiple MRC. Moreover, the antioxidant effects of Trolox and NAC enhanced the activity of both complex I and IV, but complex II-III was still compromised. It would be therefore interesting to investigate higher concentrations of Trolox and NAC to ascertain whether MRC complex II-III activity can be restored to normal levels.

To further strengthen this study, the mitochondrial ROS generation, energy charge status, and the intracellular level of GSH investigation could be carried out to assess the mitochondrial function upon antioxidants treatment. Additionally further investigation into the pharmacological efficacy of FGF21 analogue (e.g. LY2405319) and the effect of KD therapy at limiting/reversing multiple MRC complexes deficiencies would be of interest.

8.3.3 The Measurement of Mitochondrial Respiration Using O2K

The use of the O2K instrument together with a step-wise protocol has enabled us to gain information regarding the integrated mitochondrial function in cultured SH-SY5Y cells under physiological conditions. A natural progression of this work therefore is to apply this protocol to assess the integrated mitochondrial function in the neuronal cell model as well as following antioxidants and FGF21 analogue interventions. Another interesting study of future work would be the isolation of intact functional mitochondria from cultured SH-SY5Y cells based on the method of (Almeida and Medina, 1997), to allow the application of various mitochondrial substrates, thus leading to

yield further genuine information regarding the oxidative phosphorylation (OXPHOS) system.

8.3.4 FGF-21

Based on the results, it seems that FGF-21 may have the potential to be utilized as non-invasive biomarker for mitochondrial diseases. To be implemented in clinical practice, however, further work should be directed towards evaluating levels in a larger cohort of patients with confirmed diagnoses of mitochondrial disease so that it could provide more definitive evidence. Furthermore, another interesting application of this biomarker would be to measure FGF-21 concentration on CSF sample from patients with early stage of PD. Additionally, optimizing and developing a cell culture FGF21 ELISA kit would be interesting to study the effects of FGF-21 upon compromised neuronal mitochondrial function.

List of References

Abou-Sleiman, P.; Muqit, M.; Wood, N. Expanding Insights of Mitochondrial Dysfunction in Parkinson's Disease. *Nat. Rev. Neurosci.* **2006**, *7*, 207–219.

Adachi, K.; Oiwa, K.; Nishizaka, T.; Furuike, S.; Noji, H.; Itoh, H.; Yoshida, M.; Kinoshita, K. Coupling of Rotation and Catalysis in F (1)-ATPase Revealed by Single-Molecule Imaging and Manipulation. *Cell.* **2007**, *130*, 309-321.

Adam-Vizi, V.; Chinopoulos, C. Bioenergetics and the Formation of Mitochondrial Reactive Oxygen Species. *Trends Pharmacol. Sci.* **2006**, *27*, 639–645.

Ahola-Erkkila, S.; Carroll, C.; Peltola-Mjosund, K.; Tulkki, V.; Mattila, I.; Seppänen-Laakso, T.; Oresic, M.; Tyynismaa, H.; Suomalainen, A.. Ketogenic Diet Slows Down Mitochondrial Myopathy Progression in Mice. *Hum. Mol. Genet.* **2010**, *19*, 1974-1984.

Al Shahrani, M.; Heales, S.; Hargreaves, I.; Orford, M. Oxidative Stress: Mechanistic Insights into Inherited Mitochondrial Disorders and Parkinson's Disease. *J. Clin. Med.* **2017**, *6*, 100.

Alam, Z.; Jenner, A.; Daniel, S.; Lees, A.; Cairns, N.; Marsden, C.; Jenner, P.; Halliwell, B. Oxidative DNA Damage in the Parkinsonian Brain: an Apparent Selective Increase in 8-Hydroxyguanine Levels in Substantia Nigra. *J. Neurochem.* **1997**, *69*, 1196-1203.

Alexeyev, M.; Shokolenko, I.; Wilson, G.; LeDoux, S. The Maintenance of Mitochondrial DNA Integrity- Critical Analysis and Update. *Cold Spring Harb Perspect Biol.* **2013**, *5*, a012641.

Allaman, I.; Bélanger, M.; Magistretti, P. Astrocyte-Neuron Metabolic Relationships: for Better and for Worse. *Trends Neurosci.* **2011**, *34*, 76–87.

Almeida, A.; Medina, J. Isolation and Characterization of Tightly Coupled Mitochondria from Neurons and Astrocytes in Primary Culture. *Brain Res.* **1997**, *764*, 167-172.

Almeida, A.; Moncada, S.; Bolaños, J. Nitric Oxide Switches on Glycolysis through the AMP Protein Kinase and 6-Phosphofructo-2-Kinase Pathway. *Nat Cell Biol.* **2004**, *6*, 45–51.

Ambani, M.; Van Woert, M.; Murphy S. Brain Peroxidase and Catalase in Parkinson Disease. *Arch Neurol.* **1975**, *32*, 114-118.

Ambrosi, G.; Ghezzi, C.; Sepe, S.; Milanese, C.; Payan-Gomez, C.; Bombardieri, C.; Armentero, M.; Zangaglia, R.; Pacchetti, C.; Mastroberardino, P.; Blandini, F. Bioenergetic and Proteolytic Defects in Fibroblasts from Patients with Sporadic Parkinson's Disease. *Biochim. Biophys. Acta.* **2014**, *1842*, 1385-1394.

Andreasson, U.; Perret-Liaudet, A.; Van Waalwijk, L.; Iennow, K.; Chiasserini, D.; Engelborghs, S.; Fladby, T.; Genc, S.; Kruse, N.; Kuiperij, H.; Kulic, L.; Lewczuk, P.; Mollenhauer, B.; Mroczko, B.; Parnetti, L.; Vanmechelen, E.; Verbeek, M.; Winblad, B.; Zetterberg, H.; Koel-Simmelink, M.; Teunissen, C. A Practical Guide to Immunoassay Method Validation. *Frontiers in Neurology.* **2015**, *6*, 179.

Annamaki, T.; Muuronen A.; Murros, K. Low Plasma Uric Acid Level in Parkinson's Disease. *Movement Disorders.* **2007**, *22*, 1133–1137.

Atkinson, D. The Energy Charge of the Adenylate Pool as a Regulatory Parameter. Interaction with Feedback Modifiers. *Biochemistry.* **1968**, *7*, 4030-4034.

Aylett, S.; Neergheen, V.; Hargreaves, I.; Eaton, S.; Land, J.; Rahman, S.; Heales, S. Levels of 5-Methyltetrahydrofolate and Ascorbic Acid in Cerebrospinal Fluid are Correlated: Implications for the Accelerated Degradation of Folate by Reactive Oxygen Species. *Neurochem Int.* **2013**, *8*, 750-755.

Babcock, M.; Silva, D.; Oaks, R.; Davis-Kaplan, S.; Jiralerspong, S.; Montermini, L.; Pandolfo, M.; Kaplan, J. Regulation of Mitochondrial Iron Accumulation by Yfh1p, a putative Homolog of Frataxin. *Science.* **1997**, *276*, 1709-1712.

Beal, M.; Oakes, D.; Shoulson, I.; Henchcliffe, C.; Galpern, W.; Haas, R.; et al. A Randomized Clinical Trial of High-Dosage Coenzyme Q₁₀ in Early Parkinson Disease: No Evidence of Benefit. *JAMA Neurol.* **2014**, *71*, 543–552.

Bai, Y.; Park, S.; Deng, J.; Li, Y.; Hu, P. Restoration of Mitochondrial Function in Cells with Complex I Deficiency. *Annals of the New York Academy of Sciences.* **2005**, *1042*, 25-35.

Baile, M.; Lu, Y.; Claypool, S. The Topology and Regulation of Cardiolipin Biosynthesis and Remodeling in Yeast. *Chem. Phys. Lipids.* **2014**, *179*, 25-31.

Balsa, E.; Marco, R.; Perales-Clemente, E.; Szklarczyk, R.; Calvo, E.; Landázuri, M.; Enríquez, J. NDUFA4 is a Subunit of Complex IV of the Mammalian Electron Transport Chain. *Cell Metab.* **2012**, *16*, 378-386.

Barrientos, A.; Fontanesi, F.; Díaz, F. Evaluation of the Mitochondrial Respiratory Chain and Oxidative Phosphorylation System using Polarography and Spectrophotometric Enzyme Assays. *Current Protocols in Human Genetics* / editorial board, Haines, J.; et al. **2009**, Chapter: Unit19.3.

Barshop, B. Metabolomic Approaches to Mitochondrial Disease: Correlation of Urine Organic Acids. *Mitochondrion*. **2004**, 4,521-527.

Bartels, A.; Willemsen, A.; Doorduyn, J.; de Vries E.; Dierckx, R.; Leenders, K. PET: Quantification of Neuroinflammation and a Monitor of Anti-Inflammatory Treatment in Parkinson's Disease? *Parkinsonism Relat Disord*. **2010**, 16, 57–59.

Barth, P.; Scholte. H.; Berden, J.; Moorsel, J.; Luyt-Houwen, I.; Veer-Korthof, E.; Harten, J.; Sobotka-Plojhar, M. An X-linked Mitochondrial Disease Affecting Cardiac Muscle, Skeletal Muscle and Neutrophil Leucocytes. *J Neurol Sci*. **1983**, 62, 327-355.

Barth, P.; Valianpour, F.; Bowen, V.; Lam, J.; Duran, M.; Vaz. F.; Wanders, R. X-linked Cardioskeletal Myopathy and Neutropenia (Barth Syndrome): An Update. *Am. J. Med. Genet*. **2004**, 126A, 349–354.

Barth, P.; Wanders, R.; Vreken, P.; Janssen, E.; Lam, J.; Baas, F. X-linked Cardioskeletal Myopathy and Neutropenia (Barth Syndrome) (MIM 302060). *J. Inher. Metab. Dis*. **1999**, 22, 555-567.

Battisti, C.; Formichi, P.; Cardaioli, E.; Bianchi, S.; Mangiavacchi, P.; Tripodi, S.; Tosi, P.; Federico, A. Cell Response to Oxidative Stress Induced Apoptosis in Patients with Leber Hereditary Optic Neuropathy. *J. Neurol. Neurosurg. Psychiatry*. **2004**, 75, 1731–1736.

Bazán, S.; Mileykovskaya, E.; Mallampalli, V.; Heacock, P.; Sparagna, G.; Dowhan, W. Cardiolipin-dependent Reconstitution of Respiratory Supercomplexes from Purified *Saccharomyces cerevisiae* Complexes III and IV. *The Journal of Biological Chemistry*. **2013**, 288, 401–411.

Bazinet, R.; Layé, S. Polyunsaturated Fatty Acids and Their Metabolites in Brain Function and Disease. *Nat. Rev. Neurosci*. **2014**, 15, 771-785.

Beinert, H.; Kennedy, M. Aconitase, a Two-faced Protein: Enzyme and Iron Regulatory Factor. *FASEB J.* **1993**, *15*, 1442-1449.

Benecke, R.; Stumper, P.; Weiss, H. Electron Transfer Complexes I and IV of Platelets are Abnormal in Parkinson's Disease but Normal in Parkinson's-Plus Syndromes. *Brain.* **1993**, *116*, 1451–1463.

Benner, E.; Banerjee, R.; Reynolds, A.; Sherman, S.; Pisarev, V.; Tsiperson, V.; et al. Nitrated Alpha-Synuclein Immunity Accelerates Degeneration of Nigral Dopaminergic Neurons. *PLoS One.* **2008**, *3*, e1376.

Berman, S.; Hastings, T. Dopamine Oxidation Alters Mitochondrial Respiration and Induces Permeability Transition in Brain Mitochondria. *J Neurochem.* **1999**, *73*, 1127–1137.

Bernheimer, H.; Birkmayer, W.; Hornykiewicz, O.; Jellinger, K.; Seitelberger, F. Brain Dopamine and the Syndromes of Parkinson and Huntington Clinical, Morphological and Neurochemical Correlations. *Journal of the Neurological Sciences.* **1973**, *20*, 415-455.

Bezard, E.; Dovero, S.; Prunier, C.; Ravenscroft, P.; Chalon, S.; Guilloteau, D.; Crossman, A.; Bioulac, B.; Brotchie, J.; Gross, C. Relationship Between the Appearance of Symptoms and the Level of Nigrostriatal Degeneration in a Progressive 1-Methyl-4-Phenyl-1,2,3,6-Tetrahydropyridine-Lesioned Macaque Model of Parkinson's Disease. *J Neurosci.* **2001**, *21*, 6853-6861.

Betarbet, R.; Sherer, T.; Greenamyre, J. Animal Models of Parkinson's Disease. *Bioessays.* **2002**, *24*, 308–318.

Bharath, S.; Hsu, M.; Kaur, D.; Rajagopalan, S.; Andersen, J. Glutathione, Iron and Parkinson's Disease. *Biochem. Pharmacol.* **2002**, *64*, 1037-1048.

Bhatt, D.; Chen, X.; Geiger, J.; Rosenberger, T. A Sensitive HPLC-Based Method to Quantify Adenine Nucleotides in Primary Astrocyte Cell Cultures. *Journal of Chromatography B, Analytical Technologies in the Biomedical and Life Sciences*. **2012**, *890*, 110-115.

Biedler, J.; Helson, L.; Spengler, B. Morphology and growth, Tumorigenicity and Cytogenetics of Human Neuroblastoma Cells in Continuous Culture. *Cancer Research*. **1973**, *33*, 2643-2652.

Bindoff, L.; Birch-Machin, M.; Cartlidge, N.; Parker, W.; Turnbull, D. Respiratory Chain Abnormalities in Skeletal Muscle from Patients with Parkinson's Disease. *Journal of the Neurological Sciences*. **1991**, *104*, 203–208.

Birben, E.; Sahiner, U.; Sackesen, C.; Erzurum, S.; Kalayci, O. Oxidative Stress and Antioxidant Defense. *World Allergy Organ. J.* **2012**, *5*, 9–19.

Birch-Machin, A.; Briggs, H.; Saborido, A.; Bindoff, L.; Turnbull, D. An Evaluation of the Measurement of the Activities of Complexes I-IV in the Respiratory Chain of Human Skeletal Muscle Mitochondria. *Biochem. Med. Metal. Biol.* **1994**, *51*, 35-42.

Bird, I. High performance Liquid Chromatography: Principles and Clinical Applications. *British Medical Journal*. **1989**, *299*, 783-787.

Bisaglia, M.; Soriano, M.; Arduini, I.; Mammi, S.; Bubacco, L. Molecular Characterization of Dopamine-Derived Quinones Reactivity toward NADH and Glutathione: Implications for Mitochondrial Dysfunction in Parkinson Disease. *Biochim Biophys Acta (BBA) Mol Basis Dis.* **2010**, *1802*, 699–706.

Blanchet, L.; Smeitink, J.; Van, S.; Caroline, V.; Mina, P.; An, I.; Richard, R.; Lutgarde, B.; Julien, B.; Peter, W.; Werner, K. Quantifying Small Molecule Phenotypic Effects Using Mitochondrial Morpho-Functional Fingerprinting and Machine Learning. *Sci Rep.* **2015**, *5*, 8035.

Bleier, L.; Dröse, S. Superoxide Generation by Complex III: From Mechanistic Rationales to Functional Consequences. *Biochim Biophys Acta*. **2013**, *1827*, 1320-1331.

Blesa, J.; Phani, S.; Jackson-Lewis, V.; Przedborski, S. Classic and New Animal Models of Parkinson's Disease. *J. Biomed. Biotechnol.* **2012**, *2012*, 1–10.

Bolaños, J.; Heales, S. Persistent Mitochondrial Damage by Nitric Oxide and its Derivatives: Neuropathological Implications. *Frontiers in Neuroenergetics*. **2010**, *2*, 1.

Borges, N. Tolcapone-Related Liver Dysfunction. *Drug Saf.* **2003**, *26*, 743–747.

Bové, J.; Prou, D.; Perier, C.; Przedborski, S. Toxin-Induced Models of Parkinson's Disease. *NeuroRx*. **2005**, *2*, 484-494.

Boyer, P. A Model for Conformational Coupling of Membrane Potential and Proton Translocation to ATP Synthesis and to Active Transport. *FEBS Lett.* **1975**, *58*, 1-6.

Boyle, J.; Hettiarachchi, N.; Wilkinson, J.; Pearson, H.; Scragg, J.; Lendon, C.; Al-Owais, M.; Kim, C.; Myers, D.; Warburton, P.; Peers, C. Cellular Consequences of the Expression of Alzheimer's Disease-Causing Presenilin 1 Mutations in Human Neuroblastoma (SH-SY5Y) cells. *Brain Res.* **2012**, *1443*, 75-88.

Braak, H.; Rüb, U.; Gai, P.; Del Tredici, K. Idiopathic Parkinson's Disease: Possible Routes by Which Vulnerable Neuronal Types May Be Subject to Neuroinvasion by an Unknown Pathogen. *J. Neural. Transm.* **2003**, *110*, 517-36.

Brand, M.; Nicholls, D. Assessing Mitochondrial Dysfunction in Cells. *Biochemical Journal*. **2011**, *435*, 297-312.

Bresgen, N.; Eckl, P. Oxidative Stress and the Homoeodynamics of Iron Metabolism. *Biomolecules*. **2015**, *5*, 808-847.

Breydo, L.; Wub, J.; Uversky, V. α -Synuclein Misfolding and Parkinson's Disease. *Biochimica et Biophysica Acta (BBA)*. **2012**, *1822*, 261-285.

Brown, G.; Cooper, C. Nanomolar Concentrations of NO Reversibly Inhibit Synaptosomal Respiration by Competing with Oxygen at Cytochrome Oxidase. *FEBS Lett*. **1994**, *356*, 295-298.

Brück, D.; Wenning, G.; Stefanova, N.; Fellner, L. Glia and Alpha-Synuclein in Neurodegeneration: A Complex Interaction. *Neurobiol Dis*. **2015**, *85*, 262-274.

Bunker, V. Free radicals, antioxidants and ageing. *Med. Lab. Sci*. **1992**, *49*, 299–312.

Burton, G.; Joyce, A.; Ingold, K. Is vitamin E the only Lipid-Soluble, Chain-Breaking Antioxidant in Human Blood Plasma and Erythrocyte Membranes? *Arch Biochem Biophys*. **1983**, *221*, 281-290.

Cadenas, E.; Boveris, A.; Ragan, I.; Stoppani, O. Production of Superoxide Radicals and Hydrogen Peroxide by NADH–Ubiquinone Reductase and Ubiquinol–Cytochrome c Reductase from Beef-heart Mitochondria. *Arch. Biochem. Biophys*. **1977**, *180*, 248–257.

Cadenas, E.; Davies, K. Mitochondrial Free Radical Generation, Oxidative Stress, and Aging. *Free Radical Biology and Medicine*. **2000**, *29*, 222-230.

Cai, Q.; Zakaria, H.; Sheng, H. Long Time-Lapse Imaging Reveals Unique Features of PARK2/Parkin-Mediated Mitophagy in Mature Cortical Neurons. *Autophagy*. **2012**, *8*, 976-978.

Campuzano, V.; Montermini, L.; Moltò, M.; Pianese, L.; Cossée, M.; Cavalcanti, F. Friedreich's ataxia: autosomal recessive disease caused by an intronic GAA triplet repeat expansion. *Science*. **1996**, *271*, 1423-1427.

Carr, A.; Frei, B. Does vitamin C Act as a Pro-Oxidant under Physiological Conditions? *FASEB J*. **1999**, *13*, 1007-1024.

Chambial, S.; Dwivedi, S.; Shukla, K.; John, P.; Sharma, P. Vitamin C in Disease Prevention and Cure: An Overview. *Indian Journal of Clinical Biochemistry*. **2013**, *28*, 314-328.

Chan, K.; Truong, D.; Shangari, N.; O'Brien, P. Drug-Induced Mitochondrial Toxicity. *Expert Opin Drug Metab Toxicol*. **2005**, *1*, 655–669.

Chance, B.; Hollunger, G. The Interaction of Energy and Electron Transfer Reactions in Mitochondria. General Properties and Nature of the Products of Succinate-linked Reduction of Pyridine Nucleotide. *J Biol. Chem*. **1961**, *236*, 1534–1543.

Chance, B.; Williams, G. Respiratory Enzymes in oxidative phosphorylation. VI. The Effects of Adenosine Diphosphate on Azide-Treated Mitochondria. *J Biol Chem*. **1956**, *221*, 477-489.

Chandra, S.; Chen, X.; Rizo, J.; Jahn, R.; Südhof, T. A Broken Alpha -Helix in Folded Alpha -Synuclein. *J Biol Chem*. **2003**, *278*, 15313-15318.

Chappel, S. The Role of Mitochondria from Mature Oocyte to Viable Blastocyst. *Obstetrics and Gynecology International*. **2013**, *2013*, 1-10.

Chavez, A.; Molina-Carrion, M.; Abdul-Ghani, M.; Folli, F.; Defronzo, R.; Tripathy, D. Circulating Fibroblast Growth Factor-21 is Elevated in Impaired Glucose Tolerance and Type 2 Diabetes and Correlates with Muscle and Hepatic Insulin Resistance. *Diabetes Care*. **2009**, *32*, 1542–1546.

Chen, S.; He, Q.; Greenberg, M. Loss of Tafazzin in Yeast Leads to Increased Oxidative stress During Respiratory Growth. *Molecular Biology*. **2008**, *68*, 1061-1072.

Cheung, Y.; Lau, W.; Yu, M.; Lai, C.; Yeung, S.; So, K.; Chang, R. Effects of All-Trans-Retinoic Acid on Human SH-SY5Y Neuroblastoma as in Vitro Model in Neurotoxicity Research. *Neurotoxicology*. **2009**, *30*, 127-135.

Chicco, A.; Sparagna, G. Role of Cardiolipin Alterations in Mitochondrial Dysfunction and Disease. *American Journal of Physiology-Cell Physiology*. **2007**, *292*, C33-C44.

Chinnery, P.; Johnson, M.; Wardell, T.; Singh-Kler, R.; Hayes, C.; Taylor, R.; Bindoff, L.; Turnbull, D. The Epidemiology of Pathogenic Mitochondrial DNA Mutations. *Ann. Neurol*. **2000**, *48*, 188–193.

Christophe, W.; Ulrich, B.; Carola, Hu.; Volker. Z. Structure and Function of Mitochondrial Complex I. *Biochimica et Biophysica Acta (BBA) – Bioenergetics*. **2016**, *7*, 902-914.

Ciccarone, V.; Spengler, B.; Meyers, M.; Biedler, J.; Ross, R. Phenotypic Diversification in Human Neuroblastoma Cells: Expression of Distinct Neural Crest Lineage. *Cancer Research*. **1989**, *49*, 219-225.

Cino, M.; Del Maestro, F. Generation of Hydrogen Peroxide by Brain Mitochondria: The Effect of Reoxygenation Following Postdecapitative Ischemia. *Arch. Biochem. Biophys*. **1989**, *269*, 623–638.

Cleeter, M.; Cooper, J.; Darley-Usmar, V.; Moncada, S.; Schapira, H. Reversible Inhibition of Cytochrome c Oxidase, the Terminal Enzyme of the Mitochondrial Respiratory Chain, by Nitric Oxide. Implications for Neurodegenerative Diseases. *FEBS Lett.* **1994**, *345*, 50-54.

Cline, S. Mitochondrial DNA Damage and Its Consequences for Mitochondrial Gene Expression. *Biochim. Biophys. Acta Bioenerg.* **2012**, *1819*, 979–991.

Cobley, J.; Fiorello, M.; Bailey, D. 13 Reasons Why the Brain is Susceptible to Oxidative Stress. *Redox Biol.* **2018**, *15*, 490-503.

Cocco, T.; Sgobbo, P.; Clemente, M.; Lopriore, B.; Grattagliano, I.; Di Paola, M.; Villani, G. Tissue-Specific Changes of Mitochondrial Functions in Aged Rats: Effect of a Long-Term Dietary Treatment with N-Acetylcysteine. *Free Radic Biol Med.* **2005**, *38*, 796-805.

Conner, J.; and Benkovic, S. Iron Regulation in the Brain: Histochemical, Biochemical, and Molecular Considerations. *Ann. Neurol.* **1992**, *32*, 51-61.

Constantinescu, R.; Constantinescu, A.; Reichmann, H.; Janetzky, B. Neuronal Differentiation and Long-Term Culture of the Human Neuroblastoma Line SH-SY5Y. *J Neural Transm Suppl.* **2007**, *72*, 17-28.

Contreras-Sanz, A.; Scott-Ward, T.; Gill, H.; Jacoby, J.; Birch, R.; Malone-Lee, J.; Taylor, K.; Peppiatt-Wildman, C.; Wildman, S. Simultaneous Quantification of 12 Different Nucleotides and Nucleosides Released from Renal Epithelium and in Human Urine Samples Using Ion-Pair Reversed-Phase HPLC. *Purinergic Signalling.* **2012**, *8*, 741-751.

Covarrubias-Pinto, A.; Acuña, A.; Beltrán, F.; Torres-Díaz, L.; Castro, M. Old Things New View: Ascorbic Acid Protects the Brain in Neurodegenerative Disorders. *Int. J. Mol. Sci.* **2015**, *16*, 28194-28217.

Cox, G.; Jans, D.; Fimmel, A.; Gibson, F.; Hatch, L. Hypothesis. The Mechanism of ATP Synthase. Conformational Change by Rotation of the Beta-Subunit. *Biochim Biophys Acta*. **1984**, 768, 201-208.

Crofts, R.; Rose, S.; Burton, R.; Desai, A.; Kenis, P.; Dikanov, S. The Q-Cycle Mechanism of the bc₁ Complex: A Biologist's Perspective on Atomistic Studies. *The Journal of Physical Chemistry B*. **2017**, 121, 3701-3717.

Cronin-Furman, E.; Borland, M.; Bergquist, K.; Bennett, J.; Trimmer, P. Mitochondrial Quality, Dynamics and Functional Capacity in Parkinson's Disease Cybrid Cell Lines Selected for Lewy Body Expression. *Molecular Neurodegeneration*. **2013**, 8, 6.

Damier, P.; Hirsch, E.; Zhang, P.; Agid, Y.; Javoy-Agid, F. Glutathione Peroxidase, Glial Cells and Parkinson's Disease. *Neuroscience*. **1993**, 52, 1–6.

Davey, G.; Peuchen, S.; Clark, J. Energy Thresholds in Brain Mitochondria. Potential Involvement in Neurodegeneration. *J Biol Chem*. **1998**, 273, 12753-12757.

De, L.; Breteler, M. Epidemiology of Parkinson's Disease. *Lancet Neurol*. **2006**, 5, 525–535.

Deborah, E.; Haseeb, I.; Koenig, M. Mitochondrial Cardiomyopathy Pathophysiology, Diagnosis, and Management. *Tex Heart Inst J*. **2013**, 40, 385–394.

Debray, F.; Mitchell, G.; Allard, P.; Robinson, B.; Hanley, J.; Lambert, M. Diagnostic Accuracy of Blood Lactate-to-Pyruvate Molar Ratio in the Differential Diagnosis of Congenital Lactic Acidosis. *Clin Chem*. **2007**, 53, 916-921.

Desagher, S.; Glowinski, J.; Premont, J. Astrocytes Protect Neurons from Hydrogen Peroxide Toxicity. *J. Neurosci.* 1996, *16*, 2553-2562

Devenish, R.; Prescott, M.; Rodgers, A. The Structure and Function of Mitochondrial F1F0-ATP Synthases. *Int Rev Cell Mol Biol.* **2008**, *267*, 1-58.

Devi, L.; Raghavendran, V.; Prabhu, B.; Avadhani N.; Anandatheerthavarada H. Mitochondrial Import and Accumulation of Apha-Synuclein Impair Complex I in Human Dopaminergic Neuronal Cultures and Parkinson disease brain. *J. Biol. Chem.* **2008**, *283*, 9089–9100.

Dexter, D.; Carter, C.; Wells, F.; Javoy-Agid, F.; Agid, Y.; Lees, A.; Jenner, P.; Marsden, C. Basal Lipid Peroxidation in Substantia Nigra is Increased in Parkinson's Disease. *J Neurochem.* **1989a**, *52*, 381-389.

Dexter, D.; Wells, F.; Agid, F.; Agid, Y.; Lees, A.; Jenner, P.; Marsden, C. Increased Nigral Iron Content in Postmortem Parkinsonian Brain. *Lancet.* **1987**, *21*, 1219-1220.

Dexter, D.; Wells, F.; Lees, A.; Agid, F.; Agid, Y.; Jenner, P.; Marsden, C. Increased Nigral Iron Content and Alterations in Other Metal Ions Occurring in Brain in Parkinson's Disease. *J Neurochem.* **1989b**, *52*, 1830-1836.

Dias, V.; Junn, E.; Mouradian, M. The Role Oxidative Stress in Parkinson's Disease. *J. Parkinsons Dis.* **2013**, *3*, 461–491.

Distelmaier, F.; Visch, H.; Smeitink, J.; Mayatepek, E.; Koopman, W.; Willems, P. The Antioxidant Trolox Restores Mitochondrial Membrane Potential and Ca²⁺ -Stimulated ATP Production in Human Complex I Deficiency. *J Mol Med (Berl).* **2009 b**, *87*, 515-522.

Distelmaier, F.; Werner, K.; Heuvel, L.; Rodenburg, R.; Mayatepek, E.; Willems, P.; Smeitink, J. Mitochondrial Complex I Deficiency: from Organelle Dysfunction to Clinical Disease. *Brain*. **2009 a**, *132*, 833–842.

Domouzoglou, E.; Naka, K.; Vlahos, A.; Papafaklis, M.; Michalis, L.; Tsatsoulis, A.; Maratos-Flier, E. Fibroblast growth Factors in Cardiovascular Disease: The Emerging Role of FGF21. *American Journal of Physiology - Heart and Circulatory Physiology*. **2015**, *309*, 1029-1038.

Dorsey, E.; Constantinescu, R.; Thompson, J.; Biglan, K.; Holloway, R.; Kieburtz, K.; Marshall, F.; Ravina, B.; Schifitto, G.; Siderowf, A.; Tanner, C. Projected Number of People with Parkinson Disease in the Most Populous Nations, 2005 through 2030. *Neurology*. **2007**, *68*, 384–386.

Douiev, L.; Soiferman, D.; Alban, C.; Saada, A. The Effects of Ascorbate, N-Acetylcysteine, and Resveratrol on Fibroblasts from Patients with Mitochondrial Disorders. *J. Clin. Med*. **2017**, *6*, 1.

Dringen, R. Metabolism and Functions of Glutathione in Brain. *Progress in Neurobiology*. **2000**, *6*, 649-671.

Dringen, R.; Pfeiffer, B.; Hamprecht, B. Synthesis of the Antioxidant Glutathione in Neurons: Supply by Astrocytes of CysGly as Precursor for Neuronal Glutathione. *J. Neurosci*. **1999**, *19*, 562-569.

Dröse, S. Differential Effects of Complex II on Mitochondrial ROS Production and Their Relation to Cardioprotective pre- and Postconditioning. *Biochimica et Biophysica Acta (BBA) – Bioenergetics*. **2013**, *1827*, 578-587.

Duberley, K.; Heales, S.; Abramov, A.; Chalasani, A.; Land, J.; Rahman, S.; Hargreaves, I. Effect of Coenzyme Q₁₀ Supplementation on Mitochondrial Electron Transport Chain Activity and Mitochondrial Oxidative Stress in Coenzyme Q₁₀ Deficient Human Neuronal Cells. *Int. J. Biochem. Cell Biol*. **2014**, *50*, 60–63.

Duncan, A.; Heales, S.; Mills, K.; Eaton, S.; Land, J.; Hargreaves, I. Determination of Coenzyme Q10 status in Blood Mononuclear Cells, Skeletal Muscle, and Plasma by HPLC with Di-propoxy-coenzyme Q10 as an Internal Standard. *Clin Chem.* **2005**, *51*, 2380-2382.

Ebadi, M.; Srinivasan, S.; Baxi, M. Oxidative Stress and Antioxidant Therapy in Parkinson's Disease. *Prog Neurobiol.* **1996**, *48*, 1-19.

El-Bohy, A.; and Wong, B. The Diagnosis of Muscular Dystrophy. *Pediatric Annals.* **2005**, *7*, 525–530.

El-Hattab, A.; Zarante, A.; Almannai, M.; Scaglia, F. Therapies for mitochondrial diseases and current clinical trials. *Mol Genet Metab.* **2017**, *122*, 1-9.

Enns, G. Treatment of Mitochondrial Disorders: Antioxidants and Beyond. *J. Child Neurol.* **2014**, *29*, 1235-1240.

Enns, G.; and Cohen, B. Clinical Trials in Mitochondrial Disease: An Update on EPI-743 and RP103. *Journal of Inborn Errors of Metabolism and Screening.* **2017**, *5*, 1-7.

Esterbauer, H.; Dieber-Rotheneder, M.; Striegl, G.; Waeg, G. Role of Vitamin E in Preventing the Oxidation of Low-Density Lipoprotein. *Am J Clin Nutr.* **1991**, *53*, 314–321.

Fahn, S. Levodopa-Induced Neurotoxicity. *CNS Drugs.* **1997**, *8*, 376–393.

Fariss, M.; Chan, C.; Patel, M.; Houten, B.; and Orrenius, S. Role of Mitochondria in Toxic Oxidative Stress. *Mol. Interv.* **2005**, *5*, 94-111.

Farr, S.; Poon, H.; Dogrukol-Ak, D.; Drake, J.; Banks, W.; Eyerman, E.; Butterfield, D.; Morley, J. The Antioxidants α -lipoic Acid and N-Acetylcysteine

Reverse Memory Impairment and Brain Oxidative Stress in Aged SAMP8 Mice. *J. Neurochem.* **2003**, *84*, 1173–1183.

Fassone, E.; Rahman, S. Complex I Deficiency: Clinical Features, Biochemistry and Molecular Genetics. *Journal of Medical Genetics.* **2012**, *49*, 578-590.

Feldman, A.; Sokol, R.; Hardison, R.; Alonso, E.; Squires, R.; Narkewicz, M. Lactate and Lactate: Pyruvate Ratio in the Diagnosis and Outcomes of Pediatric Acute Liver Failure. *The Journal of pediatrics.* **2017**, *182*, 217-222.

Fiedor, J.; Burda, K. Potential Role of Carotenoids as Antioxidants in Human Health and Disease. *Nutrients.* **2014**, *6*, 466–488.

Fisher, F.; Chui, P.; Antonellis, P.; Bina, H.; Kharitonov, A.; Flier, J.; Maratos-Flier, E. Obesity is a Fibroblast Growth Factor 21 (FGF21)-Resistant State. *Diabetes.* **2010**, *59*, 2781–2789.

Forman, H.; Zhang, H.; Rinna, A. Glutathione: Overview of Its Protective Roles, Measurement, and Biosynthesis. *Mol Aspects Med.* **2009**, *30*, 1-12.

Frihoff, J.; Paul, Winyard, P.; Zarkovic, N.; Davies, S.; Stocker, R.; Cheng, D.; Knight, A.; Taylor, E.; Oettrich, J.; Tatiana, R.; Gasparovic, A.; Cuadrado, A.; Weber, D.; Poulsen, H.; Grune, T.; Schmidt, H.; and Ghezzi, P. Clinical Relevance of Biomarkers of Oxidative Stress. *Antioxidants and Redox Signaling.* **2015**, *23*, 1144-1170.

Fu, T.; Yuan, S.; Gao, Y.; Qu, C.; Chen, L.; Hui, Y.; Lu, G.; Gao, Y.; Guo, X. Relationship Between Fibroblast Growth Factor 21 and Thyroid Stimulating Hormone in Healthy Subjects Without Components of Metabolic Syndrome. *Family Medicine and Community Health.* **2014**, *2*, 1-6.

Gaich, G.; Chien, J.; Fu, H.; Deeg, M.; Holland, W.; Kharitononkov, A.; Bumol, T.; Schilske, H.; Moller, D. The Effects of LY2405319, an FGF21 Analog, in Obese Human Subjects with Type 2 Diabetes. *Cell Metab.* **2013**, *18*,333-340.

Gardner, P.; Fridovich, I. Superoxide Sensitivity of the Escherichia Coli Aconitase. *The Journal of Biological Chemistry.* **1991**, *266*, 19328-19333.

Gautheron, D. Mitochondrial Oxidative Phosphorylation and Respiratory Chain: Review. *J Inherit Metab Dis.* **1984**, *7*, 57-61.

Geoghegan, F.; Chadderton, N.; Farrar, G.; Zisterer, D.; Porter, R. Direct Effects of Phenformin on Metabolism/Bioenergetics and Viability of SH-SY5Y Neuroblastoma Cells. *Oncology Letters.* **2017**, *14*, 6298–6306.

Gegg, M.; Beltran, B.; Salas-Pino, S.; Bolanos, J.; Clark, J.; Moncada, S.; Heales, S. Differential Effect of Nitric Oxide on Glutathione Metabolism and Mitochondrial Function in Astrocytes and Neurones: Implications for Neuroprotection/Neurodegeneration? *J Neurochem.* **2003**, *86*, 228-237.

Gegg, M.; Burke, D.; Heales, S.; Cooper, J.; Hardy, J.; Wood, N.; Schapira, A. Glucocerebrosidase Deficiency in Substantia Nigra of Parkinson Disease Brains. *Ann Neurol.* **2012**, *72*, 455-63.

Gegg, M.; Clark, J.; Heales, S. Co-Culture of Neurones with Glutathione Deficient Astrocytes Leads to Increased Neuronal Susceptibility to Nitric Oxide and Increased Glutamate-Cysteine Ligase Activity. *Brain Res.* **2005**, *1036*, 1-6.

Gerber, J.; Muhlenhoff, U.; Lill, R. An Interaction between Frataxin and Isu1/Nfs1 that is Crucial for Fe/S Cluster Synthesis on Isu1. *EMBO Rep.* **2003**, *4*, 906-911.

Gibson, K.; Sherwood, W.; Hoffman, G.; Stumpf, D.; Dianzani, I.; Schutgens, R.; Barth, P.; Weismann, U.; Bachmann, C.; Schrynemackers-Pitance, P.

Phenotypic Heterogeneity in the Syndromes of 3-Methylglutaconic Aciduria. *J Pediatr*. **1991**, *118*, 885–90.

Giles, R.; Blanc, H.; Cann, H.; Wallace, D. Maternal Inheritance of Human Mitochondrial DNA. *Proc Natl Acad Sci USA*. **1980**, *77*, 6715–6719.

Gillis, L.; Sokol, R. Gastrointestinal Manifestation of Mitochondrial Disease. *Gastroenterol. Clin. N. Am.* **2003**, *32*, 789–817.

Giráldez-Pérez, R.; Antolín-Vallespín, M.; Muñoz, D.; Sánchez-Capelo, A. Models of α -Synuclein Aggregation in Parkinson's Disease. *Acta Neuropathologica Communications*. **2014**, *2*, 176.

Glover, V.; Sandler, M.; Owen, F.; Riley, G. Dopamine is a Monoamine Oxidase B Substrate in Man. *Nature*. **1977**, *265*, 80–81.

Gnaiger, E. Polarographic Oxygen Sensors, the Oxygraph, and High-Resolution Respirometry to Assess Mitochondrial Function. In Drug-Induced Mitochondrial Dysfunction. Dykens J, Will Y, Eds., Hoboken, John Wiley & Sons, Inc., **2008**, 327–352

Gnaiger, E.; Steinlechner-Maran, R.; Mendez, G.; Eberl, T.; Margreiter, R. Control of Mitochondrial and Cellular Respiration by Oxygen. *J Bioenerg Biomembr.* **1995**, *27*, 583-596.

Gonzalo, R.; Arumi, E.; Llige, D.; Marti, R.; Solano, A.; Montoya, J.; Arenas, J.; Andreu, A. Free Radicals-mediated Damage in Transmitochondrial Cells Harboring the T14487C Mutation in the ND6 Gene of mtDNA. *FEBS Lett.* **2005**, *579*, 6909–6913.

Götz, M.; Gerstner, A.; Harth, R.; Dirr, A.; Janetzky, B.; Kuhn, W.; Riederer, P.; Gerlach, M. Altered Redox State of Platelet Coenzyme Q10 in Parkinson's Disease. *J Neural Transm (Vienna)*. **2000**, *107*, 41-48.

Gray, M. Mitochondrial Evolution. *Cold Spring Harbor Perspectives in Biology*. **2012**, *4*, a011403.

Greenamyre, J.; MacKenzie, G.; Peng, T.; Stephans, S. Mitochondrial Dysfunction in Parkinson's Disease. *Biochem. Soc. Symp.* **1999**, *66*, 85-97.

Green, D.; Galluzzi, L.; Kroemer, G. Mitochondria and the Autophagy-Inflammation-Cell Death Axis in Organismal Aging. *Science*. **2011**, *333*, 1109-12.

Grimm, S. Respiratory Chain Complex II as General Sensor for Apoptosis. *Biochimica et Biophysica Acta (BBA) – Bioenergetics*. **2013**, *1827*, 565-572.

Guenebaut, V.; Vincentelli, R.; Mills, D.; Weiss, H.; Leonard, K. Three-dimensional Structure of NADH–Dehydrogenase from *Neurospora Crassa* by Electron Microscopy and Conical Tilt Reconstruction. *J. Mol. Biol.* **1997**, *265*, 409-418.

Guo, C.; Sun, L.; Chen, X.; Zhang, D. Oxidative stress, mitochondrial damage and neurodegenerative diseases. *Neural Regeneration Research*. **2013**, *8*, 2003-2014.

Haas, R.; Nasirian, F.; Nakano, K.; Ward, D.; Pay, M.; Hill, R.; Shults, C. Low Platelet Mitochondrial Complex I and Complex II/III Activity in Early Untreated Parkinson's Disease. *Ann. Neurol.* **1995**, *37*, 714-722.

Haas, R.; Parikh, S.; Falk, M.; Saneto, R.; Wolf, N.; Darin, N.; Wong, L.; Cohen, B.; Naviaux, R. The In-Depth Evaluation of Suspected Mitochondrial Disease: The Mitochondrial Medicine Society's Committee on Diagnosis. *Molecular genetics and metabolism*. **2008**, *94*, 16-37.

Haasio, K.; Koponen, A.; Penttila, K.; Nissinen E. Effects of Entacapone and Tolcapone on Mitochondrial Membrane Potential. *Eur J Pharmacol.* **2002 b**, *453*, 21–26.

Haasio, K.; Lounatmaa, K.; Sukura, A. Entacapone Does Not Induce Conformational Changes in Liver Mitochondria or Skeletal Muscle in Vivo. *Exp Toxicol Pathol.* **2002 a**, *54*, 9–14.

Haddad, D.; Nakamura, K. Understanding the Susceptibility of Dopamine Neurons to Mitochondrial Stressors in Parkinson's Disease. *FEBS letters.* **2015**, *589*, 3702-3713.

Hagemeier, J.; Geurts, J.; Zivadinov, R. Brain Iron Accumulation in Aging and Neurodegenerative Disorders. *Expert Rev Neurother.* **2012**, *12*, 1467-1480.

Haile, D.; Rouault, T.; Harford, J.; Kennedy, M.; Blondin, G., and Klausner, R. Cellular Regulation of the Iron-responsive Element Binding Protein: Disassembly of the Cubane Iron-sulfur Cluster Results in High Affinity RNA Binding. *Proc. Natl. Acad. Sci. U.S.A.* **1992**, *89*, 11735-11739.

Halliwell, B.; Gutteridge, J. Free radicals in biology and medicine. *4th ed.* Oxford, UK: *Clarendon Press.* **2007**.

Hara, Y.; McKeehan, N.; Dacks, P.; Fillit, H. Evaluation of the Neuroprotective Potential of N-Acetylcysteine for Prevention and Treatment of Cognitive Aging and Dementia. *J Prev Alzheimers Dis.* **2017**, *4*, 201-206.

Hargreaves, I. Coenzyme Q10 as a Therapy for Mitochondrial Disease. *Int J Biochem Cell Biol.* **2014**, *49*, 105-111.

Hargreaves, I.; Al Shahrani, M.; Wainwright, L.; Heales, S. Drug-Induced Mitochondrial Toxicity. *Drug Saf.* **2016**, *39*, 661–674.

Hargreaves, I.; Duncan, A.; Wu, L.; Agrawal, A.; Land, J.; Heales, S. Inhibition of Mitochondrial Complex IV Leads to Secondary Loss Complex II-III Activity: Implication for the Pathogenesis and Treatment of Mitochondrial Encephalomyopathies. *Mitochondrion*. **2007**, *7*, 284-287.

Hargreaves, I.; Lane, A.; Sleiman, P. The coenzyme Q10 Status of the Brain Regions of Parkinson's Disease Patients. *Neurosci Lett*. **2008**, *447*, 17-19.

Hargreaves, I.; Sheena, Y.; Land, J.; Heales, S. Glutathione Deficiency in Patients with Mitochondrial Disease: Implications for Pathogenesis and Treatment. *J Inherit Metab Dis*. **2005**, *28*, 81–88.

Hargreaves, IP. Ubiquinone: Cholesterol's Reclusive Cousin. *Ann Clin Biochem*. **2003**, *40*, 207-218.

Harrison, F.; May, J. Vitamin C Function in the Brain: Vital Role of the Ascorbate Transporter (SVCT2). *Free radical biology & medicine*. **2009**, *46*, 719-730.

Harvey, C.; Thimmulappa, R.; Singh, A.; Blake, D.; Ling, G.; Wakabayashi, N.; Fujii, J.; Myers, A.; Biswal, S. Nrf2-Regulated Glutathione Recycling Independent of Biosynthesis is Critical for Cell Survival during Oxidative Stress. *Free radical biology & medicine*. **2009**, *46*, 443-453.

Hauser, D.; Mamais, A.; Conti, M.; Christopher, T.; Kumaran, R.; Dillman, A.; Langston, G.; et al. Hexokinases Link DJ-1 to the PINK1/Parkin Pathway. *Mol Neurodegener*. **2017**, *12*, 70.

Hauser, R. Levodopa: Past, Present, and Future. *Eur Neurol*. **2009**, *62*, 1-8.

Hawkes, C.; Del Tredici, K.; Braak, H. Parkinson's Disease: a Dual-Hit Hypothesis. *Neuropathol. Appl. Neurobiol*. **2007**, *33*, 599-614.

Hayashi, G.; Cortopassi, G. Oxidative Stress in Inherited Mitochondrial Disease. *Free Radic. Biol. Med*. **2015**, *88*, 10–17.

Heales, S.; Bolaños, J.; Land, J.; Clark, J. Trolox Protects Mitochondrial Complex IV from Nitric Oxide-mediated Damage in Astrocytes. *Brain Research*. **1994**, *668*, 243-245.

Heales, S.; Bolaños, J. Impairment of Brain Mitochondrial Function by Reactive Nitrogen Species: The Role of Glutathione in Dictating Susceptibility. *Neurochem. Int*. **2002**, *40*, 469–474.

Heales, S.; Bolaños, J.; Stewart, V.; Brookes, P.; Land, J.; Clark, J. Nitric Oxide, Mitochondria and Neurological Disease. *Biochim. Biophys. Acta Bioenerg*. **1999**, *1410*, 215–228.

Heales, S.; Davies, S.; Bates, T.; Clark, J. Depletion of Brain Glutathione is Accompanied by Impaired Mitochondrial Function and Decreased N-acetyl Aspartate Concentration. *Neurochem. Res*. **1995**, *20*, 31–38.

Henchcliffe, C.; Beal, M. Mitochondrial Biology and Oxidative Stress in Parkinson Disease Pathogenesis. *Nat Clin Pract Neuro*. **2008**, *11*, 600–609.

Hinkle, C.; Butow, A.; Racker, E.; Chance, B. Partial Resolution of the Enzymes Catalyzing Oxidative Phosphorylation. XV. Reverse Electron Transfer in the Flavin-cytochrome β Region of the Respiratory Chain of Beef Heart Submitochondrial Particles. *J. Biol. Chem*. **1967**, *242*, 5169–5173.

Hinkle, P. P/O ratios of mitochondrial oxidative phosphorylation. *Biochim Biophys Acta*. **2005**, *1706*, 1-11.

Hirsch, E.; Brandel, J.; Galle, P.; Javoy-Agid, F.; Agid, Y. Iron and Aluminum Increase in the Substantia Nigra of Patients with Parkinson's Disease: an X-ray Microanalysis. *J Neurochem*. **1991**, *56*, 446-451.

Hirsch, E.; Faucheux, B. Iron Metabolism and Parkinson's Disease. *Mov. Disord*. **1998**, *13*, 39-45.

Hopfer, U.; Lehninger, A.; Thompson, T. Protonic Conductance across Phospholipid Bilayer Membranes Induced by Uncoupling Agents for Oxidative Phosphorylation. *Proc Natl Acad Sci U S A*. **1968**, *59*,484-490.

Horsen, J.; Schaik, P.; Witte, M. Inflammation and Mitochondrial Dysfunction: A Vicious Circle in Neurodegenerative Disorders? *Neurosci Lett*. **2017**, *17*, 30542-30546.

Houten, B.; Woshner, V.; Santos, J. Role of Mitochondrial DNA in Toxic Responses to Oxidative Stress. *DNA Repair (Amst)*. **2006**, *5*, 145-152.

Houtkooper, R.; Turkenburg, M.; Poll-The, B.; Karall, D.; Cerda, C.; Morrone, A.; Malyagia, S.; Wanders, R.; Kulik, W.; Vaz, F. The Enigmatic Role of Taffazzin in Cardiolipin Metabolism. *Biochimica et Biophysica Acta-Bioenergetics*. **2009**, *1788*, 2003-2014.

Houtkooper, R.; Akbarib, H.; Lenthea, H.; Kulika, W.; Wandersa, R.; Frentzenb, M.; Vaza, F. Identification and characterization of human cardiolipin synthase. *FEBS Lett*. **2006**, *580*, 3059–3064.

Howell, N. Leber Hereditary Optic Neuropathy: Respiratory Chain Dysfunction and Degeneration of the Optic Nerve. *Vis. Res*. **1998**, *38*, 1495–1504.

Hughes, S.; Kanabus, M.; Anderson, G.; Hargreaves, I.P.; Rutherford, T.; O'Donnell, M.; Cross, J.H.; Rahman, S.; Eaton, S.; Heales, S.J. The Ketogenic Diet Component Decanoic Acid Increases Mitochondrial Citrate Synthase and Complex I Activity in Neuronal Cells. *J. Neurochem*. **2014**, *3*, 426–433.

Huoponen, K.; Vilkki, J.; Aula, P.; Nikoskelainen, E.; Savontaus, M. A New mtDNA Mutation Associated with Leber Hereditary Optic Neuroretinopathy. *Am. J. Hum. Genet*. **1991**, *48*, 1147–1153.

Hurd, R.; Prime, A.; Harbour, E.; Lilley, S.; Murphy, P. Detection of Reactive Oxygen Species-sensitive Thiol Proteins by Redox Difference Gel Electrophoresis: Implications for Mitochondrial Redox Signaling. *J. Biol. Chem.* **2007**, *282*, 22040–22051.

Iglesias, P.; Selgas, R.; Romero, S.; Díez, J. Mechanisms in endocrinology: Biological Role, Clinical Significance, and Therapeutic Possibilities of The Recently Discovered Metabolic Hormone Fibroblastic Growth Factor 21. *Eur J Endocrinol.* **2012**, *167*, 301-309.

Iverson, T.; Maklashina, E.; Cecchini, G. Structural Basis for Malfunction in Complex II. *J Biol Chem.* **2012**. *42*, 35430-35438.

Itoh, N. FGF21 as a Hepatokine, Adipokine, and Myokine in Metabolism and Diseases. *Front Endocrinol (Lausanne).* **2014**, *5*, 107.

Itoh, N. Hormone-like (Endocrine) Fgfs: their Evolutionary History and Roles in Development, Metabolism, and Disease. *Cell Tissue Res.* **2010**, *342*, 1-11.

Jaber, S.; Polster, B. Idebenone and Neuroprotection: Antioxidant, Pro-Oxidant, or Electron Carrier? *J Bioenerg Biomembr.* **2015**, *47*, 111-118.

Jacobson, J.; Duchen, M.; Hothersall, J.; Clark, J.; Heales, S. Induction of Mitochondrial Oxidative Stress in Astrocytes by Nitric Oxide Precedes Disruption of Energy Metabolism. *J Neurochem.* **2005**, *95*, 388-395.

Jang, S.; Javadov, S. Current Challenges in Elucidating Respiratory Supercomplexes in Mitochondria: Methodological Obstacles. *Front Physiol.* **2018**, *9*, 238.

Jefferies, J. Barth Syndrome. *Am. J. Med. Genet. C, Semin. Med. Genet.* **2013**, *163*, 198-205.

Jenner, P.; Dexter, D.; Sian, J.; Schapira, A.; Marsden, C. Oxidative stress as a Cause of Nigral Cell Death in Parkinson's Disease and Incidental Lewy Body Disease. The Royal Kings and Queens Parkinson's Disease Research Group. *Ann. Neurol.* **1992**, *32*, 82–87.

Jensen, P. Antimycin-Insensitive Oxidation of Succinate and Reduced Nicotinamide-Adenine Dinucleotide in Electron-Transport Particles. I. pH Dependency and Hydrogen Peroxide Formation. *Biochim Biophys Acta.* **1966**, *122*, 157-66.

Jha, N.; Jurma, O.; Lalli, G.; Liu, Y.; Pettus, E.; Greenamyrel, J.; Liu, R.; Forman, H.; Anderson, J. Glutathione Depletion in PC12 Results in Selective Inhibition of Mitochondrial Complex I Activity: Implication for Parkinson's Disease. *J. Biol. Chem.* **2000**, *275*, 26096–26101.

Jin, H.; Kanthasamy, A.; Ghosh, A.; Anantharam, V.; Kalyanaraman, B.; Kanthasamy, A. Mitochondria-Targeted Antioxidants for Treatment of Parkinson's Disease: Preclinical and Clinical Outcomes. *Biochim Biophys Acta.* **2014**, *1842*, 1282-1294.

Jin, S.; Youle, R. PINK1- and Parkin-Mediated Mitophagy at a Glance. *J Cell Sci.* **2012**, *125*, 795-799.

Johansen, T.; Lamark, T. Selective Autophagy Mediated by Autophagic Adapter Proteins. *Autophagy.* **2011**, *7*, 279-296.

Jomova, K.; Valko, M. Advances in Metal-induced Oxidative Stress and Human Disease. *Toxicology.* **2011**, *10*, 65-87.

Jonckheere, A.; Smeitink, J.; Rodenburg, R. Mitochondrial ATP Synthase: Architecture, Function and Pathology. *Journal of Inherited Metabolic Disease.* **2012**, *35*, 211-225.

Joselin, A.; Hewitt, S.; Callaghan, S.; Kim, R.; Chung, Y.; Mak, T.; Shen, J.; Slack, R.; Park, D. ROS-Dependent Regulation of Parkin and DJ-1 Localization during Oxidative Stress in Neurons. *Hum Mol Genet.* **2012**, *15*, 21, 4888-4903.

Judy, H.; Joe, C.; Iain, M.; Richard, S.; John, W. The Nuclear Encoded Subunits of Complex I from Bovine Heart Mitochondria. *Biochimica et Biophysica Acta (BBA) – Bioenergetics.* **2003**, *3*, 135-155.

Judy, H.; Martin S.; Kenneth, P. The Production of Reactive Oxygen Species by Complex I. *Biochemical Society Transactions.* **2008**, *5*, 976-980.

Kaakkola, S. Clinical pharmacology, therapeutic use and potential of COMT inhibitors in Parkinson's disease. *Drugs.* **2000**, *59*, 1233–1250.

Kalia, L.; Lang, A. Parkinson's Disease. *Lancet.* **2015**, *386*, 896-912.

Kamboj, S.; Sandhir, R. Protective Effect of N-acetylcysteine Supplementation on Mitochondrial Oxidative Stress and Mitochondrial Enzymes in Cerebral Cortex of Streptozotocin-Treated Diabetic Rats. *Mitochondrion.* **2011**, *11*, 214-222.

Kanabus, M.; Fassone, E.; Hughes, S.D.; Bilooei, S.F.; Rutherford, T.; O'Donnell, M.; Heales, S.J.R.; Rahman, S. The Pleiotropic Effects of Decanoic Acid Treatment on Mitochondrial Function in Fibroblasts from Patients with Complex I Deficient Leigh Syndrome. *J. Inherit. Metab. Dis.* **2016**, *39*, 415–426.

Kaplan, J. Friedreich Ataxia is a Mitochondrial Disorder. *PNAS.* **1999**, *96*, 10948-10949.

Kawamoto, Y.; Shinozuka, K.; Kunitomo, M.; Haginaka, J. Determination of ATP and its Metabolites Released from Rat Caudal Artery by Isocratic Ion-Pair Reversed-Phase High-Performance Liquid Chromatography. *Anal Biochem.* **1998**, *262*, 33-38.

Keane, P.; Kurzawa, M.; Blain, P.; Morris, C. Mitochondrial Dysfunction in Parkinson's Disease. *Parkinson's Disease*. **2011**, *2011*, 1-18.

Keeney, P.; Xie, J.; Capaldi, R.; Bennett, J. Parkinson's Disease Brain Mitochondrial Complex I Has Oxidatively Damaged Subunits and is Functionally Impaired and Misassembled. *J. Neurosci*. **2006**, *26*, 5256–5264.

Kennedy, P.; Ormerod, M.; Singh, S.; Pande, G. Variation of Mitochondrial Size during the Cell Cycle: A Multiparameter Flow Cytometric and Microscopic Study. *Cytometry A*. **2004**, *62*, 97-108.

Kerksick, C.; Willoughby, D. The Antioxidant Role of Glutathione and N-Acetyl-Cysteine Supplements and Exercise-Induced Oxidative Stress. *Int. Soc. Sports Nutr*. **2005**, *2*, 38–44.

Kharitonkov, A.; Adams, A. Inventing New Medicines: The FGF21 Story. *Molecular Metabolism*. **2014**, *3*, 221-229.

Kim, H.; LaVaute, T.; Iwai, K.; Klausner, R.; and Rouault, T. Identification of a Conserved and Functional Iron-responsive Element in the 5'- Untranslated Region of Mammalian Mitochondrial Aconitase. *J. Biol. Chem*. **1996**, *271*, 24226-24230.

Kim, W.; Kågedal, K.; Halliday, G. Alpha-Synuclein Biology in Lewy Body Diseases. *Alzheimers Res Ther*. **2014**, *6*, 73.

Kim, Y.; Hummer, G. Proton-Pumping Mechanism of Cytochrome c Oxidase: a Kinetic Master-Equation Approach. *Biochim Biophys Acta*. **2012**, *1817*, 526-36.

King, T. Preparation of Succinate Cytochrome c Reductase, and the Cytochrome b-c1 Particle, and Reconstitution of Succinate Cytochrome c Reductase. *Methods Enzymol*. **1967**, *10*, 217–235.

Kirches, E. Do mtDNA Mutations Participate in the Pathogenesis of Sporadic Parkinson's Disease? *Current Genomics*. **2009**, *10*,585-593.

Kirches, E. LHON: Mitochondrial Mutation and More. *Curr. Genom.* **2011**, *12*, 44–54.

Klein, C.; Westenberger, A. Genetics of Parkinson's Disease. *Cold Spring Harbor Perspectives in Medicine*. **2012**, *2*, a008888.

Koene, S.; Smeitink, J. Metabolic Manipulators: a Well Founded Strategy to Combat Mitochondrial Dysfunction. *J Inherit Metab Dis.* **2011**, *34*,315-325.

Koenig, M.; Mandel, J. Deciphering the Cause of Friedreich Ataxia. *Curr. Opin. Neurobiol.* **1997**, *7*, 689-694.

Koeppen, A. Friedreich Ataxia: Pathology, Pathogenesis, and Molecular Genetics. *J. Neurol Sci.* **2011**, *303*, 1-12.

Kooncumchoo, P.; Sharma, S.; Porter, J.; Govitrapong, P.; Ebadi, M. Coenzyme Q(10) Provides Neuroprotection in Iron-Induced Apoptosis in Dopaminergic Neurons. *J Mol Neurosci.* **2006**, *28*, 125-141.

Kossoff, E.; Hartman, A. Ketogenic Diets: New Advances for Metabolism-Based Therapies. *Current opinion in neurology.* **2012**, *25*,173-178.

Kroemer, G.; Blomgren, K. Mitochondrial Cell Death Control in Familial Parkinson Disease. *PLoS Biol.* **2007**, *7*, e206.

Kudin, P.; Bimpong-Buta, Y.; Vielhaber, S.; Elger, E.; Kunz, S. Characterization of Superoxide-producing Sites in Isolated Brain Mitochondria. *J. Biol. Chem.* **2004**, *279*, 4127–4135.

Kühlbrandt, W. Structure and Function of Mitochondrial Membrane Protein Complexes. *BMC Biol.* **2015**, *13*, 89.

Kurth, M.; Adler, C. COMT Inhibition: a New Treatment Strategy for Parkinson's Disease. *Neurology.* **1998**, *50*, 3–14.

Kusmaul, L.; Hirst, J. The Mechanism of Superoxide Production by NADH:Ubiquinone Oxidoreductase (Complex I) from Bovine Heart Mitochondria. *Proc. Natl. Acad. Sci. U.S.A.* **2006**, *103*, 7607–7612.

Kuznetsov, A.; Schneeberger, S.; Seiler, R.; Brandacher, G.; Mark, W.; Steurer, W.; Saks, V.; Usson, Y.; Margreiter, R.; Gnaiger, E. Mitochondrial Defects and Heterogeneous Cytochrome c Release after Cardiac Cold Ischemia and Reperfusion. *Am J Physiol Heart Circ Physiol.* **2004**, *286*, 1633–1641.

Laar, V.; Berman, S. Mitochondrial Dynamics in Parkinson's Disease. *Exp Neurol.* **2009**, *218*, 247-256.

Lamont, P.; Surtees, R.; Woodward, C.; Leonard, J.; Wood, N.; Harding, A. Clinical and Laboratory Findings in Referrals for Mitochondrial DNA Analysis. *Arch. Dis. Child.* **1998**, *79*, 22–27.

Land, J.; Hughes, J.; Hargreaves, I.; Heales, S. Mitochondrial Disease: A Historical, Biochemical, and London Perspective. *Neurochem. Res.* **2004**, *29*, 483–491.

Langston, J.; Ballard, P.; Tetrud, J.; Irwin, I. Chronic Parkinsonism in Humans Due to a Product of Meperidine-Analog Synthesis. *Science.* **1983**, *219*, 979-980.

Lanza, I.; Nair, K. Functional Assessment of Isolated Mitochondria in Vitro. *Methods in enzymology.* **2009**, *457*, 349-372.

Leal, M.; Casabona, J.; Puntel, M.; Pitossi, F. Interleukin-1Beta and Tumor Necrosis Factor-Alpha: Reliable Targets for Protective Therapies in Parkinson's Disease? *Front Cell Neurosci.* 2013,7,53.

Le Couteur, D.; McLean, A.; Taylor, M.; et al. Pesticides and Parkinson's Disease. *Biomed. Pharmacother.* **1999**, 53,122-130.

Lechner, V.; Siess, M.; Hoffmann, P. The Effect of Uncouplers of Oxidative Phosphorylation on Oxygen Uptake, Ubiquinone Redox Status and Energy-Rich Phosphate Levels of Isolated Atria. *Eur J Biochem.* **1970**, 1,117-125.

Leeuwenburgh, C.; Hiona, A. The Role Mitochondrial DNA Mutations in Aging and Sarcopenia. *Exp. Gerontol.* **2008**, 43, 24–33.

Lehtonen, J.; Forsström, S.; Bottani, E.; Viscomi, C.; Baris, O.; Isoniemi, H.; et al. FGF21 is a Biomarker for Mitochondrial Translation and MtDNA Maintenance Disorders. *Neurology.* **2016**, 87, 2290-2299.

Lesage, S.; Drouet, V.; Majounie, E.; Deramecourt, V.; Jacoupy, M.; Nicolas, A.; et al. Loss of VPS13C Function in Autosomal-Recessive Parkinsonism Causes Mitochondrial Dysfunction and Increases PINK1/Parkin-Dependent Mitophagy. *American Journal of Human Genetics.* **2016**, 98, 500-513.

Li, N.; Ragheb, K.; Lawler, G.; Sturgis, J.; Rajwa, B.; Melendez, J.; Robinson, J. Mitochondrial Complex I Inhibitor Rotenone Induces Apoptosis through Enhancing Mitochondrial Reactive Oxygen Species Production. *J. Biol. Chem.* **2003**, 278, 8516- 8525.

Liang, L.; Ho, Y.; and Patel, M. Mitochondrial Superoxide Production in Kainate-induced Hippocampal Damage. *Neuroscience.* **2000**, 101, 563-570.

Liang, L.; Patel, M. Iron-sulfur Enzyme Mediated Mitochondrial Superoxide Toxicity in Experimental Parkinson's Disease. *J Neurochem.* **2004**, *90*, 1076-1084.

Lien, A.; Hua, H.; Chuong, P. Free Radicals, Antioxidants in Disease and Health. *Int J Biomed Sci.* **2008**, *4*, 89–96.

Lin, C.; Sharpley, M.; Fan, W.; Waymire, K.; Sadun, A.; Carelli, F.; Ross-Cisneros, F.; Baci, P.; Sung, E.; McManus, M.; et al. Mouse mtDNA Mutant Model of Leber Hereditary Optic Neuropathy. *Proc. Natl. Acad. Sci. USA.* **2012**, *109*, 20065–20070.

Lin, M.; Cantuti-Castelvetri, I.; Zheng, K.; Jackson, K.; Tan, Y.; Arzberger, T.; Lees, A.; Betensky, R.; Beal, M.; Simon, D. Somatic Mitochondrial DNA Mutations in Early Parkinson's and Incidental Lewy Body Disease. *Annals of Neurology.* **2012**, *71*, 850-854.

Lin, Z.; Zhou, Z., Liu, Y.; Gong, Q.; Yan, X.; Xiao, J.; et al. Circulating FGF21 Levels Are Progressively Increased from the Early to End Stages of Chronic Kidney Diseases and Are Associated with Renal Function in Chinese. *PLoS ONE.* **2011**, *6*, e18398.

Lionaki, E.; Markaki, M.; Palikaras, K.; Tavernarakis, N. Mitochondria, Autophagy and Age-associated Neurodegenerative Diseases: New Insights into a Complex Interplay. *Biochim Biophys Acta.* **2015**, *1847*, 1412-1423.

Lipmann, F. Biosynthetic Mechanisms. *Harvey Lect.* **1948-1949**, *44*, 99-123.

Lombes, A.; Mendell, J.; Nakase, H.; Barohn, R.; Bonilla, E.; Zeviani, M.; Yates, A.; Omerza, J.; Gales, T.; Nakahara, K.; Rizzuto, R.; Engel, W.; Dimauro, S. Myoclonic Epilepsy with Ragged-red Fibers with Cytochrome Oxidase Deficiency: Neuropathology, Biochemistry, and Molecular Genetics. *Annals of Neurology.* **1989**, *26*, 20-33.

López-Armada, M.; Riveiro-Naveira, R.; Vaamonde-García, C.; Valcárcel-Ares, M. Mitochondrial Dysfunction and the Inflammatory Response. *Mitochondrion*. **2013**, *13*,106-118.

López, L.; Quinzii, C.; Area, E.; Naini, A.; Rahman, S.; Schuelke, M.; Salviati, L.; DiMauro, S.; Hirano, M. Treatment of CoQ (10) Deficient Fibroblasts with Ubiquinone, CoQ Analogs, and Vitamin C: Time- and Compound-Dependent Effects. *PLoS One*. **2010**, *5*, e11897.

Lopez-Fabuel.; I, Le Douce, J.; Logan, A.; James, A.; Bonvento, G.; Murphy, M.; Almeida, A.; Bolaños, J. Complex I Assembly into Supercomplexes Determines Differential Mitochondrial ROS Production in Neurons and Astrocytes. *Proc Natl Acad Sci U S A*. **2016**, *15*, 13063-13068.

Lowry, O.; Rosebrough, N.; Farr, A.; Randall, R. Protein measurement with the Folin phenol reagent. *J Biol Chem*. **1951**, *193*, 265-275.

Lúcio, M.; Nunes, C.; Gaspar, D.; Ferreira, H.; Lima, J.; Reis, S. Antioxidant Activity of Vitamin E and Trolox: Understanding of the Factors that Govern Lipid Peroxidation Studies in Vitro. *Food Biophysics*. **2009**, *4*, 312-320.

Luo, X.; Pitkanen, S.; Kassovska, S.; Robinson, B.; Lehotay. Excessive Formation of Hydroxyl Radicals and Aldehydic Lipid Peroxidation Products in Cultured Skin Fibroblasts From Patients with Complex I Deficiency. *J. Clin. Investig*. **1997**, *99*, 2877–2882.

Maharaj, H.; Sukhdev, D.; Scheepers, M.; Mokokong, R.; Daya, S. L-dopa administration enhances 6-hydroxydopamine generation. *Brain Res*. **2005**, *1063*, 180–186.

Mäkelä, J.; Tselykh, T.; Maiorana, F.; Eriksson, O.; Do, H.; Mudò, G.; Korhonen, L.; Belluardo, N.; Lindholm, D. Fibroblast Growth Factor-21

Enhances Mitochondrial Functions and Increases the Activity of PGC-1 α in Human Dopaminergic Neurons via Sirtuin-1. *SpringerPlus*. **2014**, 3, 2.

Maldergem, V.; Trijbels, F.; DiMauro, S.; Sindelar, P.; Musumeci, O.; Janssen, A.; Delberghe, X.; Martin, J.; Gillerot, Y. Coenzyme Q-responsive Leigh's Encephalopathy in Two Sisters. *Ann Neurol*. **2002**, 52, 750-754.

Mancuso, M.; Orsucci, D.; Filosto, M.; Simoncini, C.; Siciliano, G. Drugs and Mitochondrial Diseases: 40 Queries and Answers. *Expert Opin Pharmacother*. **2012**, 13, 527-543.

Mandl, J.; Szarka, A.; Banhegyi, G. Vitamin C: Update on Physiology and Pharmacology. *Br J Pharmacol*. **2009**, 157, 1097–1110.

Mannella, C. Structure and Dynamics of the Mitochondrial Inner Membrane Cristae. *Biochim Biophys Acta*. **2006**, 1763, 542-548.

Männistö, T.; Kaakkola, S. Catechol-O-methyltransferase (COMT): Biochemistry, Molecular Biology, Pharmacology, and Clinical Efficacy of the New Selective COMT Inhibitors. *Pharmacol Rev*. **1999**, 51, 593–628.

Maranzana, E., Barbero, G., Falasca, I., Lenaz, G., Genova, M. Mitochondrial Respiratory Supercomplex Association Limits Production of Reactive Oxygen Species from Complex I. *Antioxid. Redox Signal*. **2013**, 19, 1469–1480.

Marí, M.; Morales, A.; Colell, A.; García-Ruiz, C.; Kaplowitz, N.; Fernández-Checa, J. Mitochondrial Glutathione: Features, Regulation and Role in Disease. *Biochim Biophys Acta*. **2013**, 1830, 3317-3328.

Martin, P.; Nicolas, J.; William, O. Quantifying Mitochondrial Dysfunction in Complex Diseases of Aging. *The Journals of Gerontology*. **2012**, 67, 1022–1035.

Martinez, L.; Forni, M.; Santos, V.; Pinto, N.; Kowaltowski, A. Cardiolipin is a Key Determinant for mtDNA Stability and Segregation during Mitochondrial Stress. *Biochimica et Biophysica Acta-Bioenergetics*. **2015**, 1847, 587-598.

Matsuda, N.; Sato, S.; Shiba, K.; Okatsu, K.; Saisho, K.; Gautier, C.; Sou, Y.; et al. PINK1 Stabilized by Mitochondrial Depolarization Recruits Parkin to Damaged Mitochondria and Activates Latent Parkin for Mitophagy. *J Cell Biol*. **2010**, 189,211-221.

Mata, M.; Maraver, J.; Cotan, D.; Cordero, M.; Avila, M.; Izquierdo, G.; Miguel, M.; Lorite, J.; Infante, E.; Ybot, P.; Jackson, S.; Alcaz, J. Recovery of MERRF Fibroblasts and Cybrids Pathophysiology by Coenzyme Coenzyme Q10. *Neurotherapeutics*. **2012**, 9, 446-463.

Mayr, J.; Haack, T.; Freisinger, P.; Karall, D.; Makowski, C.; Koch, J.; et al. Spectrum of Combined Respiratory Chain Defects. *Journal of Inherited Metabolic Disease*. **2015**; 38, 629-640.

McCoy, M.; Cookson, M. DJ-1 Regulation of Mitochondrial Function and Autophagy through Oxidative Stress. *Autophagy*. **2011**, 7, 531-532.

McGeer, P.; Itagaki, S.; Boyes, B.; McGeer, E. Reactive Microglia are Positive for HLA-DR in the Substantia Nigra of Parkinson's and Alzheimer's Disease Brains. *Neurology*. **1988**, 38, 1285–1291

McKenzie, M.; Lazarou, M.; Thorburn, D.; Ryan, M. Mitochondrial Respiratory Chain Supercomplexes Are Destabilized in Barth Patients. *J. Mol. Biol*. **2006**, 361, 462–469.

McNamara, P.; Durso, R. Neuropharmacological Treatment of Mental Dysfunction in Parkinson's disease. *Behav Neurol*. **2006**, 17, 43-51

Menéndez, R. An Electromagnetic Coupling Hypothesis to Explain the Proton Translocation Mechanism in Mitochondria, Bacteria and Chloroplasts. *Med Hypotheses*. **1996**, *47*,179-182.

Merad-Saidoune, M.; Biotier, E.; Nicole, A.; Marsac, C.; Martinou, J.; Sola, B.; Sinet, P.; Ceballos-Picot, I. Overproduction of Cu/Zn-superoxide Dismutase or Bcl-2 Prevents the Brain Mitochondrial Respiratory Dysfunction Induced by Glutathione Depletion. *Exp. Neurol*. **1999**, *158*, 428–436.

Miller, F.; Rosenfeldt, F.; Zhang, C.; Linnane, A.; Nagley, P. Precise Determination of Mitochondrial DNA Copy Number in Human Skeletal and Cardiac Muscle by a PCR-based Assay: Lack of Change of Copy Number with Age. *Nucleic Acids Res*. **2003**, *31*, e61.

Miquel, J.; Ferrándiz, M.; De Juan, E.; Sevilla, I.; Martínez, M. Acetylcysteine Protects Against Age-Related Decline of Oxidative Phosphorylation in Liver Mitochondria. *Eur J Pharmacol*. **1995**, *292*, 333-335.

Mitchell, P. Coupling of Phosphorylation to Electron and Hydrogen Transfer by a Chemiosmotic Type of Mechanism. *Nature*. **1961**, *191*,144-148.

Mitchell, P. Protonmotive Redox Mechanism of the Cytochrome bc₁ Complex in the Respiratory Chain: Protonmotive Ubiquinone Cycle. *FEBS Lett*.**1975**, *56*, 1-6.

Mizuno, Y.; Suzuki, K.; Shigeo, O. Postmortem Changes in Mitochondrial Respiratory Enzymes in Brain and a Preliminary Observation in Parkinson's Disease. *Journal of the Neurological Sciences*. **1990**, *96*, 49-57.

Monti, D.,;Zabrecky, G.; Kremens, D.; Liang, T.; Wintering, N.; Cai, J.; et al. N-Acetyl Cysteine May Support Dopamine Neurons in Parkinson's Disease: Preliminary Clinical and Cell Line Data. *PLoS ONE*. **2016**, *11*, e0157602.

Moore, D.; West, A.; Dawson, V.; Dawson, T. Molecular Pathophysiology of Parkinson's Disease. *Annu Rev Neurosci.* **2005**, *28*, 57–87.

Moos, T.; Nielsen, T.; Skjorringe, T.; Morgan, E. Iron Trafficking Inside the Brain. *Journal of Neurochemistry.* **2007**, *103*, 1730-1740.

Moreira, P.; Zhu, X.; Wang, X.; Lee, H.; Nunomura, A.; Petersen, R.; Perry, G.; Smith, M. Mitochondria: a Therapeutic Target in Neurodegeneration. *Biochim Biophys Acta.* **2010**, *1802*, 212-220.

Muller, F.; Crofts, A.; Kramer, D. Multiple Q-Cycle Bypass Reactions at the Qo Site of the Cytochrome bc₁ Complex. *Biochemistry.* **2002**, *41*, 7866-7874.

Muller, F.; Roberts, A.; Bowman, M.; Kramer, D. Architecture of the Qo Site of the Cytochrome bc₁ Complex Probed by Superoxide Production. *Biochemistry.* **2003**, *42*, 6493-6499.

Müller, S.; Bender, A.; Laub, C.; Högen, T.; Schlaudraff, F.; Liss, B.; Klopstock, T.; Elstner, M. Lewy Body Pathology is Associated with Mitochondrial DNA Damage in Parkinson's Disease. *Neurobiology of Aging.* **2013**, *34*, 2231-2233.

Muñoz, A.; Rey, P.; Soto-Otero, R.; Guerra, M.; Labandeira-Garcia, J. Systemic Administration of N-acetylcysteine Protects Dopaminergic Neurons Against 6-Hydroxydopamine-Induced Degeneration. *J Neurosci Res.* **2004**, *76*, 551-562.

Murphy, P. How Mitochondria Produce Reactive Oxygen Species. *Biochem. J.* **2009**, *417*, 1–13.

Naguib, Y. A Fluorometric Method for Measurement of Peroxyl Radical Scavenging Activities of Lipophilic Antioxidants. *Analytical Biochemistry.* **1998**, *265*, 290-298.

Nakamura, K.; Nemani, V.; Azarbal, F.; Skibinski, G.; Levy, J.; Egami, K.; et al. Direct Membrane Association Drives Mitochondrial Fission by the Parkinson Disease-Associated Protein Alpha-Synuclein. *J Biol Chem.* **2011**, *286*, 20710-20726.

Napolitano, A.; Salvetti, S.; Vista, M.; Lombardi, V.; Siciliano, G. Giraldo, C. Long-Term Treatment with Idebenone and Riboflavin in a Patient with MELAS. *Neurol Sci.* **2000**, *21*, 981-982.

Neustadt, J.; Pieczenik, S. Medication-Induced Mitochondrial Damage and Disease. *Mol Nutr Food Res.* **2008**, *52*, 780–788.

Nicholls, D.; Ferguson, S. Bioenergetics 3. San Diego, *Academic Press*, **2002**.

Nicholas J.; Frank E. The Electron Transfer Flavoprotein: Ubiquinone Oxidoreductases. *Biochimica et Biophysica Acta (BBA) - Bioenergetics.* **2010**, *12*, 1910-1916.

Ni, H.; Williams, J.; Ding, W. Mitochondrial Dynamics and Mitochondrial Quality Control. *Redox Biol.* **2015**, *4*, 6-13.

Nishimura, T.; Nakatake, Y.; Konishi, M.; Itoh, N. Identification of a Novel FGF, FGF-21, Preferentially Expressed in the Liver. *Biochim Biophys Acta.* **2000**, *21*, 203-206.

Nissinen, E.; Kaheinen, P.; Penttila, K.; Kaivola, J.; Linden, I. Entacapone, a Novel Catechol-O-Methyltransferase Inhibitor for Parkinson's Disease, Does Not Impair Mitochondrial Energy Production. *Eur J Pharmacol.* **1997**, *340*, 287–294.

Norris, H.; Giasson, I. Role of Oxidative Damage in Protein Aggregation Associated with Parkinson's Disease and Related Disorders. *Antioxid. Redox Signal.* **2005**, *7*, 672–684.

Núñez, M.; Urrutia, P.; Mena, N.; Aguirre, P.; Tapia, V.; Salazar, J. Iron Toxicity in Neurodegeneration. *Biometals*. **2012**, *25*, 761-776.

Obata, T. Dopamine Efflux by MPTP and Hydroxyl Radical Generation. *J Neural Transm (Vienna)*. **2002**, *109*, 1159-1180.

Ogasahara, S.; Engel, A.; Frens, D.; Mack, D. Muscle Coenzyme Q Deficiency in Familial Mitochondrial Encephalomyopathy. *Proc Natl Acad Sci U S A*. **1989**, *86*, 2379-2382.

Ohnishi, T.; Bandow, K.; Kakimoto, K.; Kusuyama, J.; Matsuguchi, T. Long-Time Treatment by Low-Dose N-Acetyl-L-Cysteine Enhances Proinflammatory Cytokine Expressions in LPS-Stimulated Macrophages. *PLoS ONE*. **2014**, *9*, e87229.

Oppenheimer, L.; Wellner, V.; Griffith, O.; Meister, A. Glutathione Synthetase: Purification From Rat Kidney and Mapping of Substrate Binding Sites. *J. Biol. Chem*. **1979**, *254*, 5184-5190.

O'Rourke, B. From Bioblasts to Mitochondria: ever Expanding Roles of Mitochondria in Cell Physiology. *Front Physiol*. **2010**, *1*, 7.

Orozco, D.; Skamarack, J.; Reins, K.; Titlow, B.; Lunetta, S.; Li, F.; Roman, M. Determination of Ubidecarenone (Coenzyme Q10, Ubiquinol-10) in Raw Materials and Dietary Supplements by High-Performance Liquid Chromatography with Ultraviolet Detection: Single-Laboratory Validation. *Journal of AOAC International*. **2007**, *90*, 1227-1236.

Osellame, L.; Blacker, T.; Duchon, M. Cellular and Molecular Mechanisms of Mitochondrial Function. *Best Practice & Research Clinical Endocrinology & Metabolism*. **2012**, *26*, 711-723.

Ott, M.; Zhivotovsky, B.; Orrenius, S. Role Cardiolipin in Cytochrome c Release from Mitochondria. *Cell Death and Differentiation*. **2007**, *14*, 1243-1247.

Owen, J.; Butterfield, D. Measurement of Oxidized/Reduced Glutathione Ratio. *Methods Mol Biol*. **2010**, *648*, 269-277.

Pagliarini, D.; Rutter, J. Hallmarks of a New Era in Mitochondrial Biochemistry. *Genes Dev*. **2013**, *27*, 2615-2627.

Parker, W.; Boyson, S.; Parks, J. Abnormalities of the Electron Transport Chain in Idiopathic Parkinson's Disease. *Ann. Neurol*. **1989**, *26*, 719-723.

Parker, W.; Parks, J.; Swerdlow, R. Complex I Deficiency in Parkinson's Disease Frontal Cortex. *Brain Res*. **2008**, *1189*, 215–218.

Parker, W.; Parks, J.; Swerdlow, R. Complex I Deficiency in Parkinson's Disease Frontal Cortex. *Brain Research*. **2008**, *1189*, 215-218.

Patel, K.; O'Brien, T.; Subramony, S.; Shuster, J.; Stacpoole, P. The Spectrum of Pyruvate Dehydrogenase Complex Deficiency: Clinical, Biochemical and Genetic Features in 371 Patients. *Molecular genetics and metabolism*. **2012**, *106*, 385-394.

Pedrosa, D.; Timmermann, L. Review: Management of Parkinson's Disease. *Neuropsychiatric Disease and Treatment*. **2013**, *9*, 321-340.

Perry, C.; Kane, D.; Lanza, I.; Neuffer, P. Methods for Assessing Mitochondrial Function in Diabetes. *Diabetes*. **2013**, *62*, 1041-1053.

Pesta, D.; Gnaiger, E. High-Resolution Respirometry: OXPHOS Protocols for Human Cells and Permeabilized Fibers from Small Biopsies of Human Muscle. *Methods Mol Biol*. **2012**, *810*, 25-58.

Petrosillo, G.; Benedictis, V.; Ruggiero, F.; Paradies, G. Decline in Cytochrome c Oxidase Activity in Rat-brain Mitochondria with Aging. Role of Peroxidized Cardiolipin and Beneficial Effect of Melatonin. *Journal of Bioenergetics and Biomembranes*. **2013**, *45*, 431-440.

Petrosillo, G.; Ruggiero, F.; Pistolese, M.; Paradies, G. Ca²⁺-induced Reactive Oxygen Species Production Promotes Cytochrome c Release from Rat Liver Mitochondria via Mitochondrial Permeability Transition (MPT)-dependent and MPT-independent Mechanisms: Role of Cardiolipin. *The Journal of Biological Chemistry*. **2004**, *279*, 53103-53108.

Petrosillo, G.; Ruggiero, F.; Pistolese, M.; Paradies, G. Reactive Oxygen Species Generated from The Mitochondrial Electron Transport Chain Induce Cytochrome c Dissociation from Beef-heart Submitochondrial Particles via Cardiolipin Peroxidation. Possible Role in the Apoptosis. *FEBS Lett*. **2001**, *509*, 435-438.

Pfeiffer, K.; Gohil, V.; Stuart, R.; Hunte, C.; Brandt, U.; Greenberg, M.; Schagger, H. Cardiolipin Stabilizes Respiratory Chain Supercomplexes. *The Journal of Biological Chemistry*. **2003**, *278*, 52873-52880.

Polymeropoulos, H.; Lavedan, C.; Leroy, E.; Ide, S.; Dehejia, A.; Dutra, A.; et al. Mutation in the Alpha-Synuclein Gene Identified in Families with Parkinson's Disease. *Science*. **1997**, *276*, 2045–2047.

Pope, S.; Land, J.; Heales, J. Oxidative Stress and Mitochondrial Dysfunction in Neurodegeneration; Cardiolipin a Critical Target? *Biochimica et Biophysica Acta-Bioenergetics*. **2008**, *1777*, 794–799.

Prasai, K. Regulation of Mitochondrial Structure and Function by Protein Import: A Current Review. *Pathophysiology*. **2017**, *3*, 107-122.

Quinzii, C.; DiMauro, S.; Hirano, M. Human Coenzyme Q10 Deficiency. *Neurochem Res.* **2007**, *32*, 723-727.

Racker, E. A New Look at Mechanisms in Bioenergetics, *Academic Press*, New York, **1976**.

Ragan, C.; Wilson, M.; Darley-Usmar, V.; Lowe, P. Subfractionation of Mitochondria, and Isolation of the Proteins of Oxidative Phosphorylation. In *Mitochondria: A Practical Approach* (Darley-Usmar VM, Rickwood D, Wilson MT, eds) London, IRL Press, **1987**, 79–112.

Reeve, A.; Simcox, E.; Turnbull, D. Ageing and Parkinson's Disease: Why is Advancing Age the Biggest Risk Factor? *Ageing Research Reviews.* **2014**, *14*, 19-30.

Reinehr, T.; Woelfle, J.; Wunsch, R.; Roth C. Fibroblast Growth Factor 21 (FGF-21) and Its Relation to Obesity, Metabolic Syndrome, and Nonalcoholic Fatty liver in Children: A longitudinal Analysis. *J Clin Endocrinol Metab.* **2012**, *97*, 2143–2150.

Ren, R.; Zou, L.; Zhang, X.; Branco, V.; Wang, J.; Carvalho, C.; Holmgren, A.; Lu, J. Redox Signaling Mediated by Thioredoxin and Glutathione Systems in the Central Nervous System. *Antioxid. Redox Signal.* **2017**, *27*, 989-1010.

Ribas, F.; Villarroya, J.; Hondares, E.; Giralt, M.; Villarroya, F. FGF21 Expression and Release in Muscle Cells: Involvement of MyoD and Regulation by Mitochondria-Driven Signalling. *Biochem J.* **2014**, *463*, 191-19.

Ribas, V.; García-Ruiz, C.; Fernández-Checa, J. Glutathione and Mitochondria. *Frontiers in Pharmacology.* **2014**, *5*, 151.

Rice, M.; Russo-Menna, I. Differential Compartmentalization of Brain Ascorbate and Glutathione between Neurons and Glia. *Neuroscience*. **1998**, *82*, 1213-1223.

Riederer, P.; Sofic, E.; Rausch, W.; Schmidt, B.; Reynolds, G.; Jellinger, K.; Youdim, M. Transition Metals, Ferritin, Glutathione, and Ascorbic Acid in Parkinsonian Brains. *J Neurochem*. **1989**, *52*, 515-520.

Rocha, E.; Miranda, B.; Sanders, A. Alpha-Synuclein: Pathology, Mitochondrial Dysfunction and Neuroinflammation in Parkinson's disease. *Neurobiology of Disease*. **2018**, *109*, 249-257.

Rose, C., Bode, A. Tissue-Mediated Regeneration of Ascorbic Acid: Is the Process Enzymatic? *Enzyme*. **1992**, *46*, 196–203.

Ross, M.; Kelso, G.; Blaikie, F.; James, A.; Cochemé, H.; Filipovska, A.; Da Ros, T.; Hurd, T.; Smith, R.; Murphy, M. Lipophilic Triphenylphosphonium Cations as Tools in Mitochondrial Bioenergetics and Free Radical Biology. *Biochemistry (Mosc)*. **2005**, *70*, 222-230.

Rotig, A.; Lonlay, P.; Chretien, D.; Foury, F.; Koenig, M.; Sidi, D.; Munnich, A.; Rustin, P. Aconitase and Mitochondrial Iron-sulphur Protein Deficiency in Friedreich Ataxia. *Nat. Genet*. **1997**, *17*, 215-217.

Runko, A.; Griswold, A.; Kyung-Tai, M. Overexpression of Frataxin in the Mitochondria Increases Resistance to Oxidative Stress and Extends Lifespan in *Drosophila*. *FEBS Letters*. **2008**, *582*, 715-719.

Rutter, J.; Winge, D.; Schiffman, J. Succinate Dehydrogenase—Assembly, Regulation and Role in Human Disease. *Mitochondrion*. **2010**, *10*, 393-401.

Saada, A. The Use of Individual Patient's Fibroblasts in The Search for Personalized Treatment of Nuclear Encoded OXPHOS Diseases. *Mol Genet Metab.* **2011**, *104*, 39–47.

Sadun, A.; Carelli, V.; Salomao, S.; Berezovsky, A.; Quiros, P.; Sadun, F.; DeNegri, A.; Andrade, R.; Moraes, M.; Passos, A.; et al. Extensive Investigation of a Large Brazilian Pedigree of 11778/haplogroup J Leber Hereditary Optic Neuropathy. *Am. J. Ophthalmol.* **2004**, *136*, 231–238.

Sadun, A.; Morgia, C.; Carelli, V. Leber Hereditary Optic Neuropathy. *Curr. Treat. Options Neurol.* **2011**, *13*, 109–117.

Sakamoto, S.; Putalun, W.; Vimolmangkang, S.; Phoolcharoen, W.; Shoyama, Y.; Tanaka, H.; Morimoto, S. Enzyme-Linked Immunosorbent Assay for the Quantitative/Qualitative Analysis of Plant Secondary Metabolites. *Journal of Natural Medicines.* **2018**, *72*, 32-42.

Saks, V.; Veksler, V.; Kuznetsov, A.; Kay, L.; Sikk, P.; Tiivel, T.; Tranqui, L.; Olivares, J.; Winkler, K.; Wiedemann, F.; Kunz, W. Permeabilised Cell and Skinned Fiber Techniques in Studies of Mitochondrial Function in Vivo. *Mol Cell Biochem.* **1998**, *184*, 81-100.

Saric, A.; Andreau, K.; Armand, A.; Moller, I.; Petit, P. Barth Syndrome: From Mitochondrial Dysfunctions Associated with Aberrant Production of Reactive Oxygen Species to Pluripotent Stem Cell Studies. *Frontiers in Genetics.* **2016**, *6*, 359.

Schägger, H. Respiratory chain Supercomplexes of Mitochondria and Bacteria. *Biochimica et Biophysica Acta (BBA) – Bioenergetics.* **2002**, *1555*, 154-159.

Schägger, H.; de Coo, R.; Bauer, M.; Hofmann, S.; Godinot, C.; Brandt, U. Significance of Respirasomes for the Assembly/Stability of Human Respiratory Chain Complex I. *J Biol Chem.* **2004**, *279*, 36349-36353

Schägger, H., Pfeiffer, K. Supercomplexes in the Respiratory Chains of Yeast and Mammalian Mitochondria. *EMBO J.* **2000**, *19*, 1777–1783.

Schapira, A. Evidence for mitochondrial Dysfunction in Parkinson's Disease—a Critical Appraisal. *Movement Disorders.* **1994**, *9*, 125–138.

Schapira, A. Mitochondria in the Aetiology and Pathogenesis of Parkinson's Disease. *Lancet Neurol.* **2008**, *7*, 97-109.

Schapira, A.; Cooper, J.; Dexter, D.; Jenner, P.; Clark, J.; Marsden, C. Mitochondrial Complex I Deficiency in Parkinson's Disease. *Lancet.* **1989**, *8649*, 1269.

Schlame, M.; Greenberg, R. The biosynthesis and Functional Role of Cardiolipin. *Prog. Lipid Res.* **2000**, *39*, 257-288.

Schlame, M.; Greenberg, R. The role of cardiolipin in The Structural Organization of Mitochondrial Membranes. *Biochimica et Biophysica Acta-Bioenergetics.* **2009**, *1788*, 2080–2083.

Schneider, L.; Giordano, S.; Zelickson, B.; Johnson, M.; Benavides, G.; Ouyang, X.; Fineberg, N.; Darley-Usmar, V.; Zhang, J. Differentiation of SH-SY5Y Cells to a Neuronal Phenotype Changes Cellular Bioenergetics and the Response to Oxidative Stress. *Free radical biology & medicine.* **2011**, *51*, 2007-2017.

Sekura, R.; Meister, A. γ -Glutamylcysteine Synthetase: Further Purification, 'Half of the Sites' Reactivity, Subunits, and Specificity. *J. Biol. Chem.* **1977**, *252*, 2599-2605.

Sen, C. Nutritional biochemistry of Cellular Glutathione. *J. Nutr. Biochem.* **1997**, *8*, 660–672.

Severinghaus, J.; Astrup, P. History of Blood Gas Analysis. IV. Leland Clark's Oxygen Electrode. *Journal of Clinical Monitoring*. **1986**, *2*,125–139.

Shahripour, R.; Mark, R.; Harrigan, V. N-acetylcysteine (NAC) in Neurological Disorders: Mechanisms of Action and Therapeutic Opportunities. *Brain and Behavior*. **2014**, *4*,108–122.

Sharma, L.; Lu, J.; Bai, Y. Mitochondrial Respiratory Complex I: Structure, Function and Implication in Human Diseases. *Current Medicinal Chemistry*. **2009**, *16*, 1266-1277.

Sharon, R.; Bar-joseph, I.; Frosch, P.; Walsh, M.; Hamilton, J.; Selkoe, J. The Formation of Highly Soluble Oligomers of Alpha-Synuclein is Regulated by Fatty Acids and Enhanced in Parkinson 's Disease. *Neuron*. **2003**, *37*, 583–595.

Shepherd, J.; Garland, P. Citrate Synthase from Rat Liver. *Methods Enzymol*. **1969**, *13*, 11–19.

Sherer, T.; Betarbet, R.; Stout, A.; Lund, S.; Baptista, M.; Panov, A.; Cookson, M.; Greenamyre, J. In Vitro Model of Parkinson's Disease: Linking Mitochondrial Impairment to Altered α -Synuclein Metabolism and Oxidative Damage. *Journal of Neuroscience*. **2002**, *22*, 7006-7015.

Sherer, T.; Betarbet, R.; Testa, C.; Seo, B.; Richardson, J.; Kim, J.; Miller, G.; Yagi, T.; Matsuno-Yagi, A.; Greenamyre, J. Mechanism of Toxicity in Rotenone Models of Parkinson's Disease. *Journal of Neuroscience*. **2003**, *23*, 10756-10764.

Shih, J.; Chen, K.; Ridd, M. Monoamine Oxidase: from Genes to Behavior. *Annu Rev Neurosci*. **1999**, *22*,197–217.

Shim, J.; Yoon, S.; Kim, K.; Han, J.; Ha, J.; Hyun, D.; Paek, S.; Kang, U.; Zhuang, X.; Son, J. The Antioxidant Trolox Helps Recovery from the Familial Parkinson's Disease-Specific Mitochondrial Deficits Caused by PINK1- and DJ-1-Deficiency in Dopaminergic Neuronal Cells. *Mitochondrion*. **2011**, *11*, 707-715.

Shoffner, J.; Lott, M.; Lezza, A.; Seibel, P.; Ballinger, S.; Wallace, D. Myoclonic Epilepsy and Ragged-red Fiber Disease (MERRF) is Associated with a Mitochondrial DNA tRNA(Lys) mutation. *Cell*. **1999**, *15*, 931-937.

Shoffner, J.; Wallace, D. Mitochondrial Genetics: Principle and Practice. *Am. J. Hum. Genet.* **1992**, *51*, 1179-1186.

Shoffner, J.; Watts, R.; Juncos, J.; Torroni, A.; Wallace, D. Mitochondrial oxidative phosphorylation defects in Parkinson's disease. *Ann Neurol.* **1991**, *30*, 332-339.

Shults, C.; Haas, R.; Passov, D.; Beal, M. Coenzyme Q10 Levels Correlate with the Activities of Complexes I and II/III in Mitochondria from Parkinsonian and Non-Parkinsonian Subjects. *Ann Neurol.* **1997**, *42*, 261-264.

Shults, C.; Oakes, D.; Kieburtz, K.; et al. Effects of Coenzyme Q10 in Early Parkinson Disease: Evidence of Slowing of the Functional Decline. *Arch Neurol.* **2002**, *59*, 1541-1550.

Sian, J.; Dexter, D.; Lees, A.; Daniel, S.; Jenner, P.; Marsden, C. Glutathione-related Enzymes in Brain in Parkinson's Disease. *Ann Neurol.* **1994**, *36*, 356-361.

Sies, H. Oxidative Stress. *Academic Press, London*. **1985**, 1–507.

Singh, K.; Hammachi, F.; Kunath, T. Modeling Parkinson's Disease with Induced Pluripotent Stem Cells Harboring α -Synuclein Mutations. *Brain Pathol.* **2017**, *4*, 545-551.

Sipos, K.; Lange, H.; Fekete, Z.; Ullmann, P.; Lill, R.; Kispal, G. Maturation of Cytosolic Iron-sulfur Proteins Requires Glutathione. *J Biol Chem.* **2002**, *277*, 26944-26949.

Skoog, D.; Holler, F.; Nieman, T. Principles of Instrumental Analysis. (5th edn) *Saunders College Pub*, Philadelphia. **1998**.

Smith, A.; Shenvi, S.; Widlansky, M.; Suh, J.; Hagen, T. Lipoic Acid as a Potential Therapy for Chronic Diseases Associated with Oxidative Stress. *Curr. Med. Chem.* **2004**, *11*, 1135–1146.

Smith, R.; Adlam, V.; Blaikie, F.; Manas, A.; Porteous, C.; James, A.; Ross, M.; Logan, A.; Cochemé, H.; Trnka, J.; et al. Mitochondria-Targeted Antioxidants in the Treatment of Disease. *Ann. N. Y. Acad. Sci.* **2008**, *1147*, 105–111.

Smith, R.; Hartley, R.; Cochemé, H.; Murphy, M. Mitochondrial Pharmacology. *Trends Pharmacol Sci.* **2012**, *33*, 341-352.

So, W.; and Leung, P. Fibroblast Growth Factor 21 as an Emerging Therapeutic Target for Type 2 Diabetes Mellitus. *Med. Res. Rev.* **2016**, *36*, 672-704.

So, W.; Cheng, Q.; Chen, L.; Evans-Molina, C.; Xu, A.; Lam, K.; Leung, P. High Glucose Represses Beta-klotho Expression and Impairs Fibroblast Growth Factor 21 Action in Mouse Pancreatic Islets: Involvement of Peroxisome Proliferator-activated Receptor Gamma Signalling. *Diabetes.* **2013**, *62*, 3751–3759.

Sohmiya, M.; Tanaka, M.; Tak, N.; Yanagisawa, M.; Tanino, Y.; Suzuki, Y.; Okamoto, K.; Yamamoto, Y. Redox Status of Plasma Coenzyme Q10 Indicates Elevated Systemic Oxidative Stress in Parkinson's Disease. *J Neurol Sci.* **2004**, *223*, 161-166.

Soiferman, D.; Ayalon, O.; Weissman, S.; Saada, A. The Effect of Small Molecules on Nuclear Encoded Translation Diseases. *Biochimie*. **2014**, *100*, 184–191.

Sparaco, M.; Schon, E.; DiMauro, S.; Eduardo, Bonilla. Myoclonic Epilepsy with Ragged-red Fibers (MERRF): An Immunohistochemical Study of the Brain. *Brain Pathology*. **1995**, *5*, 125-133.

Stankiewics, J.; and Brass, S. Role of Iron in Neurotoxicity: a Cause for Concern in the Elderly? *Curr. Opin. Clin. Nutr. Metab. Care*. **2009**, *12*, 22-29.

Stansley, B.; Yamamoto, B. L-Dopa-Induced Dopamine Synthesis and Oxidative Stress in Serotonergic Cells. *Neuropharmacology*. **2013**, *67*, 243–51.

Starkov, A. The Role of Mitochondria in Reactive Oxygen Species Metabolism and Signaling. *Ann N Y Acad Sci*. **2008**, *1147*,37-52.

Stein, S.; Bachmann, A.; Lössner, U.; Kratzsch, J.; Blüher, M.; Stumvoll, M.; Fasshauer, M. Serum Levels of the Adipokine FGF21 Depend on Renal Function. *Diabetes Care*. **2009**, *32*, 126-128.

Stewart, J.; Chinnery, P. The Dynamics of Mitochondrial DNA Heteroplasmy: Implications for Human Health and Disease. *Nat Rev Genet*. **2015**, *16*, 530–542.

Stewart, V.; Heales, S. Nitric Oxide-Induced Mitochondrial Dysfunction: Implication for Neurodegeneration. *Free Radic. Biol. Med*. **2003**, *34*, 287–303.

Stewart, V.; Land, J.; Clark J.; Heales, S. Pretreatment of Astrocytes with Interferon-Alpha/Beta Prevents Neuronal Mitochondrial Respiratory Chain Damage. *J. Neurochem*. **1998**, *704*, 32-34.

Štulík, K.; Pacáková, V. Electrochemical Detection Techniques in High-Performance Liquid Chromatography. *Journal of Electroanalytical Chemistry and Interfacial Electrochemistry*. **1981**, *129*, 1-24.

Suleyman, A. A Short History, Principles, and Types of ELISA, and our Laboratory Experience with Peptide/Protein Analyses Using ELISA. *Peptides*. **2015**, *72*, 4-15.

Sun, F.; Huo, X.; Zhai, Z.; Wang, A.; Xu, J.; Su, D.; Bartlam, M.; Rao, Z. Crystal Structure of Mitochondrial Respiratory Membrane Protein Complex II. *Cell*. **2005**, *121*, 1043-1057.

Suomalainen, A. Biomarkers for Mitochondrial Respiratory Chain Disorders. *Journal of Inherited Metabolic Disease*. **2011**, *2*, 277–282.

Suomalainen, A. Fibroblast Growth Factor 21: a Novel Biomarker for Human Muscle-Manifesting Mitochondrial Disorders, *Expert Opinion on Medical Diagnostics*. **2013**, *7*, 313-317.

Suomalainen, A.; Elo, J.; Pietiläinen, K.; Hakonen, A.; Sevastianova, K.; Korpela, M.; et al. FGF-21 as a Biomarker for Muscle-Manifesting Mitochondrial Respiratory Chain Deficiencies: A Diagnostic Study. *Lancet Neurol*. **2011**, *10*, 806-818.

Suomalainen, A.; Majander, A.; Haltia, M.; Somer, H.; Lönnqvist, J.; Savontaus, M.; Peltonen, L. Multiple Deletions of Mitochondrial DNA in Several Tissues of a Patient with Severe Retarded Depression and Familial Progressive External Ophthalmoplegia. *J. Clin. Invest.* **1992**, *9*, 61-66.

Swartz, M. HPLC Detectors: A Brief Review. *Journal of Liquid Chromatography & Related Technologies*. **2010**, *33*, 1130-1150.

Sykora, P.; Wilson, D.; Bohr, V. Repair of Persistent Strand Breaks in the Mitochondrial Genome. *Mech. Aging Dev.* **2012**, *133*, 169–175.

Szczepanowski, J.; Malinska, D.; Wieckowski, M.; Duszynski, J. Effect of mtDNA Point Mutations on Cellular Bioenergetics. *Biochimica et Biophysica Acta-Bioenergetics.* **2012**, *1817*, 1740-1746.

Szewczyk, A.; Wojtczak, L. Mitochondria as a Pharmacological Target. *Pharmacol Rev.* **2002**, *54*,101–127.

Tacer, K.; Bookout, A.; Ding, X.; Kurosu, K.; John, G.; Wang, L.; Goetz, R.; Mohammadi, M.; Kuro-o, M.; Mangelsdorf, D.; Kliewer, S. Research Resource: Comprehensive Expression Atlas of the Fibroblast Growth Factor System in Adult Mouse. *Mol Endocrinol.* **2010**, *24*, 2050–2064.

Toshiharu, N.; Kohichi, K. Application of Electrochemical Detection in High-Performance Liquid Chromatography to the Assay of Biologically Active Compounds. *TrAC Trends in Analytical Chemistry.* **1988**, *7*, 21-27.

Traber, M.; Stevens, J. Vitamins C and E: Beneficial Effects from a Mechanistic Perspective. *Free radical biology & medicine.* **2011**, *51*, 1000-1013.

Triepels, R.; Heuvel, L.; Loeffen, J.; Buskens, C.; Smeets, R.; Gozalbo, M.; et al. Leigh Syndrome Associated with a Mutation in the NDUFS7 (PSST) Nuclear Encoded Subunit of Complex I. *Ann Neurol.* **1999**, *45*, 787–90.

Trifunovic, A. Mitochondrial DNA and Ageing. *Biochim Biophys Acta.* **2006**, *1757*, 611-617.

Tsukihara, T.; Aoyama, H.; Yamashita, E.; Tomizaki, T.; Yamaguchi, H.; Shinzawa-Itoh, K.; Nakashima, R.; Yaono, R.; Yoshikawa, S. Structures of

Metal Sites of Oxidized Bovine Heart Cytochrome c Oxidase at 2.8 Å. *Science*. **1995**, 5227, 1069-1074.

Tuominen, E.; Wallace, C.; Kinnunen, P. Phospholipid-cytochrome c interaction. Evidence for the extended Lipid Anchorage. *The Journal of Biological Chemistry*. **2002**, 277, 8822-8826.

Turrens, J. Mitochondrial Formation of Reactive Oxygen Species. *J. Physiol.* **2003**, 552, 335–344.

Turrens, J.; Alexandre, A.; Lehninger, A. Ubisemiquinone is the Electron Donor for Superoxide Formation by Complex III of Heart Mitochondria. *Arch. Biochem. Biophys.* **1985**, 237, 408-414.

Tyynismaa, H.; Carroll, C.; Raimundo, N.; , Raimundo, N.; Ahola-Erkkilä, S.; Wenz, T.; et al. Mitochondrial Myopathy Induces a Starvation-Like Response. *Hum. Mol. Genet.* **2010**, 19, 3948-3958.

Tyynismaa, H.; Mjosund, K.; Wanrooij, S.; Lappalainen, I.; Ylikallio, E.; Jalanko, A.; Spelbrink, J.; Paetau, A.; Suomalainen, A.. Mutant Mitochondrial Helicase Twinkle Causes Multiple mtDNA Deletions and a Late-Onset Mitochondrial Disease in Mice. *Proc. Natl. Acad. Sci. USA*. **2005**, 102, 17687-17692.

Upstone, S. Ultraviolet/Visible Light Absorption Spectrophotometry in Clinical Chemistry. *Encyclopedia of Analytical Chemistry*. Chichester: John Wiley & Sons Ltd; **2013**, 1699-1714.

Valianpour, F.; Mitsakos, V.; Schlemmer, D.; Towbin, J.; Ekert, P.; Thorburn, D.; Munnich, A.; Wanders, R.; Barth, P. Vaz, F. Monolysocardiolipins Accumulate in Barth Syndrome But Do Not Lead to Enhanced Apoptosis. *J. Lipid Res.* **2005**, 46, 1182-1195.

Vanitallie, T.; Nonas, C.; Di Rocco, A.; Boyar, K.; Hyams, K.; Heymsfield, S. Treatment of Parkinson Disease with Diet-Induced Hyperketonemia: A Feasibility Study. *Neurology*. **2005**, *64*, 728–730.

Vásquez, O.; Almeida, A.; Bolaños, J. Depletion of Glutathione Up-regulates Mitochondrial Complex I Expression in Glial Cells. *J Neurochem*. **2001**, *76*, 1593-1596.

Vasquez-Vivar, J.; Kalyanaraman, B.; Kennedyl, M. Mitochondrial Aconitase is a Source of Hydroxyl Radical: An Electron Spin Resonance Investigation. *The Journal of Biological Chemistry*. **2000**, *275*, 14064-14069.

Venkateshappa, C.; Harish, G.; Mythri, R.; Mahadevan, A.; Bharath, M.; Shankar, S. Increased Oxidative Damage and Decreased Antioxidant Function in Aging Human Substantia Nigra Compared to Striatum: Implications for Parkinson's Disease. *Neurochem Res*. **2012**, *37*, 358-369.

Verschoor, M.; Ungard, R.; Harbottle, A.; Jakupciak, J.; Parr, R.; Singh, G. Mitochondria and Cancer: Past, Present, and Future. *BioMed Research International*. **2013**, *2013*, 612369.

Viscomi, C.; Bottani E.; Zeviani, M. Emerging Concepts in the Therapy of Mitochondrial Disease. *Biochimica et Biophysica Acta (BBA) – Bioenergetics*. **2015**, *1847*, 544-557.

Wakil, S.; Abu-Elheiga, L. Fatty Acid Metabolism: Target for Metabolic Syndrome. *J Lipid Res*. **2009**, *50*, 138-143.

Walker, J.; Dickson, V. The Peripheral Stalk of the Mitochondrial ATP Synthase. *Biochimica et Biophysica Acta (BBA) – Bioenergetics*. **2006**, *1757*, 286-296.

Wallace, D. The mitochondrial Genome in Human Adaptive Radiation and Disease: on the Road to Therapeutics and Performance Enhancement. *Gene*. **2005**, 354, 169–180.

Wang, Y.; Gu, Y.; Wang, J.; Tong, Y. Oxidative Stress in Chinese Patients with Leber Hereditary Optic Neuropathy. *J. Int. Med. Res.* **2008**, 36, 544–550.

Wharton, D.; Tzagoloff, A. Cytochrome Oxidase from Beef Heart Mitochondria. *Methods Enzymol.* **1967**, 10, 245–250.

White, E.; Shannon, J.; Patterson, R. Relationship between Vitamin and Calcium Supplement Use and Colon Cancer. *Cancer Epidemiol. Biomark. Prev.* **1997**, 6, 769–774.

Wiegand, G.; Remington, S. Citrate synthase: structure, control, and mechanism. *Annu Rev Biophys Biophys Chem.* **1986**, 15, 97-117.

Wills, J.; Jones, J.; Haggerty, T.; Duka, V.; Joyce, J.; Sidhu, A. Elevated Tauopathy and Alpha-Synuclein Pathology in Post-Mortem Parkinson's Disease Brains with and without Dementia. *Exp. Neurol.* **2010**, 225, 210–218.

Winkler-Stuck, K.; Wiedemann, F.; Wallesch, C.; Kunz, W. Effect of Coenzyme Q10 on the Mitochondrial Function of Skin Fibroblasts from Parkinson Patients. *J Neurol Sci.* **2004**, 220, 41-48.

Winklhofer, K.; Haass, C. Mitochondrial Dysfunction in Parkinson's Disease. *Biochimica et Biophysica Acta (BBA).* **2010**, 1, 29-44.

Winter, W.; Bazydlo, L.; Harris, N. The Molecular Biology of Human Iron Metabolism. *Lab Med.* **2014**, 45, 92-102.

Wong, A.; Cavelier, L.; Collins-Schramm, H.; Seldin, M.; McGrogan, M.; Savontaus, M.; Cortopassi, G. Differentiation-specific Effects of LHON

Mutation Introduced into Neuronal NT2 Cells. *Hum. Mol. Genet.* **2002**, *11*, 431–438.

Wong, A.; Yang, J.; Cavadini, P.; Gellera, C.; Lonnerdal, B.; Taroni, F.; Cortopassi, G. The Friedreich Ataxia Mutation Confers Cellular Sensitivity to Oxidant Stress Which is Rescued by Chelators of Iron and Calcium and Inhibitors of Apoptosis. *Hum. Mol. Genet.* **1999**, *8*, 6.

Woo, C.; Xu, A.; Wang, Y.; Lam, K. Fibroblast Growth Factor 21 as an Emerging Metabolic Regulator: Clinical Perspectives. *Clin Endocrinol.* **2013**, *78*, 489-496.

Wortmann, S.; Kluijtmans, L.; Engelke, U.; Wevers, R.; Morava, E. The 3-methylglutaconic acidurias: what's new? *J Inherit Metab Dis.* **2012**, *35*, 13–22.

Wortmann, S.; Kluijtmans, L.; Rodenburg, R.; Sass, J.; Nouws, J.; Kaauwenet, E.; et al. 3-Methylglutaconic Aciduria—Lessons from 50 Genes and 977 Patients. *Journal of Inherited Metabolic Disease.* **2013**, *6*, 913-921.

Wu, S.; Ma, Y.; Wu, Y.; Chen, Y.; Wei, Y. Mitochondrial DNA Mutation-Elicited Oxidative Stress, Oxidative Damage, and Altered Gene Expression in Cultured Cells of Patients with MERRF Syndrome. *Cell.* **1990**, *61*, 931-937.

Wu, S.; Wei, Y. AMPK-mediated Increase of Glycolysis as an Adaptive Response to Oxidative Stress in Human Cells: Implication of the Cell Survival in Mitochondrial Diseases. *Biochim Biophys Acta.* **2012**, *1822*, 233-247.

Xiao, Y.; Xu, A.; Law, L.; Chen, C.; Li, H.; Li, X.; Yang, L.; Liu, S.; Zhou, Z.; Lam, K. Distinct Changes in Serum Fibroblast Growth Factor 21 Levels in Different Subtypes of Diabetes. *J Clin Endocrinol Metab.* **2012**, *97*, 54–58.

Xicoy, H.; Wieringa, B.; Martens, G. The SH-SY5Y Cell Line in Parkinson's Disease Research: a Systematic Review. *Mol Neurodegener.* **2017**, *12*, 10.

Yan, Y.; Kang, B. The Role of Cardiolipin Remodeling in Mitochondrial Function and Human Diseases. *Journal of Molecular Biology Research*. **2012**, *2*, 1925-4318.

Yap, L.; Sancheti, H.; Ybanez, M.; Garcia, J.; Cadenas, E.; Han, D. Determination of GSH, GSSG, and GSNO Using HPLC with Electrochemical Detection. *Methods in Enzymology*. **2010**, *473*, 137-147.

Yen, M.; Kao, S.; Wang, A.; Wei, Y. Increased 8 hydroxy 2' deoxyguanosine in Leukocyte DNA in Leber Hereditary Optic Neuropathy. *Investig. Ophthalmol. Vis. Sci*. **2004**, *45*, 1688–1691.

Yi, L.; Herb, E. New Developments and Novel Therapeutic Perspectives for Vitamin C. *The Journal of Nutrition*. **2007**, *137*, 2171–2184.

Yusuf, M.; Leung, K.; Morris, K.; Volpi, E. Comprehensive Cytogenomic Profile of the in Vitro Neuronal Model SH-SY5Y. *Neurogenetics*. **2013**, *14*, 63-70.

Yuxi, S.; Schoenfeld, R.; Hayashi, G.; Napoli, E.; Akiyama, T.; Carstens, M.; Carstens E, Pook, M.; Cortopa, G. Frataxin Deficiency Leads to Defect in Expression of Antioxidants and Nrf2 Expression in Dorsal Root Ganglia of the Friedreich Ataxia YG8R Mouse Model. *Antioxid. Redox Signal*. **2013**, *19*, 1481-1493.

Zanellati, M.; Monti, V.; Barzaghi, C.; Reale, C.; Nardocci, N.; Albanese, A.; Valente, E.; Ghezzi, D.; Garavaglia, B. Mitochondrial Dysfunction in Parkinson Disease: Evidence in Mutant PARK2 Fibroblasts. *Front Genet*. **2015**, *6*, 78.

Zeevalk, G.; Manzano, L.; Sonsalla, P.; Bernard, L. Characterization of Intracellular Elevation of Glutathione (GSH) with Glutathione Monoethyl Ester and GSH in Brain and Neuronal Cultures: Relevance to Parkinson's Disease. *Exp Neurol*. **2007**, *203*, 512-520.

Zeviani, M.; Di Donato, S. Mitochondrial disorders. *Brain*. **2004**, *127*, 2153-2172.

Zhang, X.; Yeung, D.; Karpisek, M.; Stejskal, D.; Zhou, Z.; Liu, F.; Wong, R.; Chow, W.; Tso, A.; Lam, K.; Xu, A. Serum FGF21 Levels are Increased in Obesity and are Independently Associated with the Metabolic Syndrome in Humans. *Diabetes*. **2008**, *57*, 1246–1253.

Zhong, W.; Hee, S. Comparison of UV, Fluorescence, and Electrochemical Detectors for the Analysis of Formaldehyde-Induced DNA Adducts. *J Anal Toxicol*. **2005**, *29*, 182-187.

Zhou, C.; Huang, Y.; Przedorski, S. Oxidative Stress in Parkinson's Disease: A Mechanism of Pathogenic and Therapeutic Significance. *Annals of the New York Academy of Sciences*. **2008**, *1147*, 93-104.

Zhou, R.; Yazdi, A.; Menu, P.; Tschopp, J. A Role for Mitochondria in NLRP3 Inflammasome activation. *Nature*. **2011**, *469*, 221-225.

Zhu, S.; Wu, Y.; Ye, X.; Ma, L.; Qi, J.; Yu, D.; Wei, Y.; Lin, G.; Ren, G.; Li, D. FGF21 Ameliorates Nonalcoholic Fatty Liver Disease by Inducing Autophagy. *Mol Cell Biochem*. **2016**, *420*, 107.

Zhu, Y.; Carvey, P.; Ling, Z. Altered Glutathione Homeostasis in Animals Prenatally Exposed to Lipopolysaccharide. *Neurochem Int*. **2007**, *50*, 671-80.

Ziviani, E.; Tao, R.; Whitworth, A. Drosophila Parkin Requires PINK1 for Mitochondrial Translocation and Ubiquitinates Mitofusin. *Proc Natl Acad Sci U S A*. **2010**, *107*, 5018-5023.

Zitka, O.; Skalickova, S.; Gumulec, J.; Masarik, M.; Adam, V.; Hubalek, J.; Trnkova, L.; Kruseova, J.; Eckschlager, T.; Kizek, R. Redox status expressed as GSH: GSSG Ratio as a Marker for Oxidative Stress in Paediatric Tumour Patients. *Oncology Letters*. **2012**, *4*, 1247-1253.

Zorov, D.; Juhaszova, M.; Sollott, S. Mitochondrial Reactive Oxygen Species (ROS) and ROS-Induced ROS Release. *Physiol Rev.* **2014**, *94*, 909-950.

Appendix

Section 1

Validation FGF-21 kit agreement and team

Title: Validation of an enzyme linked immunosorbent assay (ELISA) kit for the measurement of human fibroblast growth factor (FGF-21). A potentially useful biomarker for the investigation of patients with mitochondrial disease.

Number: V10

Proposal: The human fibroblast growth factor (FGF-21) ELISA kit will be validated in the Clinical Immunology Laboratory. FGF-21 is a potent metabolic regulator, and it potentially serves as a sensitive indicator for mitochondrial disorders. Serum or plasma will be used to assess FGF-21. This will be achieved by using enzyme linked immunosorbent assay. It is anticipated that this test will provide us with a useful and reliable tool for the identification and monitoring of patients with suspected mitochondrial disorders. It has the potential to limit the need for invasive muscle biopsies. Additionally, assessment of FGF-21 could be offered as a test by Laboratory Medicine at GOSH. This would support the nationally commissioned mitochondrial service and provide a new avenue of external income for the Trust.

Agreed by Head of Department: Name:

Signature:

Where possible, all evaluations should be undertaken by a team of at least two people to provide continuity, cover for sickness and other absences.

Team Role	Name	Signature
Primary Investigator	Simon Heales	
Secondary Investigator	Iain Hargreaves	

Section 2

Validation FGF-21 Plan

- **Title:** Validation of an enzyme linked immunosorbent assay (ELISA) kit for the measurement of human fibroblast growth factor (FGF-21). A potentially useful biomarker for the investigation of patients with mitochondrial disease.

- **Introduction:**

The human fibroblast growth factor (FGF-21) ELISA kit will be validated in the Clinical Immunology Laboratory. FGF-21 is a potent metabolic regulator, and it potentially serves as a sensitive indicator for mitochondrial disorders. Serum will be used to assess FGF-21. This will be achieved by using enzyme linked immunosorbent assay. It is anticipated that this test will provide us with a useful and reliable tool for the identification and monitoring of patients with suspected mitochondrial disorders. It has the potential to limit the need for invasive muscle biopsies. Additionally, assessment of FGF-21 could be offered as a test by Laboratory Medicine at GOSH. This would support the nationally commissioned mitochondrial service and provide a new avenue of external income for the Trust.

- **Aim:**

The main aim is to validate the reliability of ELISA kit for the determination of FGF-21 concentration in human serum by evaluating the following parameters:

- Reference range.
- Limit of assay (linearity).
- Precision.
 - Intra-assay (Within-Run).
 - Inter-assay (Run-to-Run).

- Stability of samples.
- Accuracy.

- ***Start/ actual finish date:***

June -2015

- ***Location:***

This validation will take place at the Clinical Immunology Laboratory, Great Ormond Street Hospital.

- ***Description of the method:***

The Sandwich Enzyme- Linked ImmunoSorbent Assay (ELISA) is sensitive and reliable tool for measuring the antigen concentration between two layers of antibodies (i.e. capture and detection antibody) in unknown serum.

○ **Procedural Risk assessment:**

PROCEDURE Human FGF-21 ELISA
Procedure Details The measurement of serum Fibroblast Growth Factor-21 (FGF-21) by Enzyme Immunoassay

Substances Used	Type of Hazard	HAZARD CAT.			EXPOSURE POTENTIAL			RISK NO
		H	M	L	H	M	L	
Human serum	Biohazard ACDP 2			X			X	1
Biotin Labeled antibody	Harmful/Irritant		X				X	1
Streptavidin HRP Conjugate	Harmful/Irritant		X				X	1
Standards and QC	Harmful/Irritant Biohazard		X				X	1
Wash solution Concentrate	Harmful/Irritant		X				X	1
Substrate Solution	Harmful/Irritant		X				X	1
Stop Solution	Harmful/Irritant							
Other kit contents	-			X			X	1
MilliRo water	-			X			X	1
1% Virkon	Irritant		X				X	1

PPE and other controls	Nitrile Gloves/ Laboratory Coat Avoid heat and contact with acids.
Spillage/ Disposal	Biohazards: Use 1% Virkon or Virkon powder and dispose of into autoclave bag Chemicals: Dilute as much as possible with water, wash away down the sink or mop up with paper towels or unsafe and place for incineration. Do not pour large amounts down the sink as this maybe environmentally damaging.
Accidents	Eyes: Irrigate immediately with water for at least 10 minutes Skin: Wash with soap and rinse site immediately with water Mouth: Rinse out mouth immediately with water Lungs: Remove to fresh air immediately

Additional hazards	<p>Plate Washer: When operating, ensure plastic guard is in place to protect from moving/dispensing arm.</p> <p>Plate Reader: Take care not to trap fingers in the plate reader when inserting plate to read.</p> <p>Electrical: Electrical safety checks are made annually through the Estates department or are covered by a service contract. In case of an electrical emergency, push the red button situated on the wall. This will cut off the current to the room.</p>
	<p>Discontinue working if you feel ill or unstable. Always inform the first aid officer or seek medical advice after an accident.</p>

Refer to COSHH file, Health and Safety Policy and General Risk assessment for more information.

- **Detailed description of how aims will be assessed:**
- **Reference range:** it will be determined by assaying at least 50 normal samples from different sex and age groups. To identify the increased level, we will also evaluate at least 10 pediatric samples that are expected to have a raised FGF-21 level.
- **Limit of assay (linearity):** serum samples will be diluted in a serial two fold steps with dilution buffer and assayed.
- **Precision.**
 - Intra-assay (Within-Run): it will be evaluated by running 2 serum samples 8 times within the same run.
 - Inter-assay (Run-to-Run): it will be evaluated by running 2 serum samples 6 times on different days.

- **Stability of samples:** all serum samples will be stored at -70 °C until assayed. However, serum samples will be assayed during unseparated at room temperature, and separated at 4 °C.
- **Accuracy:** two serum samples will be spiked with a known concentration of standard and assayed.

- ***How investigators will be trained or have been trained:***

I have been trained for a year in Clinical Laboratory Department at Armed Forces Hospitals, Southern Region, Saudi Arabia. This Laboratory Department has been accredited by College of American Pathologists (CAP) and I have successfully completed this training program.

- ***Resources required and how sourced and financed.***

- The equipment and lab consumables will be provided by The Immunology and Virology Laboratories, Great Ormond Street Hospital.
- The kit components was supplied by Cambridge Bioscience Ltd, Munro House, Trafalgar way, Bar Hill, Cambridge, CB23 8SQ. The price of this kit is 528.30 GBP and is funded under the research grant.
- The Immunology Laboratory will set up a timetable in order for me to be able to assay all samples at a convenient time for them.

○ **Time line for plan:**

First run	Wednesday 22-07-15
Second run	Wednesday 29-07-15
Third run	Wednesday 05-08-15
Forth run	Wednesday 12-08-15
Fifth run	Wednesday 19-08-15
Sixth run	Wednesday 26-08-15

○ **References:**

- Denise Walshe, Kimberly Gilmour, (2013). *ISOP34 Validation and Verification Policy*.
- BioVender Research and Diagnostic Products. *Human FGF-21 ELISA*.
- Suomalainen, A., Elo, J., et al (2011). FGF-21 as a biomarker for muscle-manifesting mitochondrial respiratory chain deficiencies: A diagnostic study. *The Lancet Neurology*, 10(9), 806-818.
[http://dx.doi.org/10.1016/S1474-4422\(11\)70155-7](http://dx.doi.org/10.1016/S1474-4422(11)70155-7)

○ **Acceptance Criteria:**

Performance Qualification (PQ)

Description of test	Acceptance Criteria	Results	Comments Include action taken for any unexpected results	Sign/Date
Run 50 normal serum samples from different sex and age groups	All values to be within calibration range 30-1920 pg/ml.	Pass/ Fail		
Run 10 serum pediatric samples that are expected to have a raised FGF-21 level	All values to be higher than 1920 pg/ml.	Pass/ Fail		
Serum samples will be diluted in a serial two fold steps with dilution buffer.	All values to be shown a linear.	Pass/ Fail		
Run 2 serum samples 8 times within the same run.	Produces an acceptable CV for intra assay precision. CV to be $\pm 10\%$	Pass/ Fail		
Run 2 serum samples 6 times on different days.	Produces an acceptable CV for inter assay precision. CV to be $\pm 10\%$	Pass/ Fail		
serum samples will be assayed during unseparated at RT, and separated at 4 °C.	No decline in concentration (10%) of FGF21 will be observed in serum samples.	Pass/ Fail		
Two serum samples will be spiked with a known concentration of standard and assayed.	All values to be recovered within 80-120%.	Pass/ Fail		

- **Expected completion date:** From time line.

Agreed by Head of Department: Name:

Signature:

Where possible, all evaluations should be undertaken by a team of at least two people to provide continuity, cover for sickness and other absences.

Team Role	Name	Signature
Primary Investigator	Simon Heales	
Secondary Investigator	Iain Hargreaves	
Lab Manager	Denise Walshe	
Section Lead	Elizabeth Ralph	
PhD Student	Mesfer Al Shahrani	

Published Conference Abstracts Related to this Thesis

- ❖ **Scientific Meeting Entitled, “Chemical Biology Approaches to Assessing and Modulating Mitochondria” was Held at Royal Society Centre, Chicheley Hall, Buckinghamshire, UK. 26-27 September 2016.**

Poster 1: “Evidence of Mitochondrial Respiratory Chain Dysfunction Associated with Pathological Changes in The Early Stage of Parkinson’s Disease”.

Mesfer Al Shahrani, Sandrine C. Wauters, Christina E. Murray, Iain P. Hargreaves, Simon R. Heales, Sonia Gandhi.

Poster 2: “The Biochemical Investigation of Mitochondrial respiratory Chain Disorders”.

Mesfer Al Shahrani, Iain P. Hargreaves, Simon R. Heales

- ❖ **The 20th edition of the International Conference on “Oxidative Stress Reduction, Redox Homeostasis and Antioxidants” was held at University Pierre et Marie Curie, Paris, France. June 25-26 June 2018.**

Oral Presentation: “Biochemical Consequences of Complex I Deficiency “

Mesfer Al Shahrani, Michael Orford, Simon Heales.

Published Review Articles Related to this Thesis

- ❖ **Al Shahrani, M.**; Heales, S.; Hargreaves, I.; Orford, M. Oxidative Stress: Mechanistic Insights into Inherited Mitochondrial Disorders and Parkinson's Disease. *J. Clin. Med.* **2017**, 6, 100.
- ❖ Hargreaves, I.; **Al Shahrani, M.**; Wainwright, L.; Heales, S. Drug-Induced Mitochondrial Toxicity. *Drug Saf.* **2016**, 39, 661–674



Review

Oxidative Stress: Mechanistic Insights into Inherited Mitochondrial Disorders and Parkinson's Disease

Mesfer Al Shahrani ^{1,2,3}, Simon Heales ^{1,2,4}, Iain Hargreaves ^{1,5} and Michael Orford ^{2,*}

¹ Neurometabolic Unit, National Hospital for Neurology and Neurosurgery, Queen Square, London WC1N 3BG, UK; mesfer.shahrani.14@ucl.ac.uk (M.A.S.); s.heales@ucl.ac.uk (S.H.); i.p.hargreaves@ljamu.ac.uk (I.H.)

² Department of Genetics and Genomic Medicine, UCL Great Ormond Street Institute of Child Health, London WC1N 1EH, UK

³ College of Applied Medical Sciences, King Khalid University, Abha 61481, Saudi Arabia

⁴ Chemical Pathology, Great Ormond Street for Children Hospital NHS Foundation Trust, London WC1N 3JH, UK

⁵ School of Pharmacy and Biomolecular Sciences, Liverpool John Moores University, Liverpool L2 2AZ, UK

* Correspondence: m.orford@ucl.ac.uk

Received: 12 October 2017; Accepted: 23 October 2017; Published: 27 October 2017

Abstract: Oxidative stress arises when cellular antioxidant defences become overwhelmed by a surplus generation of reactive oxygen species (ROS). Once this occurs, many cellular biomolecules such as DNA, lipids, and proteins become susceptible to free radical-induced oxidative damage, and this may consequently lead to cellular and ultimately tissue and organ dysfunction. Mitochondria, as well as being a source of ROS, are vulnerable to oxidative stress-induced damage with a number of key biomolecules being the target of oxidative damage by free radicals, including membrane phospholipids, respiratory chain complexes, proteins, and mitochondrial DNA (mt DNA). As a result, a deficit in cellular energy status may occur along with increased electron leakage and partial reduction of oxygen. This in turn may lead to a further increase in ROS production. Oxidative damage to certain mitochondrial biomolecules has been associated with, and implicated in the pathophysiology of a number of diseases. It is the purpose of this review to discuss the impact of such oxidative stress and subsequent damage by reviewing our current knowledge of the pathophysiology of several inherited mitochondrial disorders together with our understanding of perturbations observed in the more commonly acquired neurodegenerative disorders such as Parkinson's disease (PD). Furthermore, the potential use and feasibility of antioxidant therapies as an adjunct to lower the accumulation of damaging oxidative species and hence slow disease progression will also be discussed.

Keywords: mitochondria; oxidative stress; reactive oxygen species; antioxidant

1. Introduction

Up to 90% of cellular metabolic energy is generated by mitochondria via the oxidative phosphorylation pathway [1]. In concert with glycolysis, the tricarboxylic acid (TCA) cycle additionally generates a small amount of energy via substrate level phosphorylation, although the vast proportion of metabolic energy is harnessed via the generation of reducing power and subsequent donation of high energy electron pairs through the electron carriers NADH and FADH₂, which ultimately feed directly into mitochondrial respiratory chain (MRC). The MRC is composed of four multi-subunit proteins; complex I (NADH: ubiquinone reductase; EC 1.6.5.3), complex II (succinate: ubiquinone reductase; EC 1.3.5.1), complex III (ubiquinol: cytochrome c reductase; EC 1.10.2.2), and complex IV (cytochrome c oxidase; EC 1.9.3.1) [2], each of which contain a variety of cofactors such as hemes,

flavins, and iron–sulphur clusters. In addition to these redox cofactors, two mobile electron carriers, namely coenzyme Q₁₀ (ubiquinone) and cytochrome c are involved in transferring electrons between the complexes. As a result of the passage of electrons between chains, protons are pumped out of the mitochondrial matrix and into the intermembrane space, creating a proton-motive force. It is the subsequent dissipation of these protons through the mitochondrial ATPase enzyme which results in the direct phosphorylation of ADP to ATP [3].

It has been well established that the formation of reactive oxygen species (ROS) is a significant component produced during the generation of ATP. Under normal conditions, approximately 1% of total oxygen utilized by the MRC is converted to ROS, although under pathological conditions this may increase dramatically. Mitochondrial ROS, particularly in the form of the superoxide radical ($O_2^{\bullet-}$) is mostly generated either in the matrix from complex I or both in the intermembrane space and matrix from complex III [4]. Mitochondria are additionally a site of nitric oxide (NO) synthesis which in turn may form the peroxynitrite ion ($ONOO^-$) when NO reacts with $O_2^{\bullet-}$, leading to the generation of equally undesirable reactive nitrogen species (RNS) [5]. $O_2^{\bullet-}$ is rapidly removed by conversion to hydrogen peroxide (H_2O_2) either by a manganese-dependent superoxide dismutase (Mn-SOD) or a copper, zinc-dependent superoxide dismutase (Cu, Zn-SOD), and then ultimately reduced to water by glutathione peroxidase (GPx) utilizing the active and reduced form of glutathione (GSH) as a cofactor (Figure 1) [6,7]. A large number of biomolecules have over the years been recognised as potent antioxidants. GSH itself, besides being a cofactor for the enzymatic antioxidant GPx, also serves as non-enzymatic antioxidant by directly removing free radicals as well as other oxidative agents [7]. Similarly, other powerful non-enzymatic antioxidants known to act as potent free radical scavengers include ascorbate (vitamin C) [8], α -tocopherol (vitamin E) [9], ubiquinol-10, the reduced form coenzyme Q₁₀ [10], α -lipoic acid (ALA) [11], and carotenoids (β -carotene) [12].

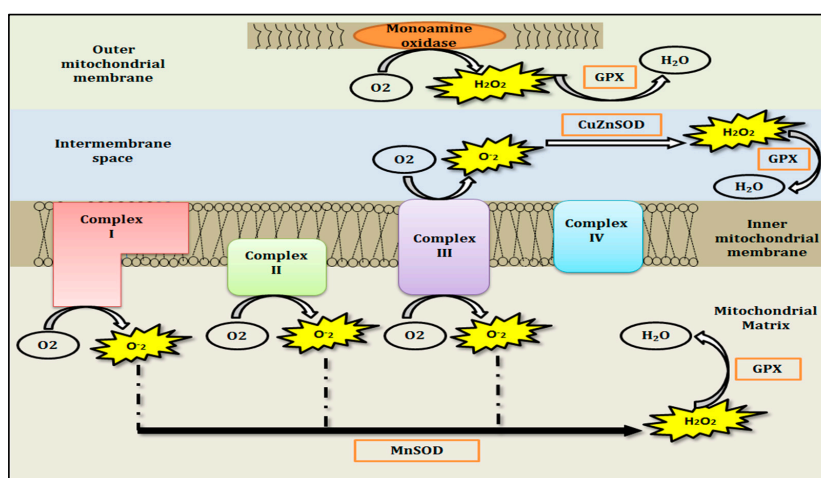


Figure 1. A schematic underlies the pathway of mitochondrial free radical generation and their enzymatic antioxidant defences. The mitochondrial $O_2^{\bullet-}$ is subsequently converted to H_2O_2 either by manganese-dependent superoxide dismutase (Mn-SOD) or copper, zinc-dependent superoxide dismutase (Cu, Zn-SOD), and then ultimately reduced to water by glutathione peroxidase (GPx).

It is the uncontrolled or overproduction of ROS (oxidative stress) or RNS (nitrosative stress) which can indiscriminately cause damage to cellular molecules, including DNA, proteins and lipids [13]. Furthermore, it is believed that the accumulation of these free radical species, resulting in oxidative/nitrosative stress, could lead to impaired MRC function and this in turn may be a major contributory factor to the pathophysiology of various inherited and acquired disorders [14,15].

In this review, the potential impact of oxidative stress and subsequent molecular and cellular damage will be discussed, including lessons learnt from our knowledge of the pathophysiology

of a number of inherited mitochondrial disorders together with our growing understanding of perturbations observed in the more commonly acquired neurodegenerative disorders. Furthermore, we will consider the potential use of antioxidant therapies as an adjunct to standard pharmacological care as a means to limit free radical accumulation and thereby attempt to slow disease progression.

2. Inherited Mitochondrial Disorders

2.1. Inherited Mitochondrial DNA (mtDNA) Disorders

Inherited mitochondrial disorders are generally believed to be one of the most common inborn errors of metabolism, with an overall birth prevalence of about 1:5000 [3], with those resulting from mitochondrial DNA (mtDNA) mutations estimated at about 1:8000 [16]. Furthermore, mtDNA mutations are rare in children, accounting for less than 10% of all mitochondrial disorders affecting infants [17]. At least 200 pathogenic point mutations affecting the mtDNA-encoded MRC complexes I, III, and IV as well as tRNAs have recently been reported [18]. In comparison with nuclear-DNA (nDNA), mtDNA is particularly vulnerable to oxidative damage since it lacks protective histones and has limited repair mechanisms, as well as being located in close proximity to the MRC which is known to be the major source of ROS generation in the cell [19,20]. Therefore, mtDNA has a potentially higher mutation rate than nDNA. A unifying hypothesis, known as “mitochondrial catastrophe”, postulates that the accumulation of mtDNA lesions results in a decline in MRC function, which in turn, leads to the generation of further ROS, and eventually cell death [21]. This phenomenon therefore provides an insightful working hypothesis that oxidative stress could be considered as a major cause of rather than as a consequence of mtDNA disorders.

Leber’s hereditary optic neuropathy (LHON) (OMIM 540000) is one of the most well-known inherited mtDNA disorders. It is caused in most cases by three mtDNA point mutations within MRC complex I subunits [22] and results predominantly in visual loss as the main clinical feature [23]. The aetiology of oxidative stress in the mechanism of LHON disorder has been described [24,25]. It is worth emphasizing that MRC complex I is one of the major sources of ROS generation, predominately in the form of $O^{\bullet 2}$, and it is this reactive species that is implicated to have significant effects in some, if not all of LHON disorders [26]. The inhibition of MRC complex I causes a significant increase in oxidative stress, which in turn promotes apoptosis and cell death. [27]. A recent study of patients with LHON demonstrated an increase in plasma free radical formation as well as a reduction in antioxidant levels compared to controls [28]. In addition to a reduction of MRC complex I activity and consequential increased $O^{\bullet 2}$ levels, increases in protein carbonyl, and lipid peroxidation have also been reported in mutant mitochondrially encoded NADH dehydrogenase 6 (MT-ND6) subunit of MRC complex I. However, the mitochondrial antioxidant enzymes Mn-SOD and GPX were not altered in this study, suggesting that the mutation threshold might not be significant [29]. Interestingly, increased lipid peroxidation and raised levels of the potent oxidant hydroxyl radical (OH^{\bullet}) together with an elevation in the activity of both Mn-SOD and Cu, Zn-SOD have also been observed [30]. Consistent with this, increased levels of chemical ROS markers have been demonstrated in LHON neurons [31] as well as the marker of oxidative DNA damage, 8-hydroxy-2'-deoxyguanosine (8-OHdG), being elevated in white blood cells of LHON patients [32]. It should be further noted that in addition to endogenous ROS production, exogenous ROS sources such as those contained in tobacco smoke have also been linked to the onset of LHON disorders [33], thereby strengthening the evidence of ROS-mediated events.

2.2. An Inherited Mitochondrial Lipid Disorder

Barth syndrome (BTHS) (OMIM 302060), is a rare X-linked genetic disorder, characterized by cardiomyopathy, neutropenia, skeletal weakness, and growth disorders [34]. In fact, it has been previously described as a mitochondrial disorder as BTHS patients show symptoms consistent with known mitochondrial disorders [35]. It is mainly caused by a mutation in the tafazzin (*TAZ*) gene,

which encodes a putative enzyme acyltransferase, an enzyme largely responsible for enzymatic remodelling of cardiolipin (CL) [36]. CL is a phospholipid component found exclusively within the inner mitochondrial membrane (IMM) and constitutes approximately 25% of the total lipid contents in mitochondria [37]. It plays a crucial role in aspects of maintaining the functional properties of mitochondrial components [38]. For example, it is required for the enhancement of the enzymatic function of the MRC complexes following CL binding [39] and its molecular interaction with all individual respiratory complexes is necessary for their assembly into super-complexes [40]. CL also plays an essential role in the retention of cytochrome *c* which protects against apoptosis [41].

The biochemical findings following MRC enzyme studies in 1983 by Barth together with other groups have indicated evidence of multiple MRC defects [42]. However, results are somewhat conflicting, suggesting the possibility that primary MRC deficiency may result in a secondary loss of other MRC activities. This latter possibility was previously been investigated in human astrocytoma cells by Hargreaves et al. in 2007 where a pharmacologically-induced MRC complex IV deficiency was found to result in a secondary loss of MRC complex II–III activity due to the progressive nature of MRC defects [43]. Interestingly, loss of CL content has been associated with mtDNA instability [44] suggesting another possible mechanism that the dysfunctional MRC encoded by mtDNA may be the consequence of oxidative damage as mtDNA structurally lacks protective histones [45]. Increased ROS levels have evidently been implicated in the TAZ mutation seen in cardiomyopathy which is a hallmark clinical feature of BTHS syndrome [46]. It is worth highlighting that CL is a susceptible target for oxidative damage for the following reasons: (1) CL has a naturally high unsaturated content, which is easily attacked by free radical species; (2) It is involved in the structural assembly of the MRC, a major intracellular site for ROS production; and (3) In addition to CL peroxidation, calcium-mediated detachment of cytochrome *c* from CL is induced by generating further ROS levels and this results in apoptotic cell death.

2.3. An Inherited Mitochondrial Protein Disorder

Friedreich ataxia (FRDA) (OMIM 229300), is a progressive neurodegenerative disorder with an autosomal recessive mode of inheritance, affecting roughly 1:50,000 live births [47]. In addition to neuronal injury in the dorsal root ganglia (DRG) and sensory peripheral nerves, FRDA patients also manifest with non-neurological symptoms including diabetes, cardiomegaly, and muscle weakness [48]. FRDA is caused by a GAA expansion in the frataxin gene, the product of which is predominantly located in mitochondria [49]. The exact role of the frataxin protein is not yet fully understood. However, it has been proposed to play crucial roles primarily in regulating iron machinery, and functioning as a mitochondrial Fe–S cluster chaperone [50,51]. In this regard, increased iron capacity and the loss of activity of mitochondrial Fe–S cluster-containing enzymes has been observed in FRDA patients, highlighting the important function of frataxin in iron metabolism [47,49,52]. In addition to its well-established role in iron metabolism, frataxin can protect against iron-mediated oxidative stress [53]. In a previous study, exposure of fibroblast obtained from patients with FRDA to ferrous ions and H₂O₂ reduced the viability of the cells compared to control patients [54]. The most direct evidence of the critical function of frataxin in protecting against oxidative stress however comes from the observation of a combined reduction in activity of nuclear factor E2-related factor 2 (Nrf2) and GSH levels in the YG8R mouse model of FRDA [55]. In contrast, an increased resistance to oxidative stress induced by the overexpression of mitochondrial frataxin has been reported in *Drosophila* [56]. Since the discovery of the gene in 1996, dysfunction of mitochondrial Fe–S cluster-containing enzymes including MRC complexes I and III as well as aconitase resulting in oxidative stress has been found to make a major contribution to the pathophysiology of FRDA [57].

Aconitase (EC 4.2.1.3) is a multi-domain enzyme, containing a closely associated iron–sulphur cluster, and exists in two slightly different structural forms: an active [4Fe-4S]²⁺ and an inactive [3Fe-4S]¹⁺ cluster [58]. The active form of aconitase is highly sensitive to oxidation by the superoxide anion, which in turn, converts it to the inactive form. This oxidation reaction is accompanied

by the release of a ferrous ion, which subsequently contributes to the generation of OH^\bullet via the Fenton reaction [59]. As a consequence, oxidative damage to mtDNA, lipids, and proteins may occur [60]. Since the aconitase enzyme is susceptible to direct attack by free radicals, it has been recognized as an oxidative stress marker in mitochondria, suggesting it may function as a mitochondrial redox sensor [61]. Aconitase exists in two isoenzyme forms in mammalian cells: the mitochondrial aconitase (m-aconitase), and cytosolic aconitase (c-aconitase), which both enzymatically catalyse the isomerization of citrate to isocitrate. In addition to its role in the TCA cycle, c-aconitase, also known as iron-responsive protein-1 (IRP1) additionally performs a dual role in the regulation of iron homeostasis through binding to iron-responsive elements (IREs) and controlling cellular iron levels [62]. Despite the m-aconitase being identical in function (with 25% sequence homology identity) to that of c-aconitase, it is clearly not recognized to have role as an IRP [63]. However, the brain is highly dependent on m-aconitase activity [64], and is regulated by a 5'IRE in its mRNA [65]. As a consequence of inactivation of m-aconitase; neurons could be highly vulnerable to free radical attack and subsequent iron overload, resulting in a dramatic increase in oxidative stress [66]. Due to its important role in TCA cycle energy metabolism, dysfunction of aconitase may consequently lead to TCA cycle impairment, a deficit in MRC activity, and a decline in ATP production, which in turn, could lead to subsequent accumulation of ROS generation, and resultant oxidative damage (Figure 2) [67].

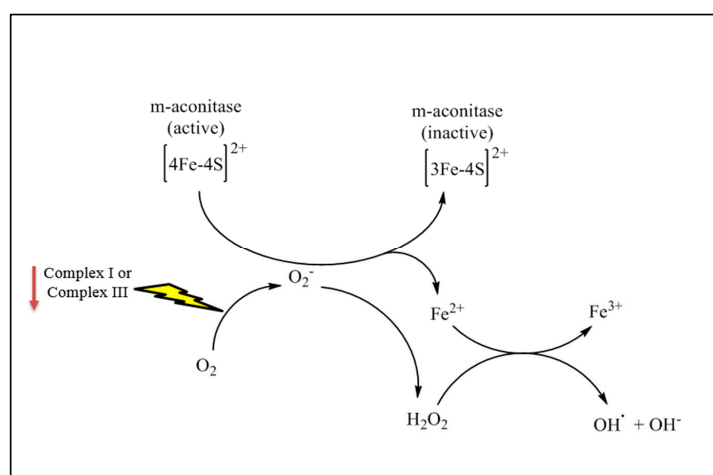


Figure 2. A potential mechanism for the oxidative inactivation of m-aconitase by mitochondrial O_2^- . This oxidation reaction is accompanied by the release of a ferrous ion, which subsequently contributes to the generation of OH^\bullet via Fenton reaction. This scenario could consequently lead to an impairment of tricarboxylic acid (TCA) cycle capacity, a deficit in mitochondrial respiratory chain (MRC) activity, and a decline in ATP production, which in turn, leads to further oxidative damage.

3. Parkinson's Disease (PD)

PD is a chronic and progressive neurological disorder. It is currently ranked as the second most common neuromuscular disorder after Alzheimer's disease, affecting roughly 1% of people almost exclusively in the over 60 age group [68]. Furthermore, the male sex is particularly susceptible to this disorder, with larger proportion of men being affected than women [69]. Clinically, PD patients commonly experience motor symptoms such as bradykinesia, tremor (particularly in the hands and/or arms), muscle stiffness (rigidity), and postural instability [70]. During later stages of the disorder, non-motor symptoms may manifest such as depression, sleep disturbances, anxiety, constipation, and in some cases dementia. Despite receiving intensive research interest over several decades and in particular with a large focus on the mechanistic aspects of PD, the exact aetiological mechanism is still poorly understood. Under normal conditions, the neurotransmitter dopamine (DA) is produced in the substantia nigra pars compacta (SNpc). However, a typical and major characteristic feature of PD is a significant depletion in its levels. The formation of intracytoplasmic eosinophilic inclusions, known

as Lewy bodies (LBs), is another pathological sign of PD observed in a majority, but not all PD cases [71]. For several decades, it was postulated that PD is likely caused by environmental factors, until 1997 when the autosomal dominant mutation in the alpha-synuclein (*SNCA*) gene was discovered [72]. Since this discovery, at least five other mutant genes that are linked to familial PD, including *parkin*, PTEN-induced putative kinase 1 (*PINK1*), *DJ-1*, High temperature requirement protein A2 (*HTRA2*), and leucine-rich-repeat kinase 2 (*LRRK2*) have also been identified [73]. These gene products appear to be in part localized to mitochondria and therefore may contribute towards mitochondrial dysfunction and oxidative stress [73].

Evidence of MRC dysfunction in PD emerged in the early 1980s following the intravenous injection of 1-methyl-4-phenyl-1,2,3,4-tetrahydropyridine (MPTP) by drug abusers, producing the neurotoxin 1-methyl-4-phenylpyridinium (MPP⁺) via the monoamine oxidase-B (MAO-B) enzyme, which consequently induced Parkinson-like symptoms [72]. Similarly, in animal models, rats and primates were shown to share Parkinson-like symptoms following the administration of MPTP [74]. In parallel with MPTP, a chronic low-dose infusion of rotenone to rats additionally induced similar features of Parkinson disorders [75]. Taken together, these MRC complex I inhibitors have become widely used to create PD models to investigate the pathogenesis and therapeutic approaches for this disorder. Further studies conducted to support the role of mitochondrial dysfunctions have shown strong links to the aetiopathogenesis of PD. Studies of post-mortem PD patient brain tissue demonstrated MRC complex I deficiency in the substantia nigra and frontal cortex [76]. Consistent with these findings, MRC complex I deficiency was also shown in platelets [77] and skeletal muscle [78] from individuals with PD. In this context, it seems that a reduction of MRC complex I activity is systemic, thereby simultaneously affecting many tissues. In addition to a decrease in the activity of MRC complex I, a reduction in MRC complex III activity was further demonstrated in lymphocytes and platelets in patients with PD [79]. Remarkably, loss of MRC complex III activity may contribute to the impairment in function of MRC complex I since the stability of MRC complex I is evidently dependent on a correctly assembled MRC complex III [80]. Taken together, inhibition of MRC complex I and III can have devastating consequences, leading to excessive free radical species generation, oxidative stress and subsequent depletion of ATP levels, elevated intracellular calcium levels, excitotoxicity, and ultimately enhanced cell death (Figure 3) [81].

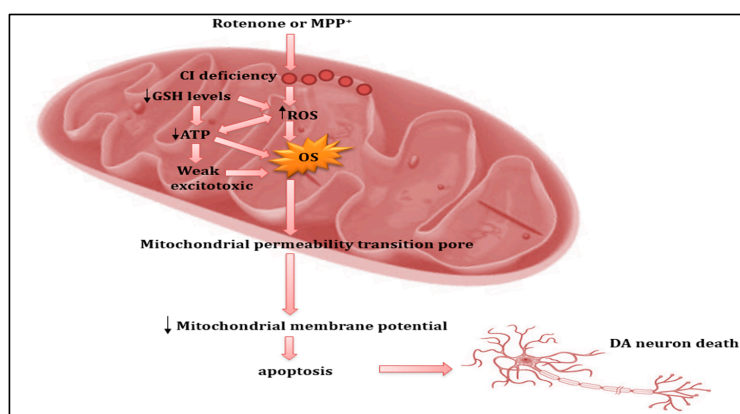


Figure 3. A schematic showing the role of mitochondrial dysfunction in the pathogenesis of Parkinson's disease (PD). Neurotoxins, such as rotenone or 1-methyl-4-phenylpyridinium (MPP⁺) elicit MRC complex I deficiency, and subsequently generate reactive oxygen species (ROS), reducing levels of the antioxidant glutathione (GSH), with resulting oxidative stress. Oxidative stress induces mitochondrial permeability by transiently opening a pore, which subsequently causes depolarization of the mitochondrial membrane potential. These events ultimately lead to neural cell death via the release of pro-apoptotic mitochondrial proteins, including cytochrome *c* and apoptosis-initiating factor. DA: dopamine.

Any discussion would be incomplete without a reference to the interplay of iron and its contribution to mitochondrial dysfunction. Amongst all transition metals, iron is considered to be the most abundant metal in the brain, predominately in the basal ganglia [82]. It significantly contributes to the proper functioning of neurotransmitters, myelination, and mitochondria [83,84]. Brain iron metabolism is primarily regulated by transferrin and ferritin [85]. It is commonly conjugated into iron–sulphur clusters in many proteins, which have the potential ability to accept or donate electrons, particularly in the MRC pathway [86]. The evidence supporting the alteration of the iron metabolism in the neuropathology of PD is also overwhelming [87–90]. In fact, the potential mitochondrial ROS toxicity due to a defect in MRC complex I activity has been widely demonstrated in PD models [91]. Nevertheless, the exact mechanism of whether an enhanced production of ROS-induced neuronal injury is yet to be fully elucidated. Neurotoxins such the product of MPTP metabolism, commonly used to create PD models [72,75,91], have been utilized to demonstrate the potential harmful effects of the inactivation m-aconitase and high amounts of iron content on dopaminergic neurons [92]. In mice, this neurotoxin has been linked to the inactivation of m-aconitase, an increase in iron content, and a depletion of DA level [93].

It appears that excess ROS production is a common denominator of these cascades. Iron and iron derivatives contribute to the generation of the most active OH^\bullet via the Fenton reaction, which in conjunction with DA autoxidation may further enhance oxidative stress, leading to degeneration of dopaminergic neurons (Figure 4) [94–96]. Post-mortem brain tissue from PD patients exhibited accumulation of iron content, which together with a reduction in the glutathione redox ratio of reduced glutathione/oxidized glutathione (GSH/GSSG) is a potential indicator of oxidative stress [96,97]. In the glutathione-depleted Δgsh1 cell model, on the other hand, the mitochondrial (Fe–S) cluster was unaffected, suggesting that m-aconitase is resistant to oxidative stress [98]. Furthermore, accumulation of iron was found to potentiate LB formation in the substantia nigra of PD patients, supporting the link between iron-mediated oxidative stress and the degeneration of dopaminergic neurons in PD [99].

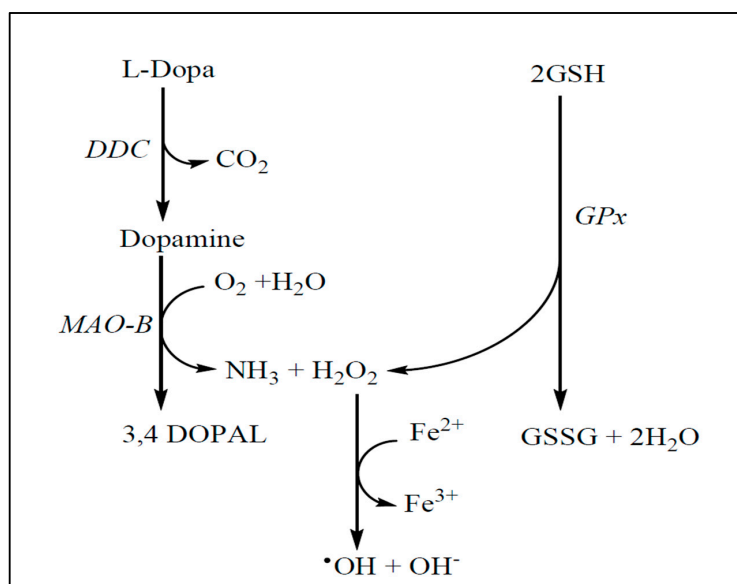


Figure 4. A potential mechanism of dopamine metabolism and OH^\bullet radical formation in the striatum of PD patients as a consequence of iron accumulation and decline in GSH levels. DDC: dopa decarboxylase; 3,4 DOPAL: 3,4-dihydroxyphenylacetaldehyde.

4. The Role of Antioxidants in the Prevention of Oxidative Damage

Despite extensive research to elucidate the underlying mechanism of mitochondrial dysfunction in various conditions, there is no currently satisfactory treatment available. According to our recent

understanding and knowledge regarding the mechanisms of mitochondrial dysfunction, it is however without doubt that mitochondrial free radical-induced oxidative damage is a plausible pathogenic facilitator in both inherited and acquired mitochondrial disorders. Alleviation of ROS/RNS free radical-mediated oxidative stress and increased availability of ATP by antioxidants could be effective therapeutic approaches to restore mitochondrial function, or at least to limit the progression of symptoms in a tremendous number of patients with mitochondrial dysfunction.

To limit free radical-induced oxidative stress, the human body is endowed with a variety of enzymatic and non-enzymatic antioxidant defence mechanisms. The two major antioxidants that protect the cell from ROS and RNS are GSH and coenzyme Q₁₀ [10,100,101]. By cooperative actions, the primary function of the antioxidants is to scavenge and eliminate harmful ROS/RNS free radicals, thereby minimizing or delaying mitochondrial damage and enhancing mitochondrial bioenergetics.

4.1. Glutathione (GSH)

The tripeptide GSH, is a major intracellular thiol-dependent antioxidant, which protects the cellular components from free radical-induced oxidative damage [102]. Consequently, a compromised cellular GSH status results in increased production of ROS and RNS [100,101]. Despite being predominantly localised in the cytosol, GSH is also present in other intracellular organelles including, mitochondria, the nucleus, and the endoplasmic reticulum [102]. It exists in two forms: a reduced (GSH) and oxidized disulphide form (GSSG), with the ratio of reduced to oxidized forms being a key indicator of OS. In addition to its vital antioxidant role, GSH also serves as a substrate for other antioxidant defences including GPx, glutaredoxin (GRX), and thioredoxin (Trx) as well as maintaining vitamins C and E to be functionally active [7]. Accumulating evidence suggests that the depletion of GSH is associated with MRC defects [103,104]. The reduction of MRC complex I activity, followed by a depletion in GSH, has been reported previously [105]. Interestingly, results from our group have recently shown that GSH levels were significantly decreased in skeletal muscle from patients with MRC defects, compared to the control group [106]. Furthermore, patients with multiple MRC defects exhibited marked reductions in GSH levels, suggesting that oxidative stress may contribute to the pathophysiology of MRC disorders. In neurological disorders, particularly PD, it is thought that GSH depletion could be an early common event in PD pathogenesis before any significant impairment of MRC complex I and iron metabolism occur [107]. With regards to the latter however, it is uncertain whether this depletion occurs as a consequence of decreased ATP availability (required for GSH biosynthesis) or is due to increased ROS levels. Thus, the replenishment of cellular GSH could hold a promising therapeutic avenue for patients with inherited or acquired mitochondrial disorders. In rat brain, the GSH ethyl ester (GEE) derivative has been subcutaneously administered to enhance GSH levels. However, elevated brain levels were only evident post-administration directly to the left cerebral ventricle [108]. Furthermore, following co-administration with neurotoxin MPP⁺, GGE has been demonstrated to partially protect dopaminergic neuron against neurotoxicity. However, complete protection was only achieved only after pre-treating with GEE [108]. As cysteine is a major component in GSH, it hinders GSH passage across the blood–brain barrier (BBB). For this reason, the modified *N*-acetyl cysteine (NAC) form, has been effectively utilized due to its increased ability to penetrate the BBB [109]. As such, it has also been shown to restore GSH level and consequently ameliorate free radical-induced oxidative stress [110]. Encouragingly, lesions in dopaminergic tissue have been reduced by approximately 30%, following administration with NAC, suggesting it is able to provide neuroprotection [111].

4.2. Coenzyme Q₁₀

For many years, the clinical use of coenzyme Q₁₀ or ubiquinone and its quinone analogues has been proven to be effective for treatment of mitochondrial disorders due to their capacity to augment electron transfer in the MRC, increase ATP, and enhance mitochondrial antioxidant activity, which in turn, can ameliorate the harmful effects of ROS [112]. In addition to its function as an electron carrier

in the MRC pathway, Coenzyme Q₁₀ also serves as a powerful free radical-scavenging antioxidant. The reduced ubiquinol form of coenzyme Q₁₀ serves this function [113].

The therapeutic potential of coenzyme Q₁₀ in the treatment of mitochondrial disorders took the spotlight in 1985 after Ogashara and colleagues reported sustained improvements in the clinical phenotype of patients with Kearns–Sayre syndrome (KSS) following administration with coenzyme Q₁₀ [114]. More recently, Maldergem also reported that coenzyme Q₁₀ therapy was beneficial to two sisters diagnosed with Leigh’s encephalopathy [115]. Remarkably, the beneficial effects of CoQ₁₀ in two patients with KSS and hypoparathyroidism were also shown to help maintain calcium levels in the serum of both patients, suggesting that treatment with coenzyme Q₁₀ restored the capacity of calcitriol, a hormone located in the mitochondria of proximal renal tubules [116]. Some degree of sustained improvement has been noted with some patients whose clinical features can be associated with mitochondrial disorders, such as ataxia, muscle stiffness, and exercise intolerance following implementation of coenzyme Q₁₀ therapy [114]. Despite the oral coenzyme Q₁₀ supplementation being significantly effective in patients with all forms of coenzyme Q₁₀ deficiency, it has been shown to be only partially effective in patients who present with neurological symptoms, suggesting that these sequelae may be somewhat refractory to coenzyme Q₁₀ supplementation [117]. The efficacy of the synthetic ubiquinone analogues such as idebenone has been reported in patients with mitochondrial disorders including, LOHN, FRDA, and MELAS (mitochondrial encephalomyopathy, lactic acidosis and stroke like episodes) [118,119]. It has also been recommended that patients with deficient levels of coenzyme Q₁₀ should be given coenzyme Q₁₀ supplementation rather than idebenone since the synthetic analogue is not a potential replacement for coenzyme Q₁₀ in the MRC [120]. However, in addition to its beneficial effects, idebenone may reduce MRC complex I activity, thereby affecting the mitochondrial bioenergetics function [121]. Hence, further clinical studies regarding the overall benefits of idebenone need to be conducted to address this issue.

Both the impairment of mitochondrial function and oxidative stress have been potentially linked to neurodegenerative pathogenesis, particularly in PD. Strategies to enhance mitochondrial function and suppress oxidative stress may therefore contribute to the development of novel therapies for PD. As coenzyme Q₁₀ performs two roles, one in mitochondrial energy metabolism and the other as a free-radical scavenger, low levels of coenzyme Q₁₀ may therefore result in the impairment of the MRC activities as well as in the accumulation of ROS levels, and thereby contribute towards the pathogenesis of PD. Coenzyme Q₁₀ deficiency associated with PD has been previously described [122,123]. A reduction in coenzyme Q₁₀ level was demonstrated in the plasma [124] and platelets [125] in patients with PD, thereby suggesting that systemic effects may be important. For the first time, a UK study demonstrated that coenzyme Q₁₀ levels were lower in the brain cortex of patients with PD [123]. The neuroprotective role of coenzyme Q₁₀ has also been investigated in both animal and human cell models [126–128]. Using in vitro models of PD, coenzyme Q₁₀ has been reported to protect dopaminergic neurons against neurotoxin-induced PD symptoms using either rotenone, paraquat or MPP⁺ [129]. Another study has shown that coenzyme Q₁₀ treatment improved both MRC complex I and complex IV activities in skin fibroblast from PD patients [128]. To investigate the neuroprotective potential of coenzyme Q₁₀ treatment in PD, 80 patients with early stage PD were randomly allocated to participate in a 16-month multicentre clinical trial [130]. Results showed that participants who received high doses of coenzyme Q₁₀ had a large improvement in their motor functions, whilst lower doses only provided mild benefits. It was therefore concluded that the beneficial effect of coenzyme Q₁₀ treatment may contribute to a reduction in the progression of PD.

4.3. Other Antioxidants

There is a considerable body of scientific literature which focuses on the beneficial effects of other antioxidants, including vitamins C and E, creatine, α -lipoic acid, urate, melatonin, and their derivatives as potential mediators in treating mitochondrial disorders [131–134]. Many patients with mitochondrial dysfunction, however, have not shown any significant clinical improvements when

treated with these antioxidants alone. However, it could be hypothesized that in combination, a cocktail therapy may improve mitochondrial conditions to an extent not seen previously with a single antioxidant agent. Several recent studies have also demonstrated some initial promise in the use of mitochondrial-targeted antioxidants with different modes of action to provide additional beneficial effects, such as mitoquinone (MitoQ) and mitotocopherol (MitoVitE) [135]. However, these compounds need to be further investigated to evaluate their full efficacy and safety as potential therapeutic treatments for mitochondrial disorders.

4.4. Ketogenic Diet (KD)

The KD, in its various forms, has successfully been used to treat patients with pharmaco-resistant epilepsy [136–138]. Whilst the exact mechanism with regards to how the diet exerts its efficacy is not known, there is growing evidence that, in part, this may occur as result of stimulation of mitochondrial biogenesis [139]. This raises the possibility of use in patients with acquired and inherited mitochondrial disorders. Recently, we have shown that a component of the medium chain triglyceride KD, decanoic acid (C10), stimulates mitochondrial biogenesis and increases MRC complex I activity and antioxidant status in neuronal cells [140]. Furthermore, cells from patients with MRC complex I deficiency have, in some cases, been shown to respond positively to C10 exposure [141].

5. Conclusion Remarks

As highlighted in this review, free radical-induced oxidative damage to the biomolecules of the mitochondria are intrinsically linked to the pathophysiology of a number of disorders (see summary in Figure 5). Despite the number of markers available to determine evidence of oxidative stress together with its pathological consequences, few clinical centres as yet include the determination of this parameter as part of the diagnostic algorithm of patient evaluation. Furthermore, in view of the vulnerability of mitochondrial biomolecules to oxidative damage by ROS or RNS, therapeutic strategies should be targeted the free radical threshold [13] and the molecular structure targeted by these radicals. Recent advances using mitochondrial-targeted antioxidants and dietary modification may hold potential promise to provide therapeutic benefit for patients with oxidative stress-associated disorders.

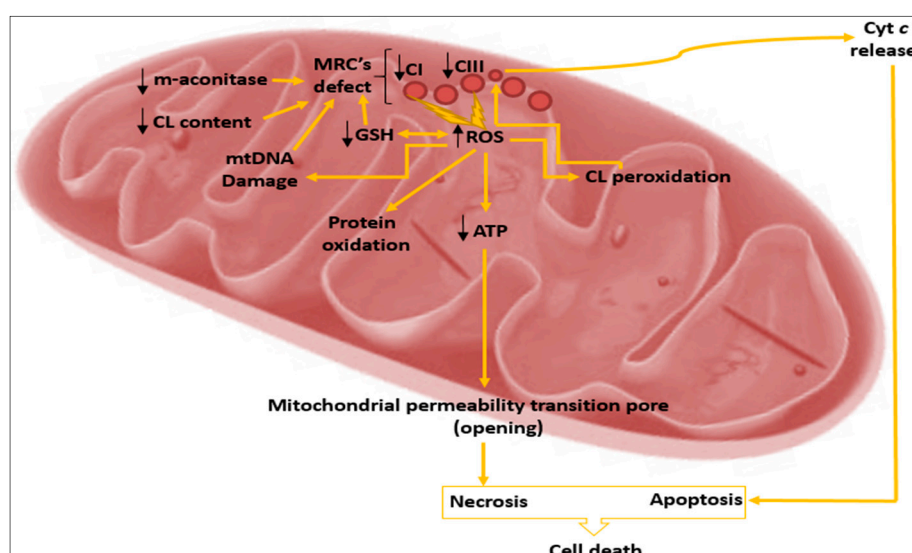


Figure 5. A summary of oxidative stress-induced mitochondrial damage is a common mechanistic link in the pathogenesis of inherited mitochondrial disorders and PD. CL: cardiolipin; mtDNA: mitochondrial DNA.

Acknowledgments: M.A.S. acknowledges support from the King Khalid University (Abha, Saudi Arabia). M.O. is in receipt of funding from the National Institute for Health Research UK (NIHR). M.O. and S.J.R.H. both acknowledge support from Great Ormond Street NIHR Research Centre.

Conflicts of Interest: The authors declare no conflict of interest.

Abbreviations

ROS	Reactive oxygen species
PD	Parkinson's disease
MRC	Mitochondrial respiratory chain
GPx	Glutathione peroxidase
GSH	Reduced glutathione
CL	Cardiolipin
mtDNA	Mitochondrial DNA
LHON	Leber's hereditary optic neuropathy
BTHS	Barth syndrome
FRDA	Friedreich ataxia
MPTP	1-methyl-4-phenyl-1,2,3,4-tetrahydropyridine

References

- Brealey, D.; Brand, M.; Hargreaves, I.; Heales, S.; Land, J.; Smolenski, R.; Dnavies, N.; Cooper, C.; Singer, M. Association between Mitochondrial Dysfunction and Severity and Outcome of Septic Shock. *Lancet* **2002**, *360*, 219–223. [[CrossRef](#)]
- Land, J.; Hughes, J.; Hargreaves, I.; Heales, S. Mitochondrial disease: A historical, biochemical, and London perspective. *Neurochem. Res.* **2004**, *29*, 483–491. [[CrossRef](#)] [[PubMed](#)]
- Hargreaves, I.; Al Shahrani, M.; Wainwright, L.; Heales, S. Drug-Induced Mitochondrial Toxicity. *Drug Saf.* **2016**, *39*, 661–674. [[CrossRef](#)] [[PubMed](#)]
- Chen, O.; Vazquez, E.; Moghaddas, S.; Hoppel, C.; Lesnefsky, E. Production of Reactive Oxygen Species by Mitochondria: Central Role of Complex III. *J. Biol. Chem.* **2003**, *278*, 36027–36031. [[CrossRef](#)] [[PubMed](#)]
- Heales, S.; Bolanos, J.; Stewart, V.; Brookes, P.; Land, J.; Clark, J. Nitric Oxide, Mitochondria and Neurological Disease. *Biochim. Biophys. Acta Bioenerg.* **1999**, *1410*, 215–228. [[CrossRef](#)]
- Turrens, J. Mitochondrial Formation of Reactive Oxygen Species. *J. Physiol.* **2003**, *552*, 335–344. [[CrossRef](#)] [[PubMed](#)]
- Birben, E.; Sahiner, U.; Sackesen, C.; Erzurum, S.; Kalayci, O. Oxidative Stress and Antioxidant Defense. *World Allergy Organ. J.* **2012**, *5*, 9–19. [[CrossRef](#)] [[PubMed](#)]
- Bunker, V. Free radicals, antioxidants and ageing. *Med. Lab. Sci.* **1992**, *49*, 299–312. [[PubMed](#)]
- White, E.; Shannon, J.; Patterson, R. Relationship between Vitamin and Calcium Supplement Use and Colon Cancer. *Cancer Epidemiol. Biomark. Prev.* **1997**, *6*, 769–774.
- Duberley, K.; Heales, S.; Abramov, A.; Chalasani, A.; Land, J.; Rahman, S.; Hargreaves, I. Effect of Coenzyme Q₁₀ Supplementation on Mitochondrial Electron Transport Chain Activity and Mitochondrial Oxidative Stress in Coenzyme Q₁₀ Deficient Human Neuronal Cells. *Int. J. Biochem. Cell Biol.* **2014**, *50*, 60–63. [[CrossRef](#)] [[PubMed](#)]
- Smith, A.; Shenvi, S.; Widlansky, M.; Suh, J.; Hagen, T. Lipoic Acid as a Potential Therapy for Chronic Diseases Associated with Oxidative Stress. *Curr. Med. Chem.* **2004**, *11*, 1135–1146. [[CrossRef](#)] [[PubMed](#)]
- Fiedor, J.; Burda, K. Potential Role of Carotenoids as Antioxidants in Human Health and Disease. *Nutrients* **2014**, *6*, 466–488. [[CrossRef](#)] [[PubMed](#)]
- Jacobson, J.; Duchon, M.; Hothersall, J.; Clark, J.; Heales, S. Induction of Mitochondrial Oxidative Stress in Astrocytes by Nitric Oxide Precedes Disruption of Energy Metabolism. *J. Neurochem.* **2005**, *95*, 388–395. [[CrossRef](#)] [[PubMed](#)]
- Hayashi, G.; Cortopassi, G. Oxidative Stress in Inherited Mitochondrial Disease. *Free Radic. Biol. Med.* **2015**, *88*, 10–17. [[CrossRef](#)] [[PubMed](#)]
- Stewart, V.; Heales, S. Nitric Oxide-Induced Mitochondrial Dysfunction: Implication for Neurodegeneration. *Free Radic. Biol. Med.* **2003**, *34*, 287–303. [[CrossRef](#)]

16. Chinnery, P.; Johnson, M.; Wardell, T.; Singh-Kler, R.; Hayes, C.; Taylor, R.; Bindoff, L.; Turnbull, D. The Epidemiology of Pathogenic Mitochondrial DNA Mutations. *Ann. Neurol.* **2000**, *48*, 188–193. [[CrossRef](#)]
17. Lamont, P.; Surtees, R.; Woodward, C.; Leonard, J.; Wood, N.; Harding, A. Clinical and Laboratory Findings in Referrals for Mitochondrial DNA Analysis. *Arch. Dis. Child.* **1998**, *79*, 22–27. [[CrossRef](#)] [[PubMed](#)]
18. Gillis, L.; Sokol, R. Gastrointestinal Manifestation of Mitochondrial Disease. *Gastroenterol. Clin. N. Am.* **2003**, *32*, 789–817. [[CrossRef](#)]
19. Sykora, P.; Wilson, D.; Bohr, V. Repair of Persistent Strand Breaks in the Mitochondrial Genome. *Mech. Aging Dev.* **2012**, *133*, 169–175. [[CrossRef](#)] [[PubMed](#)]
20. Cline, S. Mitochondrial DNA Damage and Its Consequences for Mitochondrial Gene Expression. *Biochim. Biophys. Acta Bioenerg.* **2012**, *1819*, 979–991. [[CrossRef](#)] [[PubMed](#)]
21. Leeuwenburgh, C.; Hiona, A. The Role Mitochondrial DNA Mutations in Aging and Sarcopenia. *Exp. Gerontol.* **2008**, *43*, 24–33.
22. Huoponen, K.; Vilkki, J.; Aula, P.; Nikoskelainen, E.; Savontaus, M. A New mtDNA Mutation Associated with Leber Hereditary Optic Neuroretinopathy. *Am. J. Hum. Genet.* **1991**, *48*, 1147–1153. [[PubMed](#)]
23. Sadun, A.; Morgia, C.; Carelli, V. Leber Hereditary Optic Neuroopathy. *Curr. Treat. Options Neurol.* **2011**, *13*, 109–117. [[CrossRef](#)] [[PubMed](#)]
24. Battisti, C.; Formichi, P.; Cardaioli, E.; Bianchi, S.; Mangiavacchi, P.; Tripodi, S.; Tosi, P.; Federico, A. Cell Response to Oxidative Stress Induced Apoptosis in Patients with Leber Hereditary Optic Neuroopathy. *J. Neurol. Neurosurg. Psychiatry* **2004**, *75*, 1731–1736. [[CrossRef](#)] [[PubMed](#)]
25. Lin, C.; Sharpley, M.; Fan, W.; Waymire, K.; Sadun, A.; Carelli, F.; Ross-Cisneros, F.; Baci, P.; Sung, E.; McManus, M.; et al. Mouse mtDNA Mutant Model of Leber Hereditary Optic Neuroopathy. *Proc. Natl. Acad. Sci. USA* **2012**, *109*, 20065–20070. [[CrossRef](#)] [[PubMed](#)]
26. Howell, N. Leber Hereditary Optic Neuroopathy: Respiratory Chain Dysfunction and Degeneration of the Optic Nerve. *Vis. Res.* **1998**, *38*, 1495–1504. [[CrossRef](#)]
27. Kirches, E. LHON: Mitochondrial Mutation and More. *Curr. Genom.* **2011**, *12*, 44–54. [[CrossRef](#)] [[PubMed](#)]
28. Wang, Y.; Gu, Y.; Wang, J.; Tong, Y. Oxidative Stress in Chinese Patients with Leber Hereditary Optic Neuroopathy. *J. Int. Med. Res.* **2008**, *36*, 544–550. [[CrossRef](#)] [[PubMed](#)]
29. Gonzalo, R.; Arumi, E.; Llige, D.; Marti, R.; Solano, A.; Montoya, J.; Arenas, J.; Andreu, A. Free Radicals-mediated Damage in Transmitochondrial Cells Harboring the T14487C Mutation in the ND6 Gene of mtDNA. *FEBS Lett.* **2005**, *579*, 6909–6913. [[CrossRef](#)] [[PubMed](#)]
30. Luo, X.; Pitkanen, S.; Kassovska, S.; Robinson, B.; Lehotay. Excessive Formation of Hydroxyl Radicals and Aldehydic Lipid Peroxidation Products in Cultured Skin Fibroblasts From Patients with Complex I Deficiency. *J. Clin. Investig.* **1997**, *99*, 2877–2882. [[CrossRef](#)] [[PubMed](#)]
31. Wong, A.; Cavelier, L.; Collins-Schramm, H.; Seldin, M.; McGrogan, M.; Savontaus, M.; Cortopassi, G. Differentiation-specific Effects of LHON Mutation Introduced into Neuronal NT2 Cells. *Hum. Mol. Genet.* **2002**, *11*, 431–438. [[CrossRef](#)] [[PubMed](#)]
32. Yen, M.; Kao, S.; Wang, A.; Wei, Y. Increased 8 hydroxy 2' deoxyguanosine in Leukocyte DNA in Leber Hereditary Optic Neuroopathy. *Investig. Ophthalmol. Vis. Sci.* **2004**, *45*, 1688–1691. [[CrossRef](#)]
33. Sadun, A.; Carelli, V.; Salomao, S.; Berezovsky, A.; Quiros, P.; Sadun, F.; DeNegri, A.; Andrade, R.; Moraes, M.; Passos, A.; et al. Extensive Investigation of a Large Brazilian Pedigree of 11778/haplogroup J Leber Hereditary Optic Neuroopathy. *Am. J. Ophthalmol.* **2004**, *136*, 231–238. [[CrossRef](#)]
34. Barth, P.; Scholte, H.; Berden, J.; Moorsel, J.; Luyt-Houwen, I.; Veer-Korthof, E.; Harten, J.; Sobotka-Plojhar, M. An X-linked Mitochondrial Disease Affecting Cardiac Muscle, Skeletal Muscle and Neutrophil Leucocytes. *J. Neurol. Sci.* **1983**, *62*, 327–355. [[CrossRef](#)]
35. Jefferies, J. Barth Syndrome. *Am. J. Med. Genet. C Semin. Med. Genet.* **2013**, *163*, 198–205. [[CrossRef](#)] [[PubMed](#)]
36. Barth, P.; Valianpour, F.; Bowen, V.; Lam, J.; Duran, M.; Vaz, F.; Wanders, R. X-linked Cardioskeletal Myopathy and Neutropenia (Barth Syndrome): An Update. *Am. J. Med. Genet.* **2004**, *126*, 349–354. [[CrossRef](#)] [[PubMed](#)]
37. Pope, S.; Land, J.; Heales, J. Oxidative Stress and Mitochondrial Dysfunction in Neurodegeneration; Cardiolipin a Critical Target? *Biochim. Biophys. Acta Bioenerg.* **2008**, *1777*, 794–799. [[CrossRef](#)] [[PubMed](#)]
38. Schlame, M.; Greenberg, R. The role of cardiolipin in The Structural Organization of Mitochondrial Membranes. *Biochim. Biophys. Acta Bioenerg.* **2009**, *1788*, 2080–2083. [[CrossRef](#)] [[PubMed](#)]
39. Paradies, G.; Paradies, V.; Benedictis, V.; Ruggiero, F.; Petrosillo, G. Functional Role of Cardiolipin in Mitochondrial Bioenergetics. *Biochim. Biophys. Acta Bioenerg.* **2014**, *1837*, 408–417. [[CrossRef](#)] [[PubMed](#)]

40. Pfeiffer, K.; Gohil, V.; Stuart, R.; Hunte, C.; Brandt, U.; Greenberg, M.; Schagger, H. Cardiolipin Stabilizes Respiratory Chain Supercomplexes. *J. Biol. Chem.* **2003**, *278*, 52873–52880. [[CrossRef](#)] [[PubMed](#)]
41. Vladimir, G.; Sten, O.; Boris, Z. Multiple Pathways of Cytochrome *c* Release from Mitochondria in Apoptosis. *Biochim. Biophys. Acta Bioenerg.* **2006**, *1757*, 639–647.
42. Barth, P.; Wanders, R.; Vreken, P.; Janssen, E.; Lam, J.; Baas, F. X-linked Cardioskeletal Myopathy and Neutropenia (Barth Syndrome) (MIM 302060). *J. Inher. Metab. Dis.* **1999**, *22*, 555–567. [[CrossRef](#)] [[PubMed](#)]
43. Hargreaves, I.; Duncan, A.; Wu, L.; Agrawal, A.; Land, J.; Heales, S. Inhibition of Mitochondrial Complex IV Leads to Secondary Loss Complex II–III Activity: Implication for the Pathogenesis and Treatment of Mitochondrial Encephalomyopathies. *Mitochondrion* **2007**, *7*, 284–287. [[CrossRef](#)] [[PubMed](#)]
44. Martinez, L.; Forni, M.; Santos, V.; Pinto, N.; Kowaltowski, A. Cardiolipin is a Key Determinant for mtDNA Stability and Segregation during Mitochondrial Stress. *Biochim. Biophys. Acta Bioenerg.* **2015**, *1847*, 587–598. [[CrossRef](#)] [[PubMed](#)]
45. Alexeyev, M.; Shokolenko, I.; Wilson, G.; LeDoux, S. The Maintenance of Mitochondrial DNA Integrity—Critical Analysis and Update. *Cold Spring Harb. Perspect. Biol.* **2013**, *5*, a012641. [[CrossRef](#)] [[PubMed](#)]
46. Saric, A.; Andreau, K.; Armand, A.; Moller, I.; Petit, P. Barth Syndrome: From Mitochondrial Dysfunctions Associated with Aberrant Production of Reactive Oxygen Species to Pluripotent Stem Cell Studies. *Front. Genet.* **2016**, *6*, 359. [[CrossRef](#)] [[PubMed](#)]
47. Rotig, A.; Lonlay, P.; Chretien, D.; Foury, F.; Koenig, M.; Sidi, D.; Munnich, A.; Rustin, P. Aconitase and Mitochondrial Iron-sulphur Protein Deficiency in Friedreich Ataxia. *Nat. Genet.* **1997**, *17*, 215–217. [[CrossRef](#)] [[PubMed](#)]
48. Koeppen, A. Friedreich Ataxia: Pathology, Pathogenesis, and Molecular Genetics. *J. Neurol. Sci.* **2011**, *303*, 1–12. [[CrossRef](#)] [[PubMed](#)]
49. Abeti, R.; Parkinson, M.; Hargreaves, I.; Angelova, P.; Sandi, C.; Pook, M.; Giunti, P.; Abramov, A. Mitochondrial Energy Imbalance and Lipid Peroxidation Cause Cell Death in Friedreich Ataxia. *Cell Death Dis.* **2016**, *7*, e2237. [[CrossRef](#)] [[PubMed](#)]
50. Babcock, M.; Silva, D.; Oaks, R.; Davis-Kaplan, S.; Jiralerspong, S.; Montermini, L.; Pandolfo, M.; Kaplan, J. Regulation of Mitochondrial Iron Accumulation by Yfh1p, a putative Homolog of Frataxin. *Science* **1997**, *276*, 1709–1712. [[CrossRef](#)] [[PubMed](#)]
51. Gerber, J.; Muhlenhoff, U.; Lill, R. An Interaction between Frataxin and Isu1/Nfs1 That is Crucial for Fe/S Cluster Synthesis on Isu1. *EMBO Rep.* **2003**, *4*, 906–911. [[CrossRef](#)] [[PubMed](#)]
52. Kaplan, J. Friedreich Ataxia is a Mitochondrial Disorder. *Proc. Natl. Acad. Sci. USA* **1999**, *96*, 10948–10949. [[CrossRef](#)] [[PubMed](#)]
53. Bresgen, N.; Eckl, P. Oxidative Stress and the Homeodynamics of Iron Metabolism. *Biomolecules* **2015**, *5*, 808–847. [[CrossRef](#)] [[PubMed](#)]
54. Wong, A.; Yang, J.; Cavadini, P.; Gellera, C.; Lonnerdal, B.; Taroni, F.; Cortopassi, G. The Friedreich Ataxia Mutation Confers Cellular Sensitivity to Oxidant Stress Which is Rescued by Chelators of Iron and Calcium and Inhibitors of Apoptosis. *Hum. Mol. Genet.* **1999**, *8*, 6. [[CrossRef](#)]
55. Yuxi, S.; Schoenfeld, R.; Hayashi, G.; Napoli, E.; Akiyama, T.; Carstens, M.; Carstens, E.; Pook, M.; Cortopassi, G. Frataxin Deficiency Leads to Defect in Expression of Antioxidants and Nrf2 Expression in Dorsal Root Ganglia of the Friedreich Ataxia YG8R Mouse Model. *Antioxid. Redox Signal.* **2013**, *19*, 1481–1493.
56. Runko, A.; Griswold, A.; Kyung-Tai, M. Overexpression of Frataxin in the Mitochondria Increases Resistance to Oxidative Stress and Extends Lifespan in *Drosophila*. *FEBS Lett.* **2008**, *582*, 715–719. [[CrossRef](#)] [[PubMed](#)]
57. Koenig, M.; Mandel, J. Deciphering the Cause of Friedreich Ataxia. *Curr. Opin. Neurobiol.* **1997**, *7*, 689–694. [[CrossRef](#)]
58. Beinert, H.; Kennedy, M. Aconitase, a Two-faced Protein: Enzyme and Iron Regulatory Factor. *FASEB J.* **1993**, *15*, 1442–1449.
59. Vasquez-Vivar, J.; Kalyanaraman, B.; Kennedy, M. Mitochondrial Aconitase is a Source of Hydroxyl Radical: An Electron Spin Resonance Investigation. *J. Biol. Chem.* **2000**, *275*, 14064–14069. [[CrossRef](#)] [[PubMed](#)]
60. Houten, B.; Woshner, V.; Santos, J. Role of Mitochondrial DNA in Toxic Responses to Oxidative Stress. *DNA Repair (Amst.)* **2006**, *5*, 145–152. [[CrossRef](#)] [[PubMed](#)]
61. Gardner, P.; Fridovich, I. Superoxide Sensitivity of the Escherichia Coli Aconitase. *J. Biol. Chem.* **1991**, *266*, 19328–19333. [[PubMed](#)]

62. Haile, D.; Rouault, T.; Harford, J.; Kennedy, M.; Blondin, G.; Klausner, R. Cellular Regulation of the Iron-responsive Element Binding Protein: Disassembly of the Cubane Iron-sulfur Cluster Results in High Affinity RNA Binding. *Proc. Natl. Acad. Sci. USA* **1992**, *89*, 11735–11739. [[CrossRef](#)] [[PubMed](#)]
63. Liang, L.; Ho, Y.; Patel, M. Mitochondrial Superoxide Production in Kainate-induced Hippocampal Damage. *Neuroscience* **2000**, *101*, 563–570. [[CrossRef](#)]
64. Kim, H.; LaVaute, T.; Iwai, K.; Klausner, R.; Rouault, T. Identification of a Conserved and Functional Iron-responsive Element in the 5'-Untranslated Region of Mammalian Mitochondrial Aconitase. *J. Biol. Chem.* **1996**, *271*, 24226–24230. [[CrossRef](#)] [[PubMed](#)]
65. Stankiewicz, J.; Brass, S. Role of Iron in Neurotoxicity: A cause for Concern in the Elderly? *Curr. Opin. Clin. Nutr. Metab. Care* **2009**, *12*, 22–29. [[CrossRef](#)] [[PubMed](#)]
66. Fariss, M.; Chan, C.; Patel, M.; Houten, B.; Orrenius, S. Role of Mitochondria in Toxic Oxidative Stress. *Mol. Interv.* **2005**, *5*, 94–111. [[CrossRef](#)] [[PubMed](#)]
67. Reeve, A.; Simcox, E.; Turnbull, D. Aging and Parkinson's disease: Why is Advancing Age the Biggest Risk Factor? *Aging Res. Rev.* **2014**, *14*, 19–30. [[CrossRef](#)] [[PubMed](#)]
68. Eden, S.; Tanner, M.; Bernstein, A.; Fross, R.; Leimpeter, A.; Bloch, D.; Nelson, L. Incidence of Parkinson's Disease: Variation by Age, Gender, and Race/Ethnicity. *Am. J. Epidemiol.* **2003**, *157*, 1015–1022. [[CrossRef](#)]
69. Jankovic, J. Parkinson's Disease: Clinical Features and Diagnosis. *J. Neurol. Neurosurg. Psychiatry* **2008**, *79*, 368–376. [[CrossRef](#)] [[PubMed](#)]
70. Stefanis, L. α -Synuclein in Parkinson's Disease. *Cold Spring Harb. Perspect. Med.* **2012**, *2*, a009399. [[CrossRef](#)] [[PubMed](#)]
71. Langston, J.; Ballard, P.; Tetrud, J.; Irwin, I. Chronic Parkinsonism in Humans due to a Product of Mepredine-analog Synthesis. *Science* **1983**, *219*, 979–980. [[CrossRef](#)] [[PubMed](#)]
72. Abou-Sleiman, P.; Muqit, M.; Wood, N. Expanding Insights of Mitochondrial Dysfunction in Parkinson's Disease. *Nat. Rev. Neurosci.* **2006**, *7*, 207–219. [[CrossRef](#)] [[PubMed](#)]
73. Dauer, W.; Przedborski, S. Parkinson Disease: Mechanisms and Models. *Neuron* **2003**, *39*, 889–909. [[CrossRef](#)]
74. Blesa, J.; Phani, S.; Jackson-Lewis, V.; Przedborski, S. Classic and New Animal Models of Parkinson's Disease. *J. Biomed. Biotechnol.* **2012**, *2012*, 1–10. [[CrossRef](#)] [[PubMed](#)]
75. Parker, W.; Parks, J.; Swerdlow, R. Complex I Deficiency in Parkinson's Disease Frontal Cortex. *Brain Res.* **2008**, *1189*, 215–218. [[CrossRef](#)] [[PubMed](#)]
76. Blandini, F.; Nappi, G.; Greenamyre, J. Quantitative Study of Mitochondrial Complex I in Platelets of Parkinsonian Patients. *Mov. Disord.* **1998**, *13*, 11–15. [[CrossRef](#)] [[PubMed](#)]
77. Blin, O.; Desnuelle, C.; Rascol, O.; Borg, M.; Peyro, H.; Azulay, J.; Bille, F.; Figarella, D.; Coulom, F.; Pellissier, J. Mitochondrial Respiratory Failure in Skeletal Muscle from Patients with Parkinson's Disease and Multiple System Atrophy. *J. Neurol. Sci.* **1994**, *125*, 95–101. [[CrossRef](#)]
78. Haas, R.; Nasirian, F.; Nakano, K.; Ward, D.; Pay, M.; Hill, R.; Shults, C. Low platelet Mitochondrial complex I and Complex II/III Activity in Early Untreated Parkinson's Disease. *Ann. Neurol.* **1995**, *37*, 714–722. [[CrossRef](#)] [[PubMed](#)]
79. Acín-Pérez, R.; Bayona-Bafaluy, M.; Fernández-Silva, P.; Moreno-Loshuertos, R.; Pérez-Martos, A.; Bruno, C.; Moraes, C.; Enriquez, J. Respiratory Complex III Is Required to Maintain Complex I in Mammalian Mitochondria. *Mol. Cell* **2004**, *13*, 805–815. [[CrossRef](#)]
80. Keane, P.; Kurzawa, M.; Blain, P.; Morris, C. Mitochondrial Dysfunction in Parkinson's Disease. *Parkinsons Dis.* **2011**, *2011*, 1–18. [[CrossRef](#)] [[PubMed](#)]
81. Dominic, H.; Scott, A.; Ashley, B.; Peng, L. A Delicate Balance: Iron Metabolism and Disease of the Brain. *Front. Aging Neurosci.* **2013**, *5*, 34.
82. Moos, T.; Nielsen, T.; Skjorringe, T.; Morgan, E. Iron Trafficking Inside the Brain. *J. Neurochem.* **2007**, *103*, 1730–1740. [[CrossRef](#)] [[PubMed](#)]
83. Winter, W.; Bazydlo, L.; Harris, N. The Molecular Biology of Human Iron Metabolism. *Lab. Med.* **2014**, *45*, 92–102. [[CrossRef](#)] [[PubMed](#)]
84. Conner, J.; Benkovic, S. Iron Regulation in the Brain: Histochemical, Biochemical, and Molecular Considerations. *Ann. Neurol.* **1992**, *32*, 51–61. [[CrossRef](#)]
85. Brzoska, K.; Meczynska, S.; Kruszewski, M. Iron-sulfur Cluster Proteins: Electron Transfer and Beyond. *Acta Biochim. Pol.* **2006**, *53*, 685–691. [[PubMed](#)]
86. Hirsch, E.; Faucheux, B. Iron Metabolism and Parkinson's Disease. *Mov. Disord.* **1998**, *13*, 39–45. [[PubMed](#)]

87. Dexter, D.; Wells, F.; Lees, A.; Javoy-Agid, F.; Agid, Y.; Jenner, P.; Marsden, C. Increased Nigral Iron Content and Alterations in Other Metal Ions Occurring in Brain in Parkinson's Disease. *J. Neurochem.* **1989**, *52*, 1830–1836. [[CrossRef](#)] [[PubMed](#)]
88. Dexter, D.; Wells, F.; Javoy-Agid, F.; Agid, Y.; Lees, A.; Jenner, P.; Marsden, C. Increased Nigral Iron Content in Postmortem Parkinsonian Brain. *Lancet* **1987**, *330*, 1219–1220. [[CrossRef](#)]
89. Hirsch, E.; Brandel, J.; Galle, P.; Javoy-Agid, F.; Agid, Y. Iron and Aluminum Increase in the Substantia Nigra of Patients with Parkinson's Disease: An X-Ray Microanalysis. *J. Neurochem.* **1991**, *56*, 446–451. [[CrossRef](#)] [[PubMed](#)]
90. Mazzi, E.; Soliman, K. Effects of Enhancing Mitochondrial Oxidative Phosphorylation with Reducing Equivalents and Ubiquinone on 1-methyl-4-phenylpyridinium Toxicity and Complex I-IV Damage in Neuroblastoma Cells. *Biochem. Pharmacol.* **2004**, *67*, 1167–1184. [[CrossRef](#)] [[PubMed](#)]
91. Shang, T.; Kotamraju, S.; Kalivendi, S.; Hillard, C.; Kalyanaraman, B. 1-Methyl-4-phenylpyridinium-induced Apoptosis in Cerebellar Granule Neurons is Mediated by Transferrin Receptor Iron-dependent Depletion of Tetrahydrobiopterin and Neuronal Nitric Oxide Synthase-derived Superoxide. *J. Biol. Chem.* **2004**, *279*, 19099–19112. [[CrossRef](#)] [[PubMed](#)]
92. Li-Ping, L.; Patel, M. Iron-sulfur Enzyme Mediated Mitochondrial Superoxide Toxicity in Experimental Parkinson's Disease. *J. Neurochem.* **2004**, *90*, 1076–1084.
93. Ebadi, M.; Srinivasan, K.; Baxi, M. Oxidative Stress and Antioxidant Therapy in Parkinson's Disease. *Prog. Neurobiol.* **1996**, *48*, 1–19. [[CrossRef](#)]
94. Obata, T. Dopamine Efflux by MPTP and Hydroxyl Radical Generation. *J. Neural Trans.* **2002**, *109*, 1159–1180. [[CrossRef](#)] [[PubMed](#)]
95. Jomova, K.; Valko, M. Advances in Metal-induced Oxidative Stress and Human Disease. *Toxicology* **2011**, *283*, 65–87. [[CrossRef](#)] [[PubMed](#)]
96. Nunez, T.; Urrutia, P.; Mena, N.; Aguirre, P.; Tapia, V.; Salazar, J. Iron Toxicity in Neurodegeneration. *Biomaterials* **2012**, *25*, 761–776.
97. Owen, J.; Butterfield, D. Measurement of Oxidized/Reduced Glutathione Ratio. *Methods Mol. Biol.* **2010**, *648*, 269–277. [[PubMed](#)]
98. Sipos, K.; Lange, H.; Fekete, Z.; Ullmann, P.; Lill, R.; Kispal, G. Maturation of Cytosolic Iron-sulfur Proteins Requires Glutathione. *J. Biol. Chem.* **2002**, *277*, 26944–26949. [[CrossRef](#)] [[PubMed](#)]
99. Dias, V.; Junn, E.; Mouradian, M. The Role of Oxidative Stress in Parkinson's Disease. *J. Parkinsons Dis.* **2013**, *3*, 461–491. [[PubMed](#)]
100. Heales, S.; Bolanos, J. Impairment of Brain Mitochondrial Function by Reactive Nitrogen Species: The Role of Glutathione in Dictating Susceptibility. *Neurochem. Int.* **2002**, *40*, 469–474. [[CrossRef](#)]
101. Dimonte, D.; Chan, P.; Sandy, M. Glutathione in Parkinson's Disease: A link Between Oxidative Stress and Mitochondrial Damage? *Ann. Neurol.* **1992**, *32*, 111–115. [[CrossRef](#)]
102. Mari, M.; Morales, A.; Colell, A.; Garcia-Ruiz, C.; Fernandez-Checa, J. Mitochondrial Glutathione, a Key Survival Antioxidant. *Antioxid. Redox Signal.* **2009**, *11*, 2685–2700. [[CrossRef](#)] [[PubMed](#)]
103. Heales, S.; Davies, S.; Bates, T.; Clark, J. Depletion of Brain Glutathione is Accompanied by Impaired Mitochondrial Function and Decreased N-acetyl Aspartate Concentration. *Neurochem. Res.* **1995**, *20*, 31–38. [[CrossRef](#)] [[PubMed](#)]
104. Merad-Saidoune, M.; Biotier, E.; Nicole, A.; Marsac, C.; Martinou, J.; Sola, B.; Sinet, P.; Ceballos-Picot, I. Overproduction of Cu/Zn-superoxide Dismutase or Bcl-2 Prevents the Brain Mitochondrial Respiratory Dysfunction Induced by Glutathione Depletion. *Exp. Neurol.* **1999**, *158*, 428–436. [[CrossRef](#)] [[PubMed](#)]
105. Jha, N.; Jurma, O.; Lalli, G.; Liu, Y.; Pettus, E.; Greenamyre, J.; Liu, R.; Forman, H.; Anderson, J. Glutathione Depletion in PC12 Results in Selective Inhibition of Mitochondrial Complex I Activity: Implication for Parkinson's Disease. *J. Biol. Chem.* **2000**, *275*, 26096–26101. [[CrossRef](#)] [[PubMed](#)]
106. Hargreaves, I.; Sheena, Y.; Land, J.; Heales, S. Glutathione Deficiency in Patients with Mitochondrial Disease: Implication for Pathogenesis and Treatment. *J. Inher. Dis.* **2005**, *28*, 81–88. [[CrossRef](#)] [[PubMed](#)]
107. Jenner, P.; Dexter, D.; Sian, J.; Schapira, A.; Marsden, C. Oxidative stress as a Cause of Nigral Cell Death in Parkinson's Disease and Incidental Lewy Body Disease. The Royal Kings and Queens Parkinson's Disease Research Group. *Ann. Neurol.* **1992**, *32*, 82–87. [[CrossRef](#)]

108. Zeevalk, G.D.; Manzano, L.; Sonsalla, P.K.; Bernard, L.P. Characterization of Intracellular Elevation of Glutathione (GSH) with Glutathione Monoethyl Ester and GSH in Brain and Neuronal Cultures: Relevance to Parkinson's Disease. *Exp. Neurol.* **2007**, *203*, 512–520. [[CrossRef](#)] [[PubMed](#)]
109. Farr, S.; Poon, H.; Dogrukol-Ak, D.; Drake, J.; Banks, W.; Eyerman, E.; Butterfield, D.; Morley, J. The Antioxidants α -lipoic Acid and N-Acetylcysteine Reverse Memory Impairment and Brain Oxidative Stress in Aged SAMP8 Mice. *J. Neurochem.* **2003**, *84*, 1173–1183. [[CrossRef](#)] [[PubMed](#)]
110. Kerksick, C.; Willoughby, D. The Antioxidant Role of Glutathione and N-Acetyl-Cysteine Supplements and Exercise-Induced Oxidative Stress. *Int. Soc. Sports Nutr.* **2005**, *2*, 38–44. [[CrossRef](#)] [[PubMed](#)]
111. Munoz, M.; Rey, P.; Soto, R.; Guerra, M.; Labandeira, L. Systemic Administration of N Acetylcysteine Protects Dopaminergic Neurons Against 6 Hydroxydopamine Induced Degeneration. *J. Neurosci. Res.* **2004**, *76*, 551–562. [[CrossRef](#)] [[PubMed](#)]
112. Hargreaves, I.P. Coenzyme Q₁₀ as a Therapy for Mitochondrial Disease. *Int. J. Biochem. Cell Biol.* **2014**, *49*, 105–111. [[CrossRef](#)] [[PubMed](#)]
113. Duncan, A.; Heales, S.; Mills, K.; Eaton, S.; Land, J.; Hargreaves, I. Determination of Coenzyme Q₁₀ Status in Blood Mononuclear Cells, Skeletal Muscle, and Plasma by HPLC with Di-Propoxy-Coenzyme Q₁₀. *Clin. Chem.* **2005**, *51*, 2380–2382. [[CrossRef](#)] [[PubMed](#)]
114. Ogasahara, S.; Engel, A.; Frens, D.; Mack, D. Muscle Coenzyme Q Deficiency in Familial Mitochondrial Encephalomyopathy. *Proc. Natl. Acad. Sci. USA* **1989**, *86*, 2379–2382. [[CrossRef](#)] [[PubMed](#)]
115. Maldergem, L.; Trijbels, F.; DiMauro, S.; Sindelar, P.; Musumeci, O.; Janssen, A.; Delberghe, X.; Martin, J.; Gillerot, Y. Coenzyme Q-Responsive Leigh's Encephalopathy in Two Sisters. *Ann. Neurol.* **2002**, *52*, 750–754. [[CrossRef](#)] [[PubMed](#)]
116. Papadimitriou, A.; Hadjigeorgiou, G.; Divari, R.; Papagalanis, N.; Comi, G.; Bresolin, N. The Influence of Coenzyme Q₁₀ on Total Serum Calcium concentration in Two Patients with Kearns—Sayre syndrome and hypoparathyroidism. *Neuromuscul. Disord.* **1996**, *6*, 49–53. [[CrossRef](#)]
117. Quinzii, C.; DiMauro, S.; Hirano, M. Human Coenzyme Q₁₀ Deficiency. *Neurochem. Res.* **2007**, *32*, 723–727. [[CrossRef](#)] [[PubMed](#)]
118. Koene, S.; Smeitink, J. Metabolic Manipulators: A Well Founded Strategy to Combat Mitochondrial Dysfunction. *J. Inherit. Metab. Dis.* **2011**, *34*, 315–325. [[CrossRef](#)] [[PubMed](#)]
119. Napolitano, A.; Salyetti, S.; Vista, M.; Lombardi, V.; Siciliano, G.; Giraldi, C. Long-Term Treatment with Idebenone and Riboflavin in a Patient with MELAS. *Neurol. Sci.* **2000**, *21*, 981–982. [[CrossRef](#)]
120. Mancuso, M.; Orsucci, D.; Filosto, M.; Simoncini, C.; Siciliano, G. Drugs and Mitochondrial Diseases: 40 Queries and Answers. *Expert Opin. Pharmacother.* **2012**, *13*, 527–543. [[CrossRef](#)] [[PubMed](#)]
121. Jaber, S.; Polster, B. Idebenone and Neuroprotection: Antioxidant, Pro-Oxidant, or Electron Carrier? *J. Bioenergy Biomembr.* **2015**, *47*, 111–118. [[CrossRef](#)] [[PubMed](#)]
122. Shults, C.; Haas, R.; Passov, D.; Beal, M. Coenzyme Q₁₀ Levels Correlate with the Activities of Complex I and II/III in Mitochondria From Parkinsonian and Nonparkinsonian subjects. *Ann. Neurol.* **1997**, *42*, 261–264. [[CrossRef](#)] [[PubMed](#)]
123. Hargreaves, I.; Lane, A.; Sleiman, P. The Coenzyme Q₁₀ Status of the Brain Regions of Parkinson's Disease Patients. *Neurosci. Lett.* **2008**, *447*, 17–19. [[CrossRef](#)] [[PubMed](#)]
124. Sohmiya, M.; Tanaka, M.; Tak, N.W.; Yanagisawa, M.; Tanino, Y.; Suzuki, Y.; Okamoto, K.; Yamamoto, Y. Redox Status of Plasma Coenzyme Q₁₀ Indicates Elevated Systemic Oxidative Stress in Parkinson's Disease. *J. Neurol. Sci.* **2004**, *223*, 161–166. [[CrossRef](#)] [[PubMed](#)]
125. Gotz, M.; Gerstner, A.; Harth, R.; Dirr, A.; Janetzky, B.; Kuhn, W.; Riederer, P.; Gerlach, M. Altered Redox State of Platelet Coenzyme Q₁₀ in Parkinson's Disease. *J. Neural Transm. (Vienna)* **2000**, *107*, 41–48.
126. Gille, G.; Hung, S.; Reichmann, H.; Rausch, W. Oxidative Stress to Dopaminergic Neurons as Models of Parkinson's Disease. *Ann. N. Y. Acad. Sci.* **2004**, *1018*, 533–540. [[CrossRef](#)] [[PubMed](#)]
127. Kooncumchoo, P.; Sharma, S.; Porter, J.; Govitrapong, P.; Ebadi, M. Coenzyme Q (10) Provides Neuroprotection in Iron-Induced Apoptosis in Dopaminergic Neurons. *J. Mol. Neurosci.* **2006**, *28*, 125–141. [[CrossRef](#)]
128. Winkler-Stuck, K.; Wiedemann, F.; Wallesch, C.; Kunz, S. Effect of Coenzyme Q₁₀ on the Mitochondrial Function of Skin Fibroblasts from Parkinson Patients. *J. Neurol. Sci.* **2004**, *220*, 41–48. [[CrossRef](#)] [[PubMed](#)]
129. Moreira, P.I.; Zhu, X.; Wang, X.; Lee, Y.-G.; Nunomura, A.; Peterson, R.B.; Perry, G.; Smith, M.A. Mitochondria: A Therapeutic Target in Neurodegeneration. *Biochim. Biophys. Acta* **2010**, *1802*, 212–220. [[CrossRef](#)] [[PubMed](#)]

130. Shults, C.; Oakes, D.; Kieburtz, K.; Beal, M.; Haas, R.; Plumb, S.; Juncos, J.; Nutt, J.; Shoulson, I.; Carter, J.; et al. Parkinson Study Group. Effects of Coenzyme Q₁₀ in Early Parkinson Disease: Evidence of Slowing of the Functional Decline. *Arch. Neurol.* **2002**, *59*, 1541–1550. [[CrossRef](#)] [[PubMed](#)]
131. Josef, F. Treatment of Mitochondrial Disorders. *Eur. J. Pediatr. Neurol.* **2010**, *14*, 29–44.
132. Josef, F.; Bindu, P. Therapeutic Strategies for Mitochondrial Disorders. *Pediatr. Neurol.* **2015**, *52*, 302–313.
133. Jin, H.; Kanthasamy, A.; Ghosh, A.; Anantharam, V.; Kaylanaraman, B.; Kanthasamy, G. Mitochondria-targeted Antioxidants for Treatment of Parkinson's Disease: Preclinical and Clinical Outcomes. *Biochim. Biophys. Acta* **2014**, *1842*, 1282–1294. [[CrossRef](#)] [[PubMed](#)]
134. Teodoro, G.; Baraldi, G.; Sampaio, H.; Bomfim, H.; Queiroz, L.; Passos, A.; Carneiro, M.; Alberici, C.; Gomis, R.; Amaral, G.; et al. Melatonin Prevents Mitochondrial Dysfunction and Insulin Resistance in Rat Skeletal Muscle. *J. Pineal Res.* **2014**, *57*, 155–167. [[CrossRef](#)] [[PubMed](#)]
135. Smith, R.; Adlam, V.; Blaikie, F.; Manas, A.; Porteous, C.; James, A.; Ross, M.; Logan, A.; Cochemé, H.; Trnka, J.; et al. Mitochondria-Targeted Antioxidants in the Treatment of Disease. *Ann. N. Y. Acad. Sci.* **2008**, *1147*, 105–111. [[CrossRef](#)] [[PubMed](#)]
136. Henderson, C.B.; Filloux, F.M.; Alder, S.C.; Lyon, J.L.; Caplin, D.A. Efficacy of the Ketogenic Diet as a treatment Option for Epilepsy: Meta-Analysis. *J. Child. Neurol.* **2006**, *3*, 193–198.
137. Keene, D.L. A Systematic Review of the Use of the Ketogenic Diet in Childhood Epilepsy. *Pediatr. Neurol.* **2006**, *1*, 1–5. [[CrossRef](#)] [[PubMed](#)]
138. Neal, E.G.; Chaffe, H.; Schwartz, R.H.; Lawson, M.S.; Edwards, N.; Fitzsimmons, G.; Whitney, A.; Cross, J.H. A Randomized Trial of Classical and Medium-Chain Triglyceride Ketogenic Diets in the Treatment of Childhood Epilepsy. *Epilepsia* **2009**, *5*, 1109–1117. [[CrossRef](#)] [[PubMed](#)]
139. Bough, K.J.; Wetherington, J.; Hassel, B.; Pare, J.F.; Gawryluk, J.W.; Greene, J.G.; Shaw, R.; Smith, Y.; Geiger, J.D.; Dingleline, R.J. Mitochondrial Biogenesis in The Anticonvulsant Mechanism of the Ketogenic Diet. *Ann. Neurol.* **2006**, *2*, 223–235. [[CrossRef](#)] [[PubMed](#)]
140. Hughes, S.D.; Kanabus, M.; Anderson, G.; Hargreaves, I.P.; Rutherford, T.; O'Donnell, M.; Cross, J.H.; Rahman, S.; Eaton, S.; Heales, S.J. The Ketogenic Diet Component Decanoic Acid Increases Mitochondrial Citrate Synthase and Complex I Activity in Neuronal Cells. *J. Neurochem.* **2014**, *3*, 426–433. [[CrossRef](#)] [[PubMed](#)]
141. Kanabus, M.; Fassone, E.; Hughes, S.D.; Bilooei, S.F.; Rutherford, T.; O'Donnell, M.; Heales, S.J.R.; Rahman, S. The Pleiotropic Effects of Decanoic Acid Treatment on Mitochondrial Function in Fibroblasts from Patients with Complex I Deficient Leigh Syndrome. *J. Inherit. Metab. Dis.* **2016**, *39*, 415–426. [[CrossRef](#)] [[PubMed](#)]



© 2017 by the authors. Licensee MDPI, Basel, Switzerland. This article is an open access article distributed under the terms and conditions of the Creative Commons Attribution (CC BY) license (<http://creativecommons.org/licenses/by/4.0/>).

Drug-Induced Mitochondrial Toxicity

Iain P. Hargreaves^{1,2} · Mesfer Al Shahrani^{1,3,5} · Luke Wainwright² ·
Simon J. R. Heales^{1,2,3,4}

Published online: 18 March 2016
© Springer International Publishing Switzerland 2016

